Characterisation of *ITGB3* and *ITGA2B* gene defects associated with Glanzmann thrombasthenia

Essa Mohammed E. Sabi

A thesis submitted in part fulfilment of the requirements for Doctor of Philosophy degree at the University of Sheffield

Department of Infection, Immunity & Cardiovascular Disease

July 2016

Abstract

Glanzmann thrombasthenia (GT) is a recessively inherited bleeding disorder caused by quantitative and, or, qualitative deficiencies of the platelet integrin $\alpha_{IIb}\beta_3$, which binds fibrinogen to mediate platelet aggregation at sites of vascular injury. The α- and β-subunits of $\alpha_{IIb}\beta_3$ are encoded by *ITGA2B* and *ITGB3* respectively, and many genetic defects resulting in reduced expression or dysfunction of $\alpha_{IIb}\beta_3$ have been described. A previous survey of UK GT patients that was carried out by our group identified 14 uncharacterised nonsynonymous alterations in *ITGA2B* and *ITGB3* that predicted amino acid substitutions in different domains of α_{IIb} and β_3. This study used combined *in silico* and *in vitro* approaches to confirm the pathogenicity of 13 of these alterations; eight *ITGB3* variants predicting p.Trp11Arg, p.Pro189Ser, p.Glu200Lys, p.Trp264Leu, p.Ser317Phe, p.Cys547Trp, p.Cys554Arg and p.Ile665Thr substitutions in β_3 and five *ITGA2B* variants predicting p.Asp396Asn, p.Leu492Pro, p.Ile596Thr, p.Asn670Lys and p.Glu698Asp substitutions in α_{IIb}.

With the exception of the β_3_p.Glu200Lys and α_{IIb}_p.Glu698Asp variants, *in silico* analysis predicted all variants to be pathogenic. Compared to cells expressing wild-type (WT) $\alpha_{IIb}\beta_3$, there was an almost complete absence of surface $\alpha_{IIb}\beta_3$ in cells expressing the p.Trp11Arg, p.Pro189Ser, Trp264Leu and Ser317Phe β_3 variants ($p<0.0001$). In contrast, the β_3_p.Ile665Thr variant was expressed at similar levels to WT, but showed reduced ability to bind an antibody that is specific for the active conformation of the receptor, PAC1 ($p<0.01$) and also fibrinogen ($p<0.05$), while the β_3_p.Glu200Lys variant does not appear to cause dysfunction to $\alpha_{IIb}\beta_3$. Interestingly, cells expressing the p.Cys547Trp and p.Cys554Arg β_3 variants showed moderate reductions in surface expression of $\alpha_{IIb}\beta_3$ ($p<0.0001$) that exhibited spontaneous activation ($p<0.0001$;$p<0.001$). The majority of the substitutions in β_3 resulted in greater than 90% reductions ($p<0.0001$) in membrane expression of $\alpha_v\beta_3$ with the exception of the p.Glu200Lys and p.Pro189Ser substitutions which resulted in 78% ($p<0.0001$) and 21% ($p<0.001$) reductions in membrane expression of $\alpha_v\beta_3$, respectively.

There was a severe reduction in membrane $\alpha_{IIb}\beta_3$ on cells expressing the p.Asp396Asn, the p.Leu492Pro and the p.Ile596Thr α_{IIb} variants ($p<0.0001$) while the p.Asn670Lys α_{IIb} was expressed at similar levels to wild-type α_{IIb}. Interestingly, the p.Leu492Pro and p.Asn670Lys variants showed reduced ability to bind PAC1 ($p<0.0001$;$p<0.01$) and fibrinogen ($p<0.0001$;$p<0.01$). The c.2094G>T transversion in *ITGA2B,* predicted to cause a p.Glu698Asp substitution in α_{IIb}, was associated with a

splicing defect, resulting in the deletion of exon 20 from the *ITGA2B* RNA , and the loss of $\alpha_{IIb}\beta_3$ expression.

These findings confirm the pathogenicity and demonstrate the underlying mechanisms associated with GT for the majority of the variants studied. Interestingly, while the β_3_p.Glu200Lys variant does not appear to cause $\alpha_{IIb}\beta_3$ dysfunction, it does result in a reduction in $\alpha_v\beta_3$ (vitronectin) receptor expression, though it remains unknown how this defect results in GT.

Acknowledgements

Firstly, I would like to express my profound gratitude to my PhD sponsor King Saud University, without whom none of this would have been possible.

I am truly grateful to my primary supervisor, Dr Martina Daly, for allowing me to undertake my PhD research within her group. Your advice, support and encouragement throughout the course of my PhD have been greatly appreciated. I wish you all the best for the future. I would also like to thank my secondary supervisors, Dr Jacqui Stockley and Dr Vincenzo Leo, for your support and advice during my studies. I wish you both all the best in your future careers.

To Dr Asmaa Al-Marwani, thank you for providing me with an interesting base from which to undertake my PhD research. Had it not been for your previous hard work, I don't think I would have enjoyed my project as much as I have.

I would also like to thank all members of the Haemostasis research group, both past and present, who have helped me throughout my PhD at a professional and a personal level. I have learned so much from each and every one of you and I consider you all great friends. It is because of you all that I have enjoyed my time in Sheffield so much and it will always hold a special place in my heart.

My thanks are also extended to my colleagues, the academic and technical staff in the former department of cardiovascular science and to the technical staff in the Research Core facilities for their support and help during my study. I am also hugely appreciative to Dr Alan Nurden and his group, for their suggestions about structural modelling.

Finally, I would like to thank my family for their love and support during my studies in Sheffield. To my parents, and especially my mother, I know how hard it has been for you but I have now completed my studies and am coming home! Thank you so much for all your love, help and support especially over the last few months with the arrival of my beautiful baby girl.

To my wife, your love and support has helped me through the difficult periods of my PhD studies. I am truly grateful for everything you do and you have given me the greatest gift I could possibly ask for with the birth our beautiful baby girl, Elaf.

The last acknowledgement is to Elaf, my baby girl, you have been the light of my life since your arrival. You have also been the inspiration and motivation I needed to complete my thesis so that I could return home. I love you now and always.

Alhamdulillah, all praises to Allah for the strengths and His blessing in completing this study.

Table of Contents

List of figures

List of tables

List of abbreviations

AC	adenylyl cyclase
ADMIDAS	Adjacent metal ion adhesion site
ADP	Adenosine 5'-diphosphate
APS	Ammonium persulfate
ASSEDA	Automated Splice Site and Exon Definition Analysis
ATCC	American Type Culture Collection
BDGP	Berkeley Drosophila Genome Project
BDGP	Berkeley Drosophila Genome Project
BFU-MK	Burst-forming unit megakaryocytes
BHK	baby hamster kidney
BLAST	Basic Local Alignment Search Tool
bp	Base pair
BSA	bovine serum albumin
BSS	Bernard–Soulier syndrome
C	cysteine
c.	Nucleotide alteration position
Ca^2+	Calcium
CaIDAG-GEF	diacyglycerol-regulated guanine nucleotide exchange factor I
cDNA	Complementary Deoxyribonucleic Acid
CFU-MK	Colony-forming unit megakaryocytes
CHO	Chinese hamster ovary cells
CLP	Common lymphoid progenitor
CMV	Cytomegalovirus
CMP	Common myeloid progenitor
CO_2	Carbon dioxide
COS-7	Monkey kidney tissue culture cell line
c-region	C-terminal region
DAG	Diacylglycerol
DMS	Demarcation membrane system
DMSO	Dimethyl sulfoxide
DNA	Deoxyribonucleic Acid
dNTP	Deoxynucleotide triphosphate
DPBS	Dulbecco's phosphate buffered saline
DTT	Dithiothreitol
E.coli	Escherichia coli
ECM	Extracellular matrix substances
EDTA	Ethylene diamine tetra acetic acid
EGF	Epidermal growth factor

Endo H	Endoglycosidase H
ER	Endoplasmic reticulum
ESE	Exonic splice enhancer
EtBr	ethidium bromide
FACs	Fluorescence-activated cell sorting
Factor I	Fibrinogen
Factor II	Prothrombin
Factor IX	Christmas factor
Factor VII	Proconvertin
Factor VIII	Antihemophilic factor
Factor X	Stuart-Prower factor
Factor XI	Plasma thromboplastin antecedent
Factor XII	Hageman factor
FBS	Foetal bovine serum
FCS	Fetal Calf Serum
FITC	Fluorescein isothiocyanate
FSC	Forward scatter
g	Gram
GMP	Granulocyte – monocyte progenitor
GP	Glycoprotein
GT	Glanzmann’s thrombasthenia
GTP	Guanosine-5'-triphosphate
GVGD	Align Grantham Variation Grantham Deviation
HCl	Hydrochloric acid
HEK 293T	Human embryonic kidney culture cell line
HEL	Human erythroleukaemia cells
HF	High fidelity
h-region	Hydrophobic core region
HSC	Haematopoietic stem cell
HSF	Human Splicing Finder
HUGO	Human Genome Organization
IgG	Immunoglobulin G
IL	Interleukin
IP3	Inositol 1,4,5 trisphoshate
IRDye	Infrared fluorescent dyes
IT	Inherited thrombocytopenias
ITP	Inherited thrombocytopenia
Kb	Kilobase
kDa	Kilo Dalton
L	Litre
LB	Luria-Bertani broth

LIMBS	Ligand induced metal binding site
MEP	Megakaryocyte/erythrocyte progenitor
mg	Milligram
Mg^{2+}	Magnesium ions
$MgCl_2$	Magnesium chloride
MIDAS	Metal ion adhesion site
MKs	Megakaryocyte cells
ml	Millilitre
mM	Milli molar
mRNA	Messenger RNA
NCBI	National centre for Biotechnology Information
NaCl	Sodium chloride
Neo	Neomycin
ng	Nanogram
nm	nanometers
NO	nitric oxide
n-region	N-terminal region
OCS	Open canalicular system
p.	Protein substitution position using HGVS nomenclature
P13K	phosphoinositide 3-kinase
PCR	Polymerase chain reaction
pdb	Protein Data Bank
PE	R-phycoerythrin
PGI2	prostacyclin
PIP3	hosphatidylinositol-3,4,5-trisphosphate
PKC	protein kinase C
PLCβ2	phospholipase Cβ2
PMKB	Promegakaryoblasts
pmol	Picomole
Polyphen	Polymorphism Phenotyping v2
Polyphen-v2	Polymorphism phenotyping v2
PS	Phosphatidylserine
PSI	Plexins semaphorins integrins
RGD	Arginine-Glycine-Aspartic acid
Rho-GEF	RhoA-specific guanine nucleotide exchange factor
RIAM	Rap1-interacting adaptor molecule
RIPA	Radio-Immunoprecipitation Assay
RNA	Ribonucleic acid
rpm	Revolve per minute
RPMI	Roswell Park Memorial Institute medium
RT	reverse transcriptase

rVIIa	Recombinant activated factor VII
SDS	Sodium dodecyl sulphate
SDS-PAGE	Sodium dodecyl sulphate polyacrylamide gel electrophoresis
SIFT	Sorting Intolerant From Tolerant
SRSF1	Serine/arginine-rich splicing factor 1
SSC	side scatter
SyMBS	the Synergistic metal binding site
TBE	Tris-borate EDTA
TBS	Tris-buffered saline
TEMED	Tetramethylethylenediamine
TF	tissue factor
TM	transmembrane domain
TP	Thromboxane A2 receptor
TPO	Thrombopoietin
TxA_2	Thromboxane A2
UV	Ultra violet
v	Volume
VWF	von Willebrand Factor
x g	Times gravity
α	Alpha
B	Beta
µg	Microgram
µl	Microlitre
°C	Degrees Celcius

DNA nucleotides and symbols

Nucleotide	Symbol
Adenine	A
Cytosine	C
Guanine	G
Thymine	T
Uracil	U

Amino acids and symbols

Amino acid side chain	Amino acid	Symbol
Nonpolar	Alanine	A / Ala
	Glycine	G / Gly
	Isoleucine	I / Ile
	Leucine	L / Leu
	Methionine	M / Met
	Phenylalanine	F / Phe
	Proline	P / Pro
	Tryptophan	W / Trp
	Valine	V / Val
Uncharged polar	Asparagine	N / Asn
	Cysteine	C /Cys
	Glutamine	Q / Gln
	Serine	S / Ser
	Threonine	T / Thr
	Tyrosine	Y/ Tyr
Acidic	Aspartic acid	D / Asp
	Glutamic acid	E / Glu
Basic	Arginine	R / Arg
	Histidine	H / His
	Lysine	K / Lys

Publications, Poster and oral presentations arising from this work

Laguerre, M., Sabi, E., Daly, M., Stockley, J., Nurden, P., Pillois, X. & Nurden, A.T. (2013) Molecular dynamics analysis of a novel β_3 Pro189Ser mutation in a patient with Glanzmann thrombasthenia differentially affecting alphaIIbbeta3 and alphavbeta3 expression. PLoS One, 8, e78683.

Essa Sabi, Vincenzo C. Leo, Areej Al-Musbahi, Asmaa Al-Marwani, Michael Makris, Martina E. Daly (2015) Characterization of six alterations in *ITGA2B* and *ITGB3* associated with Glanzmann thrombasthenia. Abstract and poster presentation in XXV Congress of the International Society on Thrombosis and Haemostasis and 61st Annual SSC Meeting 2015 (Toronto, Candia). Journal of Thrombosis and Haemostasis 2015; Volume 14, Supplement s2: PO517.

Essa Sabi, V Leo, A Al-Marwani, M Makris, ME Daly (2014). Characterization of five αiib integrin defects associated with Glanzmann's thrombasthenia. Abstract and oral presentation in Joint British Society for Haemostasis & Thrombosis, UK Platelet Group & United Kingdom Haemophilia Centre Doctors Organisation Group Meeting 2014 (Edinburgh, UK).

EM Sabi, J Stockley, A Al-Marwani , E Kiss-Toth, M Makris, ME Daly (2013) Characterization of four novel beta 3 integrin defects associated with Glanzmann thrombasthenia. Abstract and oral presentation in XXV Congress of the International Society on Thrombosis and Haemostasis and 61st Annual SSC Meeting 2015 (Netherlands, Amsterdam). Journal of Thrombosis and Haemostasis 2014; Volume 11, Supplement s2: OC 62.6.

Chapter 1: Introduction

1.1 Introduction

Glanzmann thrombasthenia (GT) is a recessively inherited bleeding disorder caused by defects in the integrin $\alpha_{IIb}\beta_3$, which mediates platelet aggregation at sites of injury. The $\alpha_{IIb}\beta_3$ receptor is expressed in megakaryocytes and platelets and functions by binding to several adhesive molecules such as fibrinogen and Von Willebrand factor (VWF) (Nurden*, et al* 2013). The platelet is one of the most important blood cells, having roles in inflammation, metastasis and haemostasis. Of these, the role of platelets in stemming blood loss in response to blood vessel injury is by far the most important (Broos*, et al* 2011). Platelets are derived from mature megakaryocytes in bone marrow through the process of proplatelet formation. The number of platelets circulating in the blood is normally between 150 and 400 x 10^9/L and they have a life span of between 7 and 10 days. The number of platelets produced daily is estimated to be approximately 1x 10^{11} in healthy individuals, which maintains the platelet count at a normal level (Chang*, et al* 2007, Kaushansky 2009). Inherited defects in the genes regulating megakaryocyte and platelet production and function can give rise to quantitative and/or qualitative abnormalities which may be associated with an increased bleeding tendency (Nurden and Nurden 2011). In this review, platelet production, structure and function will be described. The inherited platelet bleeding disorders will also be reviewed with the main focus being on Glanzmann Thrombasthenia.

1.2 Platelets, their production, structure and role in haemostasis

1.2.1 Megakaryocyte development and thrombopoiesis

Platelets are produced from the cytoplasm of mature megakaryocytes (MKs) which are usually located in the bone marrow. The MK is considered to be the largest haematopoietic cell in human bone marrow and also one of the rarest cells. Thus, MKs are estimated to range from 20 to 100 µm in diameter and make up 0.02 to 0.05% (4 x 10^7) of all nucleated cells residing in the bone marrow (Levine*, et al* 1982). MKs are also present in other organs, such as the spleen, liver and lung. They are produced through a complex process called megakaryopoiesis, which commences with the commitment of multipotent haematopoietic stem cells (HSCs) to become the megakaryocyte progenitors that give rise to mature MKs which in turn gives rise to platelets via cytoplasmic fragmentation from proplatelets. This process occurs in a complex microenvironment in the bone marrow and is governed by various transcriptional factors and haematopoietic growth factors, such as GATA-1 and thrombopoietin (TPO) (Chang*, et al* 2007). It is worth mentioning that the bone marrow

microenvironment, upon which megakaryopoiesis and thrombopoiesis depends, includes extracellular matrix proteins, endothelial cells and soluble haematopoietic growth factors (Kaushansky 2009).

Megakaryocytes arise from the haematopoietic stem cell (HSC). The HSC is a self-renewing haematopoietic cell that has the ability to generate all cellular blood components. In the lineage commitment, the HSC generates a progeny of cells that lose their regenerative ability and multipotent character (Chang*, et al* 2007, Metcalf 1999). Firstly, the HSC undergoes commitment to become the multipotent progenitor that lacks self-renewability and then it gives rise to the early common myeloid progenitor (CMP) and common lymphoid progenitor (CLP). The CMP has multi-lineage potential and can give rise to erythrocytes, granulocytes, monocytes and megakaryocytes (Akashi*, et al* 2000, Kondo*, et al* 1997). CMP differentiation is mainly controlled by regulatory transcription factors. Among these factors, GATA-1 and Pu.1 are considered to be the main factors with the former playing a role in the differentiation of CMP to megakaryocyte/erythrocyte progenitors (MEP), whereas the latter drives differentiation to granulocyte–monocyte progenitors (GMP) (Iwasaki*, et al* 2003, Nutt*, et al* 2005). Under the influence of micro-environmental factors, MEPs give rise to the hierarchy of high proliferation MKs, starting with burst-forming unit megakaryocytes (BFU-MK) and then colony-forming unit megakaryocytes (CFU-MK). CFU-MKs give rise to promegakaryoblasts (PMKB). At this stage, the MK progenitors lose their ability to divide but continue to replicate their DNA through endomitosis. This results in the formation of large polyploid MKs, which show an increase in cytoplasmic volume and range from 4N to 128N in chromosome content (Figure 1.1) (Chang*, et al* 2007, Odell*, et al* 1970). Simultaneously, many of the platelet proteins that are essential for both platelet formation and function are synthesised (Chang*, et al* 2007).

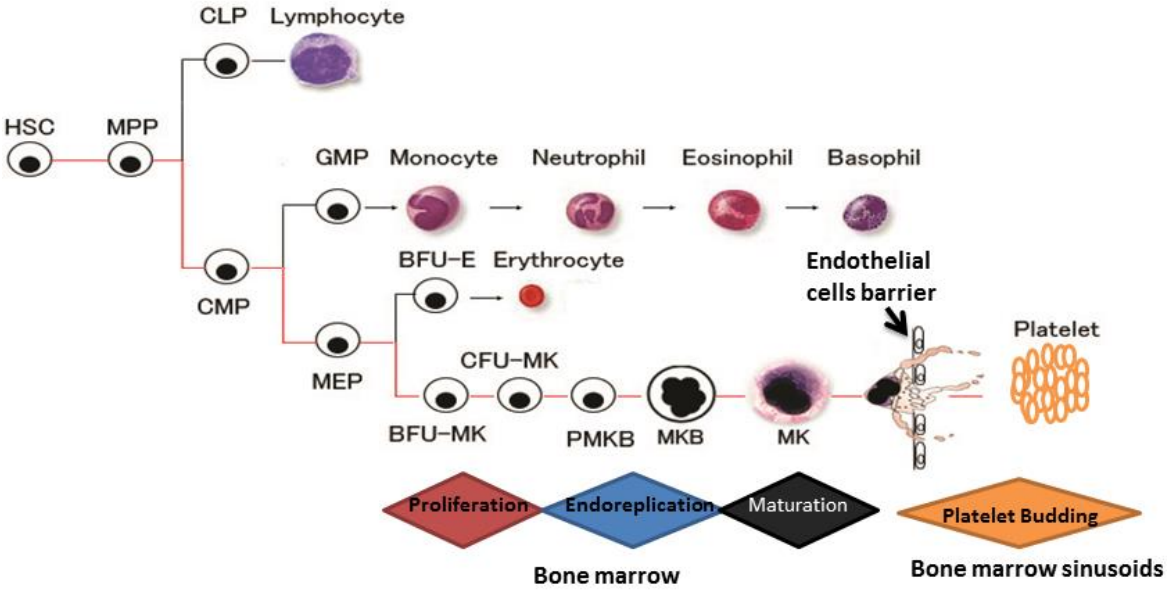

Figure 1.1 A schematic representation of megakaryocyte development and thrombopoiesis. HSC, haematopoietic stem cell; MPP, multipotent progenitor; CMP, common myeloid progenitor; CLP, common lymphoid progenitor; GMP, granulocyte/monocyte progenitor; MEP, megakaryocyte/erythrocyte progenitor; BFU-MK, burst-forming unit megakaryocyte; CFU-MK, colony-forming unit megakaryocyte; PMKB, promegakaryoblast; MKB, megakaryoblast; MK, megakaryocyte.

Platelets are released from the mature MK cytoplasm via a process of budding from MK protrusions known as proplatelets. Briefly, prior to proplatelet formation, microtubules move and aggregate in bundles at the MK cortex. In a process that is mediated by the demarcation membrane system (DMS), the MK then forms a number of thick pseudopods, which undergo elongation reducing the MK cytoplasm and leading to the formation of long, thin proplatelet structures (Patel*, et al* 2005, Radley and Haller 1982). Proplatelet formation is driven by the sliding of overlapping microtubules in a process that also leads to the movement of organelles and granules to the proplatelet ends (Cramer*, et al* 1997, Italiano*, et al* 1999a, Patel*, et al* 2005). The proplatelets also undergo branching and bending processes that are mediated by acto-myosin and lead to amplification of the proplatelet ends (Schulze*, et al* 2006). At the proplatelet tips, the nascent platelets are filled with all the materials required to form mature platelets including granules and other organelles. The platelets are released from the proplatelet tips when they are exposed to the shear forces of the blood flow as a result of emerging between the endothelial cells of the bone marrow sinusoids (Italiano*, et al* 1999b).

1.2.2 Platelet ultrastructure

Platelets are discoid shaped. Varying from 2.0 to 5.0 µm in diameter, and being about 0.5 µm in thickness, they are considered to be the smallest cells in blood. They lack nuclei and genomic DNA but have mRNA that is derived from the parental MKs, and possess the machinery required for translation of this mRNA and synthesis of platelet proteins. Microscopically, platelets appear as small, anucleate cells that have a relatively smooth membrane on Wright-Giemsa stained peripheral blood smears. While they may appear very simple, when examined by light microscopy platelets have a complex structure, which comprises three zones, the peripheral zone (outer), the sol-gel zone and the organelles (Figure 1.2) (White 2007).

The platelet periphery is comprised of three main regions, the glycocalyx, the lipid bilayer and the sub-membrane. The glycocalyx is the external surface of the platelet membrane. It acts as a separation barrier between the plasma and the internal contents of the platelet, and plays a vital role in the platelet response to blood vessel injury, by providing a scaffold for the glycoproteins that are present on the platelet outer surface, which are essential for platelet adhesion, activation and aggregation, such as glycoprotein (GP) Ib-V-IX and integrin $\alpha_{IIb}\beta_3$. Platelets also have a connected channel system known as the open canalicular system (OCS) that forms as a result of

invagination of the platelet plasma membrane into the interior platelet and is rich in various platelet receptors (White 2007). Notably, it facilitates substance exchange between the internal contents of the platelet and the surrounding media, such as the uptake of fibrinogen and the release of granule contents (Escolar and White 1991). In addition, it is involved in platelet activation and aggregation and in the expansion of the surface area of platelets.

The glycocalyx rests on a phospholipid membrane (lipid bilayer) that plays an important role in promoting coagulation due to its ability to accumulate coagulation factors, such as factors V and X, leading to conversion of prothrombin to its active form, thrombin. The acceleration of blood coagulation occurs when the platelets undergo activation leading to an increase in the level of thrombin that is essential for the activation of its receptors on the platelet surface and the subsequent conversion of fibrinogen to fibrin. This membrane also acts as the initial substrate for an enzymatic reaction that leads to the production of thromboxane A2 (TxA_2). Structurally, the lipid bilayer does not differ in appearance from a typical membrane and it is not stretchable or compressible. Therefore, any requirement to increase the platelet surface area during the spreading process that occurs upon activation is met by the tiny folds that are formed by the OCS (White 2007).

The sol-gel zone is located underneath the peripheral zone, and comprises the cytoskeleton; the framework of the platelet body. The cytoskeleton accounts for 30 to 50% of the platelet proteins and is involved in essential functions in both resting and stimulated platelets. The microtubule component of the cytoskeleton is responsible for maintaining the discoid shape of resting platelets (White and Rao 1998). In addition, the cytoskeleton works as a matrix that maintains and suspends the platelet organelles and other internal components separately from each other. The latter function is mainly conducted by the actin filament cytoskeleton (Escolar*, et al* 1986). In stimulated platelets, cytoplasmic actomyosin and cytoskeletal proteins play an important part in contractile physiology. The circumferential microtubule coils contract, allowing the platelets to change shape with dense and α granules being driven to the centre of the cytoplasm for the secretion process (White, 2007).

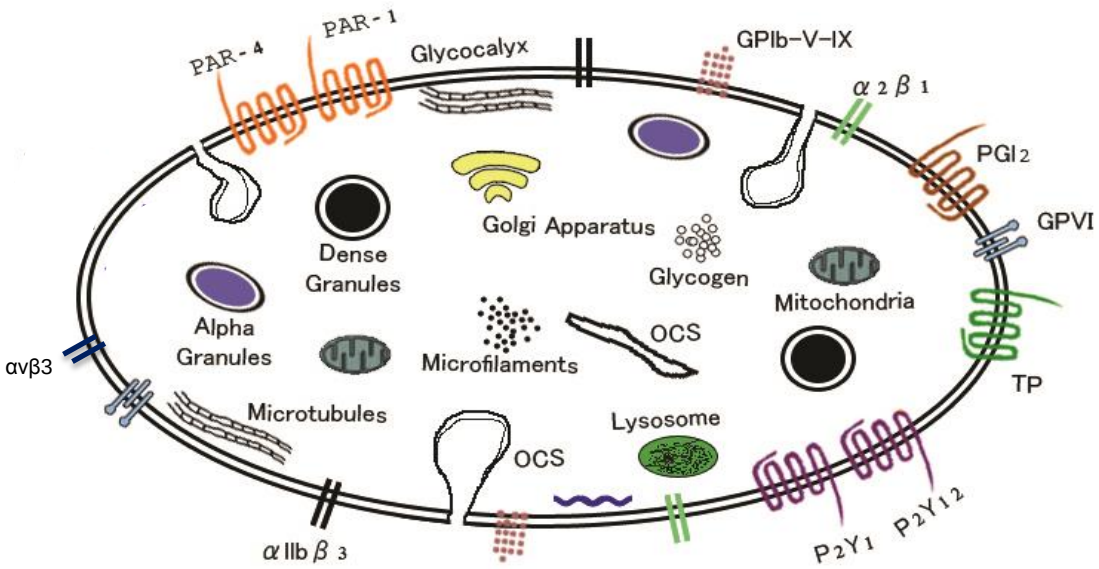

Figure 1.2 A schematic representation of the components of platelets showing the main glycoprotein receptors and integrins. Platelets are composed of three main zones, the peripheral, sol-gel and organelle zones. The peripheral zone is comprised of the glycocalyx, the lipid bilayer and the sub-membrane, while the sol-gel zone is comprised of the cytoskeleton and the organelle zone is comprised of the granules, Golgi apparatus, mitochondria and glycogen. OCS: open canalicular system, TP: Thromboxane A2 receptor.

The organelle zone comprises the granules and other cellular organelles. Platelet granules can be divided into at least three main types: α-granules, dense (δ) granules and lysosomes. The α-granules are more abundant, with the number determined by the size of the platelet. Normal platelets contain between 40 and 80 α-granules, whereas giant platelets will contain up to 100 granules. These granules contain the von Willebrand Factor (VWF), P-Selectin, the platelet derived growth factor, platelet factor 4, fibrinogen and other clotting factors (Maynard*, et al* 2007). Dense granules are present in lower numbers than α-granules with an estimated 4 to 8 per platelet. They are rich in ions, adenine nucleotides and transmitters including ADP, ATP, pyrophosphate, serotonin, magnesium and calcium (Israels*, et al* 1990, McNicol and Israels 1999, White 1969). The lysosome is the least abundant and contains proteolytic enzymes, including acid hydrolases. The process of uptake and/or release of these substances occurs through the OCS (White 2007).

1.2.3 Platelets and their role in haemostasis

Although platelets have been associated with various biological processes, such as those involved in inflammation, metastasis and response to microbial infection, their main function is to arrest bleeding at the site of injury (Broos*, et al* 2011, Leslie 2010). Haemostasis depends on several factors including endothelial cells, coagulation and platelets. Endothelial cells line blood vessels and play an important role in mediating the balance between the inhibition and activation of coagulation and platelet function by producing a number of molecules that possess either anticoagulant properties such as prostacyclin (PGI2) and nitric oxide (NO) or procoagulant properties including the platelet activating factor, the VWF and the tissue factor (Michiels 2003). In addition, endothelial cells play a role in regulating a number of anticoagulant pathways such as the protein C anticoagulant pathway, activation of which results in inactivation of the procoagulant cofactors FVIIIa and Va (Kurosawa*, et al* 1997). The intact healthy layer of endothelial cells normally promotes blood flow by abrogating the attachment of cells and protein to its surface preventing the initial stages of platelet and coagulation activation. Loss of endothelial cells after blood vessel injury leads to exposure of the subendothelial extracellular matrix, resulting in platelet attachment and activation of coagulation (Michiels 2003, Varga-Szabo*, et al* 2008). The extrinsic pathway of coagulation is activated by direct contact between FVII and the tissue factor (TF) and formation of a TF-FVIIa complex which can then catalyse the generation of FXa from its inactive precursor FX. In the presence of cofactors FV and Ca^{2+}, FXa then catalyses the conversion of prothrombin to thrombin. Thrombin cleaves fibrinogen to give rise to

fibrin which seals the aggregated platelets by generating a cross-linked fibrin mesh that stems bleeding (Riddel*, et al* 2007) (Figure 1.3).

Normally, platelets circulate freely in the bloodstream without interacting with the healthy blood vessel wall. In contrast, in a damaged vessel, the extracellular matrix (ECM) becomes exposed, facilitating interaction between platelet receptors and ECM components such as collagen, laminin and fibronectin, thereby tethering platelets to the site of injury. This mediates more stable adhesion, leading to the activation of platelets as well as the recruitment of further platelets to the sites of injury. Ultimately the platelets aggregate to form a loose platelet thrombus which is then sealed by deposition of fibrin on top of the thrombus to form the platelet fibrin plug (Broos*, et al* 2011, Stegner and Nieswandt 2011). This process can be divided into three main steps: adhesion, activation and aggregation (Figure 1.4).

1.2.3.1 Platelet adhesion

The first phase in the formation of a platelet aggregate is the tethering and adhesion of platelets at the site of injury. When damage occurs to the vascular endothelium, ECM is exposed allowing circulating platelets to interact either directly or indirectly with adhesion macromolecules such as collagen. The adhesion mechanism depends on the shear rate of the injured vessel; at low shear rates the platelets can adhere to the collagen directly via collagen receptors that are expressed on the platelet surface, namely GPVI and $\alpha_2\beta_1$ (Broos*, et al* 2011). In contrast, at very high rates (>1000 s^{-1}), such as in the microvasculature and small arteries, platelets are tethered via platelet GPIb-V-IX to VWF which is present in the subendothelium. The latter mechanism requires immobilised VWF, which can be found in the ECM, or the circulating VWF can interact with the exposed collagen via its A1 domain and become immobilised. The GPIbα-VWF interaction has fast on and off rates that allow the platelets to roll in the direction of the blood flow. Although, this interaction is not sufficient to mediate a stable adhesion of platelets, it plays an essential role in localising the platelets in the vicinity of the exposed ECM, giving other platelet receptors, such as GPVI and $\alpha_2\beta_1$, the opportunity to engage with the ECM (Hoylaerts*, et al* 1997, Savage*, et al* 1998, Varga-Szabo*, et al* 2008). Following tethering, platelets undergo more stable adhesion through processes mediated via GPVI and $\alpha_2\beta_1$ which bind directly to collagen and thereby initiate platelet activation (Stegner and Nieswandt 2011).

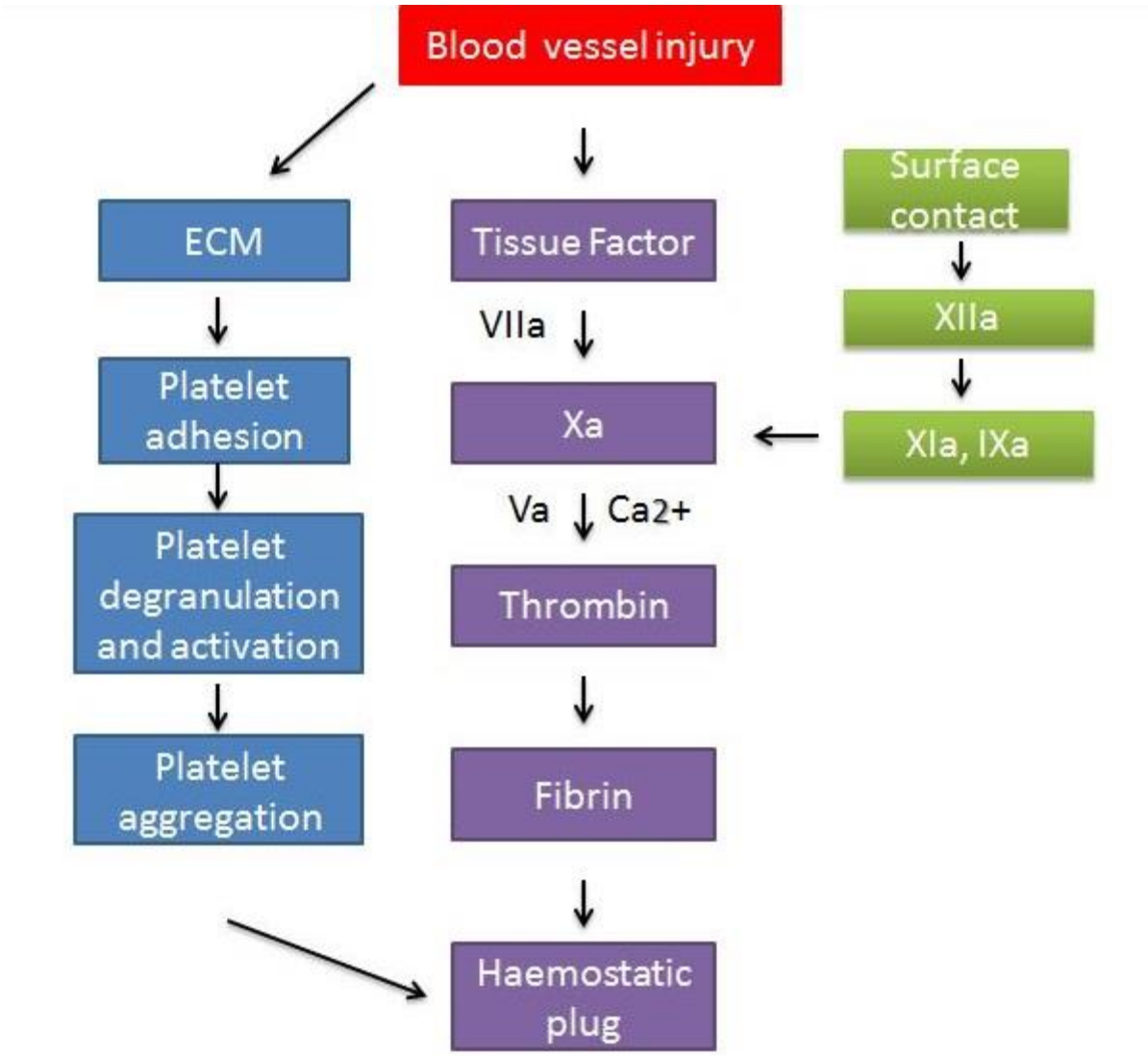

Figure 1.3 Flow diagram of normal haemostasis. The figure summarises the normal haemostatic response to blood vessel injury. The formation of a haemostatic plug requires platelet aggregation which occurs as a result of the adhesion of platelets to the extracellular matrix (ECM) leading to platelet activation, degranulation, and aggregation. The platelet thrombus is sealed by deposition of fibrin which is crosslinked by thrombin to form a platelet-fibrin clot. Fibrin is formed by activation of the coagulation cascade by the tissue factor via the extrinsic pathway, and direct contact with activated platelet surfaces, via the intrinsic pathway.

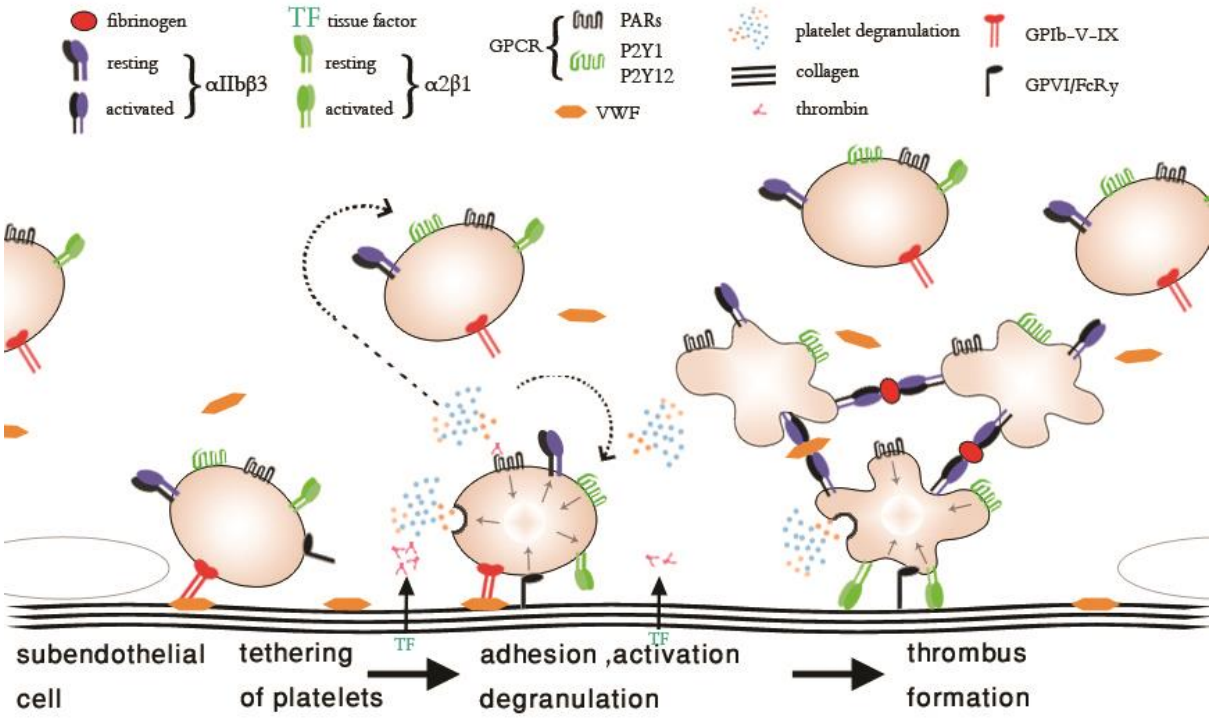

Figure 1.4 A schematic representation of the role of platelets in primary haemostasis. Following blood vessel injury, the subendothelial extracellular matrix components are exposed allowing tethering of platelets at the site of injury through the interaction between VWF and GPIb-V-IX. Stable adhesion of platelets to the ECM is mediated through the collagen receptor GPVI that triggers “outside in” signalling events leading to the activation of integrins $\alpha_2\beta_1$ and $\alpha_{IIb}\beta_3$, degranulation and platelet shape change. Following platelet activation, platelets aggregate together through $\alpha_{IIb}\beta_3$-fibrinogen and $\alpha_{IIb}\beta_3$-VWF interactions that crosslink adjacent platelets resulting in thrombus formation. Permission was obtained to reproduce this figure based on that originally published by Varga-Szabo*, et al* (2008).

1.2.3.2 Platelet activation and aggregation

GPVI plays an important role in promoting stable platelet adhesion as it triggers a strong signal through the covalently bound FcRγ-chain upon binding to its ligand. This brings FcRγ in contact with Src family tyrosine kinases Lyn and Fyn initiating a tyrosine kinase cascade via Syk that leads to the activation of phospholipase Cγ-2 (PLCγ-2) through phosphorylation of its SH2 domains (Du 2007, Watson*, et al* 2010). This signalling pathway causes an increase in the intracellular levels of both Ca^{2+} and 1,2-diacylglycerol (DAG), resulting in platelet shape change, aggregation, granule secretion and coagulation cascade activity (Figure 1.5) (Broos*, et al* 2011). The absence of the GPVI receptor or its signalling partner, FcRγ chain, causes a significant reduction in platelet adhesion to collagen under both flow and static conditions in mice, emphasising the important role of GPVI in promoting platelet adhesion and activation (Lockyer*, et al* 2006).

Integrin $\alpha_2\beta_1$ is a second collagen receptor which is engaged when it changes from a low affinity to a high affinity conformation that allows it to bind collagen. As a result, the receptor promotes platelet activation possibly by inducing and reinforcing the interaction between GPVI and collagen and prompting “outside in” signalling that results in $\alpha_{IIb}\beta_3$ activation and binding to its ligand, fibrinogen (Atkinson*, et al* 2003, Bernardi*, et al* 2006, Broos*, et al* 2011).

Following the initiation of platelet activation, particularly via GPVI, platelet activation is amplified through signal transduction by G-protein coupled receptors. These receptors are stimulated by soluble mediators that are released from activated platelets and thrombin which is localised to activated platelets. These events lead to platelet shape change, internal contraction, adenylyl cyclase inhibition and an increase in cytoplasmic Ca^{2+} (Figure 1.5) (Broos*, et al* 2011, Daniel*, et al* 1999, Stegner and Nieswandt 2011).

The increases in intracellular Ca^{2+} and diacylglycerol concentrations that occur upon platelet activation cause diacylglycerol-regulated guanine nucleotide exchange factor I (CalDAG-GEF) and protein kinase C (PKC) / phosphoinositide 3-kinase (P13K) to become activated, which in turn leads to activation and/or translocation to the plasma membrane of Rap1. The latter is a small GTP binding protein, which has been shown to play a role in regulating platelet function and integrin activation, mediating its role through its interaction with Rap1-interacting adaptor molecule (RIAM). Rap-1-GTP interacts with Rap1-GTP-interacting adaptor molecule (RIAM) which in turn leads to the recruitment of talin forming Rap-1, RIAM and talin activation complex. This activation complex interaction leads to unmasking of the binding site in talin allowing it to bind to

the β_3 cytoplasmic domain meditating $\alpha_{IIb}\beta_3$ activation (Bouaouina*, et al* 2008, Broos*, et al* 2011, Chrzanowska-Wodnicka*, et al* 2005, Crittenden*, et al* 2004). Kindlin-3 has also been implicated in mediating the activation of $\alpha_{IIb}\beta_3$. Thus, a number of studies have suggested that kindlin-3 may promote the talin binding interaction with $\alpha_{IIb}\beta_3$ and contribute with talin to inside out signalling. Defects in kindlin-3 have been associated with severe defects in integrin activation and platelet aggregation in patients diagnosed with leukocyte adhesion deficiency III and in *Fermt3* knock-out mice (Crazzolara*, et al* 2015, Malinin*, et al* 2009, Moser*, et al* 2008, Xu*, et al* 2014). In response to inside out signalling, $\alpha_{IIb}\beta_3$, the integrin that is responsible for platelet aggregation, undergoes a conformational change from its low affinity state (resting) to a high affinity state (active), enabling it to bind to its ligands, fibrinogen and VWF. Adjacent platelets are thus linked together to form loose platelet aggregates, which are sealed to form a stable thrombus by fibrin (Broos*, et al* 2011, Stegner and Nieswandt 2011). Following ligand binding, $\alpha_{IIb}\beta_3$ mediates “outside in signalling” events that amplify signal transduction resulting in more stable adhesion and the spreading of platelets, granule secretion and clot retraction (Broos*, et al* 2011).

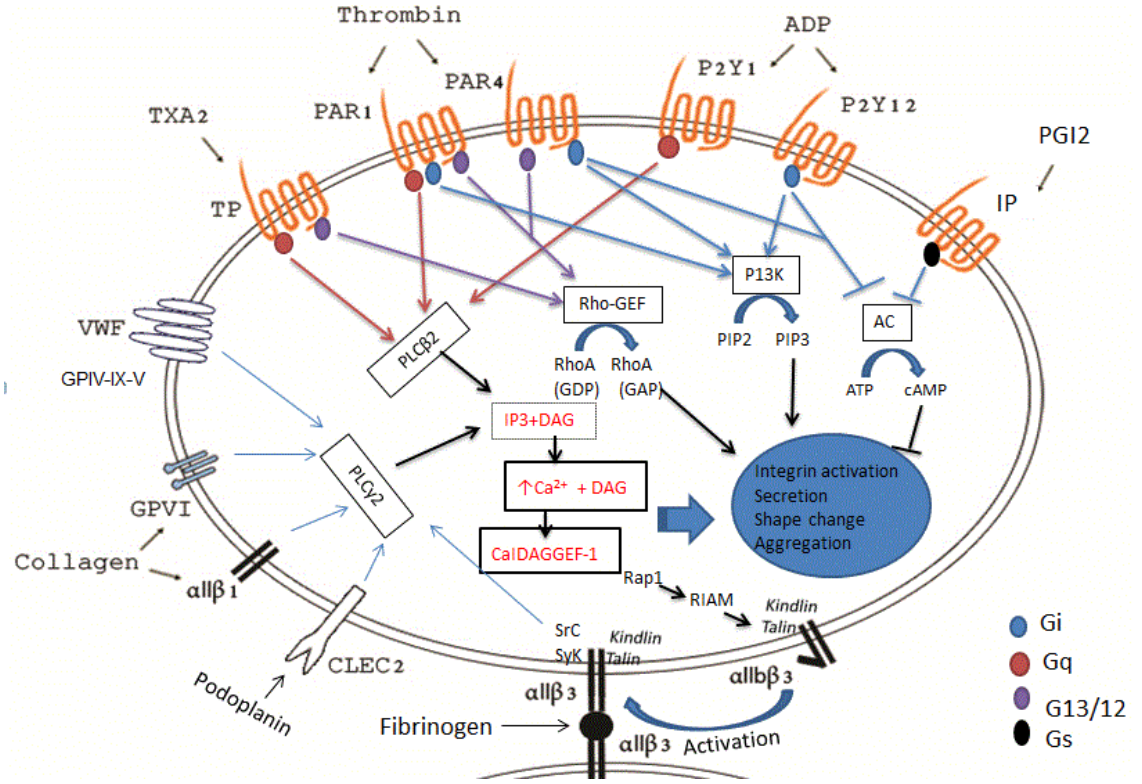

Figure 1.5 A schematic representation of the main signalling events involved in platelet activation. Binding of GPIb-V-IX, GPVI-FcRγ or CLEC2 to their ligands VWF, collagen and podoplanin results in activation of intracellular tyrosine-kinase signalling pathways that lead to the activation of PLCγ-2 through phosphorylation of its SH2 domains. PLCγ2 hydrolyses phosphatidylinositol 4,5 bisphosphate leading to production of a membrane bound 1,2-diacylglycerol (DAG) as well as inositol 1,4,5 trisphoshate (IP3). IP3 binds to its receptor IPR that is located on the dense tubular systems and is considered to be a Ca^{2+} selective channel facilitating the flow of Ca^{2+}. As a consequence, the cytoplasmic Ca^{2+} level increases. This signalling process leads to an increase in both Ca^{2+} and DAG, resulting in platelet shape change, granule secretion, activation and aggregation. Following platelet activation, second wave mediators and thrombin amplify activation by binding to their platelet surface receptors which are coupled to G-proteins (Gi, Gq G13/12). P2Y12, PAR-1 and PAR4 receptors are coupled with Gi proteins, which activate phosphoinositide 3-kinase β (P13K) resulting in the production of phosphatidylinositol-3,4,5-trisphosphate (PIP3) ultimately leading to increased Ca^{2+} mobilisation. In addition, Gi signalling also inhibits adenylyl cyclase, preventing the inhibition of platelet activation. G13/12 signalling is also activated through PAR1 and PAR4, which stimulates the RhoA-specific guanine nucleotide exchange factor (Rho-GEF) allowing platelet shape change. Gq-coupled receptors P2Y1, PAR1, PAR4 and TP result in phospholipase Cβ2 (PLCβ2) activation, which further increases Ca^{2+} mobilisation. Increased Ca^{2+} levels activate the talin via Rap-1 and RIAM. The $\alpha_{IIb}\beta_3$ integrin is then activated by talin and kindlin and binds to its ligands and triggers ‘‘outside in signaling’’ which is mediated by the activation of Src family kinases and tyrosine kinase Syk resulting in further platelet activation and clot retraction. In contrast, when prostacyclin (PGI2) binds to its receptor it causes activation of the adenylyl cyclase, inhibiting platelet activation. ADP: adenosine diphosphate, TxA2: Thromboxane A2, AC: adenylyl cyclase.

1.3 Inherited platelet bleeding disorders

Inherited platelet bleeding disorders tend to be classified into two groups: qualitative and quantitative defects. Quantitative defects refer to an abnormality in the number of platelets, either an increase (thrombocytosis) or a decrease (thrombocytopenia). Qualitative defects are defined by an abnormality in platelet function that leads to a disturbance of the normal physiological function of the platelets. However, some platelet disorders can display features of both qualitative and quantitative disorders. Generally, inherited platelet bleeding disorders cause bleeding phenotypes that vary in severity and are characterised by bleeding symptoms including mucocutaneous bleeding, epistaxis, easy bruising, menorrhagia and haemorrhage following trauma or surgery (Balduini*, et al* 2002, Nurden and Nurden 2011). In this section, some of these disorders will be discussed briefly, with the focus being on Glanzmann thrombasthenia as this disorder is the subject of this project.

1.3.1 Inherited thrombocytopenias

Inherited thrombocytopenias (IT) are rare heterogeneous disorders that are characterised by a reduction in the number of circulating platelets and result from defects in genes that have roles in megakaryopoiesis and thromobpoiesis. These gene defects result in a failure in MK production, abnormal MK proliferation and maturation, or abnormal proplatelet formation leading to reduced platelet production and release. They can be classified according to different parameters, including inheritance pattern (X-linked, autosomal recessive or dominant), clinical symptoms of the patients (syndromic or non-syndromic) and platelet size (small, large and normal) (Table 1.1). Of these, it seems that classification on the basis of platelet size is the most helpful in predicting the gene affected as it is easy to determine using a light microscope and usually remains a constant feature for most disorders. In contrast, inheritance pattern and clinical manifestations of the thrombocytopenia are less helpful since different mutations in the same gene can give rise to syndromic or non-syndromic forms of IT (Balduini*, et al* 2002).

1.3.2 Inherited platelet function disorders

Inherited platelet function disorders are caused by defects in genes' encoding platelet components which result in a failure of the physiological function of platelets and may also disturb primary haemostasis giving rise to a bleeding tendency, most notably mucocutaneous bleeding, of varying severities. The clinical manifestations also include

epistaxis, post trauma haemorrhage and menorrhagia. Platelet function defects are usually classified according to their ability to aggregate and secrete their granule contents in response to a variety of platelet stimuli. Light transmission aggregometry is considered the standard diagnostic method to identify and classify the majority of platelet function defects. For example, Bernard–Soulier syndrome (BSS), which results from a defect in the GPIb-IX-V complex, is characterised by an abnormal response to ristocetin, while Glanzmann thrombasthenia (GT), resulting from a defect in $\alpha_{IIb}\beta_3$, is characterised by impaired aggregation in response to all agonists with the exception of ristocetin. Additionally, flow cytometry can be used to determine the membrane expression levels of platelet receptors such as $\alpha_{IIb}\beta_3$, GPVI and GPIbα or degranulation markers such as P-selectin. DNA analysis is also important to confirm the diagnosis and to identify the gene defect responsible for the disease (Daly*, et al* 2014, Nurden and Nurden 2011). A more detailed list can be found in table 1.1. Given that GT is the focus of this project, this will be discussed in greater detail in section 1.3.3.

Table 1.1 Classification of a selection of inherited platelet bleeding disorders.

Inherited thrombocytopenia				
Platelet size	Syndrome	Gene mutation	Chromosomal location /Inheritance pattern	Associated phenotype
Small	Wiskott-Aldrich syndrome	*WAS*	Xp11.23-p11.22 X-linked	Immunodeficiency lymphoma, eczema, platelet and lymphocyte function defects
	X-linked thrombocytopenia	*WAS*	Xp11.23-p11.22 X-linked	No immune problems
Normal	Radioulnar synostosis with a megakaryocytic thrombocytopenia	*HOXA11*	*1* 7p15-p14.2 Autosomal dominant	Incomplete range of motion synostosis and Fused radius
	Chromosome 10/THC2	*FLJ14813*	10p12-11.2 Autosomal dominant	Bleeding
	Congenital amegakaryocytic thrombocytopenia	*c-MPL*	1p34 Autosomal recessive	Thrombocytopenia
Large	GATA-1-related thrombocytopenia	*GATA1*	Xp11.23 X-linked	Dyserythropoiesis ± anemia, Platelet dysfunction
	MYH9-related disorders	*MYH9*	22q12.3 Autosomal dominant	Thrombocytopenia with giant platelets, Cytoskeleton defect
	Mediterranean macrothrombocytopenia	*GPIBA*	17per-p12 Autosomal dominant	Enlarged platelets
Inherited platelet function disorders				
Disorder of surface components	Bernard-Soulier syndrome	*GPIBA, GP1BB GP9*	17, 22 and 3 Autosomal recessive	Failure of ristocetin induced aggregation Moderate macrothrombocytopenia
	Glanzmann thrombasthenia	*ITGA2B, ITGB3*	17q21.31-32 Autosomal recessive	No aggregation with most agonists except ristocetin
	Platelet-type VWD	*GPIBA*	17p13.2 autosomal dominant	Spontaneous binding of VWF to GP-Ibα
Disorder of intracellular components	Gray platelet syndrome	*NBEAL2*	3p21.31 autosomal recessive	Enlarged platelets Lacking α-granules, variable aggregation response
	Hermansky-pudlak syndrome	*HPS-1->HPS-8*	10q24.2 ,5q14.1, 3q24 22q12.1,11p15.1,10q24.32 6p22.3,19q13.32 autosomal recessive	Absence of dense granules, reversibility to ADP, impaired collagen response

1.3.3 Glanzmann thrombasthenia

Glanzmann thrombasthenia (GT) is a rare autosomal recessive platelet bleeding disorder characterised by a complete absence, partial deficiency or functional defect of the platelet membrane integrin receptor $\alpha_{IIb}\beta_3$ (glycoprotein IIb/IIIa). These defects cause an abrogation or reduction in platelet aggregation in response to all major agonists except ristocetin (Nurden*, et al* 2011). This integrin mediates platelet aggregation in response to blood vessel injury through binding to fibrinogen, VWF and other ligands containing arginine-glycine-aspartic acid (RGD) sequences. Upon binding to these soluble adhesive proteins, adjacent platelets are cross linked through $\alpha_{IIb}\beta_3$, forming platelet aggregates (Varga-Szabo*, et al* 2008). GT is a rare disorder, with an incidence of approximately one in one million in the UK population. Importantly, it has been shown to have a high frequency in ethnic groups where consanguinity is prevalent, such as French gypsies, Palestinians, Iraqi Jews and Jordanian Arabs (Nurden*, et al* 2011). GT can be classified into three different types according to the levels of $\alpha_{IIb}\beta_3$ expressed on the platelet surface: type I, type II and variant type. Type I GT is characterised by a complete absence of $\alpha_{IIb}\beta_3$, whereas type II is characterised by levels of $\alpha_{IIb}\beta_3$ between 5% and 20% of the normal level. Finally, the variant type of GT is characterised by a level of $\alpha_{IIb}\beta_3$ that is greater than 20% of the normal level and a receptor with reduced functional activity (Nurden et al 2011).

1.3.3.1 Historical background of GT

The first GT case was identified in 1918 by a paediatrician called Eduard Glanzmann, when he investigated a seven year old girl in Switzerland with a history of prolonged bleeding whose blood showed a failure in clot formation. Glanzmann described this condition as hereditary haemorrhagic thrombasthenia (Bellucci and Caen 2002, Jin*, et al* 1996, Nurden 2006, Stevens and Meyer 2002). Several decades later, in 1962, Caen and Cousin made the first significant breakthrough in the physiological analysis of GT when they showed that the platelets from GT cases failed to aggregate in response to ADP, thrombin, adrenaline and collagen (Bellucci and Caen 2002, Caen and Cousin 1962). Four years later, Caen identified 15 patients whose platelets showed a reduction or absence of aggregation and variable clot retraction. Moreover, the fibrinogen content in the α granules of platelets from these cases was directly correlated with the extent of platelet clot retraction (Caen*, et al* 1966). This difference led Caen and his researchers to classify GT cases into two different groups: type I and II. GT type I was the most severe form of GT and referred to patients whose platelets failed to aggregate, had low levels of fibrinogen and completely abrogated clot retraction, while platelets from type II

patients showed a complete absence of aggregation, subnormal levels of fibrinogen and mild to moderately defective clot retraction (Caen*, et al* 1966, Caen 1989). It was proposed that GT was inherited as an autosomal recessive trait as the parents of patients with the disorder were asymptomatic, the disorder affected males and females in equal numbers and because there was a history of consanguinity in approximately 25% of all cases (Boudreaux and Lipscomb 2001, Caen*, et al* 1966).

The first link between GT and a platelet glycoprotein was made by Nurden and Caen in 1974 when they showed using SDS-PAGE of platelets from three type I GT patients that one of the three glycoproteins recognised as being present in human platelets at that time was absent (Nurden and Caen 1974). Subsequently, a number of studies associated the glycoprotein IIb/IIIa ($\alpha_{IIb}\beta_3$) complex with GT. In addition, an analysis of type I and II platelets by single and two dimensional SDS-PAGE, and protein staining revealed an almost complete absence of glycoprotein IIb/IIIa in platelets from patients diagnosed as type I GT, while 10-20% of this glycoprotein was observed in type II GT platelets. This finding allowed GT to be classified based on the level of GP IIb/IIIa (Nurden and Caen 1974, Phillips and Agin 1977). In 1980, the absence of glycoprotein IIb/IIIa in GT type I was confirmed by Hagen*, et al* (1980) using crossed immunoelectrophoresis with an antiserum targeting the glycoprotein IIb/IIIa complex (Hagen*, et al* 1980). At the same time, a third type of GT was discovered and named variant GT. Patients with this form of GT were found to have platelet glycoprotein IIb/IIIa levels that were similar, or reduced by up to 50% when compared with control platelets (Caen 1989). It was also shown that the receptor level in platelets from heterozygous carriers of GT was 50% lower than in control platelets. However, platelet aggregation was relatively normal, and the carriers were asymptomatic (Caen 1989). Subsequent studies isolated and characterised GP IIb/IIIa and suggested that the receptor binds to fibrinogen, providing the first biochemical explanation for the bleeding symptoms in GT (Marguerie*, et al* 1979, Nachman*, et al* 1984). In the late 80s, the cDNAs of GP IIb and GP IIIa were isolated and linked to two different genes located on chromosome 17, *ITGA2B* and *ITGB3,* respectively (Bray*, et al* 1987, Fitzgerald*, et al* 1987). This allowed Bray and Shuman to identify the first variant resulting in GT in 1990, and since then several variants have been identified (Bray and Shuman 1990, Nurden*, et al* 2012b).

1.3.3.2 Clinical manifestations in GT

Typically, GT cases have an increased tendency to bleed that can vary greatly in severity, even between affected family members. Bleeding symptoms are only observed when patients have homozygous or compound heterozygous gene defects,

while those with the heterozygous defects are considered to be carriers and are asymptomatic (Reichert*, et al* 1975). The most common bleeding symptoms include purpura, epistaxis, easy bruising, post traumatic and surgical bleeding, gingival haemorrhage and menorrhagia, while symptoms like haematuria and gastrointestinal bleeding are considered to occur less frequently but can lead to severe complications in some cases (George*, et al* 1990, Nurden 2006, Toogeh*, et al* 2004). The clinical manifestations of GT were extensively studied by George*, et al* (1990) and Toogeh*, et al* (2004) in two large cohorts. George*, et al* (1990) studied 177 GT cases from different ethnic backgrounds, while Toogeh*, et al* (2004) investigated 382 cases recruited from a single centre in Iran.

The majority of GT cases display bleeding symptoms immediately after birth; however, some may be diagnosed as having GT later in life. In the large cohort study conducted by George*, et al* (1990), the majority of cases were diagnosed at birth or before the age of 5 years. The most common feature in neonatal cases was purpura, while excessive bruising was the most common feature in early childhood. In children, symptoms included epistaxis, gingival haemorrhage and purpura, with epistaxis being the most common cause of severe bleeding although this was unusual in adulthood. This may indicate that the risk of severe bleeding decreases with age, though another explanation is that nose-picking is a habit in young children, who have superficial blood vessels and delicate mucosa in their noses, making this condition common at this age. Another clinical feature of GT is gingival bleeding, which occurred in 55% of the French cohort and 23% of the Iranian cohort. Gingival bleeding has been associated with poor dental hygiene, and patients with good dental care regimes suffer fewer gingival bleeding events (George*, et al* 1990, Toogeh*, et al* 2004). Menorrhagia is one of the most common features of GT in women of reproductive age, and sometimes the bleeding might be severe enough to require treatment. In some cases, the onset of menstruation provides the first indication of a bleeding disorder, leading to patient diagnosis (George*, et al* 1990). Less common bleeding symptoms in GT include gastrointestinal haemorrhage, haematuria and intracranial haemorrhage, with only 12%, 6% and 2% of patients suffering from these symptoms, respectively (George*, et al* 1990).

1.3.3.3 Treatment of GT

Despite the variability in the frequency and severity of bleeding episodes in patients with GT, platelet transfusions are the standard treatment in the majority of cases, though repeated transfusions increase the risk of alloimmunization against $\alpha_{IIb}\beta_3$, leading to refractoriness to further therapy. Other forms of treatment include

compression, fibrin glue and gauze soaked with tranexamic acid. Epistaxis can be controlled by compression, nose packing, fibrin sealants, cauterisation and tranexamic acid. Menorrhagia can be controlled by high doses of progesterone and maintained by continuous use of an oral contraceptive. Severe trauma related bleeding and gastrointestinal bleeding usually requires a blood component transfusion (Di Minno*, et al* 2009, Nurden*, et al* 2012a).

Recombinant activated factor VII (rVIIa) has been widely used in the treatment of inherited and acquired platelet disorders. In GT patients, rVIIa has been used to treat bleeding episodes with some success, and it is widely used in patients who have developed alloimmunization against $\alpha_{IIb}\beta_3$ and become refractory to platelet transfusion (Nurden*, et al* 2012a).

There have also been several reports of successful stem cell transplantation to cure $\alpha_{IIb}\beta_3$ deficiency in GT patients, particularly in children suffering from severe bleeding (Bellucci*, et al* 2000, Bellucci*, et al* 1985, Johnson*, et al* 1994, McColl and Gibson 1997).

1.3.3.4 $\alpha_{IIb}\beta_3$ biogenesis and structure

$\alpha_{IIb}\beta_3$ is a calcium-dependent heterodimeric integrin that is expressed on the platelet surface and is composed of alpha and beta subunits that are associated non-covalently with each other. There are two β_3 integrin receptors in humans: $\alpha_{IIb}\beta_3$ and $\alpha_v\beta_3$. The latter is expressed widely in a number of cells, including platelets, smooth muscle cells and endothelial cells, while $\alpha_{IIb}\beta_3$ is restricted to MKs and platelets. $\alpha_{IIb}\beta_3$ is expressed abundantly in platelets, with 80,000 to 100,000 binding sites present per platelet, whereas $\alpha_v\beta_3$ is expressed in very low amounts, with approximately 100 binding sites present on each platelet (Coller*, et al* 1991, Jennings and Phillips 1982, Nurden*, et al* 2011). $\alpha_{IIb}\beta_3$ is also present in the membranes of α granules and becomes accessible when platelets are activated (Wenceldrake*, et al* 1986). Importantly, the integrin is essential for primary haemostasis, particularly for platelet aggregation due to its ability to bind various adhesive soluble proteins, most notably fibrinogen and VWF, and an absence or dysfunction of $\alpha_{IIb}\beta_3$ gives rise to GT (Hagen*, et al* 1980, Marguerie*, et al* 1979, Nachman*, et al* 1984). In addition, $\alpha_{IIb}\beta_3$ is also responsible for internalisation of fibrinogen for storage in platelet α-granules (Handagama*, et al* 1993).

1.3.3.4.1 Biogenesis of $\alpha_{IIb}\beta_3$

While the structure and function of $\alpha_{IIb}\beta_3$ have been extensively studied, little is known about its biogenesis, though it is known to commence early in hematopoietic stem cells

and continue throughout megakaryocyte maturation (Emambokus and Frampton 2003). The receptor is a calcium dependent complex that is composed of two subunits: α_{IIb} and β_3, which are both required for normal receptor assembly (Jennings and Phillips 1982) and expression on the platelet surface; otherwise the single subunit is retained intracellularly (Bray*, et al* 1986, Duperray*, et al* 1989, O'Toole*, et al* 1989, Rosa and McEver 1989). The genes that encode β_3 and α_{IIb} have been mapped to two different locations on the long arm of chromosome 17. The β3 gene, *ITGB3*, is located at 17q21-22, while *ITGA2B*, which encodes α_{IIb}, is located at 17q21.1-q21.3 (Cong*, et al* 1988, Rosa*, et al* 1988). In brief, $\alpha_{IIb}\beta_3$ is proposed to be synthesised as follows: the α- and β-subunits of $\alpha_{IIb}\beta_3$ are encoded by two distinct genes, *ITGA2B* and *ITGB3*, respectively, and thus each subunit is synthesised as a single polypeptide chain. In the Endoplasmic reticulum (ER), the N-linked glycans are attached to pro-α_{IIb} and β_3 subunits as they undergo a carbohydrate modification (Calvete*, et al* 1989, Duperray*, et al* 1987, Mitchell*, et al* 2006). Pro-α_{IIb} adopts its bent conformation before binding to the β_3 subunit to form the pro-$\alpha_{IIb}\beta_3$ complex, while the signal peptide is cleaved (Mitchell*, et al* 2007). The pro-$\alpha_{IIb}\beta_3$ complex is then transported to the Golgi apparatus for further carbohydrate modification (Duperray*, et al* 1987). In the Golgi, the α-subunit undergoes proteolytic cleavage at a specific site in the calf-2 domain producing the mature form of α_{IIb}, which comprises light and heavy chains which are linked to each other by a disulphide bond between Cys40 and Cys857 (Calvete and Gonzalez-Rodriguez 1986, Calvete*, et al* 1989, Calvete*, et al* 1990). The mature $\alpha_{IIb}\beta_3$ is then transported to the platelet membrane or the α-granule membrane (Duperray*, et al* 1989, Wenceldrake*, et al* 1986).

1.3.3.4.2 $\alpha_{IIb}\beta_3$ integrin structure

Integrins are a family of transmembrane heterodimeric proteins each containing a β- and an α-subunit. Thus, in humans, eight β- and 18 α-subunits covalently associate with each other to form 24 different integrins which have roles in cell-matrix and cell-cell interactions. Platelets express five integrin receptors. Three of these are β_1 integrins: $\alpha_v\beta_1$, $\alpha_2\beta_1$ and $\alpha_6\beta_1$. These mediate platelet adhesion to the extracellular matrix proteins, fibronectin, collagen and laminin, respectively, while the β_3 subunit associates with α_{IIb} and α_v to form $\alpha_{IIb}\beta_3$ and $\alpha_v\beta_3$, respectively. $\alpha_v\beta_3$ is expressed at a low receptor density in platelets, where it mediates platelet adhesion to vitronectin and osteopontin, while it is expressed at higher levels in smooth muscle cells, osteoclasts and endothelial cells. In contrast, $\alpha_{IIb}\beta_3$ is abundantly expressed in megakaryocytes and platelets in abundant amounts, with an estimated receptor density in excess of 80,000 per platelet. The integrin can bind to various RGD-containing ligands, including

fibrinogen, VWF and fibronectin, mediating platelet aggregation (Bennett*, et al* 2009, Kasirer-Friede*, et al* 2007).

α_{IIb} and β_3 subunits have 1008 and 762 amino acids, respectively, that are folded into three main parts: a large extracellular region (N-terminus), a trans-membrane region and a short cytoplasmic tail (C-terminus) (Zhu*, et al* 2008). The extracellular region of the α-subunit includes the calf-1 and -2 domains, the thigh domain and the β-propeller domain, while the extracellular region of β_3 comprises a β I-domain, a Hybrid domain, a Plexin-Semaphorin-Integrin (PSI) domain and four epidermal growth factor (EGF)-like domains (Figure 1.6) (Zhu*, et al* 2008). In the following sections, I will highlight the most important domains of both α_{IIb} and β_3.

1.3.3.4.3 Structure of the β_3 subunit

The β I-domain has three adjacent metal sites that are required for ligand binding. These are the metal ion adhesion site (MIDAS), the adjacent metal ion adhesion site (ADMIDAS) and the Synergistic metal binding site (SyMBS). The MIDAS is formed from amino acids Asp145, Ser147, Ser149, Glu246 and Asp277 and is located at the top of the β subunit, while the amino acid residues that form the ADMIDAS are Ser149, Asp152, Asp153 and Asp277. The SyMBS is located to the left of the MIDAS and is formed from Asp184, Asn241, Asp243, Pro245 and Glu246. The β I-domain connects with the rest of the β_3 subunit through the hybrid domain. The hybrid domain undergoes a swing out movement that is required to ensure a large conformational change of the integrin in response to activation (Xiao*, et al* 2004). The hybrid domain connects to four EGF-like domains by interacting with the PSI domain. The latter domain is composed of two antiparallel β sheets encircled by two short helices. This domain is cysteine rich, containing 8 cysteine residues that form four disulphide bonds within the domain. The PSI and hybrid domains link the head domain of β_3 with the cysteine rich epidermal growth factor (EGF)-like domains (Zhu*, et al* 2008). These domains incorporate 30 cysteines to form 15 disulphide bonds facilitating the folding of four different EGF-like domains. Each of these domains contains four disulphide bonds, which are formed between 8 cysteine residues and in very specific patterns, between cysteine residues 1 and 5, 2 and 4, 3 and 6, and 7 and 8, in all of the EGF domains apart from EGF-1, which lacks the bond between residues 2 and 4 (Figure 1.7).

The most C-terminal extracellular domain of β_3, known as the β-tail, is comprised of 86 amino acids encompassing residues 626-712 of β_3. This domain is also rich in cysteine and contains six cysteine residues at positions 634, 640, 643, 657, 661 and 681, which form three disulphide bonds (Cys634-Cys655, Cys640-Cys661 and Cys643-Cys657)

(Zhu*, et al* 2008). The transmembrane domain (TM) is comprised of 29 amino acids and has an α-helical structural that is embedded in the lipid bilayer (Yang*, et al* 2009). The cytoplasmic domain of β_3 is comprised of 47 amino acids and formed of a long α-helix that starts from the membrane and is followed by a very short loop before forming another α-helix. Interestingly, this domain has two important motifs, NPXY and NXXY. It was found that talin and kindlin-3, the cytoplasmic proteins, bind to membrane former NPXY and membrane distal NXXY motifs mediating the activation of $\alpha_{IIb}\beta_3$ (Anthis*, et al* 2009, Moser*, et al* 2008).

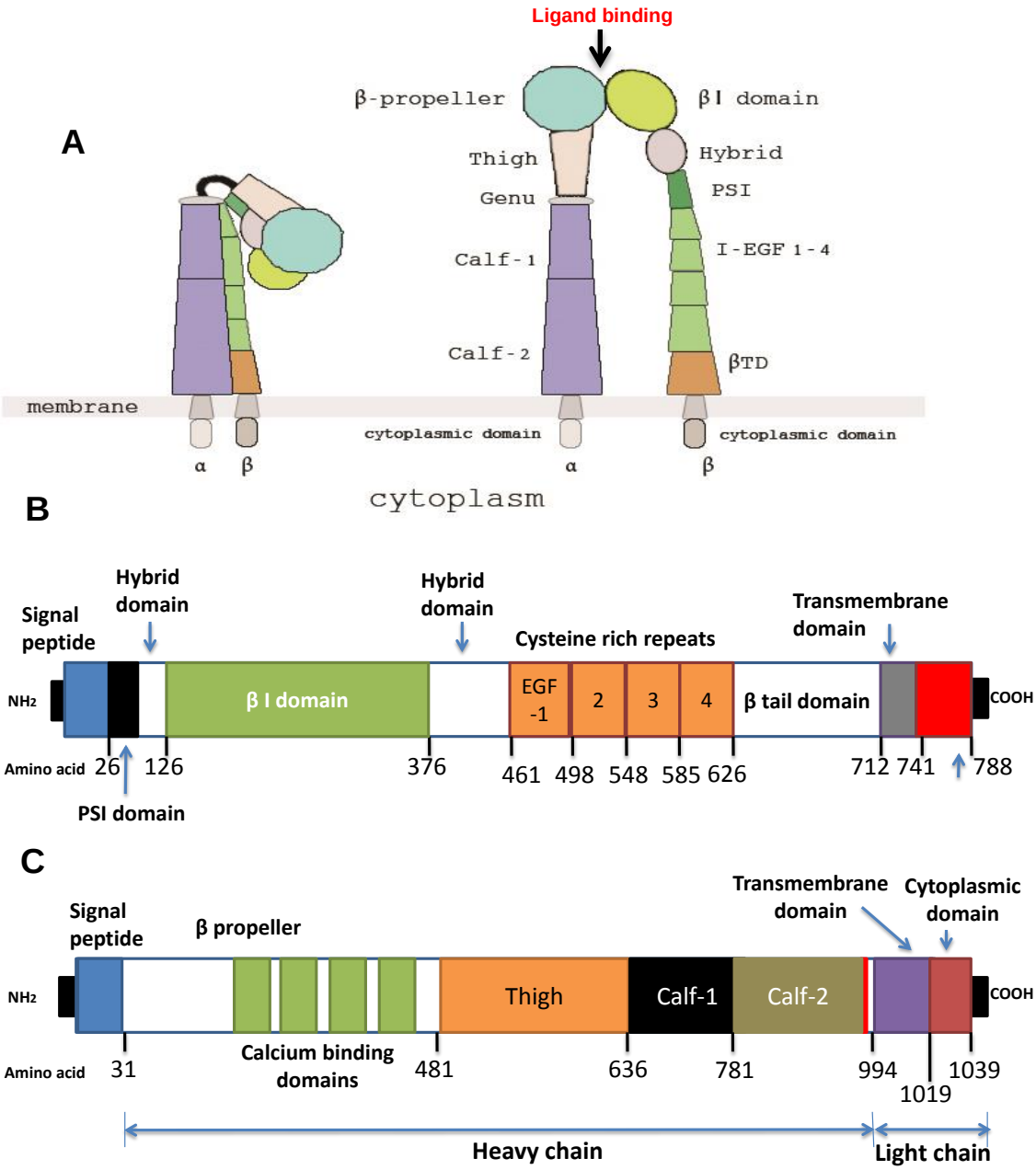

Figure 1.6 A schematic representation of $\alpha_{IIb}\beta_3$ integrin (A) in two conformations based on crystal structure studies of $\alpha_{IIb}\beta_3$ (B) β_3 and (C) α_{IIb} protein sequences. (A) Two conformations are shown, the bent conformation or low affinity state (left) and the extended conformation or high affinity state (right). In its extended form, the ligands bind at the interface between the β propeller and the I domains. (B) *ITGB3* encodes the 788 amino acid β3-subunit which comprises a signal peptide (26 amino acids), the β I domain, cysteine rich repeats, β tail, transmembrane and cytoplasmic domains. (C) *ITGA2B* encodes a protein of 1039 amino acids, which comprises a signal peptide (31 amino acids), a light chain that includes cytoplasmic and transmembrane domains, and a heavy chain that includes β propeller, thigh, calf-1 and calf-2 domains. The proteins encoded by *ITGA2B* and *ITGB3* were numbered according to Ensembl ID: ENSP00000262407 and ENSP00000452786, respectively PSI: plexins semaphorins integrin, EGF: epidermal growth factor. Permission was obtained to produce the figure based on that originally published by Zhu, *et al* (2008).

A

```
EGF-1 CQ----------AQAEPNSH-RCNNGNGTFECGVCRC-GPGW---LGSQCE 498
EGF-2 CSEEDYRPSQQDECSPREGQPVC-SQRGECLCGQCVCHSSDFGKITGKYCE 548
EGF-3 CD--DF------SCVRYKGE-MC-SGHGQCSCGDCLC-DSDW---TGYYCN 585
EGF-4 CT------TRTDTCMSSNGL-LC-SGRGKCECGSCVCIQPGS---YGDTC- 624
      1          2       3    4  5  6  7          8
```

B

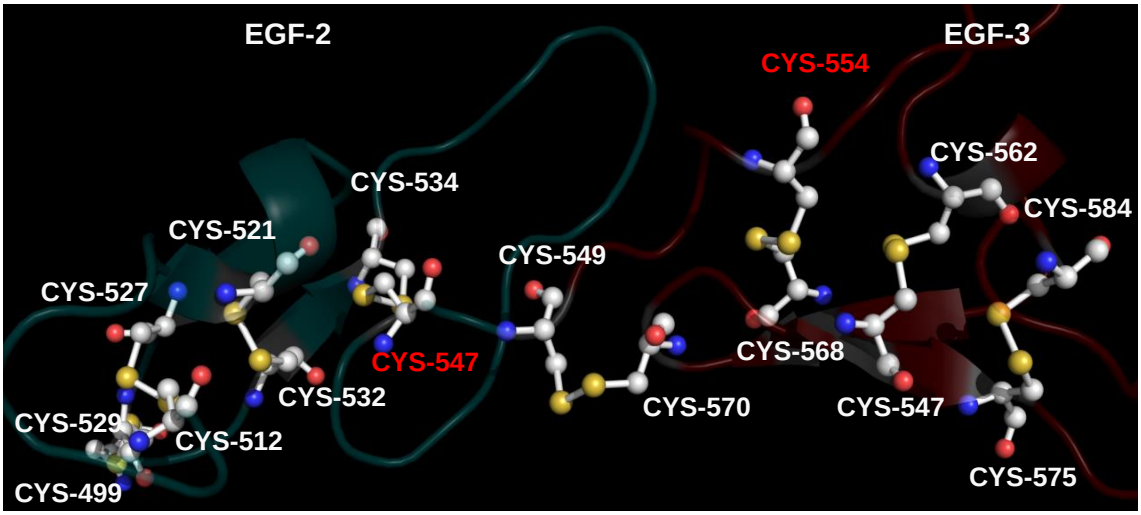

Figure 1.7 Disulphide networks in EGF domains of the β_3 protein. A) Alignment of EGF domain fragments showing the pattern of disulfide bonds. B) Computer-drawn ribbon diagrams of EGF-2 and EGF-3 showing the disulphide bonds between cysteine residues. The cysteine residues that will be studied in this project are highlighted in red. Cysteine residues are shown in balls-and-sticks. Created by Pymol using the $\alpha_{IIb}\beta_3$ crystal structure (Zhu, et al 2008).

1.3.3.4.4 Structure of the α_{IIb} subunit

The N-terminal β-propeller domain of the α_{IIb} subunit has a disc like structure and comprises a series of amino acid repeats with each repeat forming a blade like structure within the disc. The domain contains seven blades, each of which contains four antiparallel β sheets. There are four calcium binding sites in the most C-terminal four blades. The calcium binding sites contain approximately nine residues and have the following consensus sequence: Asp-h-Asp/Asn-x-Asp/Asn-Gly-h-x-Asp, where 'x' can be any residue and 'h' is a hydrophobic residue. For example, the calcium-binding residues of the third calcium binding site in blade-6 are: Asp396-Leu397-Asp-398-Arg399-Asp400-Gly401-Try402-Asn403-Asp404. The calcium ion is generally coordinated by oxygen atoms in the side chains or backbone of residues 1, 3, 5, 9 and 7 of the consensus sequence. There is extensive contact at the interface of blade-7 with the thigh domain, which may be important for maintaining a rigid interaction between the head domain (β propeller) and the thigh domain. The remaining amino acids mainly form the thigh, calf-1 and calf-2 domains, which all have a similar immunoglobulin like domain and are mainly arranged into β sheets. Importantly, a small acidic region, which coordinates a calcium binding site, and is located between the thigh and calf-1 domains, is called the genu or α_{IIb} knee. The structure of $\alpha_{IIb}\beta_3$ in its low affinity state showed a sharp bent conformation from this region, allowing the integrin to face down towards the membrane, and suggesting that this genu may give the extension required for the conformational change in response to activation (Zhu*, et al* 2008). The transmembrane domain (TM) is comprised of 25 amino acids and has an α-helical structural that is embedded in the lipid bilayer (Yang*, et al* 2009). The cytoplasmic domain of α_{IIb} is shorter than the cytoplasmic domain β_3 as it is comprised of 20 amino acids and formed of an α-helix that starts from the membrane. Importantly, the α_{IIb} tail domain contains a GFFKR motif, which plays an important role in maintaining the integrin in its low affinity state, through the formation of a salt bridge between α_{IIb}-Arg1026 and β_3-Asp749 (Li*, et al* 2014).

1.3.3.4.5 Change in integrin conformation on activation

High resolution analysis of crystallographic and electron microscopic data relating to $\alpha_{IIb}\beta_3$ and $\alpha_v\beta_3$ provided information regarding the structure and conformations of these receptors. In brief, upon platelet activation the integrin undergoes a change in conformation to bind to its ligands. There are two proposed models: the switchblade model and the deadblot model. According to the switchblade, the integrin undergoes a global change in conformation in three different steps: separation of the cytoplasmic tails and transmembrane domains, extensions at the α_{IIb} and β_3 knees and then swing

out motions of the hybrid domain. These result in the rearrangement of the β_3 I domain with displacement of the α-7 helix in the I domain allowing the hybrid and PSI domains to separate from the α_{IIb} subunit leading to α_{IIb} and β_3 separation. As a result, integrin ligands bind in a small pocket at the top of the receptor between the α_{IIb}-propeller and the β I domain. Therefore, three different conformations were proposed with this model: bent ‘‘closed’’, extended ‘‘closed’’ and extended ‘‘open’’ conformations. It has been shown that the bent and extended ‘‘closed’’ integrin conformations exist in low affinity states while the extended open conformation was in a high affinity state (Choi*, et al* 2013, Eng*, et al* 2011, Zhu*, et al* 2008). In contrast, other studies showed that $\alpha_v\beta_3$ is capable of stably binding to a physiological ligand while in the bent conformation and that integrin extension may not be required. A new model was therefore proposed, ‘‘the deadbolt’’. This model suggested that the integrin binds to its ligands when the integrin is in the bent conformation and extension occurs as a consequence of ligand binding. Based on the $\alpha_v\beta_3$ structure, it was proposed that the deadbolt in β_3 is composed of a loop located in the β_3 tail domain located between Cys689 and Cys713 that maintains the β I domain in a low affinity state which is broken due to ligand-binding (Adair*, et al* 2005, Arnaout*, et al* 2005, Xiong*, et al* 2009). However this β_3 tail loop was not found in $\alpha_{IIb}\beta_3$ and mutations or deletion of this loop did not cause spontaneous activation in $\alpha_{IIb}\beta_3$ and $\alpha_v\beta_3$ (Zhu*, et al* 2007, Zhu*, et al* 2008).

1.3.3.5 Molecular basis of GT

GT is caused by genetic defects in either *ITGA2B* or *ITGB3* that lead to qualitative and/or quantitative defects in the $\alpha_{IIb}\beta_3$ integrin, causing the absence of, or a severe reduction in, platelet aggregation in response to all major agonists, apart from ristocetin. Generally, mutations in *ITGA2B* or *ITGB3* can lead to different defects, including a severe reduction in the expression of the integrin on the platelet surface, abrogation of intracellular transport or complete absence of the integrin and abnormalities in binding to fibrinogen (Nurden*, et al* 2013). According to the GT database: http://sinaicentral.mssm.edu/intranet/research/glanzmann and the review by Nurden*, et al* (2012b), a total of 348 disease causing variations have been reported in both genes to date (accessed January, 2015). Of these, 202 defects affected *ITGA2B*, of which the majority were missense alterations (78). The remaining 146 alterations were identified in *ITGB3,* and 61 of these were missense alterations (Figure 1.8).

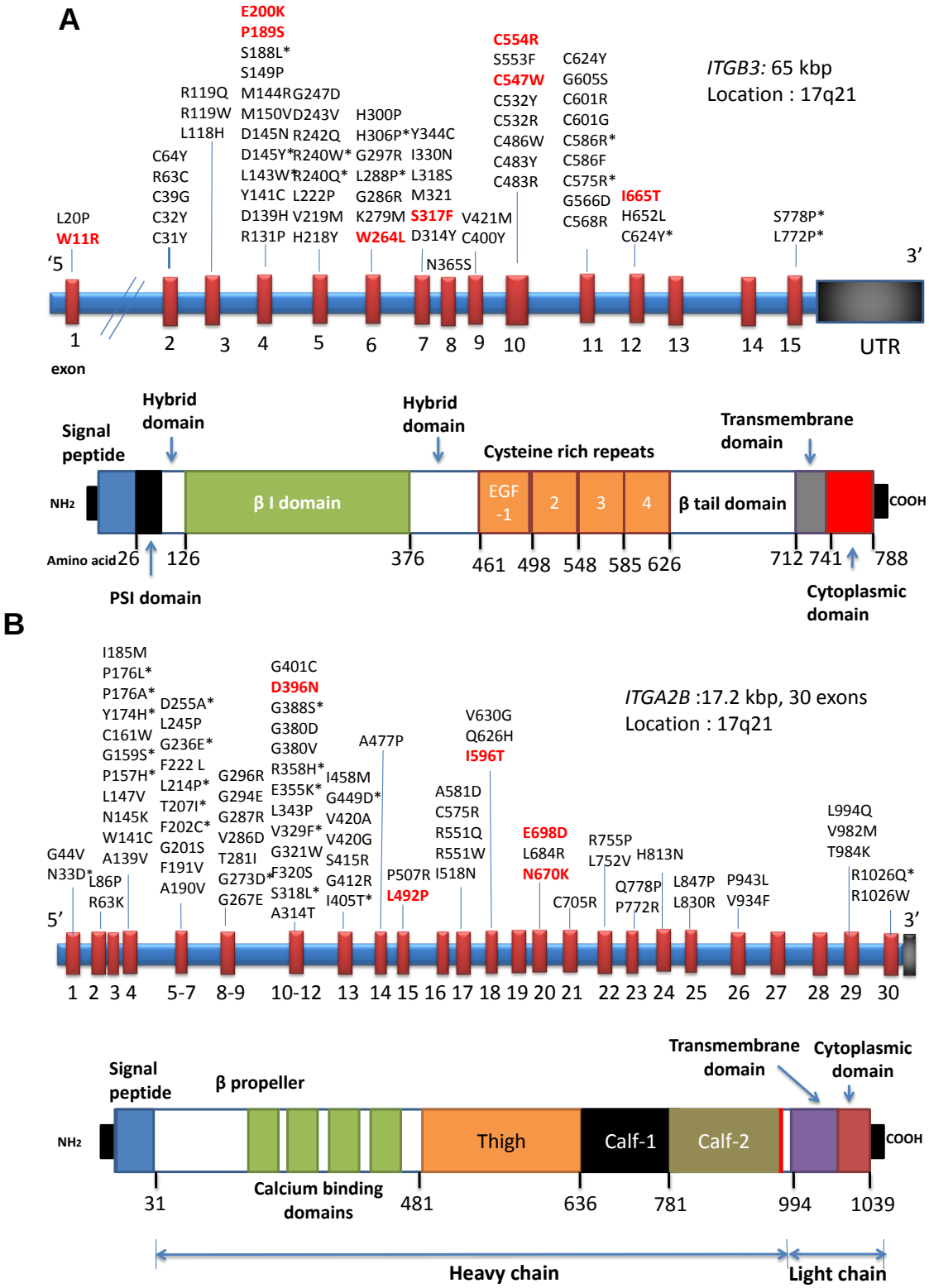

Figure 1.8 Schematic representations of A) *ITGB3* and B) *ITGA2B* and their predicted protein products showing the spectrum of approximately all reported missense substitutions reported in patients with GT. Asterisks indicate the variants that will be discussed further in this section. The variants in red have been characterised during this project. Compiled from Haghighi, *et al* (2015), Nurden, *et al* (2015), Sandrock-Lang, *et al* (2015), Tokgoz, *et al* (2015) and the online GT database (http://sinaicentral.mssm.edu/intranet/research/glanzmann).

Formation of the $\alpha_{IIb}\beta_3$ complex in the ER is considered to be a prerequisite for transport to the Golgi apparatus and the platelet membrane (Duperray*, et al* 1989, Rosa and McEver 1989). Therefore, defects in $\alpha_{IIb}\beta_3$ biogenesis may cause the α_{IIb} protein to be retained in the ER or to be rapidly degraded. Uncomplexed β_3 can either bind to α_v to form the heterodimeric $\alpha_v\beta_3$ receptor (also known as the vitronectin receptor) or be rapidly degraded (Nurden*, et al* 2013). Therefore, defects in either *ITGA2B* and/or *ITGB3* may interfere with the normal synthesis of $\alpha_{IIb}\beta_3$, causing insufficient expression of the integrin on the platelet membrane, resulting in Glanzmann thrombasthenia (Nurden and Caen 1974, O'Toole*, et al* 1989). Genetic defects which affect complex formation or integrin function may also occur (Djaffar and Rosa 1993, Hauschner*, et al* 2012, Loftus*, et al* 1990). In the following section, some examples of missense defects affecting different domains of α_{IIb} and β_3 will be highlighted.

1.3.3.5.1 Extracellular domain variants of α_{IIb}

A total of 78 missense defects have been reported in the extracellular domain of α_{IIb}, and 53 of these affected residues in the β-propeller domain, making it the most common region in α_{IIb} for missense mutations (Nurden*, et al* 2012b). Non-synonymous amino acid substitutions in the β-propeller domain can lead to defects in complex formation, or intracellular trafficking and/or integrin maturation. Amino acid residues 1 to 233, which comprise blades 1 to 3 of the β propeller, have been shown to be essential for formation of the $\alpha_{IIb}\beta_3$ complex (McKay*, et al* 1996). Nevertheless, the majority of missense substitutions in blades 1 to 3 have been associated with normal heterodimer formation, with substitution of Phe202 by Cys being the exception. An investigation of the p.Phe202Cys α_{IIb} variant, which was identified in a Cypriot patient whose platelets lacked surface expression of $\alpha_{IIb}\beta_3$, showed the p.Phe202Cys causes a failure in $\alpha_{IIb}\beta_3$ complex formation. Structural modelling suggested an interaction between Phe202 in α_{IIb} and Arg261 in the I-domain of β_3 which is disturbed when Phe202 is substituted by cysteine (Rosenberg*, et al* 2004). In contrast, several other substitutions in the β propeller, including p.Gln33Asp, p.Pro157His, p.Gly159Ser and p.Pro176Ala, did not affect $\alpha_{IIb}\beta_3$ complex formation but instead impaired the progression of pro-$\alpha_{IIb}\beta_3$ from the ER to the Golgi apparatus, leading to intracellular retention in the ER (Basani*, et al* 2000, Mansour*, et al* 2011, Nelson*, et al* 2005, Shen*, et al* 2009). Interestingly, a group of substitutions in blades 1 to 3 have been associated with the rare variant type of GT including p.Tyr174His, p.Leu214Pro, p.Thr207Ile, p.Pro176Leu and p.Asp255Vla (Basani*, et al* 2000, Grimaldi*, et al* 1998, Kiyoi*, et al* 2003, Tozer*, et al* 1999, Westrup*, et al* 2004). For example, the p.Tyr174His substitution was identified as a heterozygous defect in a 21 year old Japanese woman

with a prolonged bleeding time and a history of moderate mucocutaneous bleeding symptoms. The patient's platelets failed to aggregate in response to all physiological agonists except ristocetin, and there was a reduction in the surface expression of $\alpha_{IIb}\beta_3$ to 36%-41% of the normal levels. The integrin also failed to bind normally to its ligand. When expressed with wild-type β_3 in Chinese hamster ovary (CHO) cells, the p.Tyr174His α_{IIb} variant showed levels of surface expression of $\alpha_{IIb}\beta_3$ which were comparable to those of cells expressing the wild-type α_{IIb}, but the integrin failed to bind soluble fibrinogen or PAC-1 (the antibody that only binds to the active form of the receptor) or to immobilise fibrinogen (Kiyoi*, et al* 2003).

Many of the substitutions identified in blades 4 to 7 of the β propeller, in close proximity to or in the four calcium binding sites, result in normal production of the pro-$\alpha_{IIb}\beta_3$ complex but interfere with integrin maturation and membrane expression. Examples include the p.Gly273Asp, p.Ser318Leu, p.Val329Phe, p.Glu355Lys, p.Arg358His, p.Gly388Ser, p.IIe405The and p.Gly449Asp substitutions (Milet-Marsal*, et al* 2002b, Nelson*, et al* 2005, Poncz*, et al* 1994, Ruan*, et al* 1998, Wilcox*, et al* 1995, Wilcox*, et al* 1994). The p.Ser318Leu variant was identified as a homozygous defect in a 5 year old Indian boy with a history of gum bleeding, epistaxis and haematuria. His platelets failed to aggregate in response to epinephrine, ADP and collagen but aggregated normally in response to ristocetin, and clot retraction was also reduced. Expression of p.Ser318Leu $\alpha_{IIb}\beta_3$ receptors in Human Embryonic Kidney (HEK)-293 cells showed a reduction in surface expression of $\alpha_{IIb}\beta_3$ to 6% of the levels of the wild-type receptor, while immunoblotting analysis of cell lysates revealed a comparable level of pro-α_{IIb} when compared with the wild-type control but there was a trace of mature α_{IIb}. Immunoprecipitation of the mutated protein with antibodies to the $\alpha_{IIb}\beta_3$ complex revealed the formation of pro-$\alpha_{IIb}\beta_3$, while co-localisation studies showed that the majority of α_{IIb} was in the ER. These findings suggested that the substitution impaired progression of pro-$\alpha_{IIb}\beta_3$ to the Golgi, and results in retention of the abnormal receptor in the ER (Nelson*, et al* 2005). Outside of the β propeller domain, 22 missense defects have been identified in the extracellular regions of α_{IIb}, including in the thigh, calf-1 and calf-2 domains. The majority of the thigh, calf-1 and calf-2 domain variants which have been reported have not been characterised. However, their association with GT type I would suggest that they result in a severe reduction in membrane expression of $\alpha_{IIb}\beta_3$ (Nurden*, et al* 2012b).

1.3.3.5.2 Extracellular domain variants of β_3

Fewer genetic defects have been reported in *ITGB3* than in *ITGA2B* possibly because *ITGB3* possesses fewer exons than *ITGA2B* (15 exons in *ITGB3* versus 30 exons in

ITGA2B) and therefore there is less potential for splice site defects to occur. However, the smaller size of *ITGA2B* (17.2kb) compared to *ITGB3* (65 kb) would suggest that it should be less prone to mutation. To date, 61 missense defects have been identified in the β_3 subunit, of which 42 affect residues towards the N-terminus including in the PSI, hybrid and I domains (Nurden*, et al* 2012b). These substitutions lead to either a significant reduction in membrane expression of $\alpha_{IIb}\beta_3$, resulting in GT type I or II, or to ligand binding defects, causing variant type GT. As mentioned previously, the β I domain contains three cation binding sites. Characterisation of amino acid substitutions located in these sites (p.Asp145Tyr and p.Arg240Gln) provided essential details about the active site of the $\alpha_{IIb}\beta_3$ integrin and defined a fibrinogen binding site. The p.Asp145Tyr substitution in the β I domain, which was inherited as a homozygous defect, does not disrupt the formation of the $\alpha_{IIb}\beta_3$ heterodimer, or membrane expression of the receptor. However, the variant receptor failed to bind to fibrinogen, or to PAC-1, resulting in abrogation of the integrin function. Structural studies showed that Asp145 is located in the binding site of the MIDAS, which suggests that this cation (Mg^{2+}) binding site plays a crucial role in facilitating ligand binding. An investigation of the surrounding residues was carried out by Bajt*, et al* (1992) who substituted alanine residues for the following amino acids: Asp145, Ser147, Ser149, Asp151, Asp153 and Ser156. Analysis of CHO cells co-transfected with the recombinant β_3 and wild-type α_{IIb} showed that the p.Asp145Ala, p.Ser147Aln and Ser149Ala variants failed to bind fibrinogen and PAC-1, while the p.Asp151Ala, p.Asp153Ala and p.Ser156Ala substitutions had no effect on $\alpha_{IIb}\beta_3$ function. These results suggested that Asp145, Ser147 and Ser149 play an important role in integrin function, particularly in ligand binding (Bajt and Loftus 1994). It was found that Asp145 and Ser147 contribute to the MIDAS coordination site, while Ser149 participates in both the MIDAS and ADMIDAS binding sites (Zhu, et al 2008). Two other defects giving rise to variant GT were those caused by the substitution of p.Arg240 by either Gln or Trp. These were identified as homozygous defects in three unrelated GT patients, all of whom had moderate bleeding symptoms and platelets which expressed similar levels of $\alpha_{IIb}\beta_3$ integrin when compared to the control platelets. However, the patients' platelets failed to aggregate, and clot retraction and platelet fibrinogen content was low or absent. Furthermore, the p.Arg240Trp and p.Arg240Gln variants cause the $\alpha_{IIb}\beta_3$ complex to be unstable, highly sensitive to Ca^{2+} chelation and unable to bind to its ligands (Djaffar and Rosa 1993, Lanza*, et al* 1992, Nurden*, et al* 1987). A crystal structure revealed Arg240 to be located near a SyMBS (adjusted to the MIDAS), and the Arg240Gln or Trp substitution results in non-functional integrin indicating SyMBS also plays a role in $\alpha_{IIb}\beta_3$ in facilitating fibrinogen binding (Zhu, *et al* 2008).

In contrast to the above findings, the majority of substitutions identified in the I domain, and in the PSI and hybrid domains, such as the p.Asp143Trp, p.Ser188Leu and p.Leu288Pro defects, have been found to disrupt surface expression of $\alpha_{IIb}\beta_3$. It has been reported that the p.Asp143Trp variant (in the I domain) results in misfolded $\alpha_{IIb}\beta_3$ and causes intracellular retention of the receptor (Basani*, et al* 1997, Loftus*, et al* 1990). The p.Ser188Leu (within the I domain) was identified in an 11 year old Caucasian male with a long history of bleeding symptoms. The variant causes a significant reduction in surface expression of the receptor (to 16-27% of normal levels). Immunoblotting analysis of platelet lysates showed 30% of $\alpha_{IIb}\beta_3$ expression and the patient's platelets were unable to aggregate following stimulation and failed to bind fibrinogen (Jackson*, et al* 1998, Ward*, et al* 2000).

Several non-synonymous defects affecting residues in the cysteine rich repeats of β_3 have been reported, the majority of which disrupt disulphide bonds, and result in mild to moderate reductions in surface expression which may or may not be accompanied by constitutive activation of the receptor. In contrast, other amino acid substitutions in the cysteine rich repeats have been shown to disrupt $\alpha_{IIb}\beta_3$ biogenesis, and result in the absence of the receptor from the platelet membrane (Milet-Marsal*, et al* 2002a, Mor-Cohen*, et al* 2007). One such example would be the p.Cys575Arg variant which was identified in four Jordanian GT cases, all of whom had a history of severe bleeding symptoms. Platelets from the patients failed to aggregate in response to collagen, ADP and epinephrine, but aggregation was normal in response to ristocetin. There was a severe reduction in membrane expression of $\alpha_{IIb}\beta_3$ (to 1-14% of $\alpha_{IIb}\beta_3$ expression levels observed in control platelets), and analysis of platelet lysates showed an almost complete absence of the β_3 subunit (expression at only 5% of the control). The expression study of the p.Cys575Arg variant was carried out in baby hamster kidney (BHK) cells. Interestingly, following co-transfection of the p.Cys575Arg variant with wild-type α_{IIb}, analysis of the BHK cell lysates demonstrated a reduction in the β_3 subunit and $\alpha_{IIb}\beta_3$ complex, while the ratio of mature α_{IIb} to pro-α_{IIb} was also reduced when compared with wild-type β_3, implying that the progression of pro-$\alpha_{IIb}\beta_3$ to the Golgi was severely impaired. Subsequent staining of the transfected cells revealed that $\alpha_{IIb}\beta_3$ and β_3 were mostly retained in the ER (Mor-Cohen*, et al* 2007).

Other non-synonymous amino acid substitutions in the EGF domains, such as p.Cys586Arg and p.Cys624Tyr, result in mild to moderate reductions in the expression of constitutively active $\alpha_{IIb}\beta_3$ variants. An example would be the p.Cys586Arg variant identified in a 40 year old French male with a prolonged bleeding time, and a history of mild gum bleeding symptoms and thrombocytopenia, which was inherited as a

recessive trait. The aggregation of platelets from the patient and clot retraction were significantly reduced but not completely absent and platelets contained normal levels of fibrinogen. This indicated the residual function of $\alpha_{IIb}\beta_3$ was able to support other functions of the receptor except aggregation including clot retraction and the uptake of fibrinogen into α-granules. Membrane expression of $\alpha_{IIb}\beta_3$ on platelets from the patient was approximately 20% of that observed in control platelets. However, the platelets were found to bind spontaneously to fibrinogen and PAC-1 without activation (Ruiz*, et al* 2001). Other studies have found that substitution of Cys586 in β_3 by 12 different amino acids also results in the integrin being locked in its high affinity state, implying that this residue plays an important role in stabilising the integrin in its bent formation (Kamata*, et al* 2004). It is interesting to note that structural studies reveal Cys586 forms a disulphide bond with Cys609 in β_3, and that disruption of the bond with single and double substitutions of the cysteine residues by serine results in active $\alpha_{IIb}\beta_3$ only when Cys586 is mutated (Mor-Cohen*, et al* 2012, Zhu*, et al* 2008). It has been suggested that the free thiol group of Cys609 may be involved in integrin activation in this situation, possibly through a disulphide exchange dependent mechanism (Mor-Cohen*, et al* 2012). More recently, mouse platelets bearing the p.Cys586Arg variant of β_3 were shown to spontaneously bind PAC-1 and fibrinogen and to be associated with haemorrhage and high mortality in the affected mice (Fang*, et al* 2013).

1.3.3.5.3 Transmembrane and cytoplasmic domain variants of α_{IIb} and β_3

To date, only three missense mutations have been reported in the transmembrane and cytoplasmic domains of both β_3 and α_{IIb}, causing GT, two in β_3 and one in α_{IIb} subunit (Figure 1.8). These were predicted to cause p.Ser778Pro and Leu772Pro substitutions in β_3 and a p.Arg1026Gln substitution in α_{IIb} (Chen*, et al* 1992, Kannan*, et al* 2009, Nurden*, et al* 2015). For example, the p.Ser778Pro substitution was identified as a compound heterozygous defect along with a null allele in a patient with a life long history of bleeding symptoms. Platelets from the affected patient showed an approximate 50% reduction in $\alpha_{IIb}\beta_3$ expression when compared with control platelets and failed to aggregate in response to collagen, ADP and thrombin. The platelets also failed to bind fibrinogen following integrin activation. The p.Ser778Pro variant was characterised further by co-expressing it with wild-type α_{IIb} in CHO cells. The integrin $\alpha_{IIb}\beta_3$ bearing the p.Ser778Pro β_3 variant failed to bind PAC-1 following activation and caused a defect in cell spreading and clot retraction (Chen*, et al* 1992). Interestingly, the cytoplasmic domain of the p.Ser778Pro variant failed to bind kindlin-3, a cytoplasmic protein that is recognised to be essential for integrin activation. These findings suggest that the p.Ser778Pro variant mediates its pathogenic effects by

disturbing the interaction between kindlin-3 and the β_3 cytoplasmic domain causing a lack of receptor activation (Moser*, et al* 2008).

1.4 Dominant Glanzmann Thrombasthenia

The majority of mutations affecting *ITGA2B* and *ITGB3* have been reported in patients with normal platelet count and size. However, some patients have been diagnosed with thrombocytopenia and platelet anisocytosis. In the majority of these cases, the gene defect was inherited as a heterozygous form causing a GT like phenotype, also known as a dominant GT (Nurden*, et al* 2013). Most of these mutations, such as α_{IIb}-p.Arg1026Gln, β_3-p.Asp749His and β_3-p.Leu744Pro affect the transmembrane and cytoplasmic domains of α_{IIb} and β_3. Briefly, a heterozygous variant, p.Arg1026Gln α_{IIb} was reported in five Japanese patients with large platelets and mild thrombocytopenia. The patients' platelets showed 50-70% of surface $\alpha_{IIb}\beta_3$ receptor levels when compared to control platelets. In addition, platelet aggregation was reduced; though the platelets also spontaneously bound to PAC-1 indicating constitutive activation. In an *in vitro* study of CHO cells expressing the p.Arg1026Gln variant, the cells displayed cytoplasmic protrusions containing abnormally large swellings at the tip. This also corresponded to a reduction in the number of proplatelet tips with the formation of enlarged proplatelets in murine megakaryocytes (Kunishima*, et al* 2011). Ghevaert*, et al* (2008) identified a heterozygous variant, β_3-p.Asp749His, in five patients of a single family. The propositus was a 49 year old female with thrombocytopenia and platelet anisocytosis but did not have a bleeding history. Similar to the p.Arg1026Gln variant, the p.Asp749His variant was found to be partially activated and has been associated with a defect in proplatelet formation, causing macrothrombocytopenia in the patients (Ghevaert*, et al* 2008). Interestingly, Arg1026 in α_{IIb} forms a salt bridge with p.Asp749 in β_3, maintaining the bent conformation and therefore loss of this interaction is likely to cause a change in conformation and integrin activation (Yang*, et al* 2009). A heterozygous β_3-p.Leu744Pro substitution was inherited in a 43 year old Caucasian female with a history of frequent and severe mucocutaneous bleeding and menorrhagia. The patient had moderate thrombocytopenia and platelet anisocytosis. Platelets from the patient expressed 47-78% of the control $\alpha_{IIb}\beta_3$ surface levels, and also bound spontaneously to fibrinogen. Co-expression of the p.Leu744Pro β_3 variant with wild-type α_{IIb} in CHO cells was characterised by normal membrane expression of $\alpha_{IIb}\beta_3$ receptors which bound spontaneously to both PAC-1 and fibrinogen. The transfected CHO cells also aggregated spontaneously in the presence of soluble fibrinogen and formed long protrusions containing large swellings when spread on immobilised fibrinogen. In addition, the mutation promoted abnormal clustering of $\alpha_{IIb}\beta_3$

in transfected CHO cells. These results suggested that spontaneous activation of the integrin can disturb platelet production and morphology and results in receptor clustering (Jayo*, et al* 2010).

A recent report identified the possible mechanism behind the proplatelet defect in patients with gain-of-function mutations in β_3. A heterozygous variant, c.2134+G>C in *ITGB3,* which is predicted to give rise to a 40 amino acid deletion (del647-686) in the tail domain of β_3, was identified in two patients, resulting in a dominant form of GT. The mutation results in a reduction of membrane expression with sustained integrin activation. *In vitro* studies on MKs derived from CD45+ stem cells showed normal megakaryocyte maturation but impaired proplatelet development with a significant reduction in tip number and an increase in size (Bury*, et al* 2012). Very recently, the mechanism behind the latter effect was extensively studied by the same group, showing that spontaneous activation of $\alpha_{IIb}\beta_3$ continuously triggers outside-in signalling events leading to impaired cytoskeletal rearrangement, possibly through preventing actin turn over at the stage of polymerization (Bury*, et al* 2016). The study also showed that integrin internalisation may be responsible for the integrin reduction in gain-of-function mutations in dominant GT like syndrome. Therefore, this work may explain why some cases present with thrombocytopenia as a result of gain-of-function mutations in *ITGA2B* and *ITGB3* genes.

1.5 The effects of non-synonymous *ITGB3* defects on the $\alpha_v\beta_3$ Integrin

In addition to forming a receptor with α_{IIb}, the β_3 subunit also has the ability to bind to α_v forming the vitronectin receptor, $\alpha_v\beta_3$, which is expressed on the platelet surface at low levels (50-100 copies) compared to $\alpha_{IIb}\beta_3$. A high degree of homology exists between α_{IIb} and α_v; however it has been shown that mutations in β_3 can affect $\alpha_v\beta_3$ differently to $\alpha_{IIb}\beta_3$. $\alpha_v\beta_3$ is highly expressed in cells such as endothelial cells, smooth muscle and osteoclasts and has been associated with angiogenesis and cancer. However, there is no clear phenotypic difference between patients with defects in *ITGB3* and those with *ITGA2B* defects (Nurden*, et al* 2013). It has been reported that defects in *ITGB3* had a range of effects on the expression and function of $\alpha_v\beta_3$, while the same was not always true for $\alpha_{IIb}\beta_3$. The p.His306Pro β_3 variant was identified in a Japanese patient who was diagnosed with type I GT. Flow cytometry analysis of the patient's platelets revealed a 94% reduction in membrane expression of $\alpha_{IIb}\beta_3$ compared to the control platelets, while a modest reduction of 47% was observed for $\alpha_v\beta_3$ (Tadokoro*, et al* 2002). However, some variants, including the p.Leu143Trp and p.Cys400Tyr variants, have

been associated with severe parallel reductions in expression of both integrins (Ambo*, et al* 1998, Basani*, et al* 1997). Accordingly, several variants were created by mutating cysteine residues in the EGF domains of β_3, which resulted in a variety of structural and functional differences between $\alpha_{IIb}\beta_3$ and $\alpha_v\beta_3$. *In vitro* expression studies showed that cells expressing p.Cys463Ser and p.Cys483Ser variants had severely reduced surface levels of $\alpha_{IIb}\beta_3$ while only mild reductions were observed for $\alpha_v\beta_3$. In contrast, cells expressing p.Cys619Ser and p.Cys627Ser variants displayed parallel reductions in both $\alpha_v\beta_3$ and $\alpha_{IIb}\beta_3$. The majority of these variants also resulted in spontaneous activation of both $\alpha_v\beta_3$ and $\alpha_{IIb}\beta_3$. Therefore, cysteine residues in the EGF domain are likely to be important to maintain both receptors in a resting state, while the structural roles required for surface expression can be unique to each receptor (Mor-Cohen*, et al* 2012).

1.6 Work leading up to this study and aims of this project

This project continues on the work carried out as part of a previous study by Al-Marwani (2009) in the Haemostasis Research Group, the University of Sheffield, which aimed to identify the genetic alterations underlying GT in a UK patient cohort. The spectrum of *ITGA2B* and *ITGB3* defects underlying GT was investigated in 37 unrelated index cases with GT who were all recruited through UK haemophilia centres. This work identified several novel mutations in the two genes and a number of previously identified variants, which had not yet been characterised. Attempts were made to recall patients as well as affected and unaffected family members in order to confirm the cosegregation of variants with disease and to further assess their effect on platelet function. Unfortunately, the patients and family members were unavailable for further studies. Therefore, the current study aimed to reproduce the patient phenotypes using alternative methods such as *in vitro* expression studies.

Genetic analysis of the UK GT cohort identified 31 different mutations affecting *ITGB3* and *ITGA2B* in 34 of 37 index cases, 23 of which were novel. Seventeen different mutations in *ITGA2B* were found in 21 unrelated index cases, while 14 *ITGB3* mutations were detected in 13 unrelated cases. In *ITGA2B*, ten were either deletions or duplications predicted to cause splicing defects or frameshift mutations. In addition, two nonsense mutations and five missense changes were identified. In *ITGB3*, 14 different genetic defects were predicted to cause 12 non-synonymous variants and two frameshift defects. Importantly, 23 of these mutations were novel with the majority being non-synonymous changes (Al-Marwani 2009).

Of the defects identified in the cohort, 17 were predicted to cause amino acid substitutions in the receptor, 12 in *ITGB3* and 5 in *ITGA2B*. The majority of these variants were previously unreported or uncharacterised, 9 in *ITGB3* and 5 in *ITGA2B*. This project aimed to study these novel and uncharacterised missense mutations to identify their effects on platelet function and further our understanding of the molecular basis of this disease. The genetic alterations in *ITGB3* that were investigated in this study were c.31T>C, c.356G>A, c.565C>T, c.598G>A, c.791G>T, c.950C>T, c.1641C>G, c.1660T>C and c.1994T>C transitions, which were predicted to cause the following amino acid substitutions in β_3: p.Trp11Arg, p.Arg119Gln, p.Pro189Ser, p.Glu200Lys, p.Trp264Leu, p.Ser317Phe, p.Cys547Trp, p.Cys554Arg and p.Ile665Thr, respectively. The genetic alterations in *ITGA2B* that were investigated were c.1186G>A, c.1475T>C, c.1787T>C, c.2010C>A and c.2094G>T transitions, which were predicted to cause the following amino acid substitutions in α_{IIb}: p.Asp396Asn, p.Leu492Pro, p.IIe596Thr, p.Asn670Lys and p.Glu698Asp, respectively. All of these variants have been associated with variable clinical symptoms and bleeding severities (Table 1.2).

A combined *in silico* and *in vitro* approach was adopted in this study. First, a number of computational tools were used to predict the effects of non-synonymous *ITGB3* and *ITGA2B* defects on β_3 and α_{IIb} structure and function. These initial studies, which are described in detail in chapter 3 of this thesis, allowed several hypotheses to be generated (see chapter 3). These hypotheses were then tested experimentally, by expression and characterisation of the corresponding recombinant integrin subunits *in vitro*. The results of these studies are detailed in chapters 4, and 5 which summarise the findings on *ITGB3* and *ITGA2B* respectively. *ITGA2B* and *ITGB3* defects were characterised by expressing the corresponding recombinant integrin subunits in CHO cells since they do not express α_{IIb} and β_3 subunits endogenously. Furthermore, the *in vitro* biogenesis, expression and function of $\alpha_{IIb}\beta_3$ in CHO cells have previously been shown to correlate strongly with the expression of $\alpha_{IIb}\beta_3$ on platelets from GT patients (Nurden*, et al* 2013). In addition, the use of CHO cells provides an opportunity to evaluate the impact of of both homozygous and compound heterozygous defects.

While this work was in progress, the p.Cys547Trp and p.Arg119Gln β_3 variants were investigated under my supervision by Ms A Almusbahi, a master's student in the haemostasis research group. Work relating to the p.Arg119Gln variant has been included in chapter 3 (*in silico* analysis). Further characterisation of the p.Cys547Trp variant has been undertaken as part of this project and therefore the findings obtained during the master's project, have been reproduced here for reasons of completeness.

It was expected that the results of this project would allow confirmation of the pathogenicity of the candidate genetic defects that were studied in patients with bleeding tendencies, provide insights into the structure and function of $\alpha_{IIb}\beta_3$, and advance our understanding of the molecular basis of GT.

Table 1.2 Candidate *ITGA2B* and *ITGB3* defects identified in UK patients with GT. Details of 13 candidate gene defects that will be investigated in this study are shown.

Gene	Nucleotide change	Predicted amino acid substitution	Genotype	Treatment	Anti-$\alpha_{IIb}\beta_3$*	Bleeding symptoms/ score[x]
ITGB3	**c.31T>C-c.565C>T**	p.Trp11Arg, p. Pro189Ser	Compound heterozygous	Platelets, rVIIa	Unknown	Epistaxis / 5
	c.356G>A	p.Arg119Gln	Compound heterozygous	RBC, Platelets, rVIIa	No	Epistaxis and menorrhagia / 3
	c.598G>A	p.Glu200Lys	Homozygous	Platelets	No	Epistaxis / 3
	c.791G>T	p.Trp264Leu	Homozygous	RBC, Platelets, rVIIa	Yes	Epistaxis / 10
	c.950C>T	p.Ser317Phe	Homozygous	Platelets, rVIIa	Yes	Epistaxis and menorrhagia / 8
	c.1641C>G	p.Cys547Trp	Homozygous	Platelets, rVIIa	No	Epistaxis / 3
	c.1660T>C	p.Cys554Arg	Homozygous	Platelets, rVIIa	No	Epistaxis / 3
	c.1994T>C	p.Ile665Thr	Homozygous	RBC, Platelets, rVIIa	No	Epistaxis – Gastrointestinal bleeding / 7
ITGA2B	**c.1186G>A**	p.Asp396Asn	Homozygous	RBC, Platelets, rVIIa	Unknown	Epistaxis / 5
	c.1186G>A	p.Asp396Asn	Homozygous	Platelets, rVIIa	Unknown	Epistaxis / 7
	C.1475T>C	p.Leu492Pro	Compound heterozygous	None	No	Epistaxis / 1
	C.1787T>C	p.Ile596Thr	Homozygous	Platelets	Unknown	Epistaxis, Menorrhagia and Gastrointestinal bleeding / 7
	C.1787T>C	p.Ile596Thr	Homozygous	RBC, Platelets, rVIIa	No	Epistaxis, Menorrhagia and Gastrointestinal bleeding / 7
	C.2010C>A	p.Asn670Lys	Homozygous	None	Unknown	Epistaxis / 7
	C.2094G>T	p.Glu698Asp	Homozygous	Platelets	No	Epistaxis and Menorrhagia / 4

*Indicates whether patients developed antibodies to $\alpha_{IIb}\beta_3$ in response to platelet transfusion. [x]Bleeding severity, assessed subjectively by the referring clinician on a scale of 1 to 10, where 1 is minor and 10 is severe bleeding. RBC: red blood cells and rVIIa is recombinant factor VIIa. The *ITGB3* and *ITGA2B* cDNA and amino acid were numbered according to Ensembl ID: ENSP00000452786 and ENSP00000262407.

Chapter 2:
Materials and methods

Materials and methods

2.1 Materials

2.1.1 Plasmids

ITGA2B and *ITGB3* cDNAs were subcloned into pcDNA3.1 (-) Neo from Invitrogen (California, USA) and made available as a kind gift by Professor Nelly Kieffer, University of Luxembourg (**Appendix 1**). The exontrap (pET01) vector was purchased as lyophilized DNA from Mo Bi Tec Molecular Biotechnology (Goettingen, Germany) while pcDNA 3.1 Dup plasmid was derived from pcDNA3.1 (-) Neo, Invitrogen (California, USA) and made available as a kind gift by Dr Isabelle Tournier, University of Rouen, France.

2.1.2 Primers

Oligonucleotide primers were obtained from Eurofins MWG Operon (Ebersberg, Germany) and Sigma-Aldrich (Missouri, USA). All primers were supplied lyophilized and were resuspended in distilled water at a concentration of 100 pmol/µl before use and stored at -20°C. The final working concentrations were 1 pmol/µl, 10 pmol/µl and 2.5 ng/µl for sequencing, PCR and mutagenesis, respectively.

2.1.3 Preparation of plasmids and mutagenesis kits

Mini- and maxi-preparations of plasmids were carried out using the QIAprep Miniprep and QIAprep Maxiprep kits purchased from Qiagen (Venlo, Netherlands), respectively. Mutagenesis was performed using a QuikChange® Lightning Site-Directed Mutagenesis Kit purchased from Agilent Technologies (California, USA). Luria-Bertani (LB) broth and agar were purchased from Merck© (Darmstadt, Germany) while NZY$^+$ broth was purchased from Thermo Fisher Scientific (Massachusetts, USA).

2.1.4 Cell lines, tissue culture media and transfection reagent

Human erythroleukaemia (HEL) and Chinese hamster ovary (CHO) cells were purchased from American Type Culture Collection (ATCC) (Manassas, USA). HEL and CHO cells were cultured in Roswell Park Memorial Institute (RPMI) 1640 Medium GlutaMAX™ supplemented with 10% fetal bovine serum (FBS). The RPMI 1640 Medium GlutaMAX™ and FBS were purchased form Gibco® (California, USA).

Lipofectamine® LTX reagent was purchased from Life Technologies (California, USA) and used to transfect CHO cells with the desired plasmids.

2.1.5 Antibodies and fluorescent labelled protein

Monoclonal mouse anti human CD61 (β_3) conjugated with R-phycoerythrin (PE) (Cat No. 555754) and PE-mouse IgG1 isotype control (Cat. No. 555749) were obtained from BD Bioscience (California, USA). Monoclonal mouse anti human CD41 (α_{IIb}) conjugated with fluorescein isothiocyanate (FITC) (Cat. No. MCA467F) and FITC-mouse IgG1 isotype control (Cat. No. MCA928) were purchased from AbD Serotec (Kidlington, UK) (Table 2.1). A list of the antibodies and fluorescent proteins which were used in the study can be seen in table 2.1.

Table 2.1 Antibodies and fluorescent labelled protein used in the study and their working dilutions

Antibody	Dilution	Company	Catalogue No.
Anti human CD61(β_3) - PE	1:16	BD Bioscience	555754
PE mouse IgG1 isotype control	1:16	BD Bioscience	555749
Anti human CD41(α_{IIb}) - FITC	1:16	AbB Serotec	MCA467F
Anti human $\alpha_v\beta_3$ - FITC	1:5	Mili-Mark	FCMAB282F
PE mouse IgG1 isotype control	1:16	AbB Serotec	MCA928
Fibrinogen from human plasma, Alexa Fluor® 488 conjugate	1:10	Molecular Probes	F-13191
Anti human CD41a ($\alpha_{IIb}\beta_3$ complex)	1:8	Beckman Coulter	A07781
PAC-1 antibody -FITC	1:2	BD Bioscience	340507
Rabbit anti β_3	1:250	Millipore	AB2984
Rabbit anti α_{IIb}	1:250	Santa Cruz Biotechnology	SC-15328
Mouse anti β tubulin	1:1000	Sigma-Aldrich	T7816
Infrared fluorescent dyes (IRDye) ® 680 Donkey anti-Rabbit	1:10000	Li-Cor	926-68073
Infrared fluorescent dyes (IRDye) ®800CW Donkey anti-Mouse	1:10000	Li-Cor	926-32212

2.1.6 Enzymes

All restriction enzymes used in this study were obtained from New England Biolabs (Massachusetts, USA). T4 DNA ligase and 10x ligase buffer were purchased from Promega (Fitchburg, USA). Q5® High-Fidelity DNA Polymerase, OneTaq® DNA Polymerase and Endoglycosidase (Endo) H were obtained from New England Biolabs (Massachusetts, USA).

2.1.7 Other commercial kits and reagents

Table 2.2 provides a list of the main commercial kits and reagents used in this study.

Table 2.2 Commercial kits, chemicals and reagents.

Kit / Chemical / Reagent	Supplier
Acrylamide 30% solution	Sigma-Aldrich
Agarose	Bioline Laboratories
Ammonium persulfate (APS)	BDH Merck Ltd
Ampicillin	Sigma-Aldrich
boric acid	BDH Merck Ltd
Bovine serum albumin (BSA)	Sigma-Aldrich
Bradford reagent	Sigma-Aldrich
Calcium chloride	BDH Merck Ltd
Chameleon™pre-stained protein ladder	Li-Cor
Diethylpyrocarbonate (DEPC)-treated Water	Thermo Fisher Scientific
Dimethyl sulfoxide (DMSO)	Sigma-Aldrich
Dithiothreitol (DTT)	Sigma-Aldrich
Dulbecco's Phosphate-Buffered Saline (DPBS)	Life Technologies Ltd
Ethylenediaminetetraacetic acid (EDTA)	Sigma-Aldrich
Fixation/Permeabilization Solution	BD Bioscience
Glycerol	BDH Merck Ltd
Hybond extra nitrocellulose membrane	GE Healthcare
Hyper Ladder™ I	Bioline Laboratories
Hyper Ladder™ VI	Bioline Laboratories
Isopropanol (Propan-2-ol)	Fisher Scientific
Luria-Bertani (LB) broth	Fisher Scientific
Luria-Bertani (LB) agar	Fisher Scientific
Methanol	Fisher Scientific
MG-132	Sigma-Aldrich
NZY+ broth	Fisher Scientific
Odyssey Blocking buffer	Li-Cor
Protease Inhibitor Cocktail	Sigma-Aldrich
QIAquick Gel Extraction Kit	Qiagen
QuantiTect® Reverse Transcription kit	Qiagen
Radio-Immunoprecipitation Assay (RIPA) lysis buffer	Thermo Fisher Scientific
Sodium dodecyl sulfate (SDS)	BDH Merck Ltd

Tetramethylethylenediamine (TEMED)	BDH Merck Ltd
Total RNA isolation kit (EZ-RNA II)	Biological industries
Tris-base	Fisher Scientific
Triton® X-100	BDH Merck Ltd
Trypsin-EDTA solutions	Sigma-Aldrich
Tween® 20	BDH Merck Ltd

2.2 Methods

2.2.1 *In silico* analysis

2.2.1.1 Cross-species comparisons of integrin β_3 and α_{IIb} protein sequences

Cross-species comparisons of integrin β_3 and α_{IIb} protein sequences were carried out to examine the degree of conservation of amino acid sequences encompassing the sites of non-synonymous substitutions identified in patients with Glanzmann thrombasthenia, nine in β_3 and five in α_{IIb}. In brief, β_3 (ENSP00000452786) and α_{IIb} (ENSP00000262407) amino acid sequences were obtained from Ensembl (http://www.ensembl.org). The sequences were then queried using Standard Protein BLAST (http://blast.ncbi.nlm.nih.gov) (accessed April, 2013). The β_3 and α_{IIb} sequences were compared across 12 different vertebrate species that were selected from the BLAST results. These sequences were selected by removing paralogue sequences, avoiding redundancy and adding as much variability as possible without introducing low sequence coverage. Alignment and identification of conserved regions were achieved using the ClustalW2 (http://www.ebi.ac.uk) and Boxshade3.1 (http://www.ch.embnet.org) tools (accessed April, 2015).

2.2.1.2 Comparisons of integrin β_3 and α_{IIb} protein sequences with other human β and α integrin family members

Comparisons of β_3 and α_{IIb} protein sequences with other β and α integrin family members were performed to examine the degree of conservation of amino acid sequences encompassing the sites of non-synonymous substitutions identified in GT patients. The approach was similar to that described in section 2.2.1.1. β_3 (ENSP00000452786) and α_{IIb} (ENSP00000262407) amino acid sequences were obtained from Ensembl (http://www.ensembl.org). The protein sequences were submitted to BLAST and all similar proteins were selected, avoiding duplication and low sequence coverage. Alignment and identification of conserved regions were achieved

using the ClustalW2 (http://www.ebi.ac.uk) and Boxshade3.1 (http://www.ch.embnet.org) tools (accessed April, 2015).

2.2.1.3 Predicting the effects of non-synonymous substitutions

The impact of amino acid substitutions on the structure and function of the β_3 and α_{IIb} integrin subunits were predicted using a number of online prediction tools. The wild-type amino acid sequences of human β_3 and α_{IIb} were obtained as described above. The potential effects of each substitution were predicted using Polymorphism phenotyping v2 (Polyphen-v2) (http://genetics.bwh.harvard.edu/pph2/), Sorting Intolerant From Tolerant (SIFT) (http://sift.jcvi.org/), Align Grantham Variation Grantham Deviation (GVGD) (http://agvgd.iarc.fr/agvgd_input.php) and SNPs&GO (http://snps-and-go.Biocomp.unibo.it/snps-and-go/) (accessed May, 2013). Similarly, transcript sequences for the human *ITGB3* (ENST00000559488) and *ITGA2B* (ENST00000262407) genes were obtained from Ensembl and used to predict the effects of single nucleotide substitutions using MutationTaster (http://www.mutationtaster.org/) (accessed May, 2013).

2.2.1.4 Prediction of signal peptide cleavage

The online prediction tool SignalP 4.0 (http://www.cbs.dtu.dk/services/SignalP) (accessed May, 2012) was used to predict the effect of the p.Trp11Arg substitution in the β_3 subunit on signal peptide cleavage. SignalP was used with the default settings to analyse the wild-type and variant sequences.

2.2.1.5 Prediction of effects of single nucleotide substitutions on ITGA2B and ITGB3 RNA splicing

The potential effects of single nucleotide substitutions on *ITGB3* and *ITGA2B* RNA splicing were predicted using NetGene (http://www.cbs.dtu.dk/services/NetGene2/), Berkeley Drosophila Genome Project (BDGP) (http://wwwfruitfly. org/), Human Splicing Finder (HSF) (http://www.umd.be/HSF/) and Automated Splice Site and Exon Definition Analysis (ASSEDA) (http://www.splice.uwo.ca/) (accessed May, 2013).

2.2.1.6 Protein structure modelling

The crystal structures of the extracellular domains of $\alpha_{IIb}\beta_3$ (3FCS) and $\alpha_v\beta_3$ (1JV2) were obtained from the Research Collaboratory for Structural Bioinformatics Protein Data Bank (pdb) (http://www.rcsb.org/pdb) (Xiong*, et al* 2001, Zhu*, et al* 2008). Visualisation and analysis of these structures were carried out using Pymol molecular graphic software version 1.3 (Schrödinger, New York, USA). In brief, the pdb file was uploaded into Pymol, visualised as a cartoon and secondary structure coloured as follows: α-helices in red, β-sheets in yellow and loops in green. The cationic binding

sites were shown as spheres and coloured in grey. Residues of interest and surrounding residues (within 5 angstroms) were shown as sticks to study the effects of amino acid substitutions. Chemical interactions were also displayed for these residues and those considered relevant were highlighted. To examine the effects of non-synonymous substitutions, mutagenesis was performed on the sequence to substitute selected amino acids within the protein structure. The orientation of the side chain of the substituted residue was selected based on the highest frequency of occurrence of this amino acid in the protein, shown in Pymol as a percentage at mutation object panel.

2.2.1.7 Primer design

The QuikChange® Primer Design Program (www.genomics.agilent.com) (accessed April, 2015) was used to design primers for site-directed mutagenesis. For each missense mutation, two overlapping primers containing the corresponding single nucleotide substitution were used to introduce the desired change into the *ITGA2B* or *ITGB3* cDNA which had been cloned into pcDNA3.1 (-) Neo (Section 2.1.1). The sequences of these primers are presented in Table 2.3. The sequencing and cloning primers were designed using the Primer 3 tool (http://frodo.wi.mit.edu) (accessed May, 2014). Details of the primers used for sequencing the *ITAG2B* and *ITGB3* cDNAs are provided in Table 2.4 and those used for cloning inserts into the vectors pcDNA-Dup and pET-01 are provided in Tables 4.3 and 5.2.

Table 2.3 Sequences of oligonucleotide primers used to introduce single nucleotide changes into the *ITGA2B* and *ITGB3* cDNAs. The single nucleotide substitutions are highlighted in red.

Mutation / Gene	Exon	Nucleotide substitution	Forward primer (5' to 3')	Reverse primer (5' to 3')
p.W11R / *ITGB3*	1	c.31T>C	CGGCCCCGGCCGCTCCGGGCGACTGTGCTG	CAGCACAGTCGCCCGGAGCGGCCGGGGCCG
p.P189S / *ITGB3*	4	c.565C>T	GGACAAGCCTGTGTCATCATACATGTATATCTCCCCAC	GTGGGGAGATATACATGTATGATGACACAGGCTTGTCC
p.E200K / *ITGB3*	4	c.598G>A	CCACCAGAGGCCCTCAAAAACCCCTGCTATG	CATAGCAGGGGTTTTTGAGGGCCTCTGGTGG
p.W264L / *ITGB3*	6	c.791G>T	CTGTGATGAAAAGATTTGCTGGAGGAATGATGCATCCCAC	GTGGGATGCATCATTCCTCCAGCAAATCTTTTCATCACAG
p.S317F / *ITGB3*	7	c.950C>T	CTACCATGGATTATCCCTTTTTGGGGCTGATGACTG	CAGTCATCAGCCCCAAAAAGGGATAATCCATGGTAG
p.C554R / *ITGB3*	10	c.1660T>C	TGTGACGACTTCTCCCGTGTCCGCTACAAGG	CCTTGTAGCGGACACGGGAGAAGTCGTCACA
p.I665T / *ITGB3*	12	c.1994T>C	CGTTACTGCCGTGACGAGACTGAGTCAGTGAAAGA	TCTTTCACTGACTCAGTCTCGTCACGGCAGTAACG
p.D396N / *ITGA2B*	12	c.1186G>A	CACCCCTGGGCAACCTCGACCGG	CCGGTCGAGGTTGCCCAGGGGTG
p.I596T / *ITGA2B*	18	c.1787T>C	ACAAGCTGAGCCCCACTGTGCTCAGCCTC	GAGGCTGAGCACAGTGGGGCTCAGCTTGT
p.N670K / *ITGA2B*	20	c.2010C>A	GCAGATGGACGCAGCCAAAGAGGGCGAGG	CCTCGCCCTCTTTGGCTGCGTCCATCTGC
p.L492P / *ITGA2B*	15	c.1475T>C	GCCTCTGTCCAGCTACCGGTGCAAGATTCACTG	CAGTGAATCTTGCACCGGTAGCTGGACAGAGGC
p.E698D / *ITGA2B*	20	c.2094G>T	GGCCCTAAGCAATGTCGATGGCTTTGAGAGAC	GTCTCTCAAAGCCATCGACATTGCTTAGGGCC

Table 2.4 Oligonucleotide primers used to sequence the cDNA sequence of *ITGA2B* and *ITGB3*

Sequencing	Direction	Primer
T7F	Forward	TAATACGACTCACTATAGGG
BGH	Reverse	TAGAAGGCACAGTCGAGG
ITGB3-1	Forward	GGCAAGTACTGCGAGTGTGA
ITGB3-2	Forward	GATGCCATCATGCAGGCTAC
ITGB3-3	Reverse	CTGCAGACGGGCTGACCCTC
ITGA2B-1	Forward	CGTAGGTAGCTGCTTTTTGG
ITGA2B-2	Forward	TGACTGGCACACAGCTCTAT
ITGA2B-3	Forward	AATGTGTCCCTACCGCCCAC
ITGA2B-4	Reverse	CACCTCAGCATCCACCTTCC
ITGA2B-5	Reverse	AGCCTACACTATTCTAGCAG

2.2.2 Laboratory methods

2.2.2.1 Agarose gel electrophoresis of DNA

Agarose gel electrophoresis is used to separate DNA fragments on the basis of size and charge by applying an electric current across an agarose gel. DNA is negatively charged and therefore moves from a negative towards a positive electrode. The smaller DNA fragments migrate faster than larger fragments allowing their separation based on size. The percentage of agarose used in the gel is determined by the size of fragments being analysed and ranges from 0.7% to 2%. DNA fragments of 5kb or greater were electrophoresed in 0.7% gels while fragments of 1kb or less were analysed in 2% gels.

An appropriate quantity of Multi-Purpose agarose (Bioline Ltd, London, UK) was dissolved by heating in 50 ml of 0.5x Tris-borate EDTA (TBE) buffer (89 mM Tris, 89 mM boric acid, 2 mM EDTA, pH 8.3) in a conical flask. The agarose solution was allowed to cool slightly before adding ethidium bromide (EtBr) to a final concentration of 0.2 µg/ml.

The gel solution was poured into a perspex electrophoresis tray (Bio-Rad laboratories, Hercules, USA), with a well former positioned at one end, and the gel was allowed to solidify at room temperature.

Once solidified, the gel was transferred to an electrophoresis tank and submerged in 0.5 x TBE. The well former was removed and the samples were loaded into the wells after adding 2 µl of loading dye (Bioline Ltd, London, UK) to 2-5 µl of each DNA sample. DNA markers, hyperladders I and IV (Bioline Ltd, London, UK) were used to estimate DNA fragment sizes and 5 µl of the marker was loaded per well. Samples were electrophoresed at 100V for 45 minutes or until the dye had migrated 70-80% of the length of the gel. Images were captured using a Bio-Rad Gel Doc 2000 ultra violet (UV) transilluminator and Quantity One imaging software from Bio-Rad laboratories (Hercules, USA).

2.2.2.2 Extraction and purification of DNA from agarose gel

Following DNA separation by agarose gel electrophoresis (see section 2.2.2.1), a slab of agarose containing the DNA fragment of interest was excised from the gel using a clean, sharp scalpel, and transferred to a 1.5 ml tube and weighed. DNA was extracted from the gel using the QIAquick gel extraction kit (Qiagen, Venlo, Netherlands). Three volumes of QG buffer was added to 1 volume of gel (i.e. 300 µl QG for every 100 mg gel). The mixture was incubated at 50°C for 10 minutes, vortexing for 10 seconds every 2 minutes. When the gel was completely dissolved, 1 volume of isopropanol was added and the mixture transferred to a spin column and centrifuged at 13,000 x g for 1 minute allowing DNA to bind to the column membrane. The flow-through was discarded, and the spin columns washed by adding 750 µl of buffer PE and centrifuging for 1 minute at 13,000 x g. The flow-through was discarded and residual PE buffer removed by an additional centrifugation step at 13,000 x g for 1 minute. DNA was collected by adding 50 µl of buffer EB and centrifuging the column at 13,000 x g for one minute. The concentration of DNA was measured using a Nano Drop 1000 Microfluid Spectrophotometer as described in section 2.2.2.3.

2.2.2.3 Nucleic acid quantification

Nucleic acid concentration and purity were determined using a Nano Drop 1000 Microfluid Spectrophotometer (Thermo Fisher Scientific, Massachusetts, USA). Nucleic acid concentrations were based on absorbance at a wavelength of 260nm, while nucleic acid purity was assessed using ratios of sample absorbance at 260nm, 280nm and 230nm. To assess the degree of protein contamination, the 260/280nm absorbance ratio was used, with the expected ratios for pure DNA and RNA being ~1.8

and ~2, respectively. The presence of contaminating organic compounds such as phenol was assessed using the 260/230nm absorbance ratio, which ranges from 2.0 to 2.2 for pure nucleic acid.

2.2.2.4 Total RNA extraction

Total RNA was isolated from CHO cells using the EZ-RNA II kit. CHO cells were cultured in a 6-well plate and transfected as described in section 2.2.2.13. Forty-eight hours following transfection, cells were washed twice in Dulbecco's phosphate buffered saline (DPBS) (Life Technologies Ltd, California, USA) before lysis of the cells in 0.5 ml denaturing solution. The cell lysates were homogenized by passing the lysate several times through a pipette tip before incubation at room temperature for a further 5 minutes. A 0.4 ml aliquot of water-saturated phenol was then added to each homogenate and the sample shaken vigorously for 15 seconds. The mixtures were allowed to stand at room temperature for 10 minutes before being centrifuged at 12,000 x g for 15 minutes at 4°C to separate into two phases, red and colourless.

The aqueous colourless phase containing the RNA was transferred into a new 1.5 ml Eppendorf tube and RNA precipitated by adding 0.5 ml isopropanol per 0.5 ml denaturing solution. Samples were stored at room temperature for 10 minutes. To increase yield, samples were also stored at -20°C overnight. Samples were then centrifuged at 12,000 x g for 8 minutes at 4°C, the supernatants were removed and the RNA pellets were washed with 1 ml 75% ethanol. The samples were then centrifuged at 7,500 x g for 5 minutes at 4°C. The ethanol wash was removed and the RNA pellets were allowed to dry for 5 minutes. The RNA pellets were then dissolved in 50 µl of Diethylpyrocarbonate (DEPC)-treated water (Thermo Fisher Scientific, Massachusetts, USA). The concentration of RNA was measured using a Nano Drop as described in section 2.2.2.3.

2.2.2.5 Removal of DNA from RNA sample

In order to investigate the RNA expression in transfected CHO cells, the total RNA sample should be free of any contaminating DNA, in particular cDNA derived from the plasmid. Thus, genomic and plasmid DNA were removed after RNA isolation, which was achieved using the gDNA Wipeout buffer (Qiagen, Venlo, Netherlands). One µg of isolated RNA was incubated with gDNA Wipeout Buffer in RNase-free water in a final volume of 14 µl for 5 minutes at 42°C before being immediately placed on ice, and then stored at -20°C until further use.

2.2.2.6 Reverse transcription

RNA was transcribed to cDNA using the QuantiTect Reverse Transcription Kit (Qiagen, Venlo, Netherlands). Following removal of DNA, the purified RNA (14 µl) was mixed with 4 µl of Quantiscript reverse transcriptase (RT) Buffer (5x), and 1 µl of RT Primer Mix. The sample was mixed and 1 µl Quantiscript reverse transcriptase added. The reaction was incubated for 15 minutes at 42°C followed by 3 minutes at 95°C to inactivate the reverse transcriptase. The reaction was placed on ice and then stored at -20°C.

2.2.2.7 DNA transformation into competent E.coli

Competent *E.coli* cells were obtained from Promega (Fitchburg, USA) and stored at -80°C before use. An aliquot (45 µl) of *E.coli* cells was thawed on ice before mixing with 1 ng plasmid DNA. The sample was incubated on ice for 30 minutes. The cells were then subjected to a heat-pulse at 42°C for 60 seconds, before being incubated on ice for a further 2 minutes. A 0.5 ml aliquot of preheated (42°C) LB broth (22 g/L) was added, and the samples incubated at 37°C, with rotation at 200 rpm, for 30 minutes before being plated on LB agar (11.1g/300ml) plates containing 100 µg/ml ampicillin. Agar plates were incubated overnight at 37°C to allow growth of colonies.

2.2.2.8 Plasmid DNA purification using the QIAprep Spin Miniprep kit

Plasmid DNA was purified using the QIAprep Spin Miniprep kit following the manufacturer's instructions. Briefly, 5 ml of Luria-Bertani (LB) broth containing 100 µg/ml ampicillin was inoculated with a single colony and incubated at 37°C, with rotation at 200 rpm for 16-18 hours. Following incubation, the bacterial cells were harvested by centrifugation for 5 minutes at 6000 x g in a bench-top microcentrifuge. The bacterial pellets were resuspended in 250 µl of buffer P1. Bacteria were lysed by adding 250 µl of buffer P2 and gently mixing by inversion. The samples were incubated for 5 minutes at room temperature before 350 µl of buffer N3 was added. After mixing by inverting the tubes 4–6 times until the solution became cloudy, the samples were centrifuged for 10 minutes at 17,900 x g. The supernatants were applied to QIAprep spin columns, which were then centrifuged for one minute at 17,900 x g. The flow-through was discarded, and the spin columns were washed twice by adding 750 µl of buffer PE and centrifuging for one minute at 17,900 x g. The flow-through was discarded, and the residual PE buffer was removed by an additional centrifugation step at 17,900 x g for one minute. Finally, the plasmid DNA was collected by adding 50 µl of distilled water and centrifuging the column at 17,900 x g for one minute. The concentration of each plasmid was then determined using a Nano Drop 1000 Microfluid Spectrophotometer, section 2.2.2.3.

2.2.2.9 Plasmid DNA purification using the Qiagen plasmid Maxi kit

Plasmid DNA was purified using the Qiagen maxi kit (Qiagen, Venlo, Netherlands), according to the manufacturer's instructions. Briefly, 250 ml LB broth containing 100 µg/ml ampicillin was inoculated with a sample from a glycerol stock of a bacterial colony bearing the desired plasmid and incubated for 16-18 hours at 37°C, 200 rpm. The bacterial cells were harvested by centrifugation at 6000 x g for 15 minutes at 4°C before resuspending the bacterial pellet in 10 ml of buffer P1. The cells were then lysed by adding 10 ml of buffer P2 and mixing by inverting the sample 4-6 times. Following incubation for 5 minutes at room temperature, 10 ml of chilled N3 was added and the samples again mixed by inversion. Samples were incubated on ice for 20 minutes to enhance the precipitation of cellular debris and then centrifuged at 20,000 x g for 30 minutes. The supernatant was removed and applied to a Qiagen tip-500 column, allowing it to move through by gravity. The column was washed with 30 ml wash buffer, and the DNA then eluted using 15 ml of elution buffer. DNA was precipitated by adding 10.5 ml of isopropanol to the eluate, and centrifuging the sample at 20,000 x g for 30 minutes. The DNA pellet was washed using 5 ml of 70% ethanol and the sample centrifuged again at 20,000 x g for 15 minutes. The supernatant was removed, and the DNA pellet allowed to dry before being resuspended in an appropriate volume (300-500 µl) of distilled water. The concentration of each plasmid was determined using a Nano Drop 1000 Microfluid Spectrophotometer (Section 2.2.2.3) prior to storage of the samples at -20^{0}C until required.

2.2.2.10 Plasmid DNA sequencing

When sequencing was required, the template DNA and primer were sent to sequencing facility as 50 ng/µl and 1 pmol/µl, respectively. The sequencing was performed in Applied Biosystems 3730 DNA Analyzer (Applied Biosystems, Massachusetts, USA) in the Core Genomics Facility, University of Sheffield. The results were analysed using the Staden Package (http://staden.sourceforge.net) and FinchTV v1.4 software (Geospiza inc., Seattle, USA).

2.2.2.11 Site-directed mutagenesis and transformation of E.coli

Desired nucleotide substitutions were introduced into wild-type pcDNA3.1 (-) neo-*ITGB3* and pcDNA3.1 (-) neo-*ITGA2B* using the Quikchange lightning site-directed mutagenesis kit (Agilent Technologies, California, USA) according to the manufacturer's instructions (Figure 2.1). Briefly, the PCR was carried out in a volume of 50 µl containing 5 µl of reaction buffer (10x), 100 ng of dsDNA template, 125 ng of each oligonucleotide primer, 1 µl of dNTP mix, 1.5 µl of Quiksolution reagent and 1 µl of Quikchange Lightning Enzyme (*Pfu*-based DNA polymerase). Using an Applied

Biosystems® (Massachusetts, USA) thermal cycler the reaction was subjected to an initial denaturation step at 95°C for 2 minutes, followed by 18 cycles of denaturation at 95°C for 20 seconds, annealing at 60°C for 10 seconds and extension at 68°C for 4 minutes, and a final extension step at 68°C for 5 minutes. The amplification products were then treated with 2 µl of *Dpn*I for 5 minutes at 37°C to digest the parental DNA template.

Ultracompetent XL10-Gold cells (45 µl) were then transformed with 2 µl of *Dpn*I-treated DNA. The DNA was introduced into the competent cells with gentle mixing, before incubating the sample on ice for 30 minutes. The cells were then subjected to a heat-pulse at 42°C for 30 seconds, before being incubated on ice for a further 2 minutes. Following the addition of 0.5 ml preheated (42°C) NZY+ broth (22 g/L), the samples were incubated at 37°C, with rotation at 200 rpm for 1 hour and then plated onto LB agar (11.1g/300ml) plates containing 100 µg/ml ampicillin. Agar plates were incubated overnight at 37°C to allow the growth of colonies. Plasmid DNA was purified from transformed cells (Section 2.2.2.8) and screened for the presence of the desired nucleotide substitutions by sequence analysis. Sequencing was undertaken using the plasmid DNA sequencing primers (Table 2.4) as described in section 2.2.2.10.

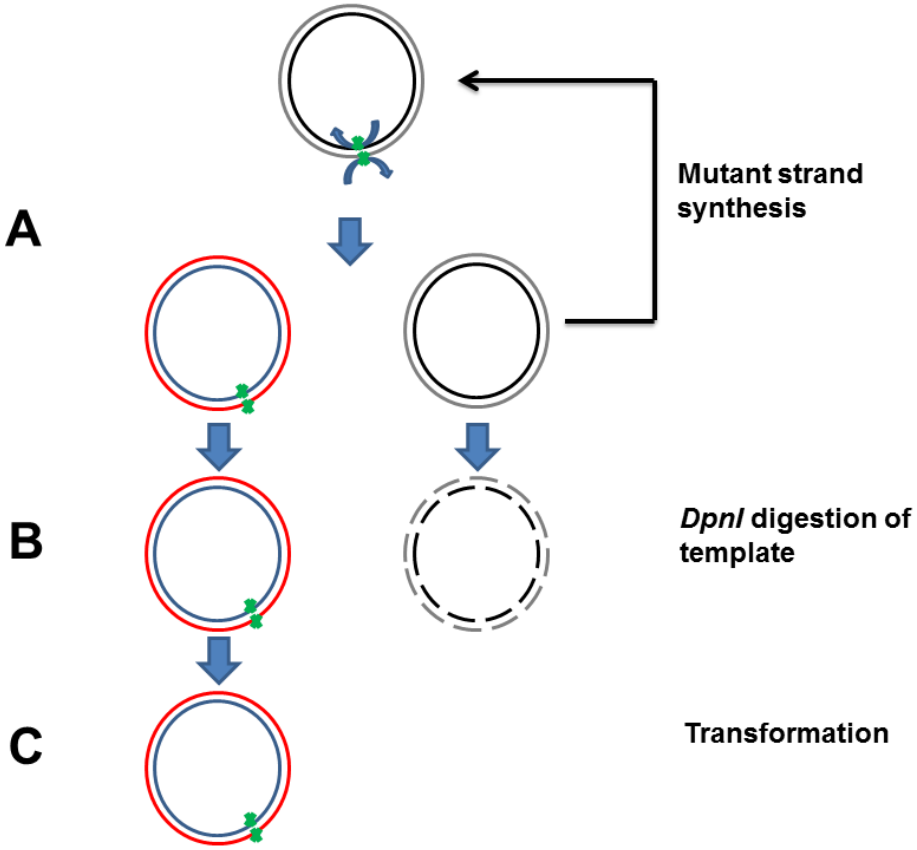

Figure 2.1 Overview of the quickchange site-directed mutagenesis approach. Site-directed mutagenesis is used to introduce single nucleotide changes in plasmids of interest. **A**) The plasmid is denatured before annealing a pair of complementary primers containing the desired nucleotide to the separate strands. The primers are then extended and the mutated nucleotide incorporated into the DNA using *Pfu*-based polymerase, resulting in nicked circular strands containing the desired change. **B**) The product is then subjected to treatment with *DpnI* enzyme whichtargets the methylated parental plasmid (non-mutated). **C**) Plasmids were then transformed into ultracompetent XL10-Gold cells for nick repair and plasmid replication.

2.2.2.12 Mammalian cell culture

The human erythroleukaemia (HEL) and Chinese hamster ovary (CHO) cell lines were used in this study. Human erythroleukaemia cells were derived from erythroblasts in the bone marrow of an erythroleukaemia patient and have lymphoblast like morphology. The cells grow in suspension and were used as a positive control for surface and intracellular detection of the $\alpha_{IIb}\beta_3$ receptor. CHO cells are originally derived from the ovary of an adult female Chinese hamster and have epithelial like morphology. They grow as an adherent monolayer and since their introduction in 1957 have become widely used due to their high yields of heterologous protein production and rapid growth (Tjio JH and Puck 1958). In this project, the CHO cell line, which does not express $\alpha_{IIb}\beta_3$, was used to examine expression of the $\alpha_{IIb}\beta_3$ receptor following transient transfection with plasmids bearing *ITGA2B* and *ITGB3* cDNAs. The cells were thawed at 37°C and then seeded in full RPMI 1640- GlutaMAX™ medium supplemented with 10% Fetal Calf Serum (FCS) and maintained in an incubator at 37°C in the presence of 5% CO_2.

2.2.2.12.1 Passaging cells

All manipulations of mammalian cell lines were carried out in a class II tissue culture laminar flow cabinet using aseptic techniques. Adherent CHO cells were grown to subconfluence (70-90% confluence) in a 75 cm^2 flask and passaged as follows: RPMI media 1640-GlutaMAX™ (Life Technologies Ltd, California USA), Dulbecco's phosphate buffered saline (DPBS) and Trypsin-EDTA solutions (0.25% trypsin and 0.02% EDTA) (Sigma-Aldrich, Missouri, USA), were prewarmed to 37°C. The medium was removed from the cells before washing with 8 ml of DPBS. Following aspiration of the DPBS, the cells were detached by incubation with 2 ml Trypsin-EDTA for 5 minutes at 37°C. The trypsin was neutralized by the addition of 8 ml RPMI containing 10% FCS and the cells then collected by centrifugation at 500 x g for 5 minutes. Following removal of the supernatant by aspiration, the cells were resuspended in 8 ml medium, and 1 ml of this suspension was transferred to a new 75 cm^2 flask containing 14 ml of fresh medium. Subconfluent HEL cells, which grow in suspension, were passaged as follows: RPMI media 1640-GlutaMAX™ was prewarmed. The cells were collected by centrifugation at 500 x g for 5 minutes before resuspension in 8 ml medium. One ml of the suspension was then transferred to a new 75 cm^2 flask containing 14 ml of medium which was then placed in the incubator.

2.2.2.12.2 Freezing and thawing of cells

Mammalian cell lines were stored long-term in liquid nitrogen after resuspension of the cells in 90% FCS and 10% dimethyl sulfoxide (DMSO) (Sigma-Aldrich, Missouri, USA). In brief, the medium was removed from the flask containing a monolayer of cells and the cells washed with DPBS before being harvested as described in section 2.2.2.12.1. Prior to centrifugation, cells were counted using a haemocytometer and following collection, the cell pellet was resuspended in freezing medium at a density of $1x10^6$ cells/ml before aliquoting into cryopreservation vials and placing in a Mr Frosty™ freezing container (Thermo Fisher Scientific, Massachusetts, USA) at -80ºC for 24 hours. Vials were then transferred to liquid nitrogen.

Cells which were frozen in liquid nitrogen were thawed by incubation at 37°C for 1-2 minutes before transfer to 5 ml RPMI containing 10% FCS in a sterile falcon tube. Cells were centrifuged at 500 x g for 5 minutes and resuspended in 5 ml of medium. The cell suspension was then transferred to a new 75 cm^2 flask containing 10 ml of medium and maintained at 37°C in a 5% CO_2 incubator.

2.2.2.12.3 Cell counting

To count cells manually, they were first suspended in an appropriate volume of medium (1ml). Twenty µl of the cell suspension was then added to the chambers of a haemocytometer. As a result of capillary action, the cell suspension flows into the narrow area between the coverslip and chamber. The cells present in 4 large squares of the chamber slide were then counted microscopically using a 10x objective on an inverted phase contrast microscope (Zeiss, Jena, Germany) as demonstrated in figure 2.2 and the total number of cells determined using the following equation:

$$\text{Number of cell (cells/µl)} = \frac{\text{Number of cells in large squares}}{\text{Number of squares}} \text{ X Dilution factor X } 10$$

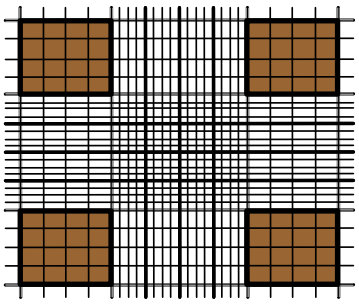

Figure 2.2 Haemocytometer grid as seen under a microscope. Cells lying in the 4 corner squares (highlighted in brown) are counted.

2.2.2.13 Co-transfection of CHO cells with ITGA2B (α_{IIb}) and ITGB3 (β_3) cDNAs

CHO cells were co-transfected with pcDNA derivatives bearing mutated *ITGA2B*, or *ITGB3* cDNAs, in the presence of wild-type cDNA for either *ITGB3* or *ITGA2B* respectively. For each transfection, 1 µg of the α_{IIb} expression plasmid and 1 µg of the β_3 expression plasmid were diluted in 500 µl of serum-free RPMI medium. Five µl Lipofectamine LTX (Invitrogen, California, USA) was added to the diluted DNA, and the solution incubated at room temperature for 25 minutes to allow the formation of Lipofectamine-DNA complexes. In the meantime, CHO cells were harvested as described in section 2.2.2.12.1 and counted using a haemocytometer. The lipofectamine-DNA complexes (500 µl) were added to the wells of a 6-well plate before adding 1.5 ml of full RPMI medium containing 2.5 x 10^5 cells into each of the wells. Cells were incubated at 37°C in the presence of 5% CO_2 for 48 hours before further analysis.

2.2.2.14 Flow cytometry

Flow cytometry is a laser based technology that is used to measure multiple parameters that describe the chemical and physical properties of small particles such as cells. It allows rapid analysis of large cell populations. In order to detect the protein of interest on a cell surface, cells must be labelled with fluorescent dyes (fluorochrome) before being injected into the flow cytometer. When hit by a light source, the dye absorbs the light, which results in a change in energy state from a low stable state to a high unstable state, known as the excitation state. The molecule then emits energy returning to a low energy stable state, while the emitted light is collected by specific fluorescence channels in the flow cytometer.

Following injection into the flow cytometer, a stream of single cells pass through a number of light beams resulting in light scattering and fluorescent emission. Forward scatter (FSC) provides details about cell size while light in side scatter (SSC) indicates cell granularity. Light emitted by different fluorochromes is detected at the corresponding emission wavelengths (Table 2.5). The detectors convert this light into voltage that is amplified by a series of linear or logarithmic amplifiers before being converted to electronic signals, which are then graphically plotted on histograms or dot plots. Flow cytometry was used in this study to assess the surface expression of $\alpha_{IIb}\beta_3$, total expression of β_3 and the ability of $\alpha_{IIb}\beta_3$ to bind to PAC-1 and fibrinogen, as described in the following sections.

Table 2.5 Maximum excitation and emission wavelengths of FITC, Alexa fluor®488 and PE fluorochromes

Fluorochrome	Maximal Excitation (nm)	Maximal Emission (nm)	Band pass Filter
Fluorescein isothiocyanate (FITC)	490	525	530/30
Alexa Fluor® 488	495	519	530/30
R-phycoerythrin (PE)	490,565	578	575/26

2.2.2.15 Assessment of cell surface expression of the $\alpha_{IIb}\beta_3$ receptor complex by flow cytometry

The expression of cell surface $\alpha_{IIb}\beta_3$ was assessed by flow cytometry using monoclonal antibodies targeting the α_{IIb} and β_3 subunits. Forty-eight hours post transfection, the culture medium was removed from the 6-well plates by aspiration and the cells were washed using 700 µl of prewarmed DPBS before adding 200 µl of trypsin-EDTA (0.25% trypsin and 0.02% EDTA) to detach the cells. The plate was incubated for 5 minutes at 37°C and then 800 µl of RPMI containing 10% FCS was added to each well to neutralize the trypsin. The cells were transferred to a fluorescence-activated cell sorting (FACs) tube and collected by centrifugation at 500 x g for 5 minutes. The

supernatant was removed, and the cells washed twice with 300 µl of FACs buffer (2% FBS in DPBS). Monoclonal antibodies were diluted 1:16 in a final volume of 40 µl for each test sample using FACs buffer as the diluent. Antibodies used included mouse anti-human CD61 conjugated to R-phycoerythrin (PE) and mouse anti-human CD41 conjugated to fluorescein isothiocyanate (FITC). In addition, two isotypes were used as negative controls to allow correction for nonspecific binding of the primary antibodies, and these were PE-mouse IgG1 isotype control and FITC-mouse IgG1 isotype control. The cells were stained by adding 40 µl (1:16) of the appropriate antibody and incubating the sample on ice, in the dark for 30 minutes. The cells were then collected by centrifugation and washed twice with 300 µl FACs buffer to remove any unbound antibody. Finally, the cells were resuspended in 250 µl of FACs buffer and analysed using the FACsCalibur (BD Bioscience, California, USA) located in the Flow Cytometry Core Facility, Medical School. HEL cells were used as a positive control for the detection of $\alpha_{IIb}\beta_3$ receptor and were stained alongside CHO cells following the same protocol.

2.2.2.16 Assessment of total expression of the $\alpha_{IIb}\beta_3$ receptor complex by flow cytometry

Forty-eight hours post transfection, cells were harvested and resuspended in 300 µl of FACs buffer as previously described (see section 2.2.2.12.1). They were then fixed by incubation in 50 µl of Fixation/Permeabilization solution (BD Bioscience, California, USA) for 20 minutes on ice. The cells were collected by adding 500 µl of DPBS and centrifugation at 500 x g for 5 minutes and then permeabilised by treatment with 0.1% (v/v) Triton X-100 in FACs buffer for 5 minutes at room temperature. The cells were recovered by centrifugation for 5 minutes at 500 x g. They were then washed twice in Perm/Fix buffer before being stained using the protocol described in section 2.2.2.15, substituting Perm/Fix buffer for FACs buffer as the antibody diluent. The stained cells were washed twice with 250 µl FACs buffer before being resuspended in 250 µl FACs buffer and analysed using the FACsCalibur. HEL cells were used as a positive control and were treated in the same way as the CHO cells in terms of fixation, permeabilization and staining.

2.2.2.17 Assessment of $\alpha_{IIb}\beta_3$ activation by flow cytometry

Assessment of $\alpha_{IIb}\beta_3$ activation was carried out using either PAC-1 antibody which is specific for the activated conformation of $\alpha_{IIb}\beta_3$, or fluorescently labelled fibrinogen. Forty-eight hours post-transfection, cells were harvested as previously described (see section 2.2.2.12.1) and incubated in FACs buffer at room temperature for 30 minutes to allow them to recover. The cell suspension was diluted by adding 250 µl of DPBS and

the cells were then collected by centrifugation at 500 x g for 5 minutes. To induce $\alpha_{IIb}\beta_3$ activation, cells were treated with 20mM Dithiothreitol (DTT), for 5 minutes at 37°C and then washed twice in DPBS. For the PAC-1 binding assay, cells were stained by adding 40 µl of FITC-labelled PAC-1 antibody, diluted1:2 in DPBS and incubating the sample at room temperature, in the dark for 30 minutes. For the fibrinogen binding assay, cells were stained by adding 50 µl containing 120µg/ml Alexa Fluor® 488-labelled fibrinogen and 1mM $CaCl_2$ in DPBS. Cells were incubated at room temperature, in the dark for 30 minutes. The cells were then collected by centrifugation and washed twice with 300 µl FACs buffer to remove any unbound antibody or fibrinogen before being resuspended in 250 µl of FACs buffer and analysed using the FACsCalibur.

2.2.2.18 Sodium dodecyl sulphate polyacrylamide gel electrophoresis (SDS-PAGE) and Western blotting

2.2.2.18.1 Protein extraction

SDS-PAGE and western blot analysis of CHO cell lysates was carried out to examine the expression of α_{IIb} and β_3 subunits following transfection. CHO cells were transfected as previously described (Section 2.2.2.13). Forty-eight hours post-transfection, cells were washed with DPBS and then lysed by the addition of 100 µl RIPA Lysis buffer (Thermo Fisher Scientific, Massachusetts, USA) containing 1% protease inhibitor cocktail (Sigma-Aldrich, Missouri, USA). Cell lysates were incubated on ice for 10 minutes and then centrifuged at 13,000 x g for 10 minutes at 4°C. Supernatants were transferred to fresh sample tubes and stored at -80°C until further analysis.

2.2.2.18.2 Total Protein concentration using Bradford Assay

Sample protein concentrations were determined prior to electrophoresis using the Bradford assay. This is a colorimetric assay that takes advantage of the ability of proteins to bind to Coomassie brilliant blue. The concentration of the test protein sample was estimated by comparison with a series of standard solutions containing known concentrations of bovine serum albumin (BSA) (Sigma Aldrich, Missouri, USA). Thus, eight BSA samples were used to create a standard curve with concentrations ranging from 0 µg/ml to 30 µg/ml. The protein samples were incubated with 100 µl Bradford reagent (Sigma Aldrich, Missouri, USA) for 5 minutes in a total volume of 500 µl. Absorbance was measured at a wavelength of 590nm using the Eppendorf

biophotometer spectrophotometer (Eppendorf, Hamburg, Germany). The standard curve was then used to derive protein concentrations.

2.2.2.18.3 Sample preparation

Samples of the cell lysates, containing 25 µg protein, were mixed with 4x loading buffer (50% glycerol, 500mM Tris-HCl (pH 6.8), 100 mg/ml SDS, 25 mg/ml bromophenol blue, 20% of DTT) to make 1x final dilution. Samples were denatured by boiling at 100°C for 5 minutes.

2.2.2.18.4 SDS- PAGE

Electrophoresis was carried out in 64mm x 83mm x 1.5 mm (height x width x depth) SDS-polyacrylamide gels. The stacking gel comprised 6% acrylamide gel while the resolving gel comprised 10% polyacrylamide gels. They were mixed with 50% resolving buffer (0.749 M Tris, pH 8.8, 7 mM SDS) or stacking buffer (250 mM Tris, pH 6.8, 7 mM SDS), 0.1% (w/v) Ammonium persulfate (APS) and 0.2% (v/v) Tetramethylethylenediamine (TEMED). The acrylamide solutions for the resolving and stacking gels were poured separately into the gel cassette, and allowed to polymerise. The gel cassette was then placed into a Mini-protean®3 electrophoresis (Bio-Rad laboratories, Hercules, USA) tank and submerged in reservoir buffer (125 mM Tris, 0.947 M glycine and 17.3 mM SDS). Ten µl of protein ladder (including 11 proteins ranging in size from 8 to 260 kDa) and 25 µg samples were loaded into the wells of the gel and samples separated by electrophoresis at 180 V for an hour.

2.2.2.18.5 Electrophoretic transfer

Following SDS-PAGE, proteins were transferred to a nitrocellulose membrane. Care was taken to avoid the formation of air bubbles between the membrane and the gel during assembly of the blotting cassette, which was then placed into a transfer tank and submerged in transfer buffer (1.5 M Glycine and 250 mM Tris and 10% (v/v) methanol). Electrophoretic transfer of proteins was carried out at 30 V overnight.

2.2.2.18.6 Detection of β_3 and α_{IIb} subunits

Following transfer, the nitrocellulose membrane was blocked with Odyssey® blocking Buffer (Li-Cor, Nebraska, USA) for one hour with agitation. The membrane was then incubated in blocking buffer containing a 1:250 dilution of either rabbit anti-human α_{IIb} antibody (H-160) or rabbit anti-human β_3 antibody and a 1:1000 dilution of mouse anti β-tubulin overnight at 4°C with agitation. The membrane was then washed twice with 0.1% (v/v) Tween20® in Tris-buffered saline (TBS) (146.2g/L NaCl, pH 7.5 and 12.1 g/L Tris) before being incubated in blocking buffer containing a 1:10,000 dilution of IRDye®680-labelled donkey anti-rabbit and IRDye®800CW-labelled donkey anti-

mouse (LI-COR, UK) secondary antibodies for an hour with agitation. The membrane was then washed twice with 0.1% Tween20-TBS and once with TBS before labelled proteins were detected using the Odyssey®Sa Infrared Imaging System (LI-COR, Nebraska, USA) using 700nm and 800nm detection channel.

2.2.2.19 Statistical analysis

The majority of numerical data show mean values with standard deviation. Data are largely presented as bar charts which were prepared and analysed using Microsoft Excel 2010 (Microsoft Software, Washington, USA) and GraphPad Prism version 5 (GraphPad Software, San Diego, CA). Comparison of mean values was performed using One-way ANOVA (Dunnett's test), Two-way ANOVA or an unpaired student t test. P values of less than 0.05 were considered statistically significant.

2.2.2.20 Nomenclature and numbering of ITGA2B and ITGB3 sequences

Gene nomenclature (for example, *ITGA2B* and *ITGB3*) followed the guidelines of the Human Genome Organization (HUGO), using italicised Latin symbols for genes to distinguish them from proteins. Nucleotide positions in cDNA sequences were numbered according to the reference *ITGA2B* and *ITGB3* sequences, NM_000419 and NM_000212, respectively, following the recommendations of the Human Genome Variation Society (first "A" of the translation initiation codon ATG denoted as c.1). Nucleotide substitutions were described using a ">" character (indicating "changes to") between the original and substituted nucleotide. Amino acids were numbered according to the reference sequences NP_000410 (α_{IIb}) and NP_000203 (β_3) with the first amino acid corresponding to the methionine encoded by the translation initiation codon. Amino acids were mainly referred to using the three letter code, with the exception of figures where the one letter code was utilised. Substitutions are described following the recommendations of the Human Genome Variation Society, using "p." followed by the reference amino acid symbol the codon number and the substituted amino acid.

Chapter 3: *In silico* predictions of the effects of non-synonymous *ITGB3* and *ITGA2B* alterations identified in patients with Glanzmann thrombasthenia in the UK cohort

3.1 Introduction

The detailed investigation of the underlying candidate gene defects in the UK GT cohort that was previously carried out by the Haemostasis Research Group at the University of Sheffield identified 17 different candidate gene defects in *ITGA2B* in 21 unrelated index cases and 14 candidate *ITGB3* defects in a further 13 unrelated index cases. Twenty-three of these defects were previously unreported and of these, 10 were non-synonymous alterations. This study will focus on the characterisation of a subset of non-synonymous candidate gene defects in order to investigate their possible pathogenic mechanisms, and to further our understanding of the molecular basis of GT. The novel candidate defects which were investigated predicted the following amino acid substitutions in the β3 subunit: p.Trp11Arg, p.Pro189Ser, p.Glu200Lys, p.Trp264Leu, p.Ser317Phe, p.Cys554Arg and p.Ile665Thr and the following substitutions in α_{IIb}: p.Leu492Pro, p.Asn670lys and p.Glu698Asp. In addition, four non-synonymous candidate gene defects described previously, but which have not been characterised to any extent, were studied. These defects predicted p.Arg119Gln and p.Cys547Trp substitutions in β_3 and p.Asp396Asn and p.Ile596Thr substitutions in α_{IIb} (D'Andrea*, et al* 2002, Kannan*, et al* 2009, Peretz*, et al* 2006, Ruan*, et al* 1998, Vijapurkar*, et al* 2009). This chapter describes the results of work in which *in silico* approaches were used to predict the possible pathogenic effects of each candidate defect on the expression, structure and function of the $\alpha_{IIb}\beta_3$ receptor. The results of these *in silico* investigations allowed hypotheses to be generated which formed the basis for the studies described in Chapters 4 and 5.

A range of bioinformatic tools, designed to facilitate the interpretation of biological data, were used to predict the effects of candidate gene defects within *ITAG2B* and *ITGB3* on the $\alpha_{IIb}\beta_3$ receptor structure and function. These tools help to further our understanding of the underlying molecular mechanisms by which candidate gene defects mediate their pathogenicity. The tools used allowed an assessment of the amino acid sequence conservation at sites of non-synonymous substitutions, and prediction of their potential effects at both the transcriptional (on RNA splicing) and protein (structure and function) levels. The effects of the non-synonymous p.Trp11Arg substitution on signal peptide cleavage were also predicted.

The degree of protein conservation across human and other species allows inferences to be made regarding the importance of specific amino acids to protein structure and function. Highly conserved amino acids are usually associated with the structure or essential functions of a protein. Therefore, non-synonymous substitutions of highly

conserved amino acids are more likely to be pathogenic than those involving less conserved residues. In addition, the degree of conservation of specific amino acid residues across species allows the prediction of those amino acids that may be tolerated in place of the original one without having deleterious effects on the protein. The degree of conservation is investigated through multiple alignments of paralogous and orthologous proteins and the presence of the same amino acid at a specific position in a protein across different species or among closely related proteins indicates a high level of conservation (Briscoe*, et al* 2004, Miller and Kumar 2001, Mooney and Klein 2002).

There are several *in silico* tools available online that predict the effects of non-synonymous substitutions on protein structure and function. These can be divided into three main categories based on the methods that are used for prediction. First are sequence and evolutionary conservation-based methods, which are used by the Sorting Intolerant From Tolerant (SIFT) and Align Grantham Variation Grantham Deviation (GVGD) tools and make predictions by assessing the degree of sequence conservation in multiple sequence alignments of protein homologues (Ng and Henikoff 2001, Tavtigian*, et al* 2008). Second protein sequence and structure methods, such as those used by Polymorphism phenotyping v2 (Polyphen-v2), make predictions based on the properties such as charge, hydrophobicity and size of the wild-type and substituted amino acid residue (Sunyaev*, et al* 2001). Finally, supervised-learning methods, as exemplified by SNPs&GO and MutationTaster, utilise two different data sets, one for variants that have been associated with disease and another for variants with no disease associations, and make predictions based on similarities to those with known associations (Calabrese*, et al* 2009, Schwarz*, et al* 2014). It has been shown that the use of several *in silico* tools for the prediction of the effects of non-synonymous substitutions can increase the prediction accuracy and help to draw reliable inferences about the effects of each substitution (Tavtigian*, et al* 2008, Thusberg and Vihinen 2009).

While single nucleotide substitutions in the exonic regions of *ITGA2B* and *ITGB3* can lead to amino acid substitutions in the integrin subunits, it is also possible for single nucleotide substitutions to cause defects in the splicing of the *ITGA2B* and *ITGB3* RNAs. In brief, RNA splicing is the process involved in removing intervening sequences, known as introns, from gene transcripts and joining together exons to form the mRNA transcript encoding the protein of interest (Reed 2000). This complex process is facilitated by the spliceosome, a large complex comprised of five small nuclear RNA molecules and over 100 proteins (Rappsilber*, et al* 2002, Zhou*, et al*

2002). The process involves two chemical steps. First, following assembly of the spliceosome in the region of the intron targeted for splicing, cleavage of the RNA occurs at the 5' end of the intron (splice donor site) and the intron then loops back on itself to form a lariat structure by ligating to the 2′ hydroxyl group of an adenosine at the branch point of the intron which is located approximately 20-30 nucleotides from the 3' end of the intron. The second step involves cleavage at the 3' end of the intron (the splice acceptor site) followed by ligation of the two exons to each other, while the lariat intron dissociates from the spliceosome and is degraded (Bauren and Wieslander 1994, Kessler*, et al* 1993).

Where protein structures are available, it is sometimes possible to predict the effects of amino acid substitutions using structural modelling. Thus, protein modelling structures provide information about the location and the physical and chemical properties of both the wild-type and substituted residues. In addition, where available, the structure facilitates the identification of any differences in the structures, interactions or chemical bonds between the original and substituted amino acid side chains, allowing the consequences of specific substitutions to be predicted. An advantage of using Pymol for protein modelling is that it allows for the evaluation of amino acid contacts and the assessment of whether a substitution leads to steric clashes with adjacent residues. Steric clashes are defined as unfavourable interactions that occur when the atoms of a molecule become too close or overlap with adjacent atoms, while the contacts are defined as those interactions between amino acids in a protein such as peptide, hydrogen and ionic bonds. Importantly, the three dimensional structure of the extracellular domains of $\alpha_{IIb}\beta_3$ and $\alpha_v\beta_3$ integrins have been resolved and made available online through the protein data bank (PDB: 3FCS and 1JV2) (Xiong*, et al* 2001, Zhu*, et al* 2008).

One of the candidate *ITGB3* defects predicted a non-synonymous p.Trp11Arg substitution in the signal peptide of β_3. A signal peptide is a short amino acid sequence (11-27 amino acids) that is located at the N-terminus of an immature protein, and targets the protein towards subcellular compartments where the signal peptide is cleaved to release the mature protein. Signal peptides are typically comprised of three different regions: a positively charged amino terminal region (n-region), a hydrophobic core region (h-region) and a polar carboxyl-terminal region (c-region) (Heijne, 1990; von Heijne, 1998). The β_3 subunit has a 26 amino acid signal peptide, while the α_{IIb} signal has 31 amino acids.

3.2 Aims

The aim of the work described in this chapter was to investigate and predict the potential effects of genetic alterations identified in *ITGB3* and *ITGA2B* in patients with GT using a variety of *in silico* methods, as described in Section 2.2.1. In addition, structural modelling was undertaken to investigate the effects of candidate amino acid substitutions on the three dimensional structure of $\alpha_{IIb}\beta_3$. It was anticipated that the results of these studies would generate hypotheses about the effects of candidate gene defects on the β_3 and α_{IIb} structure, function and expression which would then be tested in the subsequent results in Chapters 4 and 5.

3.3 Results

3.3.1 Comparison of β_3 and α_{IIb} integrins across species and with other α and β family members

In this study, 14 candidate gene defects that were identified in patients with GT and predicted amino acid substitutions in either the β_3 or α_{IIb} subunits were investigated (Figure 3.1). Of the 14 candidate mutations studied, nine predicted substitutions in β_3, while the remaining five predicted substitutions in the α_{IIb} subunit (Table 1.2). Four of the substitutions in β_3, p.Pro189Ser, p.Glu200Lys, p.Trp264Leu and p.Ser317Phe, affected residues located in the ligand-binding domain, while the p.Trp11Arg and p.Arg119Gln substitutions occurred within the signal peptide and hybrid domains of β_3, respectively. Two of the candidate defects predicted p.Cys547Trp and p.Cys554Arg substitutions within the cysteine rich repeat domain while the p.Ile665Thr substitution occurred in the β tail domain of β_3. One of the α_{IIb} substitutions, p.Asp396Asn, was predicted to occur in the β propeller domain. Two others, p.Leu492Pro and p.Ile596Thr, affected residues in the thigh domain, while the p.Asn670Lys and p.Glu698Asp substitutions both affected residues in the calf-1 domain. The degree of conservation of the amino acids that were predicted to be substituted was examined by aligning the sequences of the human β_3 and α_{IIb} subunits with the corresponding sequences from 12 different vertebrate species and homologous proteins in human (Figures 3.2, 3.3, 3.4 and 3.5).

The tryptophan (W) residue at amino acid position 11 of the β_3 subunit was conserved across 7 species. In *Cavia porcellus*, *Gallus gallus* and *Danio rerio,* the tryptophan residue was replaced by proline, leucine and serine residues, respectively, while in

Camelus bactrianus and *Ovis aries,* no corresponding signal peptide sequences were found. In humans, the tryptophan residue at position 11 in the β_3 subunit was conserved in three other β integrins, β_1, β_4 and β_8, and replaced by alanine in β_2 and β_5, by phenylalanine in β_6, and by valine in β_7. The arginine (R) residue at position 119 of β_3 was conserved across all species examined apart from *Ovis aries,* where it was replaced by a tryptophan residue. Arg119 was also conserved in all other human β integrin proteins examined. The glutamate (E) residue at position 200 was not conserved across species. Furthermore, the conserved amino acid at position 200 in 8 species is lysine (K), which is the amino acid that is predicted to be substituted for glutamic acid as a result of the candidate missense mutation identified in the patient with GT. Glu200 was also not conserved in several of the β integrins examined, being replaced by an arginine residue in β_1, β_2 and β_7. In β_5, β_6 and β_8, it was replaced by threonine, alanine and histidine residues, respectively. The proline (P), tryptophan (W), serine (S), and isoleucine (I) residues at positions 189, 264 317 and 665 respectively, were conserved across all species examined, suggesting important roles for these amino acids in the β_3 subunit. Both Pro189 and Trp264 were conserved among other members of the β integrin family of proteins, while the serine residue at position 317 in β_3 was conserved in other β integrins apart from β_6 where it was replaced by a threonine residue. In contrast, the isoleucine residue at position 665 was not conserved among other β integrin family members. The cysteine (C) residues at positions 547 and 554 in human β_3 were conserved across all the species and among other human β integrins, supporting an important role for these residues in $\alpha_{IIb}\beta_3$ and other β proteins (Figure 3.2 and 3.4).

The aspartate (D) and isoleucine (I) residues at positions 396 and 596 of α_{IIb}, were conserved across all species examined and in other α integrin family members in humans, suggesting an important role for these amino acids in α_{IIb}. In contrast, the proline (P) residue at position 492 of α_{IIb} was not conserved. The asparagine (N) residue located at position 670 was conserved in 11 species, being replaced by threonine in *Cavia porcellus*, while the glutamate (E) residue position 698 was conserved in 8 species, being replaced by either lysine or arginine in *Sus scrofa, Rattus norvegicus, Gallus gallus and Cavia porcellus.* The asparagine residue at position 670 in human α_{IIb} was conserved in five other α-integrin proteins, but not in α3, α6 and α7 which have arginine, lysine and alanine residues at same position, respectively. Glu698 was not conserved in other human α-integrin family members examined except in α4 protein (Figure 3.3 and 3.5).

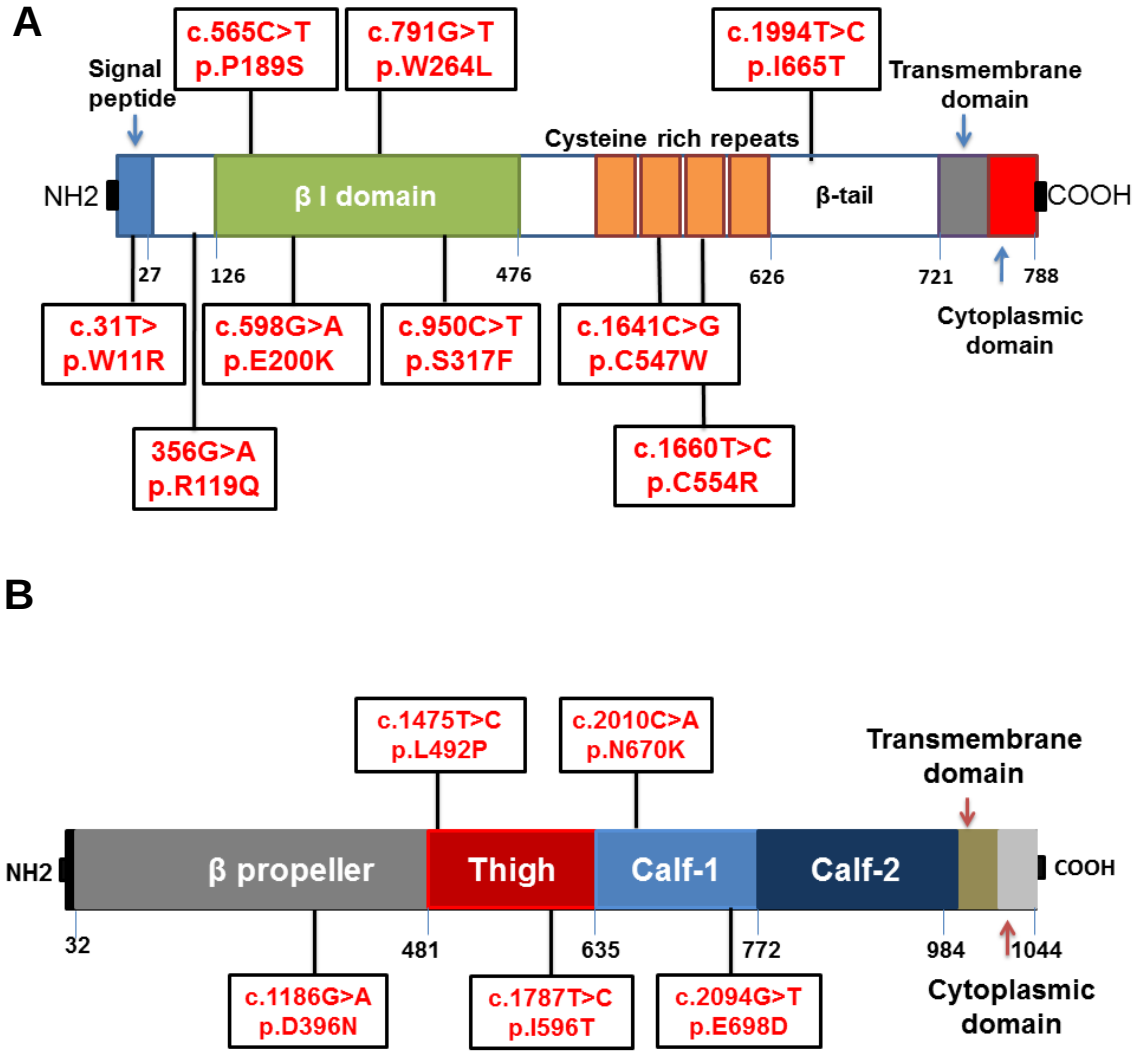

Figure 3.1 A schematic representation of β_3 (A) and α_{IIb} (B) proteins showing the location of 14 variants identified in UK patients with GT.

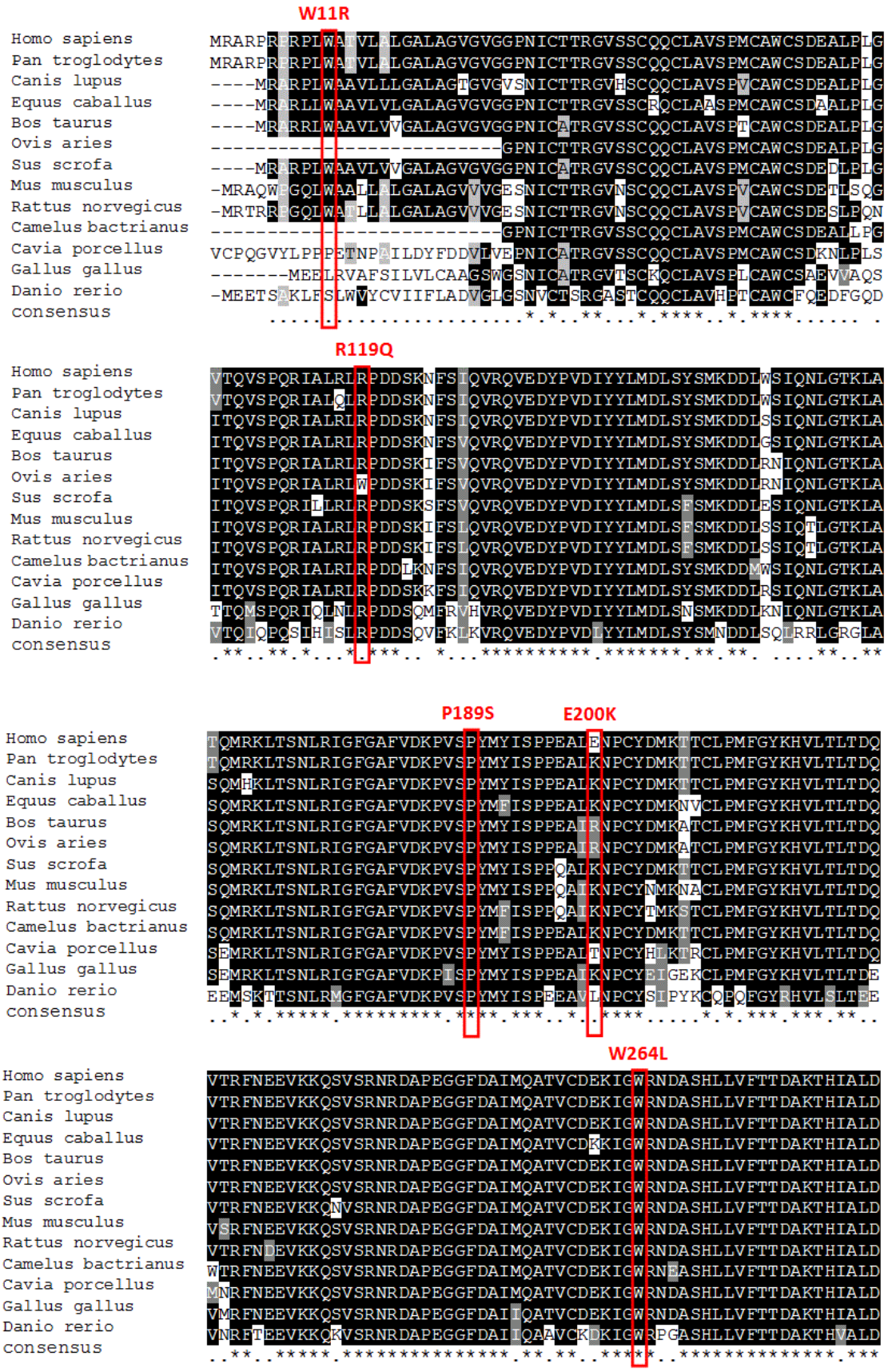
W11R
R119Q
P189S
E200K
W264L
Homo sapiens
Pan troglodytes
Canis lupus
Equus caballus
Bos taurus
Ovis aries
Sus scrofa
Mus musculus
Rattus norvegicus
Camelus bactrianus
Cavia porcellus
Gallus gallus
Danio rerio
consensus

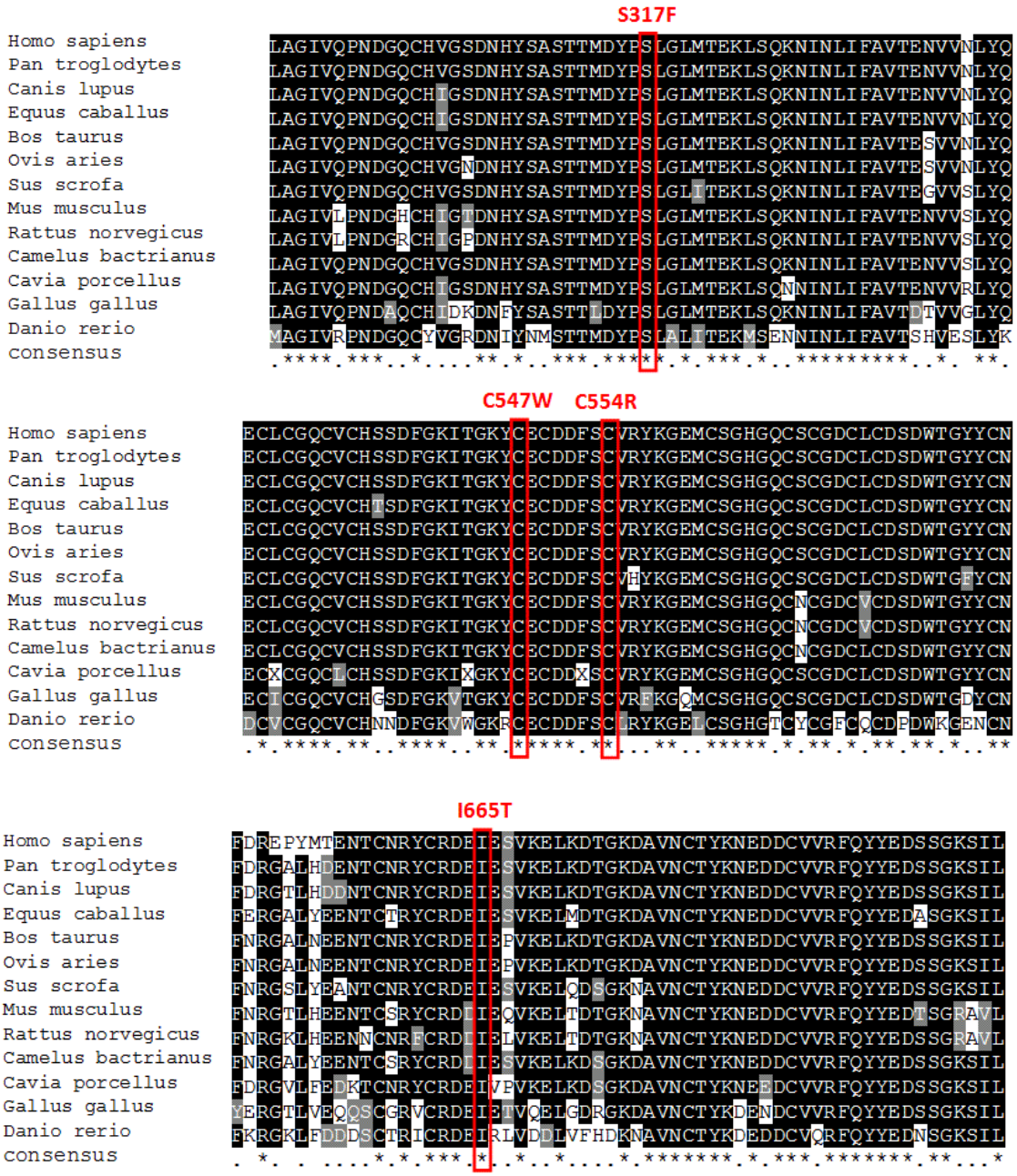

Figure 3.2 Alignment of fragments of the human β_3 amino acid sequence with the corresponding β_3 sequence from 12 other species. The red boxes indicate the positions of the amino acid substitutions identified in patients with GT and studied here.* : highly conserved residue; . : semi-conserved residue.

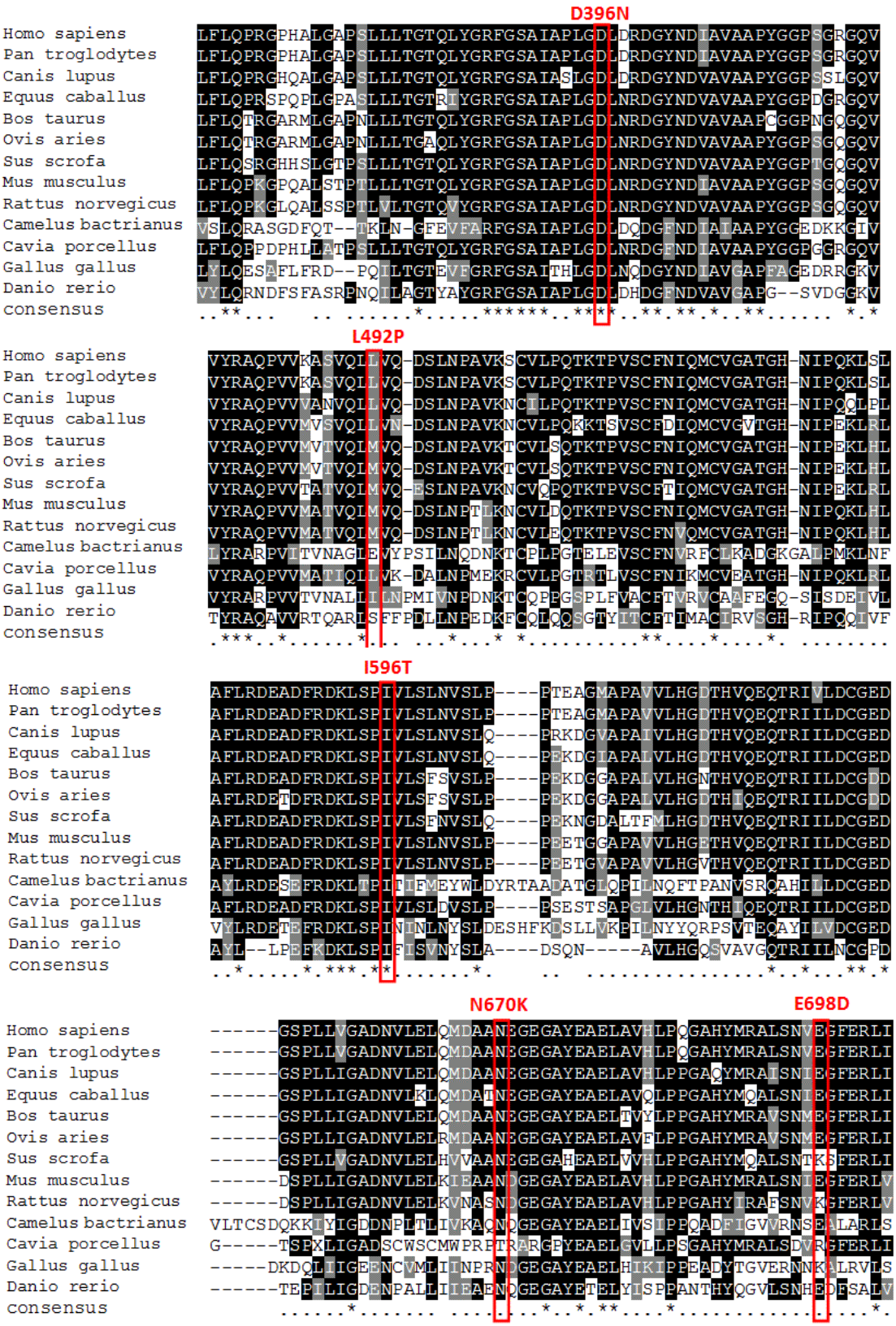

Figure 3.3 Alignment of fragments of the human α_{IIb} amino acid sequence with the corresponding α_{IIb} sequence from 12 other species. The red boxes indicate the positions of the amino acid substitutions.* : highly conserved residue; . : semi-conserved residue.

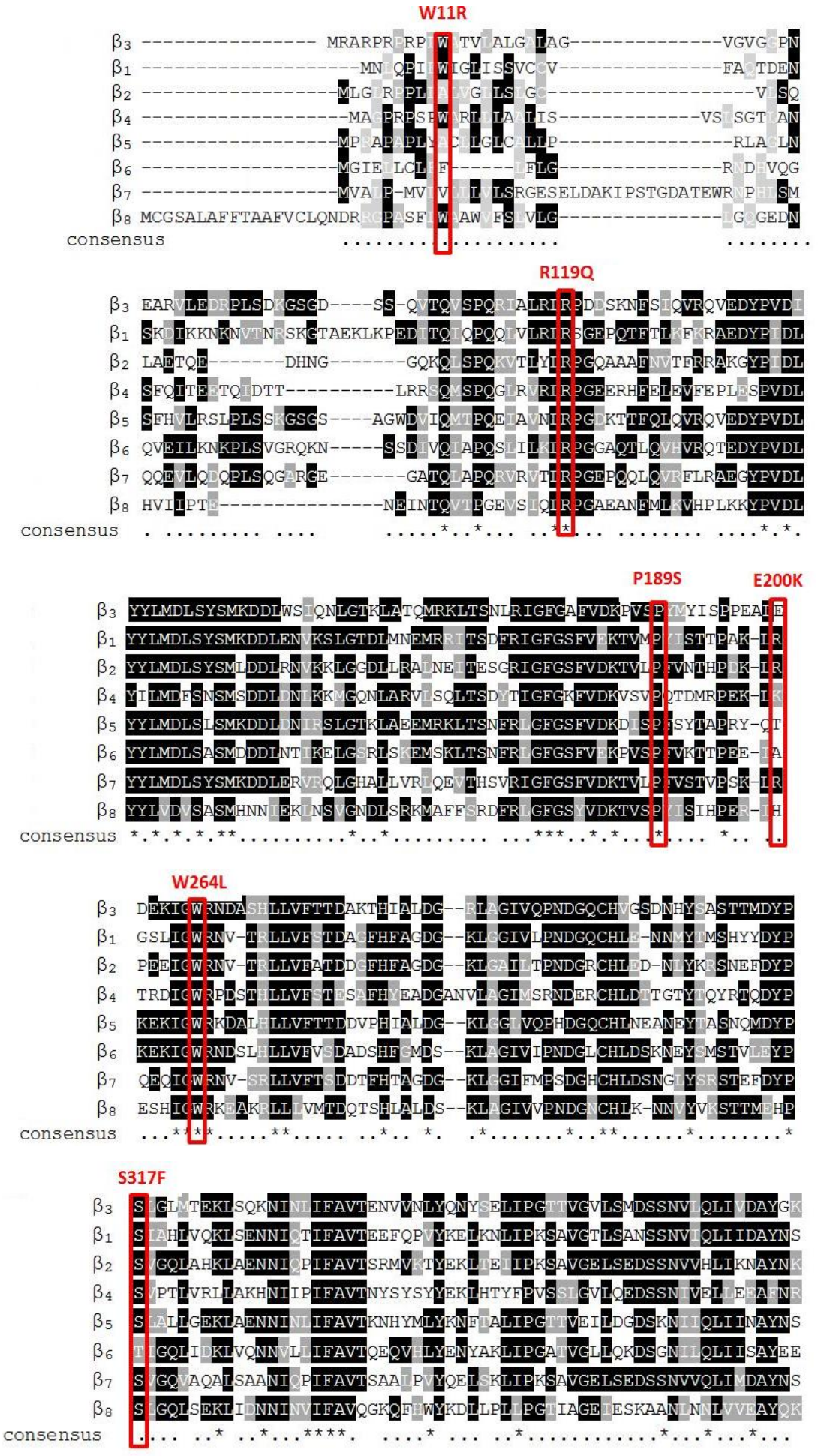
W11R
R119Q
P189S
E200K
W264L
S317F

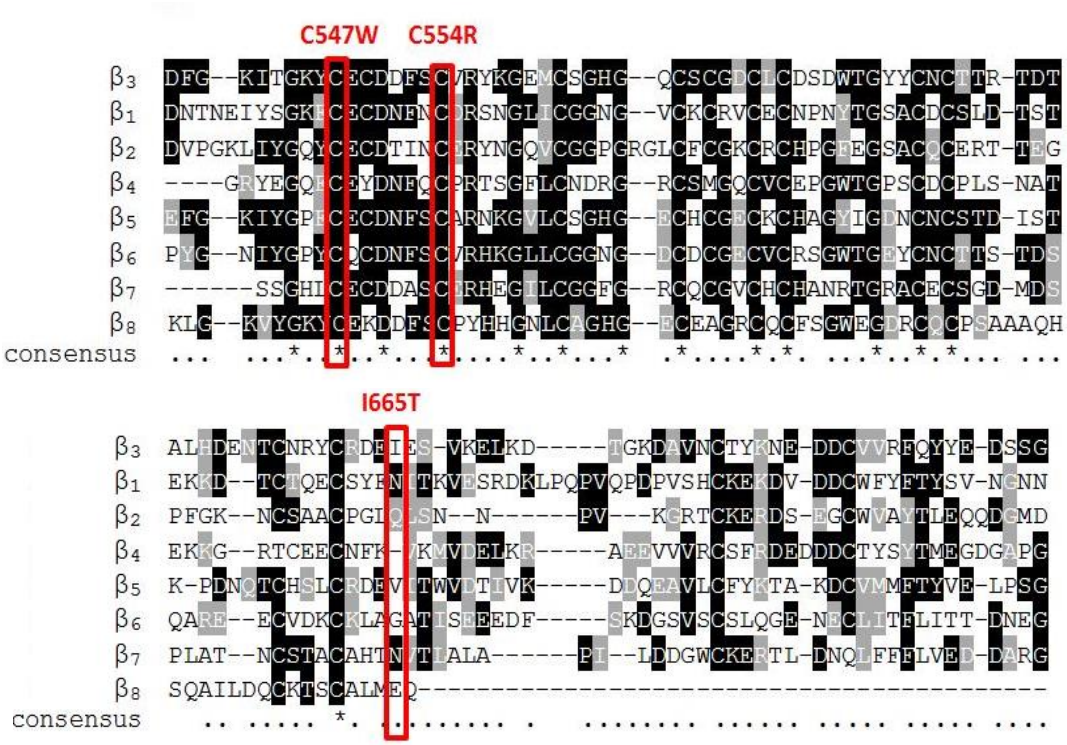

Figure 3.4 Alignment of fragments of the human β_3 amino acid sequence with the corresponding fragments from 7 other β integrin family members. The red boxes indicate the positions of the amino acid substitutions.* : highly conserved residue; . : semi-conserved residue.

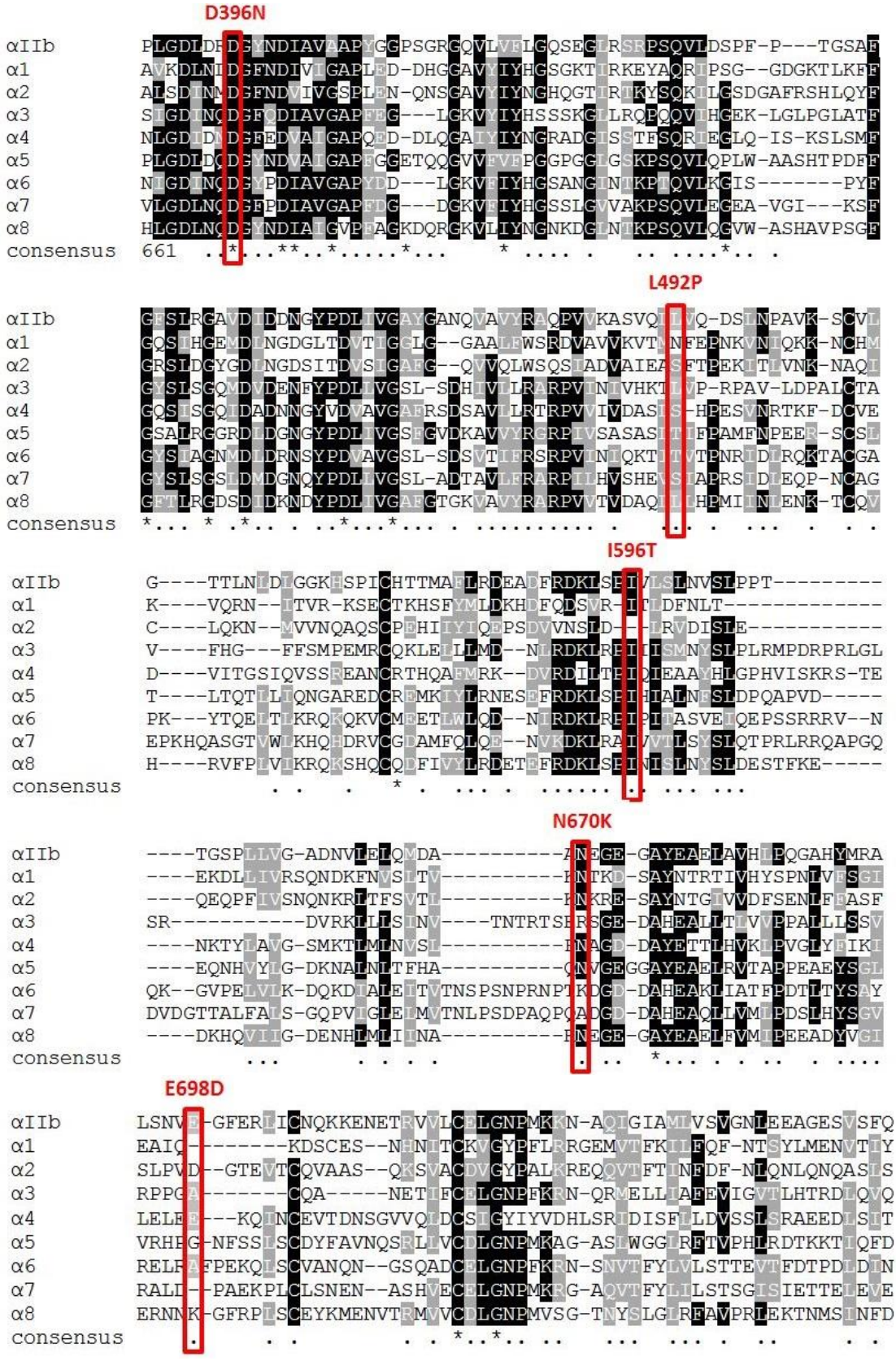

Figure 3.5 Alignment of fragments of the human α_{IIb} amino acid sequence with the corresponding fragments from 8 other α integrin family members. The red boxes indicate the positions of the amino acid substitutions.* : highly conserved residue; . : semi-conserved residue.

3.3.2 Predicting the effects of amino acid substitutions in β_3 and α_{IIb}

A number of online prediction tools were used to examine the possible structural and functional effects of the 14 candidate missense mutations on the β_3 and α_{IIb} integrin subunits. These tools were Polyphen, SIFT, GVGD, SNPs&GO and MutationTaster. The results of these analyses are summarised in tables 3.1 and 3.2.

The p.Trp11Arg substitution in β_3 was predicted to have damaging, or possibly damaging effects on β_3 protein by three of the five prediction tools used, Polyphen, GVGD and SNPs&GO, while the remaining two tools, SIFT and MutationTaster, predicted the substitution to be tolerated. The p.Arg119Gln substitution was predicted to have damaging effects on β_3 integrin by Polyphen, SIFT and MutationTaster, while GVGD and SNPs&GO predicted the change to be less damaging or neutral. Three of the tools, SIFT, GVGD and MutationTaster, predicted the p.Ile665Thr substitution to be detrimental to β_3 while SNPs&GO and Polyphen predicted it to be benign. Importantly, the p.Pro189Ser, p.Trp264Leu, p.Ser317Phe, p.Cys547Trp, p.Cys554Arg substitutions were predicted to have detrimental effects on β_3 using all five prediction tools. In contrast, the p.Glu200Lys substitution was predicted to be a benign change with all but the GVGD tool which predicted that this amino acid substitution may interfere with its normal function (Table 3.1).

The p.Asp396Asn substitution in integrin α_{IIb} was predicted to be detrimental using SIFT, Polyphen, MutationTaster and SNPs&GO, while GVGD predicted the change to be less damaging. Similarly, the p.Leu492Pro substitution was predicted to be detrimental to α_{IIb} by all except the Polyphen tool which found the change to be benign. The p.Ile596Thr and p.Asn670Lys substitutions were predicted to be deleterious to α_{IIb} by all tools used. In contrast, the p.Glu698Asp substitution in α_{IIb} was predicted to be a benign change by Polyphen, SNPs&GO and GVGD, while SIFT and MutationTaster predicted this change to be damaging (Table 3.2).

Table 3.1 The predicted effects of candidate amino acid substitutions on the β_3 subunit.

Amino acid substitution	Polyphen v2	SIFT	GVGD	SNPs&GO	MutationTaster	Pathogenic predictions*
p.Trp11Arg	Possibly damaging	Tolerated	Most likely to interfere with function	Disease	Neutral	**3**
p.Arg119Gln	Damaging	Possibly damaging	Moderately likely to interfere with function	Neutral	Disease	**3**
p.Pro189Ser	Probably damaging	Damaging	Most likely to interfere with function	Disease	Disease	**5**
p.Glu200Lys	Benign	Tolerated	Likely to interfere with function	Neutral	Neutral	**1**
p.Trp264Leu	Probably damaging	Damaging	Likely to interfere with function	Disease	Disease	**5**
p.Ser317Phe	Probably damaging	Damaging	Most likely to interfere with function	Disease	Disease	**5**
p.Cys547Trp	Damaging	Damaging	Most likely to interfere with function	Disease	Disease	**5**
p.Cys554Arg	Damaging	Possibly damaging	Most likely to interfere with function	Disease	Disease	**5**
p.Ile665Thr	Benign	Damaging	Most likely to interfere with function	Neutral	Disease	**3**

* Pathogenic predictions shows number of tools predicting substitution is deleterious

Table 3.2 The predicted effects of candidate amino acid substitutions on the α_{IIb} subunit.

Amino acid substitution	Polyphen V2	SIFT	GVGD	SNPs&GO	MutationTaster	Pathogenic Predictions*
p.Asp396Asn	Damaging	Damaging	Less likely to interfere with function	Disease	Disease	**4**
p.Leu492Pro	Benign	Damaging	Most likely to interfere with function	Disease	Disease	**4**
p.Ile596Thr	Damaging	Damaging	Most likely to interfere with function	Disease	Disease	**5**
p.Asn670Lys	Damaging	Damaging	Most likely to interfere with function	Disease	Disease	**5**
p.Glu698Asp	Benign	Possibly damaging	Less likely to interfere with function	Neutral	Disease	**2**

* Pathogenic predictions shows number of tools predicting substitution is deleterious

3.3.3 Predicted effects of candidate mutations on RNA splicing

The potential for the candidate single nucleotide substitutions in *ITGA2B* and *ITGB3* to affect RNA splicing was investigated using a combination of four bioinformatic tools, Automated Splice Site and Exon Definition Analysis (ASSEDA), NetGene, Berkeley Drosophila Genome Project (BDGP) and Human Splicing Finder (HSF). The results of these analyses are summarised in table 3.3.

Eleven of the 14 single nucleotide substitutions in *ITGA2B* and *ITGB3* which were investigated were predicted to have no effect on RNA splicing by all four tools, while the remaining three substitutions, c.356G>A, c.2010C>A and c.2094G>T, were all predicted to affect splicing (Table 3.3). Thus, the c.356G>T and c.2010C>A transversions were predicted to create an additional acceptor site by HSF. Interestingly, the c.2094G>T transversion in *ITGA2B* was predicted to remove a donor splice site using all four tools (Table 3.3). Further examination of the location of this alteration revealed that it occurred in the last nucleotide of exon 20 in the donor splice site consensus sequence (Figure 3.6), which suggested that the c.2094G>T was more likely to mediate its pathogenic effects by disrupting *ITGA2B* splicing.

Table 3.3 Prediction of potential effects of candidate nucleotide alterations on splicing of *ITGB3* or *ITGA2B* RNA.

Gene / Nucleotide* / Amino acid substitution	ASSEDA	NetGene	BDGP	HSF
***ITGB3* / c.31T>C / p.W11R**	No effect	No effect	No effect	No effect
***ITGB3* / c.356G>A / p.R119Q**	No effect	No effect	No effect	New acceptor site
***ITGB3* / c.565C>T / p.P189S**	No effect	No effect	No effect	No effect
***ITGB3* / c.598G>A / p.E200K**	No effect	No effect	No effect	No effect
***ITGB3*/ c.791G>T / p.W264L**	No effect	No effect	No effect	No effect
***ITGB3*/ c.950C>T / p.S317F**	No effect	No effect	No effect	No effect
***ITGB3* / c.1641C>G/p.C547W**	No effect	No effect	No effect	No effect
***ITGB3* / c.1660T>C / p.C554R**	No effect	No effect	No effect	No effect
***ITGB3* / c.1994T>C / p.I665T**	No effect	No effect	No effect	No effect
***ITGA2B* /c.1186G>A/p.D396N**	No effect	No effect	No effect	No effect
***ITGA2B* / c.1475T>C/p.L492P**	No effect	No effect	No effect	No effect
***ITGA2B* / c.1787T>C /p.I596T**	No effect	No effect	No effect	No effect
***ITGA2B*/c.2010C>A /p.N670K**	No effect	No effect	No effect	New acceptor site
***ITGA2B* /c.2094G>T/p.E698D**	Decrease (donor site)	Donor site broken	Donor site broken	Decrease (donor site)

*Transcript sequences for the human *ITGB3* (ENST00000559488) and *ITGA2B* (ENST00000262407).

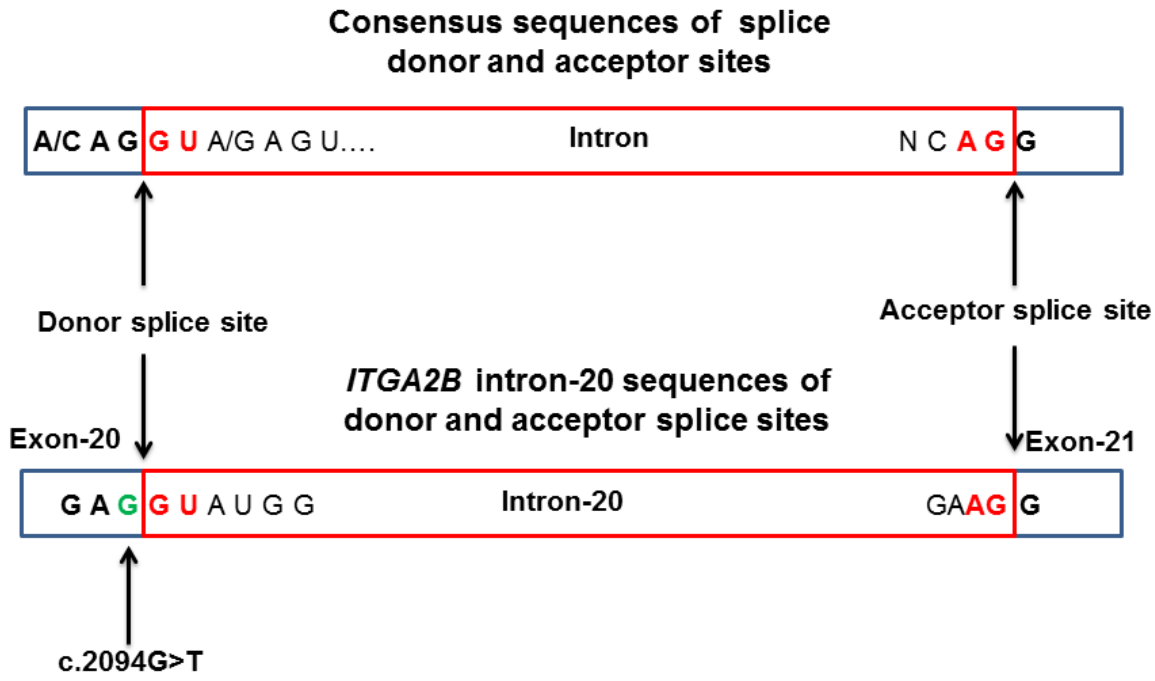

Figure 3.6 Comparsion betweeen human splice site consensus sequences and the sequence of *ITGA2B* at the junction between intron 20 and its flanking exons. The c.2094G>T transversion in *ITGA2B* occurs at the last nucleotide position of exon 20 in the donor splice site that is required for exon-20 definition and appropriate splicing of intron-20.

3.3.4 Effect of the p.Trp11Arg substitution in β_3 on signal peptide cleavage

As the p.Trp11Arg substitution occurs within the signal peptide of β_3, the predicted effects of this amino acid substitution on signal peptide cleavage were examined using SignalP. As expected, signal peptide cleavage of the wild-type β_3 subunit was predicted to occur between amino acids 26 and 27. Similarly, cleavage of the signal peptide from the p.Trp11Arg β_3 variant was predicted to be between amino acids 26 and 27 Thus, the highest cleavage site scores were at position 27 for both the p.Trp11Arg variant (0.48) and wild-type β_3 (0.53) (Figure 3.7).The tryptophan residue at amino acid position 11 is located within the hydrophobic region of the signal peptide. Thus, its substitution by arginine will lead to an increase in positive charge and loss in hydrophobicity in this region (Figure 3.7).

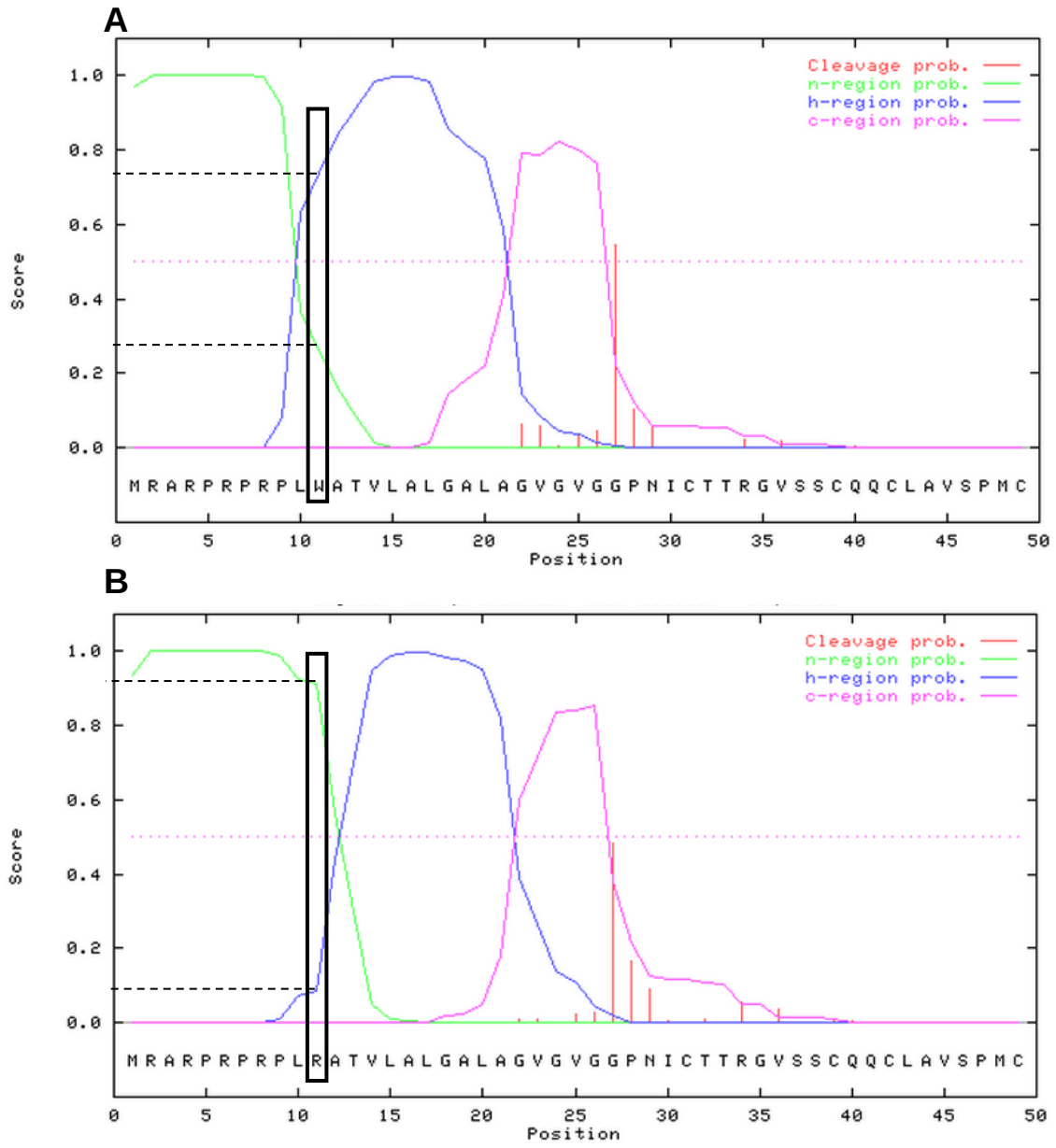

Figure 3.7 Prediction of signal peptide cleavage sites and location of the signal peptide regions in wild-type β_3 (A) and in the p.Trp11Arg variant (B) using SignalP. The highest scores for the probability of cleavage were at position 27 in both the p.Trp11Arg variant (0.48) and wild-type β_3 (0.53) indicating that the p.Trp11Arg substitution did not affect the capacity of the signal peptidase to remove the signal peptide. The graphic also shows that the tryptophan (W) residue at amino acid position 11 (boxed in panel A) is located within the hydrophobic (h) region of the β_3 signal peptide (probability score 0.74). In the case of the p.Trp11Arg variant (panel B) the arginine (R) at amino acid position 11 (boxed in panel B) reduces the likelihood of this residue being in a hydrophobic region, and increases the likelihood that it is in the n-terminal (n) region of the signal peptide. The results indicate that the p.Trp11Arg substitution does not alter the site of signal peptide cleavage but reduces hydrophobicity in the β_3 signal peptide. n-region: N-terminal region (Green), h-region: hydrophobic (Red), c- region: C-terminal region (Pink), Cleavage site (Red).

3.3.5 Predicted effects of substitutions on the molecular structure of β_3 and α_{IIb}

Three dimensional structural models were used to investigate the location and orientation, chemical properties and function of amino acid residues which were predicted to be substituted in patients with GT. The effects of the substituted amino acid residues on protein stability, complex formation and ligand-binding were also examined. This was conducted using published 3D structures for $\alpha_{IIb}\beta_3$ (3FCS) and $\alpha_v\beta_3$ (1JV2) which were downloaded from the protein data bank and visualized using Pymol software (Xiong*, et al* 2001, Zhu*, et al* 2008). The 3D structure for $\alpha_v\beta_3$ was examined in those cases where substitutions in β_3 were predicted to occur in regions of β_3 that were involved in heterodimer formation.

3.3.5.1 β_3 variants

3.3.5.1.1 Hybrid and ligand binding domains variants

The arginine residue at amino acid position 119 of β_3 is located in the hybrid domain and forms hydrogen bonds with 5 residues (Ser46, Pro47, Pro83, Leu43 and Cys49) in β3. Substitution of Arg119 by glutamine causes the loss of 4 hydrogen bonds and also causes steric hindrance in the region leading to destabilisation of the β_3 protein (Figure 3.8). Pro189 forms part of the β I domain that is located in the β_3 headpiece that interacts with the β propeller of α_{IIb}. In addition, it has a role in the formation of the turn between two β sheets, which may be important for normal folding and engagement with α_{IIb}. In the wild-type conformation, the carbonyl group of Pro189 forms a hydrogen bond with Arg242 in β_3. Furthermore, it shows an interaction between β_3 and α_{IIb} residues where Arg242 in β_3 forms a salt bridge with Glu154 in α_{IIb} and the residue adjacent to Pro189, Ser188 forms a hydrogen bond with His143 in α_{IIb}. The substitution of Pro189 by serine does not appear to cause any notable changes in the structure of β_3 (Figure 3.9). Interestingly, Pro189 in β_3 was also not predicted to have a role in engaging with α_V as it is located in an area that does not engage directly with α_V (figure 3.10, lower panel). However, when Pro189 is replaced by serine, this allows hydrogen bond formation between the substituted serine residue and tryptophan 210 in α_V, which might be predicted to result in preferential binding of β3 to α_V rather than α_{IIb} (Figure 3.10).

Glu200 is located on the surface of β_3 in the β I domain, though its side chain does not appear to interact with any residues in either α_{IIb} or β_3. When substituted with lysine, no structural differences are observed for the variant conformation (Figure 3.11). Trp264 is located in the core of the β I domain of the β_3 subunit. It forms a hydrogen bond with Ala255 and is surrounded by a number of hydrophobic amino acids, including Leu222,

Ile262 and Leu272. The substitution of Trp264 by leucine leads to the loss of the hydrogen bond with Ala255 (Figure 3.12), possibly leading to a less stable protein and affecting the normal ability of the integrin to fold correctly. Ser317 is located in the β I domain, at the interface with α_{IIb} where it forms hydrogen bonds with the amino group of Leu320 and the side chain of Glu355 in β_3 and α_{IIb}, respectively. Substitution of Ser317 by phenylalanine causes a loss of both hydrogen bonds and steric hindrance that may disrupt dimerization of β_3 with α_{IIb} and alter receptor trafficking (Figure 3.13). Similarly, Ser317 is located in a region that has direct contact with αv and would appear to be important for $\alpha_V\beta_3$ receptor formation. The wild-type $\alpha_V\beta_3$ structure shows that Ser317 forms a hydrogen bond with Glu342 in α_V, which is lost when Ser317 is substituted by phenylalanine, thus disrupting the interaction with α_V and causing steric hindrance (Figure 3.14).

3.3.5.1.2 Cysteine rich repeats and β tail domains

Cysteine residues 547 and 554 are located in the cysteine rich repeats of β_3, in epidermal growth factor-like domains 2 (EGF-2) and 3 (EGF-3), respectively. Cys547 and Cys554 form disulphide bonds with Cys534 and 568, respectively. Substitution of these cysteine residues with tryptophan at position 547 and arginine at position 554 abrogates the formation of the disulphide bonds and is predicted to cause steric hindrance, possibly leading to destabilisation of the β_3 protein. In addition, the loss of cysteine residues 547 and 554 releases free thiol groups on cysteine residues 534 and 568 (Figure 3.15 and 3.16).

Ile665 is located within the β tail domain of β_3 and in an area with number of hydrophobic amino acids, including Leu705, Val707 and Val641. Importantly, six cysteine residues at, 634, 640, 643, 657, 661 and 681 form three disulphide bonds and are located in the vicinity of isoleucine 665. Substitution of isoleucine with threonine is predicted to disturb the hydrophobicity in this region of the protein. In addition, the side chain of threonine can hydrogen bond with neighbouring residues (Figure 3.17).

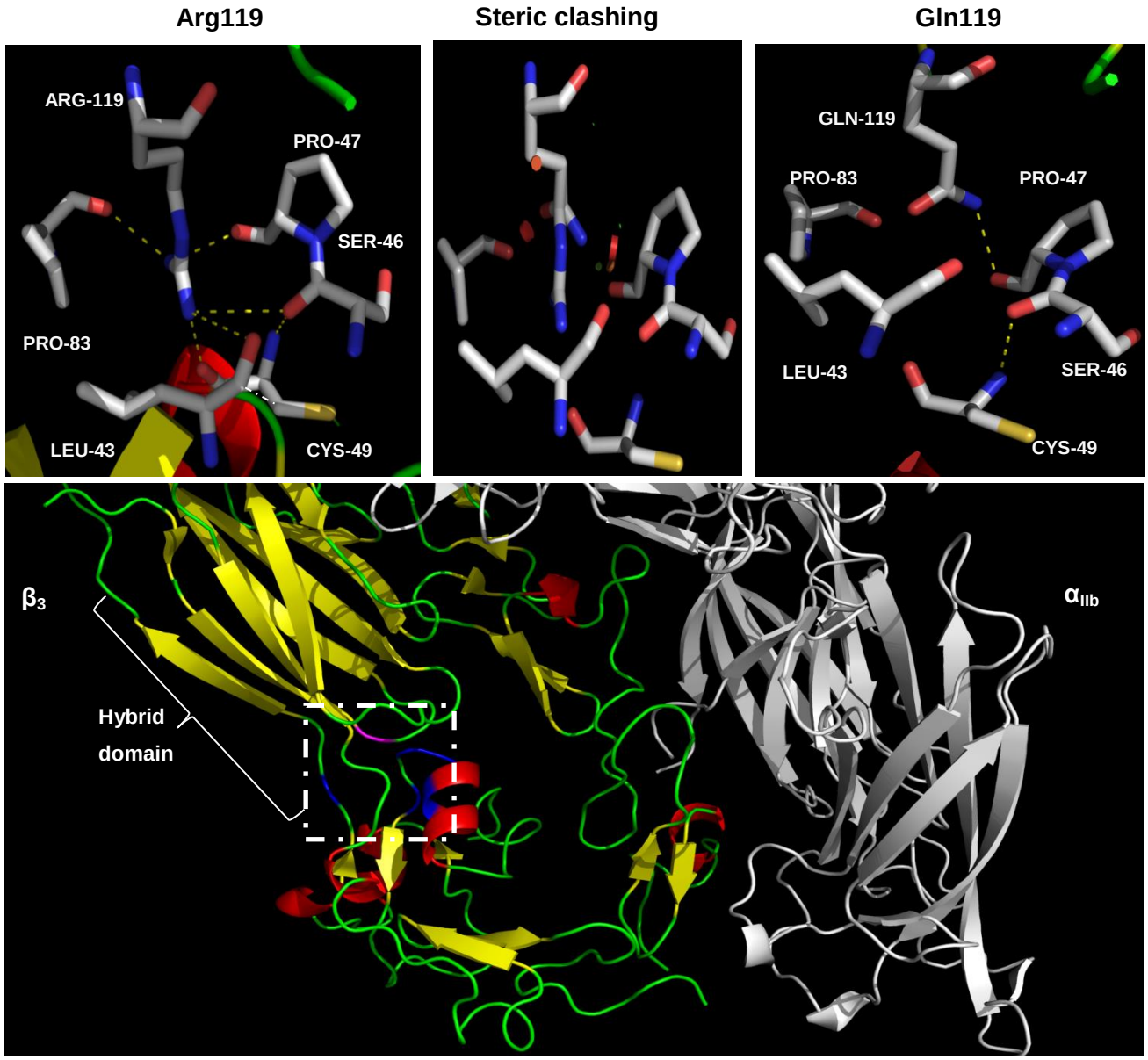

Figure 3.8 Computer-drawn ribbon diagrams of the α_{IIb} (in white) β_3 complex showing the positions of Arg119 in β_3 and the effect of the p.Arg119Gln substitution. Arg119 is located in the hybrid domain of β_3 (lower panel) and a zoomed image shows that it is likely to form five hydrogen bonds through its side chain with the carbonyl oxygen of residues Ser46, Pro47, Pro83, Leu43 and Cys49 (top left panel). This amino acid would therefore seem to be important for receptor stability and function. Interactions modified by the p.Arg119Gln substitution are highlighted in the upper right panel and indicate that glutamine at position 119 abrogates the formation of four hydrogen bonds and thereby affects the stability of the protein. The upper middle panel highlights the steric clashing that occurs as a result of the p.Arg119Gln substitution as represented by graphical 'bumps' (red discs). Affected amino acids are represented as sticks (blue: nitrogen, red: oxygen yellow: sulfhydryl group), Graphical "bumps" (red discs) indicate adverse steric interactions. α-helices are shown as red coils, β-strands as yellow arrows and loops as green tubes. H-bonds are represented by dashed yellow lines.

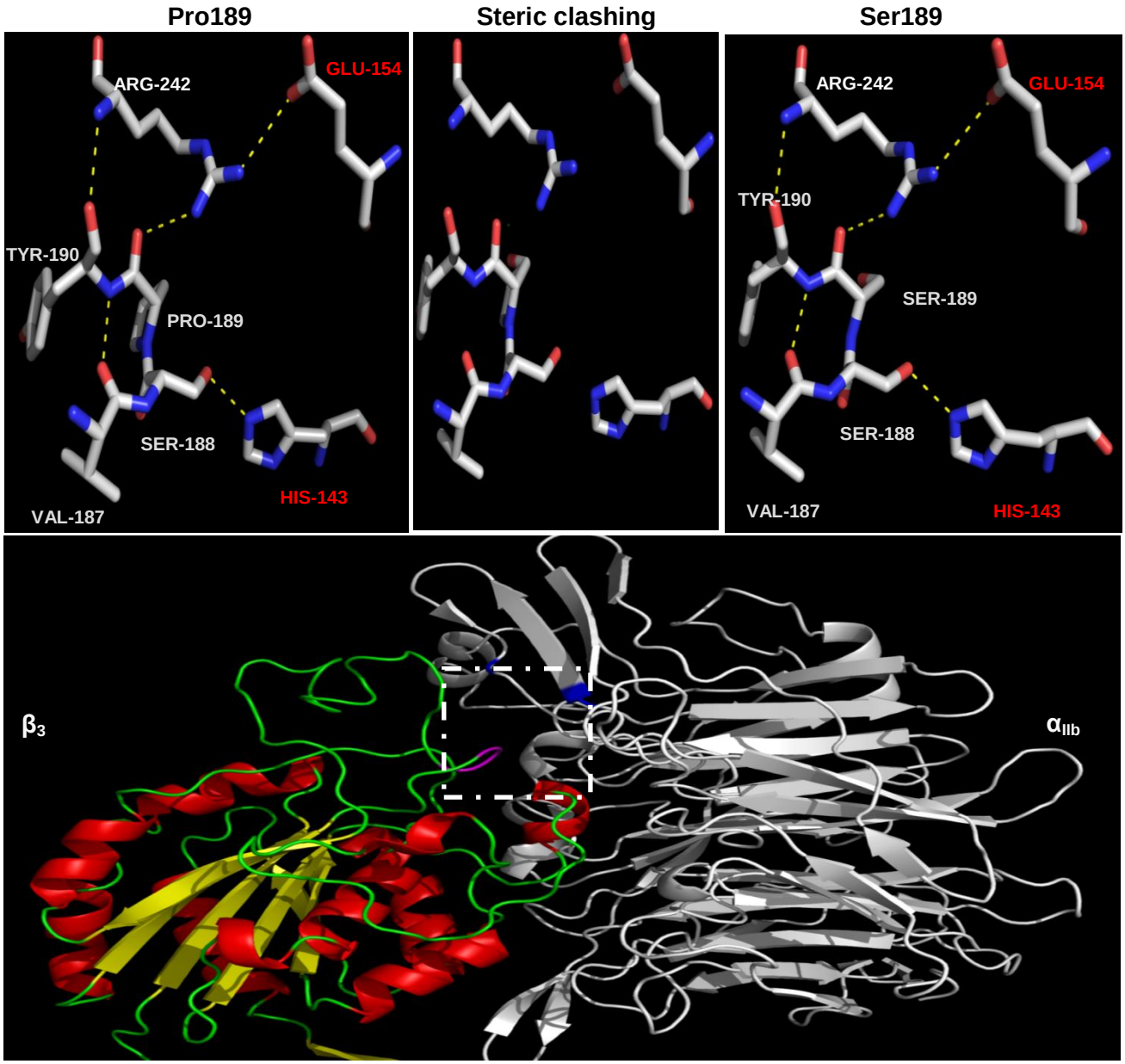

Figure 3.9 Computer-drawn ribbon diagrams of the of β_3 and α_{IIb} (in white) headpieces showing the positions of Pro189 in β_3 and the effect of p.Pro189Ser variant. Pro189 is located in the ligand-binding domain of β_3, at the interface with α_{IIb} subunit (lower panel). In the upper left panel, a zoomed image of the wild-type conformation shows an interaction between β_3 and α_{IIb} in which Arg242 and Ser188 of β_3 form ionic (salt bridge) and hydrogen bonds with Gln154 and His143 of α_{IIb}, respectively. Arg242 also forms hydrogen bonds with the carbonyl groups of Pro189. Pro189 is present in the vicinity of the dimerization area and is important for the bend formation of the turn, which would be important for normal folding and engagement with α_{IIb}. The substitution of Pro189 by serine (upper right panel) may not directly affect interactions between β_3 and α_{IIb} but may affect the normal formation of the β turn leading to a loss of binding between β_3 and α_{IIb}. The p.Pro189Ser substitution does not result in any steric clashing as is shown by the figure in the upper middle panel. Affected amino acids are represented as sticks (blue: nitrogen, red: oxygen yellow: sulfhydryl group), Graphical “bumps” (red discs) indicate adverse steric interactions. α-helices are shown as red coils, β-strands as yellow arrows and loops as green tubes. H-bonds are represented by dashed yellow lines.

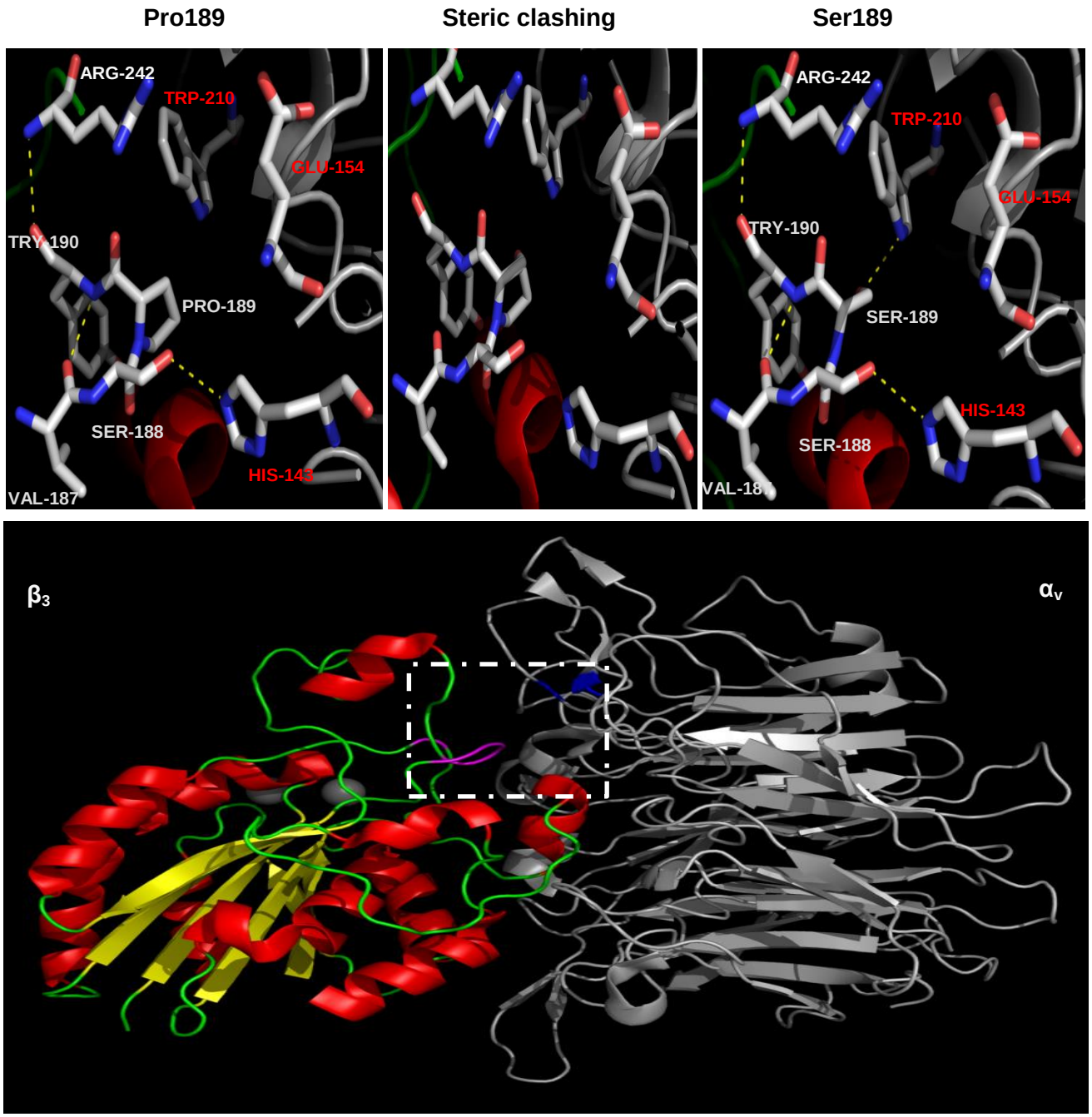

Figure 3.10 Computer-drawn ribbon diagrams of the β_3 and α_V (in white) headpieces showing the positions of Pro189 in β_3 and the effect of p.Pro189Ser variant. Pro189 is located in the ligand-binding domain of β_3 and at the interface with the α_V subunit (lower panel). The upper left panel, shows a zoomed image of the wild-type conformation showing an interaction between β_3 and α_V residues where Ser188 forms a hydrogen bond with His143 of α_v. The substitution of Pro189 by Serine (upper right panel) predicts the formation of an additional bond with Trp210 of α_V suggesting a strengthened interaction between the two subunits. The p.Pro189Ser substitution is not predicted to cause any steric clashes as is shown in the upper middle panel. Affected amino acids are represented as sticks, α-helices are shown as red coils, β-strands as yellow arrows and loops as green tubes. H-bonds are represented by dashed yellow lines. Grey Spheres are Ca^{2+} and Mg^{2+} of the SyMBS MIDAS and ADMIDAS domains.

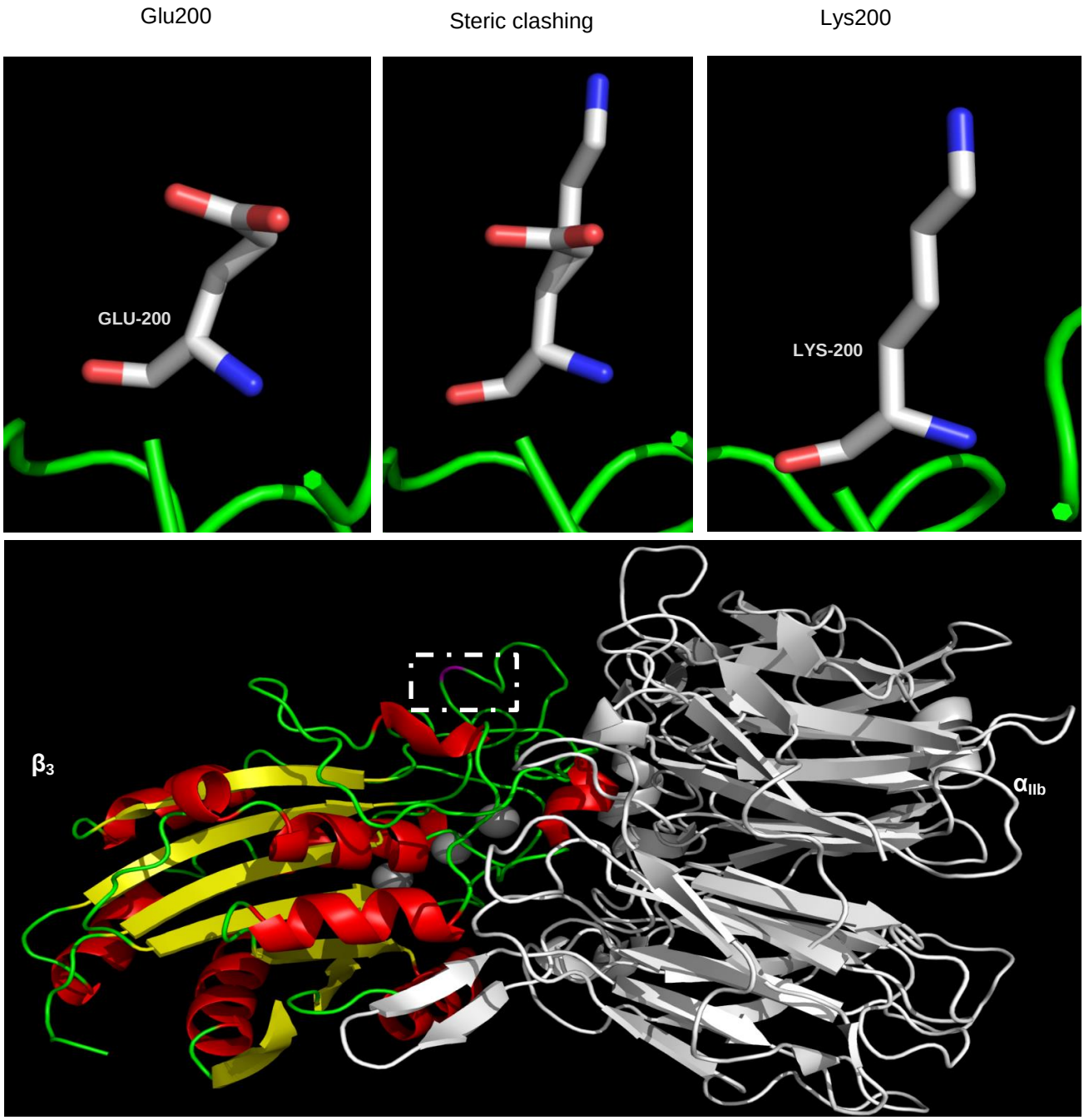

Figure 3.11 Computer-drawn ribbon diagrams of the α_{IIb} (in white) and β_3 complex showing the positions of Glu200 in β_3 and the effect of the p.Glu200Lys subsititution. Glu200 is located within the β_3 ligand-binding domain, but not a part of the dimerization or ligand binding areas. In the upper left panel is a zoomed image of wild-type conformation showing Glu200 is located on the surface of β_3 subunit and its side chain dose not participate in any interaction with β_3 or α_{IIb} residues. The substitution of Glu200 by lysine (upper right panel) does not indicate any deleterious effects on the β_3 subunit and no steric clashing occurs (upper middle panel). Affected amino acids are represented as sticks (blue: nitrogen, red: oxygen yellow: sulfhydryl group), Graphical "bumps" (red discs) indicate adverse steric interactions. α-helices are shown as red coils, β-strands as yellow arrows and loops as green tubes. H-bonds are represented by dashed yellow lines. Grey Spheres are Ca^{2+} and Mg^{2+} of the SyMBS, MIDAS and ADMIDAS domains.

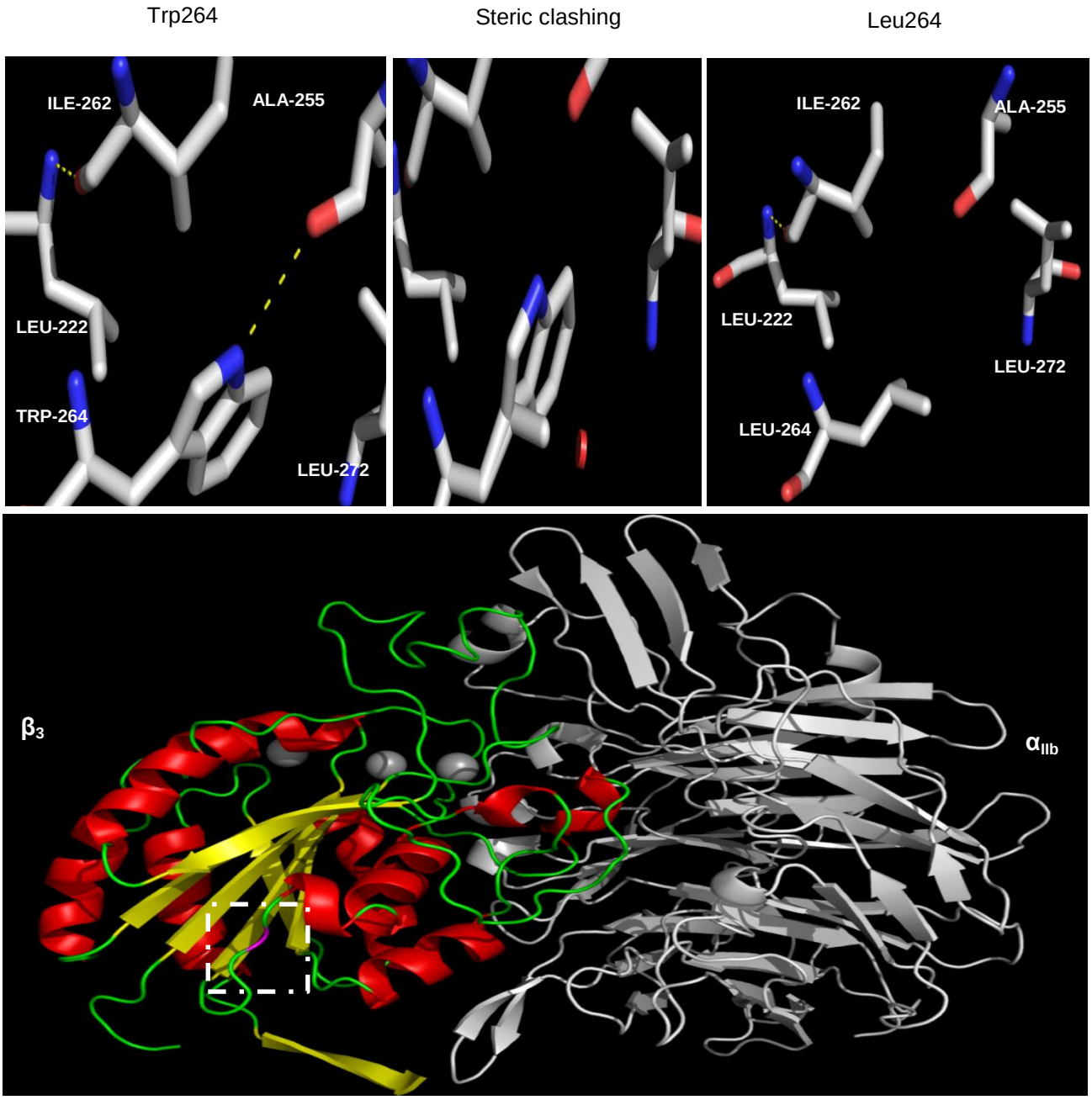

Figure 3.12 Computer-drawn ribbon diagrams of the α_{IIb} (in white) and β_3 complex showing the positions of Trp264 in β_3 and the effect of p.Trp264Leu variant. Trp238 is located within the β_3 ligand-binding domain, but not a part of the dimerization or ligand binding areas. The upper left panel shows a zoomed image of the wild-type conformation showing Trp264 binds directly to Ala255 of β_3 and is also surrounded by a number of hydrophobic amino acid such as Leu222, Leu272 and Ile262. The substitution of Trp264 by leucine (upper right panel) causes the loss of a hydrogen bond between Ala255 and Trp264, possibly resulting in a less stable protein and affecting protein folding. The substitution is not predicted to cause any steric clashes (upper middle panel). Affected amino acids are represented as sticks (blue: nitrogen, red: oxygen yellow: sulfhydryl group), Graphical "bumps" (red discs) indicate adverse steric interactions. α-helices are shown as red coils, β-strands as yellow arrows and loops as green tubes. H-bonds are represented by dashed yellow lines. Grey Spheres are Ca^{2+} and Mg^{2+} of the SyMBS MIDAS and ADMIDAS domains.

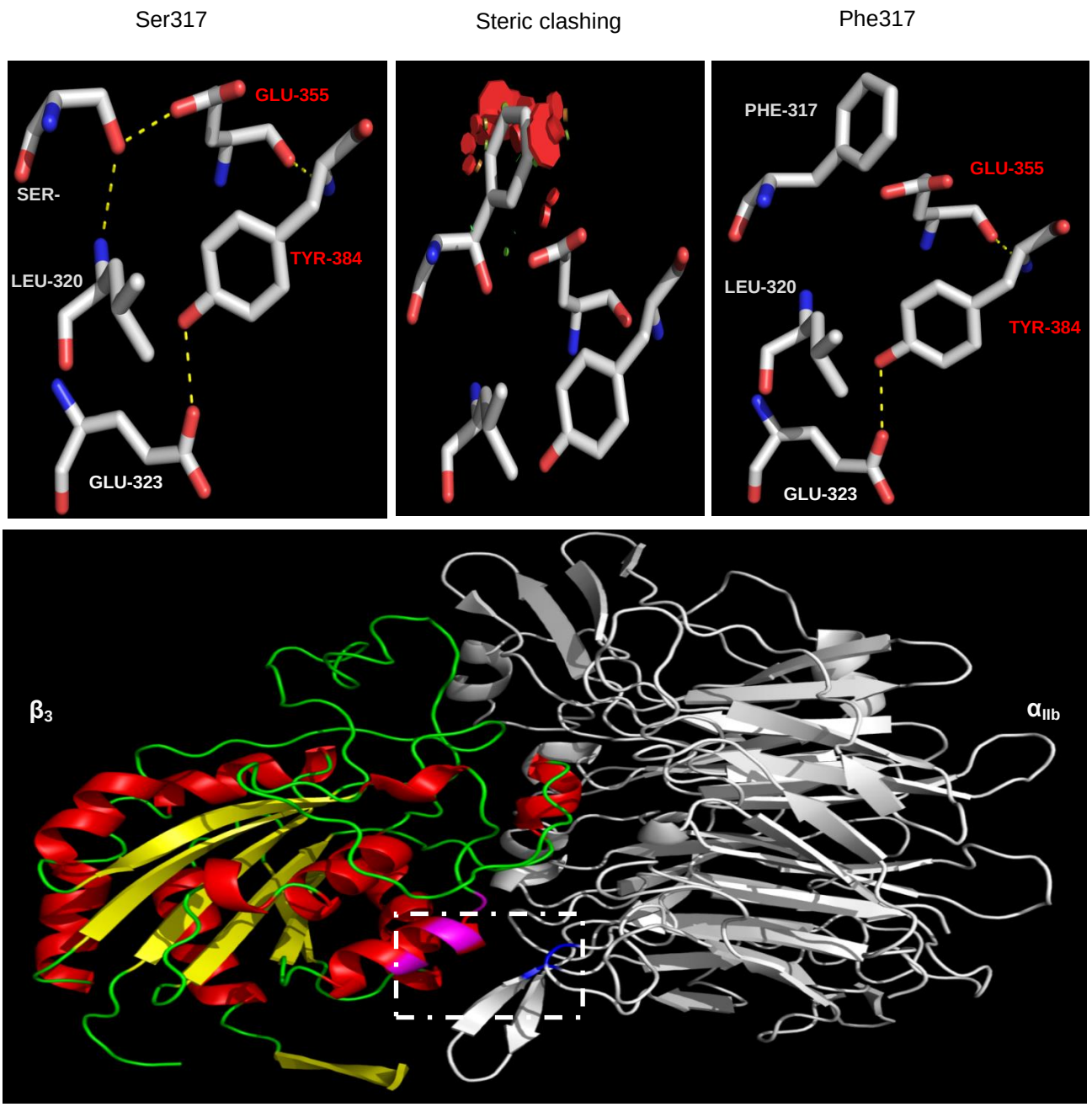

Figure 3.13 Computer-drawn ribbon diagrams of the α_{IIb} (in white) and β_3 headpieces showing the positions of Ser317 in β_3 and the effect of p.Ser317Phe variant. Ser317 is located in the ligand-binding domain of β_3 and at the interface with α_{IIb} subunit (lower panel). The upper left panel is a zoomed image of wild-type conformation showing that the Ser317 forms two hydrogen bonds with the amine group of Leu320 and side chain of Glu355 in β_3 and α_{IIb}, respectively. The substitution of Ser317 by phenylalanine (upper right panel) abrogates both bonds. The upper middle panel highlights the steric clashes which occur as a result of the p.Ser317Phe substitution. The loss of hydrogen bonds and steric hindrance caused by the substitution are likely to destabilize the dimer and interfere with protein trafficking. Affected amino acids are represented as sticks (blue: nitrogen, red: oxygen yellow: sulfhydryl group), Graphical “bumps” (red discs) indicate adverse steric interactions. α-helices are shown as red coils, β-strands as yellow arrows and loops as green tubes. H-bonds are represented by dashed yellow lines.

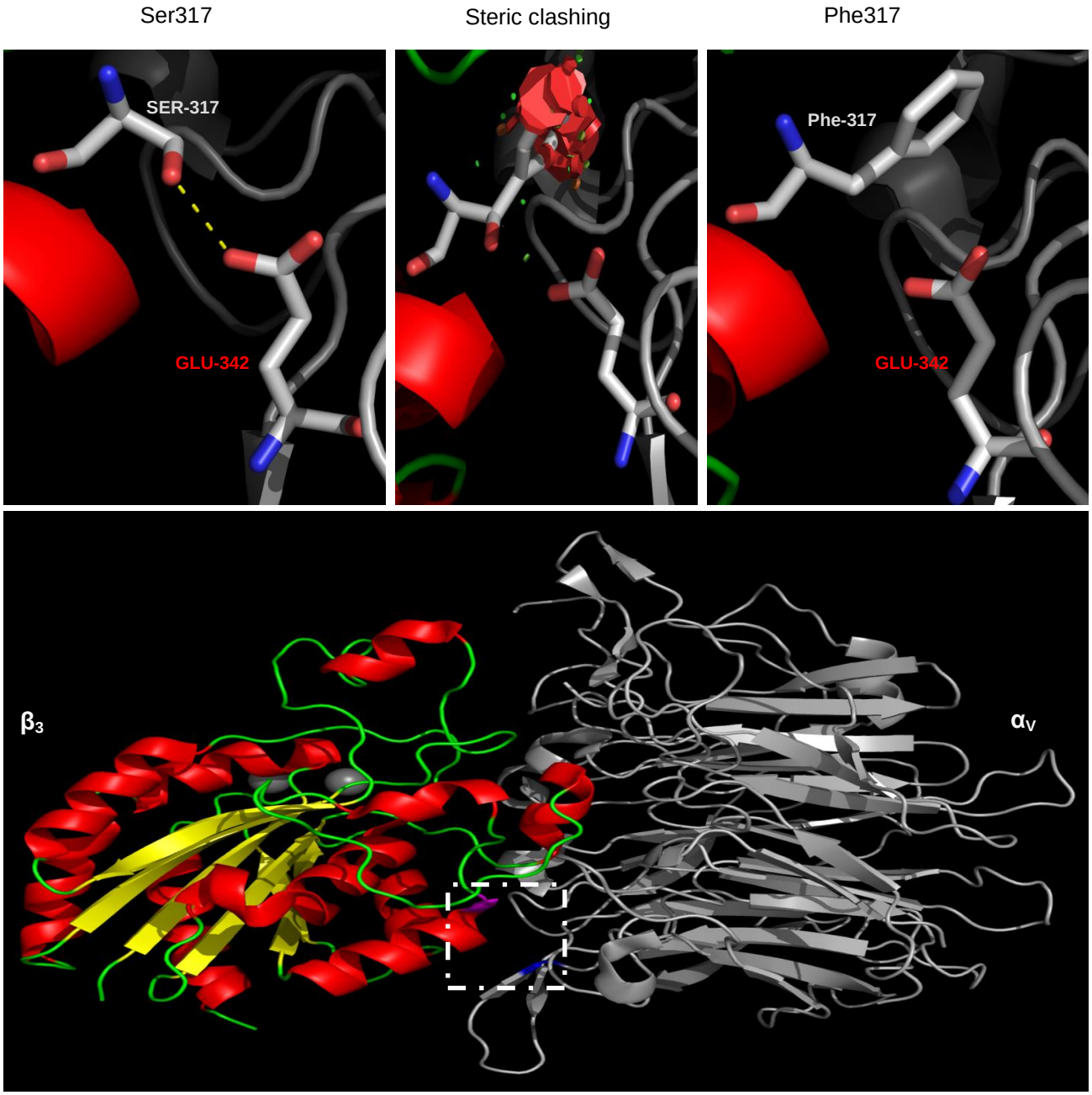

Figure 3.14 Computer-drawn ribbon diagrams of the α_v (in white) and β_3 headpieces showing the positions of Ser317 in β_3 and the effect of p.Ser317Phe variant. Ser317 is located in the ligand-binding domain of β_3 and at the interface with α_v. The upper left panel is a zoomed image of the wild-type conformation showing that Ser317 forms a hydrogen bond with Glu342 in α_v. Whereas the substituted conformation (upper right panel) indicates the substitution by phenyalanine causes a loss of the hydrogen bond in the interface region of the heterodimer suggesting dimer destabilisation and altered protein trafficking. The upper middle panel highlights the steric clashes that occur as a result of the p.Ser317Phe substitution causing steric hindrance in the region. Affected amino acids are represented as sticks (blue: nitrogen, red: oxygen yellow: sulfhydryl group), Grey Spheres are Ca^{2+} and Mg^{2+} of the SyMBS MIDAS and ADMIDAS domains, Graphical “bumps” (red discs) indicate adverse steric interactions. α-helices are shown as red coils, β-strands as yellow arrows and loops as green tubes. H-bonds are represented by dashed yellow lines.

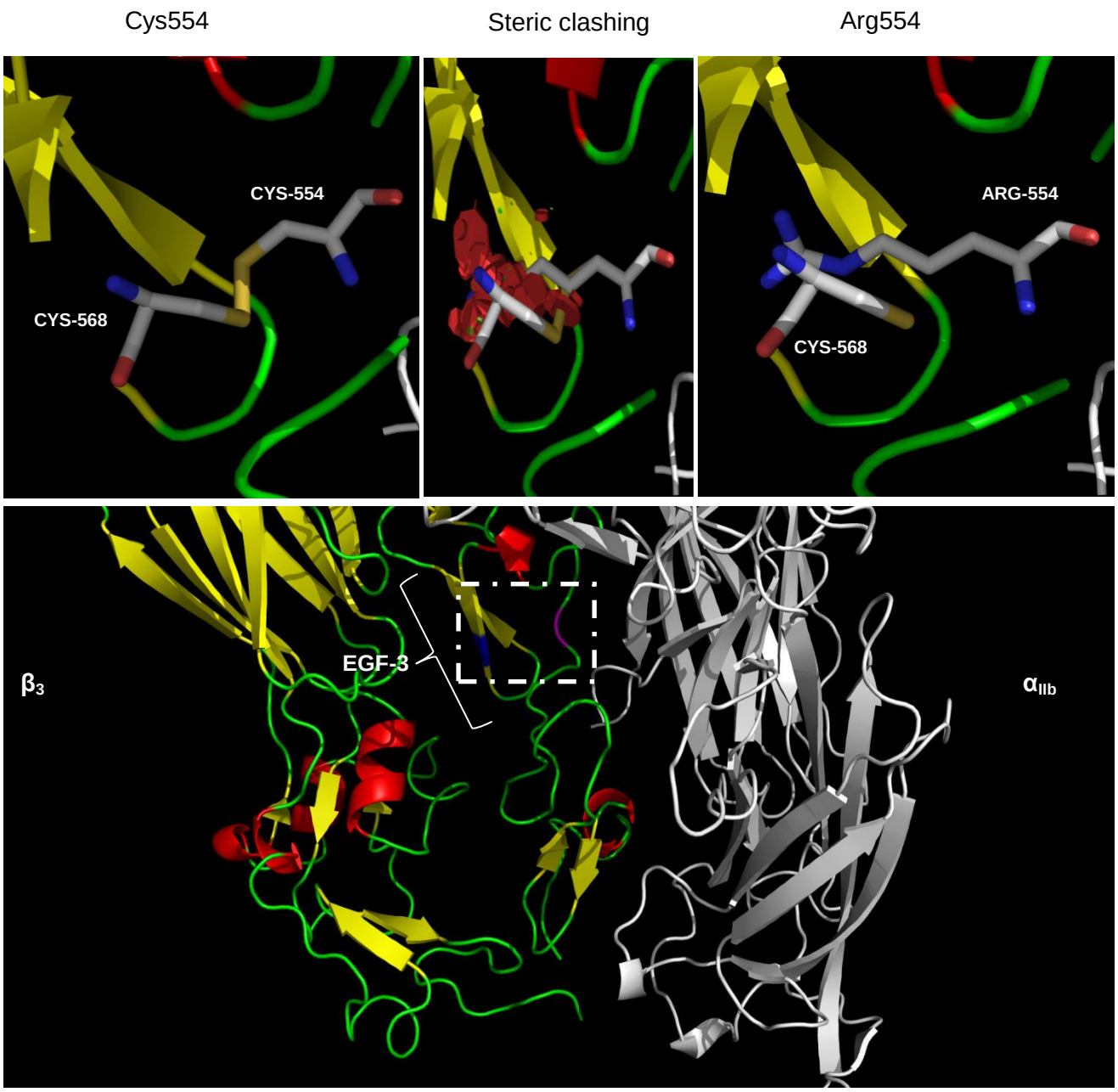

Figure 3.15 Computer-drawn ribbon diagrams of the α_{IIb} (in white) β_3 complex showing the positions of Cys554 in β_3 and the effect of p.Cys554Arg variant. Cys554 is located in epidermal growth factor-like domain 3 (EGF-3) of the cysteine rich repeats domain of the β_3 subunit (lower panel). In the upper left panel, a zoomed image of the wild-type conformation shows the ability of Cys554 to form a disulphide bond to Cys568. The substitution of Cys554 by arginine (top right panel) abrogates the disulphide bond and also leads to release of a free thiol group of its partner residue (Cys568) that, in turn, might disturb another disulphide bond through binding with surrounding cysteine residue. The upper middle panel highlights the steric clashes which occur as a result of the p.Cys554Arg substitution. Affected amino acids are represented as sticks (blue: nitrogen, red: oxygen yellow: sulfhydryl group), Graphical "bumps" (red discs) indicate adverse steric interactions. α-helices are shown as red coils, β-strands as yellow arrows and loops as green tubes. H-bonds are represented by dashed yellow lines.

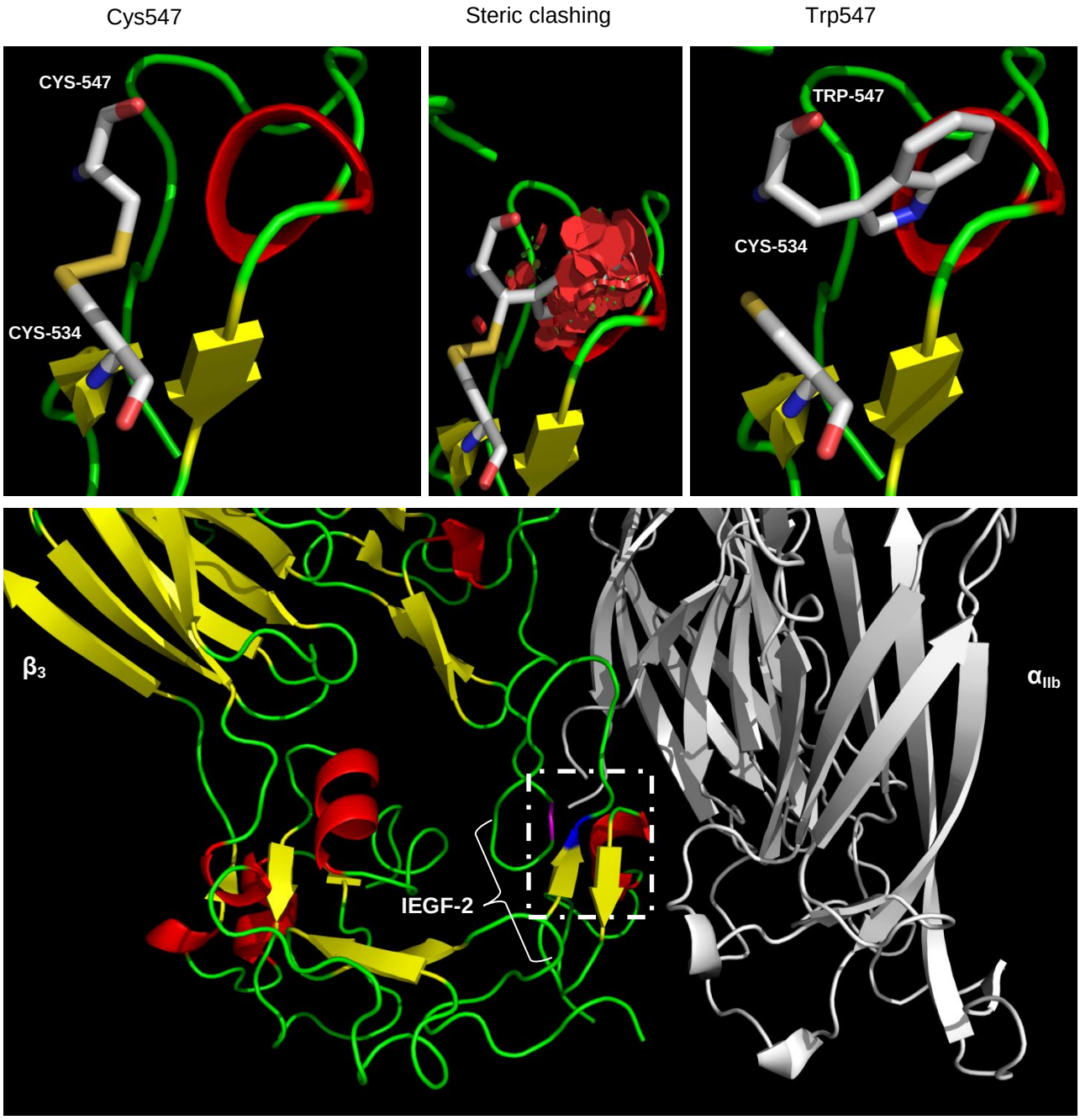

Figure 3.16 Computer-drawn ribbon diagrams of the α_{IIb} (in white) β_3 complex showing the positions of Cys547 in β_3 and the effect of p.Cys547Trp substitution. Cys547 is located in epidermal growth factor-like 2 (EGF-2) of the cysteine rich repeat domains of the β_3 subunit. In the upper left panel, a zoomed image of the wild-type conformation shows the ability of Cys547 to form a disulphide bond to Cys534. The substitution of Cys547 by tryptophan (top right panel) abrogates the disulphide bond and also leads to the release of a free thiol group of partner residue (Cys534) that might disturb an alternative disulphide bond through binding to surrounding cysteine residues. The upper middle panel highlights the steric clashes which occur as a result of the substitution. Affected amino acids are represented as sticks (blue: nitrogen, red: oxygen yellow: sulfhydryl group), Graphical "bumps" (red discs) indicate adverse steric interactions. α-helices are shown as red coils, β-strands as yellow arrows and loops as green tubes. H-bonds are represented by dashed yellow lines.

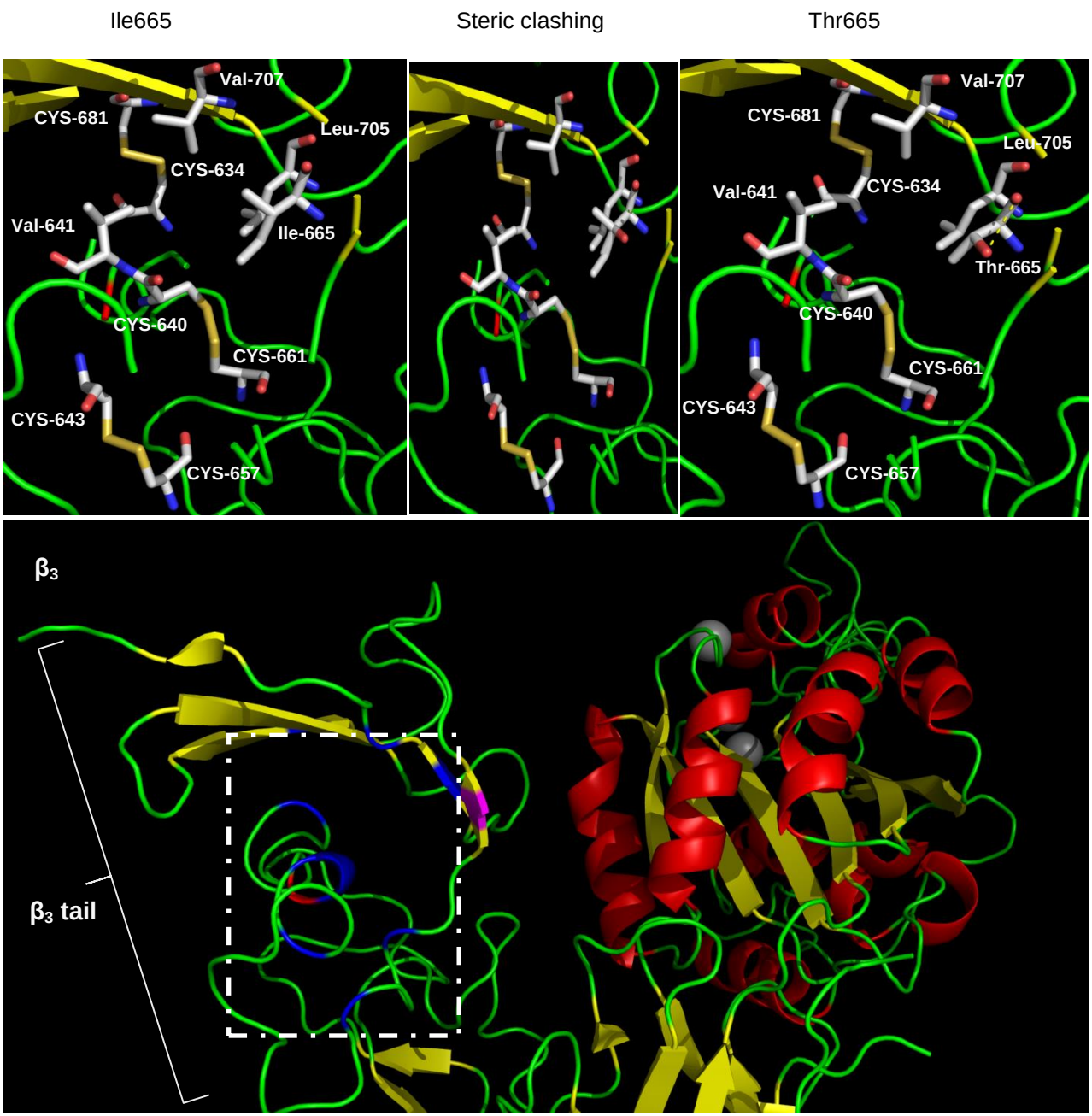

Figure 3.17 Computer-drawn ribbon diagrams of the β_3 protein showing the position of Ile665 in β_3 and the effect of the p.Ile665Thr variant. Ile665 is located within the β tail domain of the β_3 protein. Wild-type conformation (top left panel) shows number of hydrophobic amino acids, including Ile705, Val707 and Val641 in the vicinity of Ile665. Importantly, three different disulphide bonds are located in nearby region to Ile665 indicating β tail domain also rich in cysteine residues. Substitution by threonine, polar neutral amino acid, may affect this hydrophobic region (top right panel) causing a less stable protein. The p.Ile665Thr substitution is not predicted to cause any steric clashes (upper middle panel). Affected amino acids are represented as sticks (blue: nitrogen, red: oxygen yellow: sulfhydryl group), Graphical "bumps" (red discs) indicate adverse steric interactions. Grey Spheres are Ca^{2+} and Mg^{2+} of the SyMBS MIDAS and ADMIDAS domains. α-helices are shown as red coils, β-strands as yellow arrows and loops as green tubes.

3.3.5.2 α_{IIb} variants

3.3.5.2.1 β-propeller and thigh domains

The aspartate residue at amino acid position 396 of α_{IIb} is located in the sixth blade of the β-propeller domain, and forms part of the third calcium binding site. In the wild-type α_{IIb} subunit, calcium ion 3 of α_{IIb} is coordinated by one backbone oxygen in Tyr402 and the oxygen atoms in the carboxyl groups of four Aspartate residues at positions 396, 398, 400 and 404. Replacement of the negatively charged Asp396 by the neutral amino acid asparagine leads to a disturbance of the chemical properties in the vicinity of the substituted residue and affects coordination of the calcium binding site. In addition, the p.Asp396Asn substitution is predicted to cause steric hindrance and clashes with other residues in the vicinity including those in the calcium binding site (Figure 3.18). Leu492 is located in one of the β-strands that form a three stranded antiparallel β–sheet within the thigh domain of α_{IIb}. It forms two hydrogen bonds with Gln519, one of which is disturbed by its replacement with proline. Furthermore this substitution is also predicted to cause steric clashing with neighbouring residues (Figure 3.19). Similarly, Ile596 is mapped to the thigh domain of α_{IIb}, and located within a β-sheet in a region containing several hydrophobic residues, including Leu583 and Val552. Examination of the structure of wild-type α_{IIb} shows that Asp542 and Ser594 form three hydrogen bonds and one salt bridge with Arg551 in the vicinity of Ile596. Substitution of isoleucine by threonine results information of an additional hydrogen bond with Arg551 and may disturb the hydrophobicity of this region (Figure 3.20).

3.3.5.2.2 Calf-1 domains

Asn670 is located at the top of the calf-1 domain of α_{IIb} in the vicinity of a small calcium binding site that is located between the thigh and calf-1 domains in the genu (or knee) of α_{IIb} where it forms hydrogen bonds with 4 nearby residues, Gln642, Gly672, Met724 and Glu673. Its replacement by the positively charged amino acid lysine leads to the loss of these hydrogen bonds, and introduces a positive charge in acidic area and results in steric hindrance (Figure 3.21). Modelling of Glu698 was not possible due to the poorly defined structural features in the α_{IIb} model in the region where this residue is located.

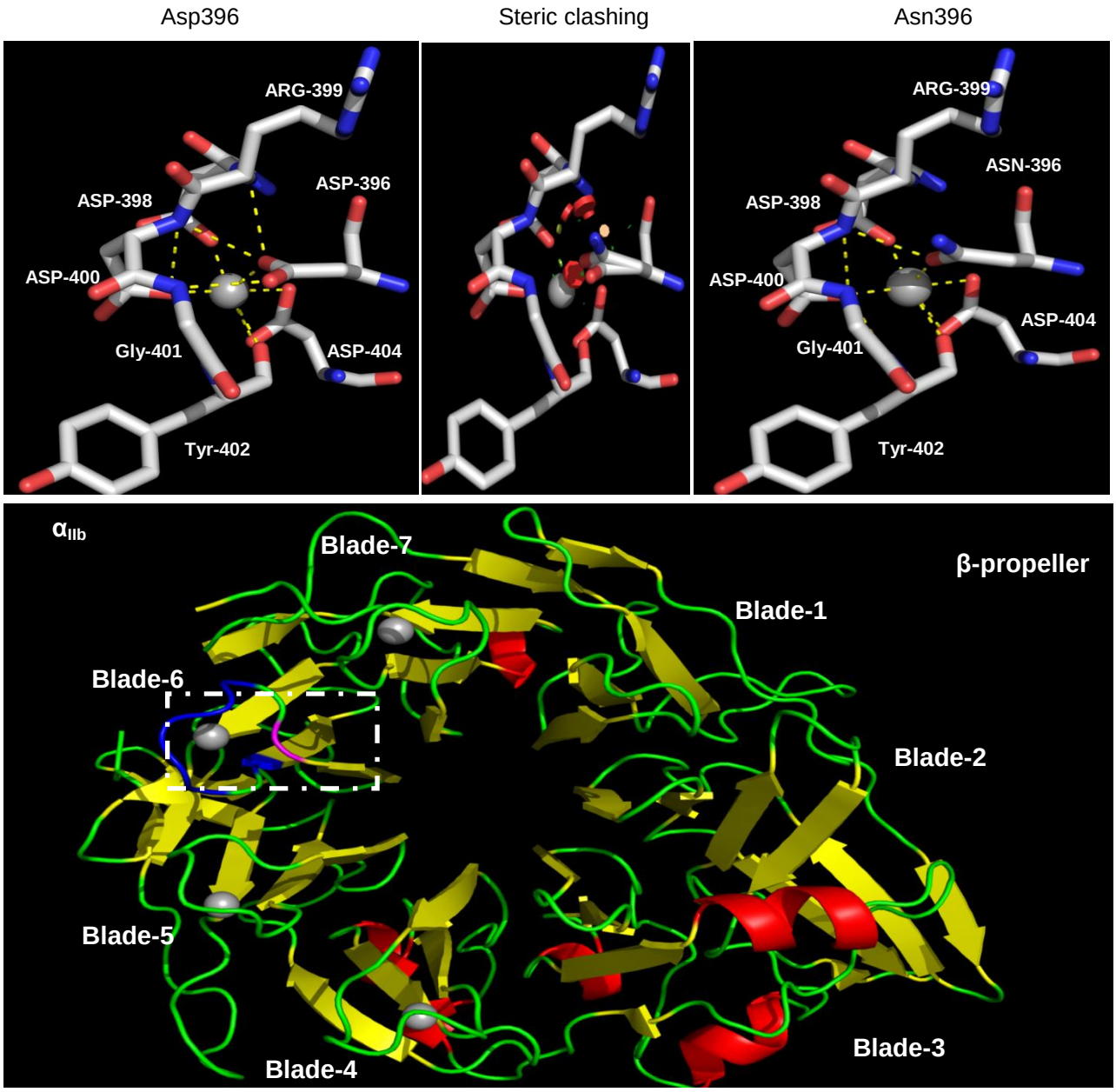

Figure 3.18 Computer-drawn ribbon diagrams of the α_{IIb} headpiece showing the position of Asp396 in α_{IIb} and the effect of the p.Asp396Asn substitution. Asp396 is located in the sixth blade of the β-propeller domain of α_{IIb} within one of 4 α_{IIb} cation binding sites. The wild-type conformation (top left panel) shows calcium ion 3 of α_{IIb} is coordinated by the backbone oxygen of tyrosine-402 and four oxygen of carboxyl groups present in Aspartate residues 396, 398, 400 and 404. Substitution of Asp396 with Asn (upper right panel) abrogates the bond to the divalent ion binding site that is important for the interface between the thigh and β-propeller domains. The upper middle panel highlights the steric clashes that occur as a result of the p.Asp396Asn substitution and cause steric hindrance in the vicinity of the calcium binding site. Affected amino acids are represented as sticks (blue: nitrogen, red: oxygen yellow: sulfhydryl group), Graphical “bumps” (red discs) indicate adverse steric interactions. Grey Spheres are Ca^{2+} ions, α-helices are shown as red coils, β-strands as yellow arrows and loops as green tubes. H-bonds are represented by dashed yellow lines.

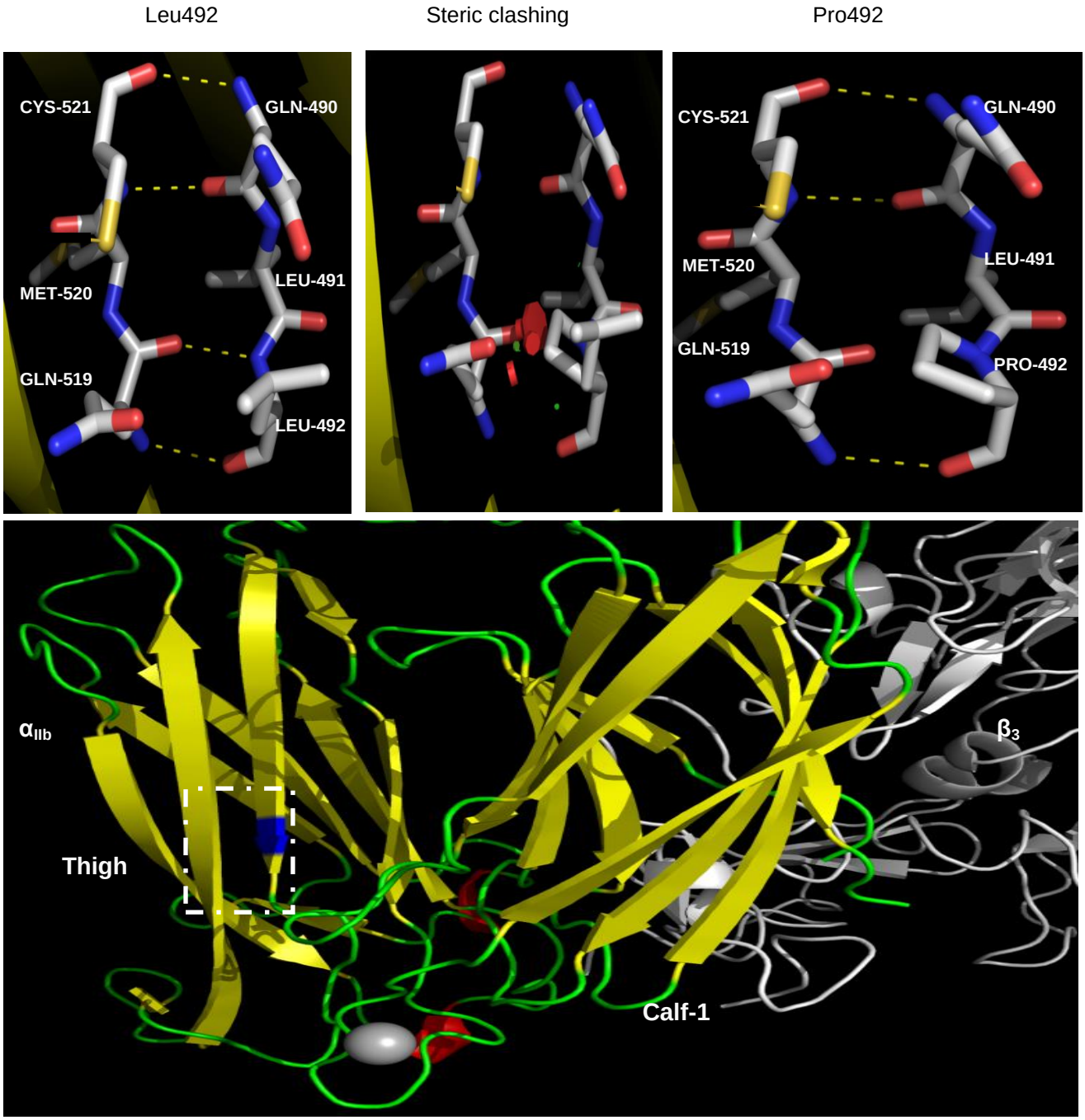

Figure 3.19 Computer-drawn ribbon diagrams of the α_{IIb} (in coloured) β_3 (in white) complex showing the position of Leu492 in α_{IIb} and the effect of the p.Leu492Pro substitution. Leu492 is located in the thigh domain of α_{IIb} and forms β-strand which is a part of three-stranded antiparallel β-sheet. In the upper left panel is a zoomed image of wild-type conformation showing the location of Leu492 within a β-strand where each amino acid forms a hydrogen bond between the amine and carbonyl groups in a regular pattern. The amine and carbonyl groups of Leu492 forms 2 hydrogen bonds with Gln519. The substitution of Leu492 with proline results in forming only one hydrogen bond with Gln519. The upper middle panel highlights the steric clashes that occur as a result of the substitution. Affected amino acids are represented as sticks (blue: nitrogen, red: oxygen yellow: sulfhydryl group), graphical "bumps" (red discs) indicate adverse steric interactions. Grey Spheres are Ca^{2+} ions, α-helices are shown as red coils, β-strands as yellow arrows and loops as green tubes. H-bonds are represented by dashed yellow lines.

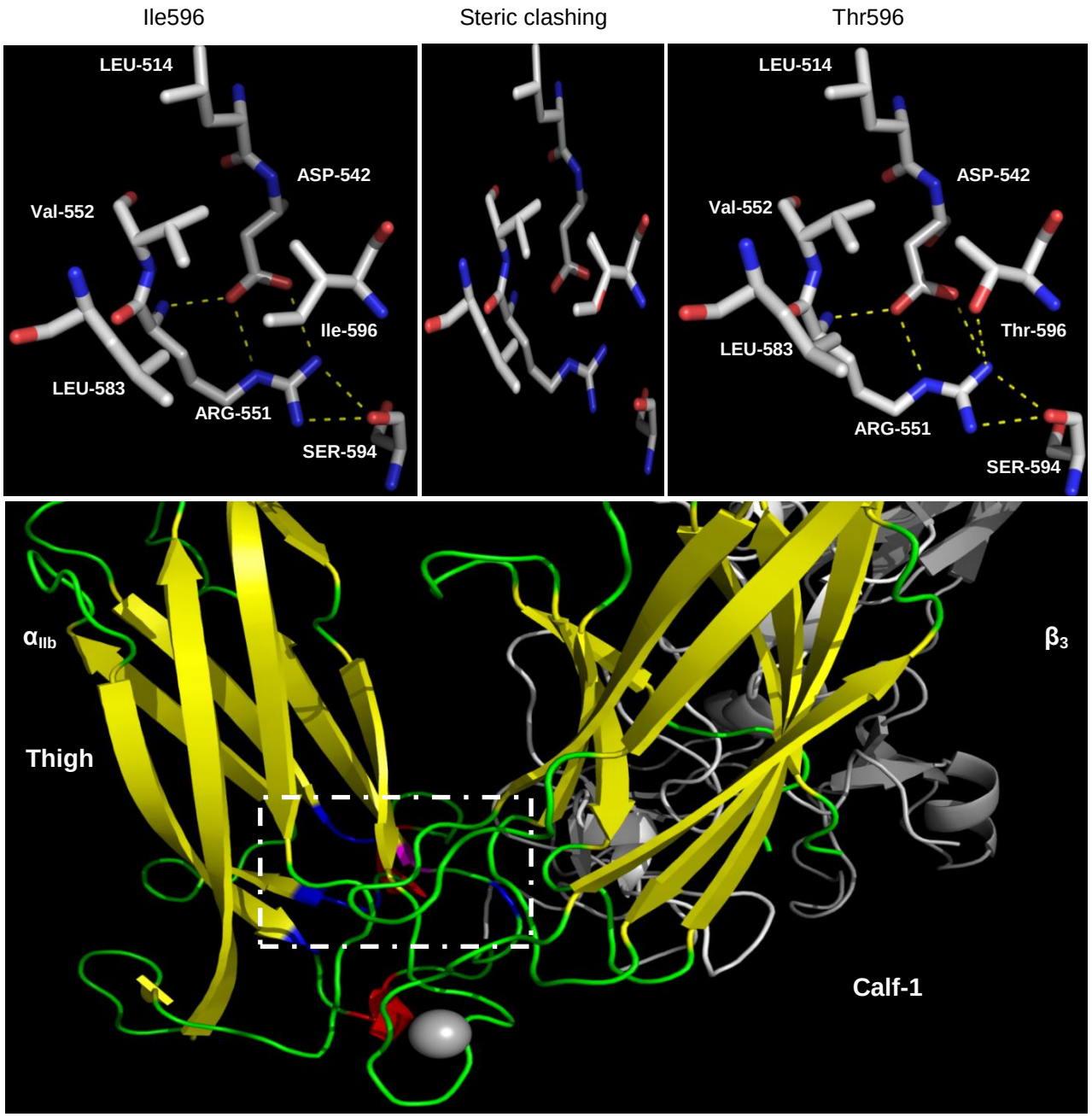

Figure 3.20 Computer-drawn ribbon diagrams of the α_{IIb} (in coloured) and β_3 (in white) complex showing the position of Ile596 in α_{IIb} and the effect of the p.Ile596Thr substitution. Ile596 is located in the thigh domain of α_{IIb} (lower panel). The wild-type conformation (upper left panel) shows number of hydrophobic amino acids, including Ile596, Leu583 and Val552, forming a hydrophobic region. It also shows that Asp542 and Ser594 form four interactions (three hydrogen bonds and one salt bridge) with Arg551. The substitution of Ile596 by threonine, polar neutral amino acid (upper right panel) leads to form a new hydrogen bond with Arg551. No steric clashing is predicted by this substitution (upper middle panel). Affected amino acids are represented as sticks (blue: nitrogen, red: oxygen yellow: sulfhydryl group), Graphical "bumps" (red discs) indicate steric interactions. Grey Sphere is Ca^{2+} ion, α-helices are shown as red coils, β-strands as yellow arrows and loops as green tubes. H-bonds are represented by dashed yellow lines.

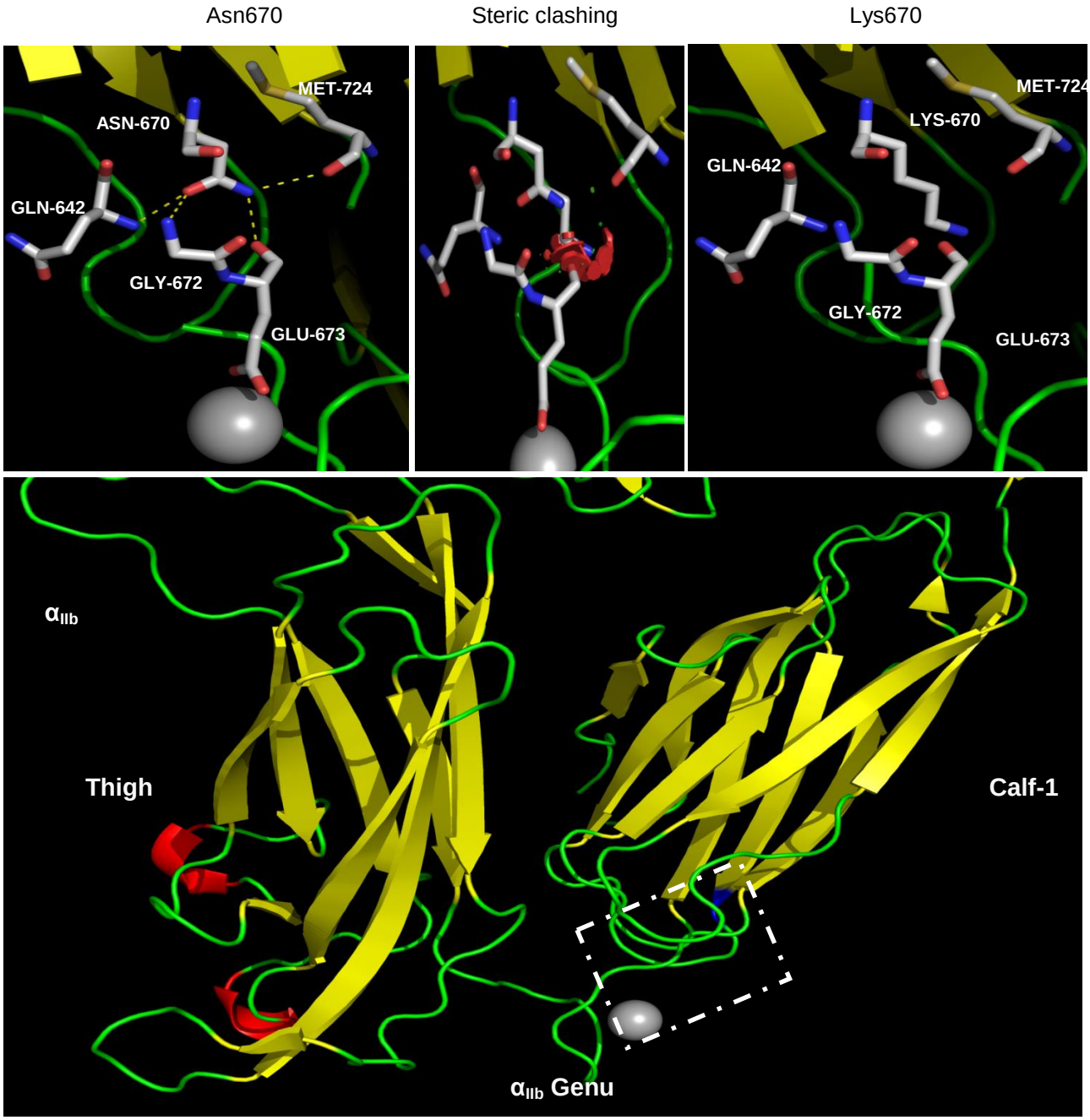

Figure 3.21 Computer-drawn ribbon diagrams of the α_{IIb} subunit showing the positions Asn670 in α_{IIb} and the effect of p.Asn670Lys substitution. Asn670 is located on the top of calf-1 domain, at the c-terminus of the β-sheet that closes to α_{IIb} genu and in the vicinity of calcium binding site. The wild-type conformation (upper left panel) shows the side chain of Asn670 forms four hydrogen bonds with Gln642, Gly672, Glu673 and Met724 where Glu673 is part of a divalent ion binding site. The substitution of Asn670 by lysine (upper right panel), positively charge amino acid, predicts to cause a loss of four hydrogen bonds and introducing a positive charge in calcium coordination region. The upper middle panel highlights the steric clashes which occur as a result of the p.Asn670Lys substitution. Affected amino acids are represented as sticks (blue: nitrogen, red: oxygen yellow: sulfhydryl group), Graphical "bumps" (red discs) indicate adverse steric interactions. Grey Sphere are Ca^{2+} ion, α-helices are shown as red coils, β-strands as yellow arrows and loops as green tubes. H-bond is represented by dashed yellow line.

3.4 Discussion

In this chapter, the possible pathogenic effects of 14 candidate defects identified in GT patients, 9 affecting *ITGB3* and 5 affecting *ITGA2B* were investigated using a variety of computational methods. Of the 9 *ITGB3* defects, 4 predicted amino acid substitutions in the ligand-binding domain of β3 (p.Pro189Ser, p.Glu200Lys, p.Trp264Leu, and p.Ser317Phe), while the fifth predicted an amino acid substitution in the signal peptide (p.Trp11Arg). The remaining 4 predicted substitutions in the cysteine rich domain (p.Cys547Trp, and p.Cys554Arg), the hybrid domain (p.Arg119Gln) and the β-tail (p.Ile665Thr) of β_3. The 5 *ITGA2B* defects predicted amino acid substitutions in the thigh domain (p.Leu492Pro and p.Ile596Thr), the calf-1 domain (p.Asn670Lys and p.Glu698Asp), and in the β-propeller domain (p.Asp396Asn) of α_{IIb}. In the majority of cases the candidate gene defects were predicted to be detrimental to the $\alpha_{IIb}\beta_3$ receptor. The gene defects predicting the p.Glu200Lys and p.Glu698Asp substitutions in β_3 and α_{IIb} were assessed as less deleterious. Importantly, the genetic defect that predicts the p.Glu698Asp substitution, c.2094G>T in *ITGA2B*, is likely to be associated with altered *ITGA2B* RNA splicing. In this section, I will discuss the implications of the findings for each variant, focusing solely on the computational aspects of the work, and I will explain how these led to the generation of hypotheses which formed the basis for *in vitro* studies, the results of which will be presented and discussed further in Chapters 4 and 5.

The c.31T>C transition in *ITGB3* predicted the substitution of a hydrophobic tryptophan (Trp) residue by a polar, positively charged arginine (Arg) residue at position 11 of the signal peptide of β_3. Signal peptides are recognised to comprise three regions: a positively charged amino terminal region (n-region), a hydrophobic core region (h-region) and a polar carboxy-terminal region (c-region). The hydrophobic core region is usually located at the centre of the signal peptide and encompasses 5 to 15 hydrophobic amino acids. This central region is considered to play a crucial role in signal peptide function. Therefore, a significant defect in this region is likely to impair the ability of the protein to enter the endoplasmic reticulum (Heijne 1990, Oliver 1985, von Heijne 1998). SignalP analysis showed that Trp11 is located within the hydrophobic region of the β_3 signal peptide and that the p.Trp11Arg substitution significantly disturbs this region. However, the signal cleavage site for both wild-type β_3 and the p.Trp11Arg variant was predicted to be between residues 26 and 27, indicating that the substitution does not interfere with signal peptide cleavage. In addition, 3 out of 5 bioinformatic software tools predicted that this substitution was likely to be pathogenic to the β_3 protein. However, it was found that Trp11 is only conserved in 7

species out of 12 and in 3 human β integrins out of 7. In *Cavia porcellus* and *Gallus gallus*, the tryptophan residue was replaced by hydrophobic amino acid, proline and leucine residues, respectively, while in *Danio rerio*, it was replaced by polar uncharged amino acid, serine residue. In *Camelus bactrianus* and *Ovis aries*, no corresponding signal peptide sequences were found. In human β_2, β_6, β_5 and β_7 integrins, the tryptophan residues were replaced by hydrophobic amino acid, alanine, phenylalanine alanine, and valine residues, respectively. These results suggested that the presence of hydrophobic amino acid at position 11 of β_3 or at the corresponding position in other β family members seems important and semi-conserved. Therefore, introducing a positive charge amino acid such as arginine at this position would be pathogenic and would interfere with signal peptide function. Collectively, the presence of tryptophan at amino acid position 11 may be essential for normal β_3 protein biogenesis which leads us to hypothesise that **the p.Trp11Arg substitution is deleterious to the β_3 subunit and will result in a severe reduction or complete absence of membrane surface expression of the $\alpha_{IIb}\beta_3$ and $\alpha_v\beta_3$ receptors**.

Three *ITGB3* defects predicted substitutions of residues within the ligand-binding domain of β_3; the c.565C>T transition which predicted the substitution of proline (Pro) 189 with a polar uncharged serine (Ser) residue, the c.791G>T transversion predicting the replacement of the hydrophobic tryptophan residue at position 264 with leucine (Leu) which is also hydrophobic, and the c.950C>T transition predicting the substitution of serine residue at position 317 with a hydrophobic phenylalanine (Phe) residue. Pro189, Trp264 and Ser317 are all highly conserved residues, which suggests they may be important for the structural and functional integrity of the integrin. Supporting this, substitutions of these residues with Ser at position 189, Leu at position 264 and Phe at position 317, were predicted to be deleterious to β_3 integrin using a panel of 5 online computational tools.

Structural modelling showed that both Pro189 and Ser317 are located at the interface between β_3 and α_{IIb}, unlike Trp264, which occurs at the core of the β_3 protein. Although the Pro189 side chain does not directly bind to any neighbouring residues, it is located close to residues which are involved in interactions between β_3 and α_{IIb}, including the adjacent Ser188 which forms a hydrogen bond with His143 in α_{IIb} and Arg242 which forms an ionic salt bridge with Glu154 in α_{IIb}. These interactions may be important for $\alpha_{IIb}\beta_3$ heterodimer formation. Proline is a unique amino acid as it has an amide group instead of a normal amino group. For this reason, proline residues are usually located in turns and α-helices where they give the polypeptide chains their ability to change direction. Substitution of Pro189 with serine may affect this function, leading to a

disturbance in the normal engagement of Ser188 with His143 in α_{IIb} and of Arg242 with Glu154 in α_{IIb}. Interestingly, Pro189 may be less important for $\alpha_v\beta_3$ dimerization as it is located in a region of β_3 that does not directly interact with α_v and there is only one amino acid residue, Ser188, which binds to His143 in α_v. In addition, the substitution of Pro189 with Ser would facilitate hydrogen bonding with the indole nitrogen of Trp210 in α_v, potentially increasing the likelihood of engagement with α_v, and $\alpha_v\beta_3$ receptor stability. These findings would support the results obtained with the online computational tools which predict that the p.Pro189Ser variant would be pathogenic to $\alpha_{IIb}\beta_3$ and would preferentially form the $\alpha_v\beta_3$ complex. In concurrence with our findings, p.Ser188Leu and p.Arg242Gln substitutions caused severe reductions in the membrane expression of $\alpha_{IIb}\beta_3$, while they were tolerated and did not have deleterious effects on $\alpha_v\beta_3$ membrane expression. These results suggested that this region may be important for $\alpha_{IIb}\beta_3$ but not $\alpha_v\beta_3$ heterodimer formation (Jackson*, et al* 1998, Tadokoro*, et al* 2002). In contrast, Ser317 seems to be important for the interaction of β_3 with both α integrins as it forms hydrogen bonds with Glu355 and Glu342 of α_{IIb} and α_v, respectively, as well as with Leu320 in β_3. Modelling of β_3 in which Ser 317 is replaced by Phe shows that there is a loss of hydrogen bonding and a steric hindrance with surrounding residues that may disturb receptor formation between β_3 and either α_{IIb} or α_v. These findings indicate that this variant would be pathogenic to α_{IIb} and α_v and would disturb the formation of $\alpha_{IIb}\beta_3$ and $\alpha_v\beta_3$. Trp264 is located at the core of the β I domain of β_3 where it forms a hydrogen bond with Ala255 and is surrounded by a number of hydrophobic amino acids, including Leu222, Leu272 and Ile262, creating a hydrophobic region in the protein. Its substitution by Leu abrogates hydrogen bond formation with Ala255 and may disturb protein stability. Importantly, the previously described p.Leu222Pro variant, which involves the same region of β_3, has been associated with GT and is shown to interfere with the expression and function of $\alpha_{IIb}\beta_3$, suggesting that the integrity of this region is essential for the structure and function of $\alpha_{IIb}\beta_3$ (Morel-Kopp*, et al* 2001, Ruiz*, et al* 2001). **Therefore, we hypothesised that p.Trp264Leu and p.Ser317Phe substitutions are deleterious to the β_3 subunit and result in a severe reduction or complete absence of membrane surface expression of the $\alpha_{IIb}\beta_3$ and $\alpha_v\beta_3$ receptors. The p.Pro189Ser substitution results in an absence or reduction of $\alpha_{IIb}\beta_3$ receptor expression, while it has less deleterious effects on heterodimer formation between β_3 and α_v.**

The c.1641C>G and c.1660T>C alterations identified in *ITGB3* were predicted to lead to the substitution of cysteine (Cys) residues with tryptophan and arginine at positions 547 and 554 in β_3 respectively. Cys547 and Cys554 are both highly conserved in β_3

across species and among other β integrin family members which would suggest that they play an important role in the structure and function of β_3. This suggestion is supported by the results obtained with five online prediction tools, all of which predicted the p.Cys547Trp and p.Cys554Arg substitutions to be deleterious to β_3. Cys547 and Cys554 are located in the cysteine rich repeats of β_3 in the epidermal growth factor (EGF)-like domains 2 and-3, respectively. Furthermore, Cys547 and Cys554 form disulphide bridges with Cys534 and Cys568, respectively. Importantly, the substitution of these residues not only prevents the formation of these disulphide bonds but also releases a free thiol group in a cysteine-rich region of the protein, which could potentially disturb other disulphide bonds in the vicinity. Several studies have characterised GT-associated defects in the cysteine-rich domains of β_3, causing a range of different effects from the complete absence of the expression of β_3 to constitutively active integrin (Milet-Marsal*, et al* 2002a, Mor-Cohen*, et al* 2007, Ruan*, et al* 1999, Ruiz*, et al* 2001). For example, p.Cys542Arg and p.Cys575Arg substitutions resulted in severe reductions in $\alpha_{IIb}\beta_3$ receptor expression, while other substitutions, such as p.Cys586Arg and p.Cys624Tyr, allowed moderate expression of constitutively active $\alpha_{IIb}\beta_3$ receptors (Chen*, et al* 2001, Mor-Cohen*, et al* 2012, Mor-Cohen*, et al* 2007, Ruan*, et al* 1999). These results suggest that this region of $\alpha_{IIb}\beta_3$, and thus, p.Cys547Trp and Cys554Arg are important for both normal expression and activation. **Therefore, we hypothesised that the p.Cys547Trp and p.Cys554Arg substitutions result in reduced or normal membrane surface expression of $\alpha_{IIb}\beta_3$ receptors which do not signal normally.**

The c.356G>A transition in *ITGB3* predicted the substitution of Arg119 with glutamine (Gln) in β_3. Arg119 is highly conserved across species and among other human β integrins, which suggests it may play an important role in the β_3 subunit. However, only three of the five computational tools that were used in this study predicted this variant to be deleterious. Structural modelling showed that Arg119 is located in the hybrid domain of β_3 where it forms hydrogen bonds with nearby residues Leu43, Ser46, Pro47, Cys49 and Pro83. Previous studies have shown that the formation of multiple hydrogen bonds in this manner is likely to play an important role in protein structure and function (Borders*, et al* 1994). Substitution of Arg119 with Gln results in the loss of four of these hydrogen bonds and also causes steric hindrance in the vicinity of the substituted residue, leading to the destabilisation of the β_3 protein. **Thus, we hypothesised that the p.Arg119Gln variant is pathogenic to the β_3 subunit and results in a complete absence or severe reduction of membrane surface expression of the $\alpha_{IIb}\beta_3$ and $\alpha_v\beta_3$ receptors.**

The c.1994T>C transition in *ITGB3* predicted the substitution of isoleucine (Ile) 665 with a threonine (Thr) residue. Ile665 is highly conserved in β_3 across all the species examined but poorly conserved among other human β integrins and only three of the five computational tools that were used in this study predicted this variant to be deleterious. Structural modelling showed that Ile665 is located in the extracellular β tail domain of the β_3 subunit, in a region comprised of several hydrophobic amino acids, including Val641, Leu705 and Val707. Notably, six cysteine residues at 681, 634, 640, 661, 643 and 657 form three disulphide bonds, all of which are located in close proximity to Ile665. Substitution of the non-polar isoleucine residue, with the polar threonine residue, could therefore cause structural disturbances in this region, potentially affecting protein function. Although little is known about the β tail domain, a p.His652Leu substitution in this region has previously been associated with variant type GT (Nurden*, et al* 2012b, Vinciguerra*, et al* 2001), although a separate study showed that the deletion of amino acids in the β tail domain did not have deleterious effects on $\alpha_{IIb}\beta_3$ membrane expression which would suggest that this domain may be less important for β_3 integrity (Butta*, et al* 2003). **Therefore, we hypothesised that the p.Ile665Thr substitution results in a qualitative abnormality of $\alpha_{IIb}\beta_3$.**

In contrast to the above findings, the substitution of the negatively charged Glutamate (Glu) residue with the positively charged Lysine (Lys) residue at amino acid position 200 in the ligand binding domain of β_3 (p.Glu200Lys) which was predicted by the c.598G>A transition in *ITGB3*, was predicted to be benign using *in silico* methods. Glu200 was not conserved in any of the vertebrate β_3-integrin sequences examined. Moreover, the conserved amino acid at this position in 8 out of the 12 species examined was lysine, including in *Pan troglodytes*, *Canis lupus* and *Equus caballus*. In *Bos taurus* and *Ovis aries*, Glu200 was replaced by arginine, while threonine and leucine were found at the corresponding positions in *Cavia porcellus* and *Danio rerio*, respectively. Similarly, Glu200 is not conserved among other human β integrin family members and it was replaced by arginine in β_1, β_2 and β_7, while in β_4, β_5, β_6 and β_8 integrins it was substituted by lysine, threonine, alanine and histidine, respectively. These results suggested that the substitution of Glu200 with positively charged amino acids such as arginine and lysine would be tolerated. In support of this, the p.Glu200Lys substitution was predicted to be tolerated in β_3 with four out of five computational tools used. The structural modelling showed that Glu200 is located on the surface of the I domain of β_3 and does not directly interact with residues in α_{IIb} and β_3. The substitution of glutamate with lysine was not predicted to cause changes to the structure of β_3. Thus, the association of this variant with GT is unclear, although it

remains possible that Glu200 is required for some other functional aspect of β_3 that has not been examined here. However, our investigations to date would lead us to hypothesise that **the p.Glu200Lys variant does not have any deleterious effects on $\alpha_{IIb}\beta_3$ and $\alpha_v\beta_3$**.

The effects of five candidate *ITGA2B* defects were also evaluated using *in silico* approaches. The c.1186G>A transition in *ITGA2B* was predicted to lead to the substitution of aspartate (Asp) with asparagine (Asn) at position 396 in α_{IIb}. Asp396 is highly conserved across species and in other α integrin family members in humans, which would suggest that it plays an important role in the structure and function of α_{IIb}. Its substitution with Asn was predicted to be deleterious to α_{IIb} by 4 of the 5 computational tools used in the study, suggesting that this is an important amino acid in α_{IIb}. Structural modelling showed that Asp396 is located in the sixth blade of the β-propeller domain of α_{IIb} and within the third calcium binding site. More specifically, it is situated in the calcium binding loop, which forms a β-hairpin structure between two β-strands. This calcium binding site is coordinated by four oxygens atoms in the carboxy groups of Aspartate residues 396, 398, 400 and 404 and one backbone oxygen atom in Tyr402. Substitution of the negatively charged Asp residue by the uncharged polar Asn residue is likely to disturb the chemical properties of this region and could possibly interfere with calcium binding since, although asparagine is hydrophilic, its neutral side chain is unable to contribute to binding calcium, thereby affecting coordination of the metal ion in the binding site. The p.Asp396Asn substitution was also predicted to cause steric hindrance in the vicinity of the substituted residue. Previously it has been shown that substitution of other amino acids located in proximity to the four calcium binding sites, in the β-propeller, causes GT by disrupting the biogenesis and surface expression of the $\alpha_{IIb}\beta_3$ receptor (Mitchell*, et al* 2003, Ruan*, et al* 1998). Interestingly, deletion of each of the calcium binding sites in the β-propeller causes a dramatic reduction in the surface expression of the receptor, indicating that these calcium binding domains play an important role in biogenesis and surface expression of $\alpha_{IIb}\beta_3$ (Basani*, et al* 1996). **Therefore, we hypothesised that the p.Asp396Asn substitution results in a severe reduction or complete absence of membrane expression of the $\alpha_{IIb}\beta_3$ receptor.**

The c.1475T>C and c.1787T>C transitions in *ITGA2B* predicted the substitution of Leu492 and Ile596 with proline (Pro) and threonine (Thr) respectively. Both substitutions were predicted to be deleterious to α_{IIb}. It was shown here that Leu 492 is not conserved across species, only being present in 4 of the 12 α_{IIb} integrins examined from other species, and in only 2 of 8 other members of the human α integrin family of

proteins, unlike Ile596, which is highly conserved across species and in other α integrins. These findings suggest that the substitution of Ile596 might be more deleterious to the α_{IIb} subunit than that of Leu492. Importantly, structural modelling showed that Leu492 and Ile596 map onto different regions of the thigh domain of α_{IIb}. Leu492 is located on a β-strand which is part of a three stranded anti-parallel β-sheet and forms two hydrogen bonds with Gln519, which is also located in the thigh domain. One of these hydrogen bonds is lost when Leu492 is substituted with proline, an amino acid which has limited ability to form hydrogen bonds. Its introduction in the middle of this β-strand may therefore not be favoured as it blocks the formation of the hydrogen bonding network that is required to maintain the normal structure of the β-strand. Structural modelling also revealed that the introduction of proline was likely to cause steric clashing with the neighbouring Gln519 residue, which might be predicted to destabilise the α_{IIb} protein. Similarly, Ile596 maps onto the thigh domain of α_{IIb}, and is also part of the β-strand. This amino acid side chain is found within a number of hydrophobic residues, including Leu583 and Val552. The replacement of isoleucine by threonine at position 596 may result in a loss of hydrophobicity in this region, and the formation of new hydrogen bonds between the substituted threonine residue and neighbouring residues, including Arg551, which might be predicted to disturb the normal conformation of the region. A number of studies have characterised GT-associated defects in the thigh domain of α_{IIb}, causing a complete absence of membrane $\alpha_{IIb}\beta_3$ such as p.Ala550Asp and p.Ile518Asn (D'Andrea*, et al* 2002, Nurden*, et al* 2015). **Therefore, we hypothesised that the p.Leu492Pro and p.Ile596Thr amino acid substitutions result in a severe reduction or complete absence of membrane surface expression of the $\alpha_{IIb}\beta_3$ receptor**.

The remaining *ITGA2B* variants studied were two transversions, c.2010C>A and c.2094G>T predicting p.Asn670Lys and p.Glu698Asp substitutions, in the calf-1 domain of α_{IIb}. The p.Asn670Lys substitution was predicted to be deleterious to α_{IIb} with all five computational tools used. In contrast, the p.Glu698Asp substitution was predicted to be deleterious using only two tools, suggesting this substitution is more likely to be benign. Glu698 is conserved in α_{IIb} in 8 of the 12 species examined, but poorly conserved among other α integrin family members, while Asn670 was conserved in 11 species, and in 5 of the 8 other α-integrin proteins. Structural modelling of α_{IIb} shows Asn670 is located at the top of the calf-1 domain, in the genu region of α_{IIb}, between the thigh and calf-1 domains. According to Xie*, et al* (2004), the genu-calf-1 interaction is rigid and maintained during integrin activation, but the interface between the genu-thigh is rearranged to provide the extension required for

activation. This suggests that the genu region and the genu-calcium binding site are important for activation. Asn670 forms hydrogen bonds with neighbouring residues, including Gln642, Gly672, Met724 and Glu673. Importantly, these residues are located in the vicinity of the genu-calcium binding site, with Glu673 forming part of the site. The replacement of asparagine by the positively charge amino acid lysine leads to a loss of hydrogen bonding and introduces a positive charge in the acidic area and steric clashing with surrounding residues, especially Glu673. These findings suggest that the p.Asp670Lys substitution disturbs the normal coordination of the calcium binding site and the genu domain. Thus, this variant may exert deleterious effects on α_{IIb} which could lead to altered $\alpha_{IIb}\beta_3$ activation. **Therefore, we hypothesised that the p.Asn670Lys substitution results in a reduced or normal membrane surface expression of $\alpha_{IIb}\beta_3$ accompanied by altered integrin function.**

Modelling of Glu698 was not possible due to poorly defined structural features in the α_{IIb} model in the region where this residue is located. Interestingly, a re-evaluation of the c.2094G>T transversion in *ITGA2B* that predicts the p.Glu698Asp substitution revealed that this nucleotide alteration occurred at the last position in exon 20 of *ITGA2B* and was likely to have a deleterious effect on RNA splicing, and result in exon-skipping, the activation of a cryptic splice site or intron retention. These consequences can result in forming an alternative protein sequence or the introduction of a stop codon and can lead to the formation of a truncated protein or result in nonsense-mediated decay, hence mRNA degradation (Gonzalez-Manchon*, et al* 2003, Nurden*, et al* 2012b). These findings suggest that the c.2094G>T defect is more likely to mediate its pathogenicity through abnormal splicing. **Therefore, we hypothesised that the c.2094G>T results in a splicing defect of *ITGA2B*-mRNA**.

3.5 Conclusion

In summary, the findings presented in this chapter suggest that 13 of the *ITGA2B* and *ITGB3* variants which were studied were deleterious to the $\alpha_{IIb}\beta_3$ receptor and were likely to be responsible for the bleeding tendency that was seen in the GT cases in which they were identified. In contrast, the *ITGB3* defect predicting the Glu200Lys variant was predicted to be a benign alteration via *in silico* analysis. Therefore, we hypothesise that:

- The β_3-p.Trp11Arg, β_3-p.Arg119Gln, β_3-p.Pro189Ser, β_3-p.Trp264Leu, β_3-p.Ser317Phe, α_{IIb}-p.Asp396Asn, α_{IIb}-p.Leu492Pro and α_{IIb}-p.Ile596Thr variants result in severely reduced or absent membrane expression of the $\alpha_{IIb}\beta_3$ receptor.
- The β_3-p.Cys547Trp, β_3-p.Cys554Arg and α_{IIb}-p.Asn670Lys variants result in normal or reduced membrane expression of $\alpha_{IIb}\beta_3$ accompanied by altered integrin function.
- The p.Ile665Thr substitution in β3 causes a qualitative defect of the $\alpha_{IIb}\beta_3$ receptor.
- The c.2094G>T transversion in *ITGA2B* results in an aberrant splicing of *ITGA2B*-mRNA.
- The p.Glu200Lys substitution in β_3 does not have any deleterious effects on $\alpha_{IIb}\beta_3$ biogenesis and expression.
- The p.Trp11Arg, p.Arg119Gln, p.Trp264Leu and p.Ser317Phe substitutions in β_3 will result in a severe reduction or complete absence of membrane expression of the $\alpha_v\beta_3$ receptor, while the p.Pro189Ser, p.Glu200Lys and p.Ile665Thr substitutions will be less deleterious to $\alpha_v\beta_3$ expression.

The above hypotheses have been investigated using a variety of *in vitro* approaches and the findings are presented in Chapters 4 (β_3 variants) and 5 (α_{IIb} variants). While the p.Arg119Gln variant was not taken any further as part of this study, it was further characterised by another student in our laboratory as part of a Masters level project which was co-supervised by the candidate. Some of the results are reproduced here where appropriate, and for the sake of comparison (Almusbahi 2014).

Chapter 4: Functional Characterisation of β_3 Variants

4.1 Introduction

Previous analysis of the *ITGA2B* and *ITGB3* genes encoding the $\alpha_{IIb}\beta_3$ receptor which was undertaken as part of a survey of UK patients with GT identified 14 candidate defects in *ITGB3*. In this study, the potential effects of some of these candidate defects on the structure and function of $\alpha_{IIb}\beta_3$ were predicted using a variety of online computational tools and the results were summarised in the previous chapter.

Of the defects identified in the survey, 17 were predicted to cause amino acid substitutions in the receptor, 12 in *ITGB3* and 5 in *ITGA2B*. The majority of these variants were previously unreported or uncharacterised, 8 in *ITGB3* and 5 in *ITGA2B*. Further investigation of the effects of these substitutions on the expression and function of the $\alpha_{IIb}\beta_3$ receptor is therefore warranted. In this chapter, further studies to investigate the pathogenicity of the missense defects identified in *ITGB3* are described, while the results of further work aimed to characterise the defects identified in *ITGA2B* are summarised in Chapter 5.

The genetic alterations in *ITGB3* were c.31T>C, c.356G>A, c.565C>T, c.598G>A, c.791G>T, c.950C>T, c.1641C>G, c.1660T>C, and c.1994T>C which were predicted to cause the following amino acid substitutions in β_3: p.Trp11Arg, p.Arg119Gln, p.Pro189Ser, p.Glu200Lys, p.Trp264Leu, p.Ser317Phe, p.Cys547Trp, p.Cys554Arg and p.Ile665Thr, respectively. Six of the candidate missense defects were novel. The c.1641C>G and c.356G>A variants predicting the p.Cys547Trp and p.Arg119Gln variants had been described previously but had not been not characterised to any extent (Kannan*, et al* 2009, Peretz*, et al* 2006). The c.31T>C variant predicting the p.Trp11Arg was novel at the outset of the study as it has recently been identified in the international cohort but was not characterised (Nurden*, et al* 2015). These amino acid substitutions occurred in different domains of the β_3 subunit including the signal peptide (p.Trp11Arg), the hybrid domain (p.Arg119Gln), the ligand binding domain (p. Pro189Ser, p.Glu200Lys, p.Trp264Leu and p.Ser317Phe), the cysteine rich repeats (p.Cys547Trp and p.Cys554Arg) and the β tail domain (p.Ile665Thr). The eight variants investigated in this chapter were associated with variable clinical symptoms and bleeding severities (Table 1.2). Thus, studying these mutations will further our understanding of the molecular basis of Glanzmann thrombasthenia in addition to highlighting the roles of specific residues in the structure and function relationships of the $\alpha_{IIb}\beta_3$ integrin.

Here it is worth noting that the remaining three missense variants identified by Al-Marwani (2009) which predicted substitutions in β_3 (p.Leu143Trp, p.Asp145Asn and

p.Arg240Gln) had been previously reported and characterised in other studies (Bajt*, et al* 1992, Basani*, et al* 1997, Loftus*, et al* 1990). In brief, the p.Asp145Asn and p.Arg240Gln substitutions do not affect the membrane expression of $\alpha_{IIb}\beta_3$ but they do disturb integrin function and abrogate fibrinogen binding. Interestingly, Asp145 and Arg240 are located at the top of the ligand binding domain and characterisation of these variants helped to identify the key residues involved in fibrinogen binding on the $\alpha_{IIb}\beta_3$ receptor (Bajt*, et al* 1992, Loftus*, et al* 1990). In contrast, the p.Leu143Trp substitution which occurs in the ligand binding domain of the β3 subunit caused severe reductions in the membrane expression of $\alpha_{IIb}\beta_3$ (Basani*, et al* 1997). Therefore, these three variants were excluded from the current studies.

A further two variants, p.Arg119Gln and p.Cys547Trp, the expression of which was predicted by the c.356G>A and c.1641C>G *ITGB3* defects respectively, were investigated under my supervision by a master's student in the haemostasis research group; of which the surface expression of $\alpha_{IIb}\beta_3$, total β_3 expression, PAC-1 and fibrinogen binding was examined (Almusbahi 2014). In addition, further examination of the p.Cys547Trp variant has been undertaken as part of this project and therefore the findings for the p.Cys547Trp variant, obtained as part of the master's project, have been presented in this chapter for the reason of completeness. However, the p.Arg119Gln variant resulted in a severe reduction of $\alpha_{IIb}\beta_3$ expression and was therefore not taken any further as part of this study (Almusbahi 2014).

Table 4.1 Clinical features of index cases with inherited defects in *ITGB3*.

Nucleotide change	Predicted amino acid substitution	Genotype	Treatment	Anti-$\alpha_{IIb}\beta_3$*	Bleeding symptoms/ score[x]
c.31T>C-c.565C>T	p.Trp11Arg, p. Pro189Ser	Compound heterozygous	Platelets, rVIIa	Unknown	Epistaxis / 5
c.598G>A	p.Glu200Lys	Homozygous	Platelets	No	Epistaxis / 3
c.791G>T	p.Trp264Leu	Homozygous	RBC, Platelets, rVIIA	Yes	Epistaxis / 10
c.950C>T	p.Ser317Phe	Homozygous	Platelets, rVIIA	Yes	Epistaxis and menorrhagia / 8
c.1641C>G	p.Cys547Trp	Homozygous	Platelets, rVIIa	No	Epistaxis / 3
c.1660T>C	p.Cys554Arg	Homozygous	Platelets, rVIIa	No	Epistaxis / 3
c.1994T>C	p.Ile665Thr	Homozygous	RBC, Platelets, rVIIa	No	Epistaxis – Gastrointestinal bleeding / 7

*Indicates whether patients developed antibodies to $\alpha_{IIb}\beta_3$ in response to platelet transfusion. [x]Bleeding severity, assessed subjectively by the referring clinician on a scale of 1 to 10, where 1 is minor and 10 is severe bleeding. RBC: red blood cells; rVIIa:recombinant factor VIIa.

4.2 Hypotheses and Aims

Based on the *in silico* analyses presented in Chapter 3, and published data relating to β3 structure and function, we hypothesise that:

1. The p.Trp11Arg, p.Trp264Leu and p.Ser317Phe amino acid substitutions are deleterious to the β_3 subunit and will result in a severe reduction or complete absence of membrane surface expression of the $\alpha_{IIb}\beta_3$ and $\alpha_v\beta_3$ receptors.
2. The p.Pro189Ser substitution results in abnormal heterodimer formation between β_3 and α_{IIb} and the absence of $\alpha_{IIb}\beta_3$ receptor expression, while it has less deleterious effects on heterodimer formation between β_3 and α_v.
3. The p.Cys547Trp and p.Cys554Arg substitutions result in reduced or normal membrane surface expression of the $\alpha_{IIb}\beta_3$ receptors which do not signal normally.
4. The p.Ile665Thr substitution results in qualitative abnormality of $\alpha_{IIb}\beta_3$.
5. The p.Glu200Lys substitution does not have any deleterious effects on $\alpha_{IIb}\beta_3$ and $\alpha_v\beta_3$.
6. The p.Cys547Trp and p.Cys554Arg substitutions result in normal or reduced membrane expression of $\alpha_v\beta_3$.

To investigate the above hypotheses, Chinese Hamster Ovary (CHO) cells were co-transfected with recombinant *ITGB3* and wild-type (WT)-*ITGA2B* expression vectors before using flow cytometry and western blotting to assess membrane and intracellular expression of $\alpha_{IIb}\beta_3$ in the cells. CHO cells are widely used in *in vitro* studies of GT as they show no endogenous expression of the $\alpha_{IIb}\beta_3$ receptor (Jayo*, et al* 2006, Shen*, et al* 2009). In addition, the ability of the recombinant integrin to undergo the conformational change that is required to allow ligand binding was assessed in those cases where the receptor was expressed stably on the cell membrane.

4.3 Methods

CHO cells were co-transfected with recombinant *ITGB3* and WT-*ITGA2B* expression vectors as described in section 2.2.2.13. After allowing the cells to recover for 48 hours, cell surface and total expression of $\alpha_{IIb}\beta_3$ were analysed using flow cytometry and expression of β_3 and α_{IIb} was assessed in cell lysates by Western blotting (see sections 2.2.2.14 and 2.2.2.18). The activation of $\alpha_{IIb}\beta_3$ receptors was assessed using the ligand-mimetic antibody, PAC-1 and labelled fibrinogen (see section 2.2.2.17).

4.3.1 Proteasome inhibition of cells expressing p.Trp11Arg

CHO cells were co-transfected with the p.Trp11Arg expression construct and wild-type β3 as described in section 2.2.2.13. Forty eight hours following transfection, cells were treated with 10µm or 20µm MG-132, a cell-permeable proteasome inhibitor (Sigma-Aldrich, Missouri, USA). The cells were treated with 10 µm for various time points, 1,2,4,6 hours, and 20µm for 1 and 3 hours. The cells were then fixed and permeabilized as described in section 2.2.2.16 to allow intracellular staining of the of total β_3 using a monoclonal antibody.

4.3.2 Detection of p.Trp11Arg cDNA using PCR

CHO cells were co-transfected with either wild-type or p.Trp11Arg *ITGB3* cDNA and wild-type *ITGA2B* cDNA expression plasmids as described in section 2.2.2.13 and allowed to recover by incubation at 37°C for 48 hours. RNA was then extracted from the cells and cDNA generated as described in sections 2.2.2.4, 2.2.2.5 and 2.2.2.6. cDNA derived from the p.Trp11Arg and wild-type expression plasmids was amplified using primers that were complementary to exon 1 of *ITGB3* and as a negative control primers were designed to amplify a fragment of the parental pcDNA3.1 expression plasmid backbone (see Table 4.2). PCR was performed using OneTaq® DNA Polymerase (NEB, Massachusetts, USA) and carried out using a GeneAmp ABI9700 Thermal cycler (Life Technologies Ltd, California, USA). The PCR mixture comprised the following: 1x OneTaq standard reaction Buffer, 200 µM of dNTPs, 0.2 µM forward primer, 0.2 µM reverse primer, 100 ng of cDNA template and 0.025 U/µl *OneTaq*® DNA polymerase. Thermocycling began with an initial denaturation step at 94°C for 30 seconds (secs), followed by 35 cycles of denaturation at 94°C for 10 secs, annealing at 55°C for 30 secs and extension at 68°C for 30 secs, followed by a final extension step at 68°C for 5 minutes. PCR products were then subjected to agarose gel electrophoresis to assess the efficiency of the reaction (see section 2.2.2.1).

The intensities of stained DNA fragments derived from the p.Trp11Arg and wild-type *ITGB3* expression plasmids were compared using densitometry.

Table 4.2 Oligonucleotide primers used to amplify p.Trp11Arg and wild-type cDNAs

Primer	Direction	Primer (5'to 3')
***ITGB3*-cDNA-F**	Forward	GGACCTTTGAGTGTGGGGTA
***ITGB3*-cDNA-R**	Reverse	CTTGCCAAAGTCACTGCTGT
pCDNA3.1	Forward	ACCCACTGCTTACTGGCTTA
pCDNA3.1	Reverse	GGTACAGATGTTGGGCCCT

4.3.3 Cloning of the 31 bp fragment of *ITGB3* into the pcDNA-Dup vector

The plasmid, pcDNA 3.1 Dup is designed to deliver highly level expression in most common cell lines. It is derived from pcDNA 3.1 and has the same elements and features of pcDNA3.1 (see Appendix 1, Table A1 for further details) but has been modified by Tournier et al (2008) for use in an exonic splicing enhancer (ESE)-dependent splicing assay. The plasmid has been generated by cloning a 670bp DNA sequence corresponding to three exons and two introns between the CMV promoter cassette and the poly (A) tail of pcDNA3.1. The outer 5' and 3' exons correspond to exons 3 and 4 of the human β-globin gene while the intervening exon contains EcoRI and BamHI restriction sites to facilitate cloning of putative ESE sequences, and has the donor and acceptor splice sites at the 5' and 3' ends of the exon. The middle exon is flanked both upstream and downstream by 130 nucleotides corresponding to intron 1 of the β -globin gene. The native pcDNA 3.1 Dup plasmid was used as a negative control, while the positive control plasmid included a sequence inserted between the EcoRI and BamHI sites that was known to contain ESE elements, Serine/arginine-rich splicing factor 1 (SRSF1) (Tournier*, et al* 2008). In the current study, 31 nucleotides spanning positions c.583 to c.613 of *ITGB3* and corresponding to either the wild-type or mutated c.598G>A variants was cloned into the middle exon of pcDNA 3.1 Dup. The plasmid map and cloning strategy discussed in Figure 4.1 and sequence is included in **appendix 2**.

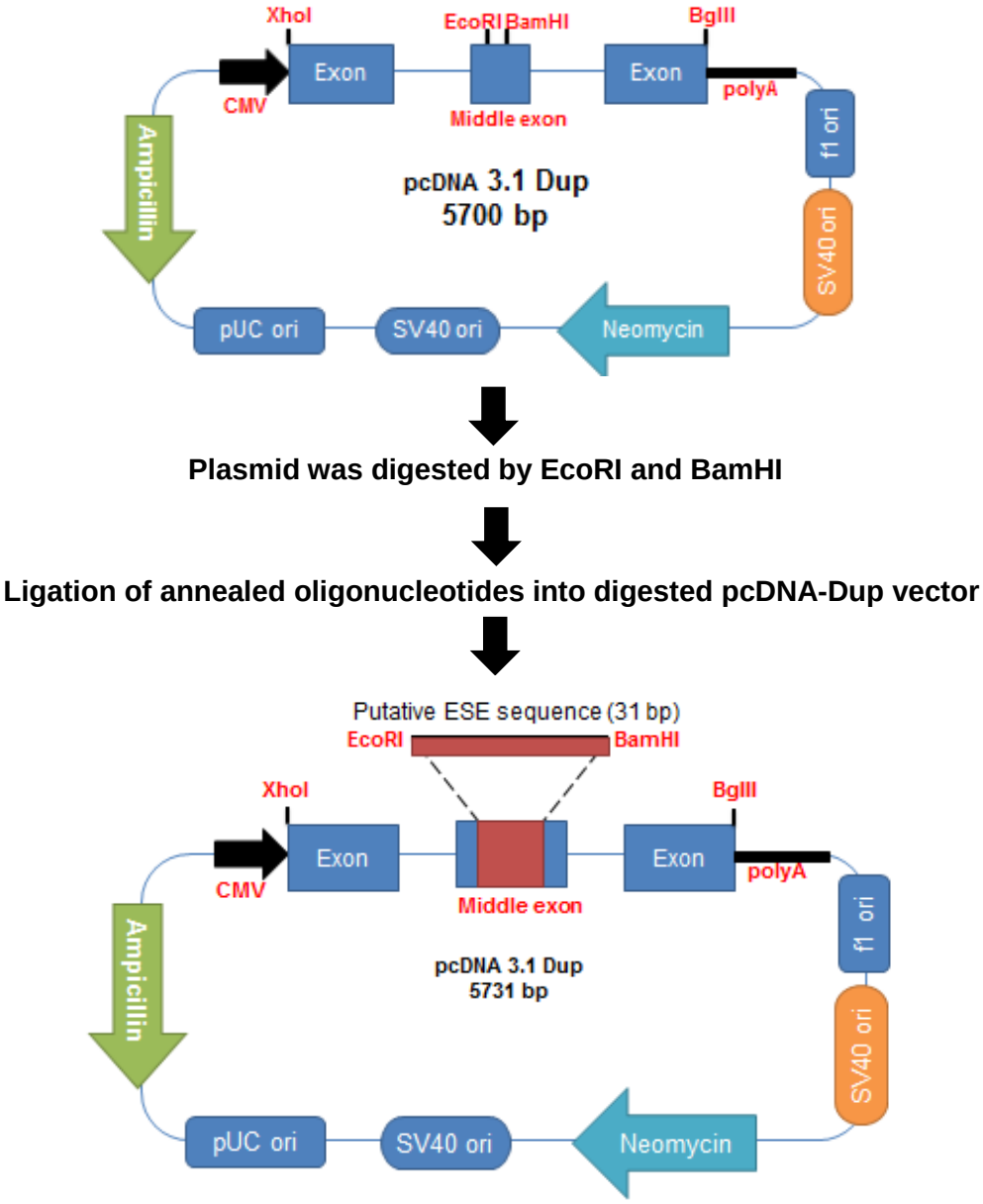

Figure 4.1 Strategy for cloning putative ESE sequence into pcDNA 3.1 Dup. A 31bp annealed double stranded DNA sequence, spanning nucleotides c.583 to c.613 of *ITGB3*, was cloned into pcDNA 3.1 Dup by ligation following restriction with EcoRI and BamHI.

4.3.3.1 Restriction digestion of pcDNA-Dup

The pcDNA-Dup plasmid was received in a glycerol stock which was used to inoculate 250 ml LB broth (25 g/L) containing 100 µg/ml ampicillin to grow the bacteria before purifying the plasmid DNA using a QIAprep Maxiprep kit (Section 2.2.2.9). The restriction digestion was performed used BamHI and EcoRI (NEB, Massachusetts, USA). Five µg of pcDNA-Dup was digested with 50 units of BamHI and, or 50 units of EcoRI in NEB cutsmart buffer for 2 hours at 37ºC. Digested plasmids were analysed by electrophoresis in 0.7% agarose (see Section 2.2.2.1).

4.3.3.2 Generation of insert

Complementary 37-mer oligonucleotides corresponding to the wild-type c.598G or mutated c.598G>A sequence of exon 4 in *ITGB3*, were obtained from Eurofins MWG Operon (Ebersberg, Germany). The oligonucleotides were designed to have overhangs that facilitated directional cloning into pcDNA-Dup digested with EcoRI and BamHI (Table 4.3).

Table 4.3 Oligonucleotide primers used to form insert that is ligated with digested pcDNA-Dup. The c.598G>A substitution is highlighted in underlined bold text whereas the restriction site overhangs are highlighted in red.

Primer	Direction	Primer (5' to 3')	Restriction site
c.598G	Forward	AATTCCCACCAGAGGCCCTC**G**AAAACCCCTGCTATGG	EcoRI
c.598G	Reverse	GATCCCATAGCAGGGGTTTT**C**GAGGGCCTCTGGTGGG	BamHI
c.598A	Forward	AATTCCCACCAGAGGCCCTC**A**AAAACCCCTGCTATGG	EcoRI
c.598A	Reverse	GATCCCATAGCAGGGGTTTT**T**GAGGGCCTCTGGTGGG	BamHI

Samples containing 20 pmol/µl of both the forward and reverse strand oligonucleotides in 500mM NaCl/100mM Tris solution (pH: 8.0) were heated at 95°C for 5 minutes, and then slowly allowed to cool to 25°C. The double stranded product was diluted to 1 pmol/µl before cloning into pcDNA-Dup.

4.3.3.3 Cloning of double stranded oligonucleotide into pcDNA-Dup

A ligation reaction containing 0.22 ng of digested pcDNA-Dup, 0.1 pmol of double stranded oligonucleotide, 1x ligase buffer and 1 unit of T4 DNA ligase in a final volume of 45 µl was incubated for 10 minutes at room temperature before deactivating the DNA ligase by incubation at 70°C for 10 minutes. The ligation reactions were then introduced into competent *E.coli* as described earlier (see section 2.2.2.7). Following overnight growth of the transformed bacteria, a single colony was used to inoculate 5 ml of LB-broth before carrying out minipreps to harvest the plasmid DNA (section 2.2.2.8). The presence of the insert in the plasmid was confirmed by DNA sequence analysis as described in section 2.2.2.10.

4.3.4 Transfection and PCR analysis

CHO cells were transfected with pcDNA-Dup plasmids containing the wild-type and mutated *ITGB3* sequences or with the native pcDNA-Dup as a negative control as previously described 2.2.2.13. The RNA was harvested as described in section 2.2.2.4 and transcribed to cDNA using the QuantiTect Reverse Transcription Kit (see Section 2.2.2.6). PCR was performed as described in section 4.3.2 using OneTaq® DNA Polymerase and the primers listed in table 4.4, with an annealing temperature of 44°C. The PCR products were then subjected to agarose gel electrophoresis to assess the efficiency of the reaction, and estimate product size (Section 2.2.2.1).

Table 4.4 Oligonucleotide primers used to amplify the cDNA products of pcDNA-Dup plasmids.

Primer	Direction	Primer (5'to 3')
T7-Pro	Forward	TAATACGACTCACTATAGGG
Dup-2R	Reverse	GGACTCAAAGAACCTCTGGG

4.4 Results

4.4.1 Optimization experiments

Prior to characterising the variants identified in the GT patients, preliminary experiments were undertaken to determine the optimal conditions for transfection of CHO cells and detection of α_{IIb}, β_3 and $\alpha_{IIb}\beta_3$, and to generate the expression plasmids bearing the candidate *ITGB3* alterations, and that this work will be described in this section.

4.4.1.1 Determination of optimal antibody dilutions for detection of α_{IIb} and β_3

The Human Erythrocyte Leukaemia (HEL) cell line was used in experiments to determine the optimal antibody dilutions for detection of β_3, α_{IIb} and the $\alpha_{IIb}\beta_3$ complex, as these cells possess megakaryocyte-like properties and express a number of platelet proteins including the $\alpha_{IIb}\beta_3$ receptor, thus making them a suitable positive control. Cells were harvested and stained with different antibody dilutions as described in section 2.2.2.15. Flow cytometric analysis of HEL cells stained with 1:20 and 1:16 dilutions of anti-α_{IIb} (CD41) monoclonal antibody revealed 96% and 98% of the cell population to be positively stained, respectively (Figure. 4.2A). The cells stained with 1:20 and 1:16 dilutions of anti-β_3 (CD61) showed 81% and 92% of the cell population to be positively stained, respectively (Figure. 4.2B). While the cells stained with 1:20, 1:16, 1:12 and 1:8 dilutions of anti-$\alpha_{IIb}\beta_3$ (CD41/CD61) antibody showed approximately 75%, 79%, 85% and 92% of the cells to be positively stained, respectively (Figure 4.2C). Therefore, 1:16 dilutions of the α_{IIb} and β_3 antibodies were used to detect the α_{IIb} and β_3 subunits in subsequent experiments, while a 1:8 dilution of the anti-CD41/CD61 complex was used to detect the $\alpha_{IIb}\beta_3$ receptor.

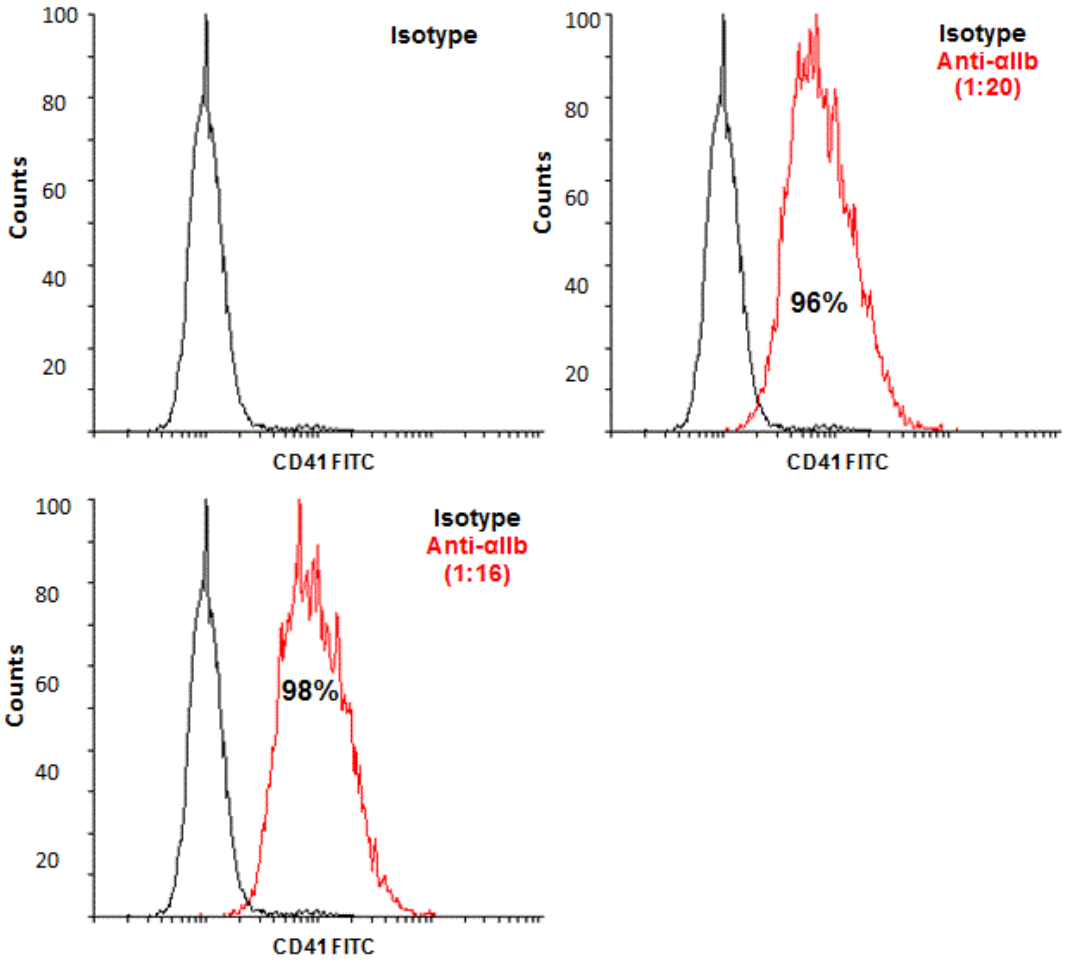

Figure 4.2A Detection of α_{IIb} subunit on HEL cells by flow cytometry. HEL cells were incubated with two dilutions of anti-α_{IIb} antibody, 1:20 and 1:16. Flow cytometric analysis showed approximately 96% and 98% of cells stained positive for α_{IIb} subunit at the indicated dilutions of antibody. X-axis represents fluorescent intensity and y-axis represents the number of events (cell count).

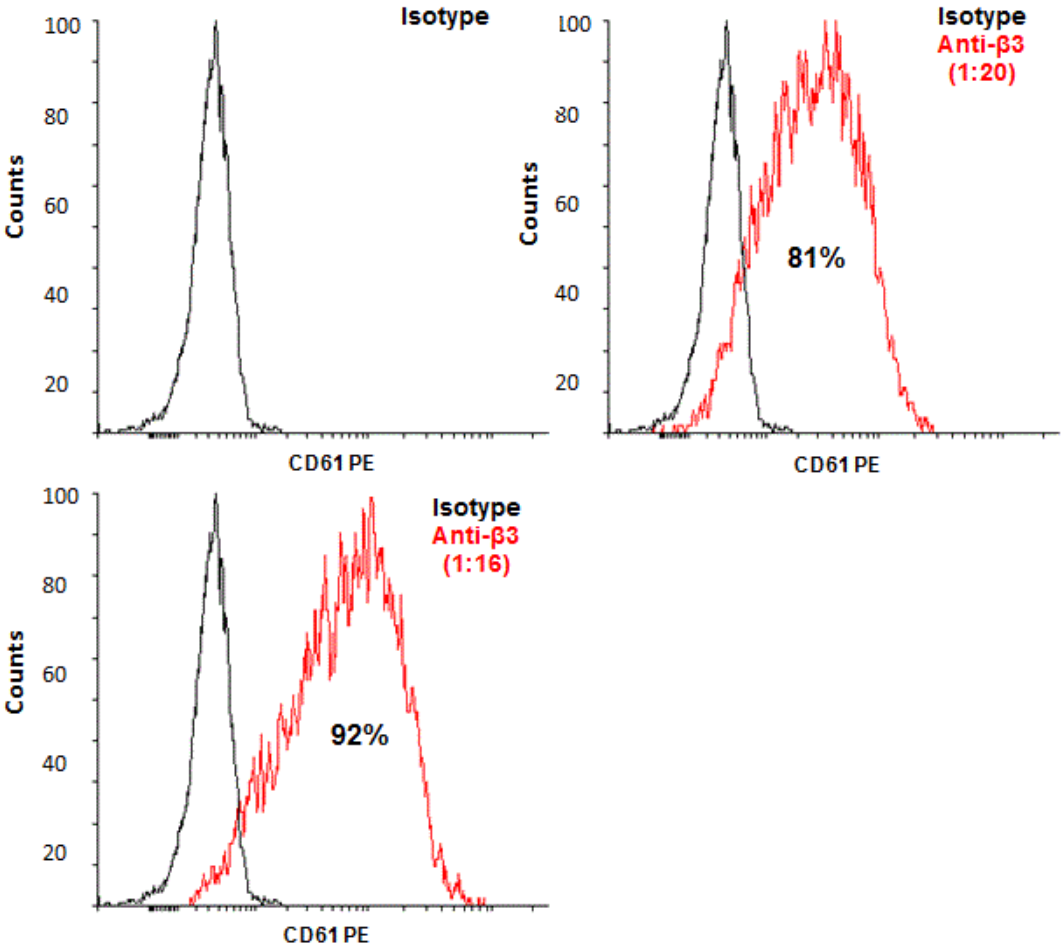

Figure 4.2B Detection of β_3 subunit on HEL cells by flow cytometry. HEL cells were incubated with two dilutions of anti-β_3 antibody, 1:20 and 1:16. Flow cytometric analysis showed approximately 81% and 92% of cells stained positive for β_3 subunit at the indicated dilutions of antibody. X-axis represents fluorescent intensity and y-axis represents the number of events (cell count).

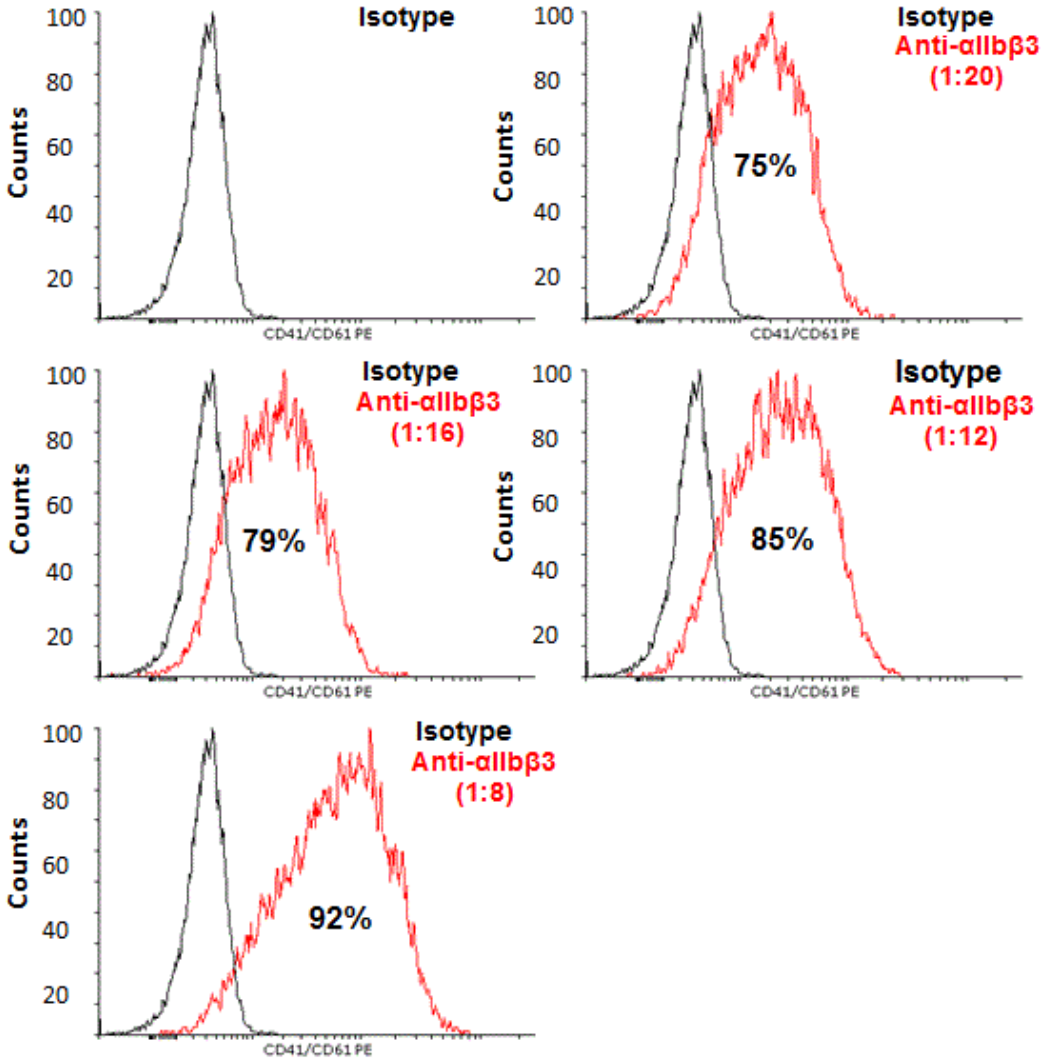

Figure 4.2C Detection of $\alpha_{IIb}\beta_3$ complex on HEL cells by flow cytometry. HEL cells were incubated with four dilutions of anti-$\alpha_{IIb}\beta_3$ antibody, 1:20, 1:16, 1:12 and 1:8. Flow cytometric analysis showed approximately 75% 79%, 85% and 92% of cells stained positive for $\alpha_{IIb}\beta_3$ receptor at the indicated dilutions of antibody. X-axis represents fluorescent intensity and y-axis represents the number of events (cell count).

.

4.4.1.2 Determination of the optimal volume of lipofectamine® for transfection of CHO cells

CHO cells were transiently transfected with fixed amounts (1 µg) of wild-type *ITGA2B*-pcDNA and *ITGB3*-pcDNA expression plasmids using varying volumes (3.0 to 5.5 µl) of lipofectamine® ltx as described in section 2.2.2.13. Importantly, the transfected cells appeared similar to untransfected cells when examined by inverted light microscopy at all concentrations of lipofectamine used (data not shown). Cell surface expression of β_3 and α_{IIb} was examined 48 hours after transfection by flow cytometry. The analysis showed that 20% to 63% of CHO cells expressed α_{IIb} over the range of lipofectamine® ltx concentrations used. Similarly, between 23% and 66% of cells were positive for β_3 over the same range of volumes of lipofectamine® ltx used (Table 4.5 and Figure 4.3). There was very little increase in expression of α_{IIb} and β_3 when the volume of lipofectamine® ltx was increased from 5.0 to 5.5 µl. For this reason, subsequent transfections were undertaken using 5 µl of the transfection reagent.

Table 4.5 The percentage of CHO cells staining positive for α_{IIb} and β_3 following transfection with *ITGA2B*-pcDNA and *ITGB3*-pcDNA using various volumes of lipofectamine® ltx

Lipofectamine® ltx (µl)	% of β_3 positive cells	% of α_{IIb} positive cells
3	23	20
3.5	28	27
4	40	47
4.5	42	48
5	65	61
5.5	66	63

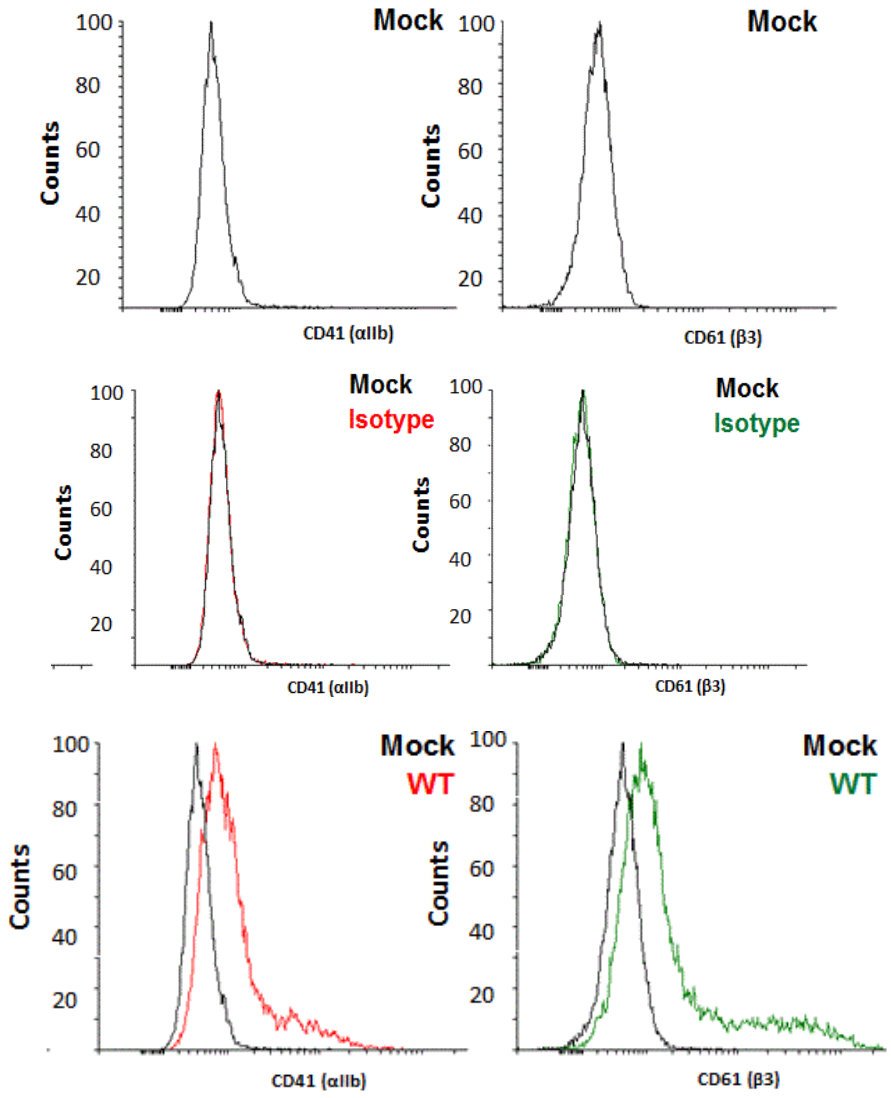

Figure 4.3 Flow cytometric analysis to determine the optimal concentration of lipofectamine®ltx for transfection of CHO cells. CHO cells were co-transfected with wild-type *ITGA2B* and *ITGB3* cDNAs or mock transfected with empty pcDNA3.1 as a negative control using 5 µl of lipofectamine®ltx to facilitate transfection. Forty eight hours following transfection, the cells were incubated with PE- and FITC-conjugated monoclonal antibodies against α_{IIb} (CD41) and β_3 (CD61), respectively. In addition, cells were stained with PE and FITC labelled mouse IgG1 isotype control antibodies to assess non-specific binding and confirm the specificity of the primary antibody. Flow cytometric analysis showed 61% of transfected cells expressed α_{IIb} while 65% of cells were positive for β_3. The detection of α_{IIb} and β_3 subunits is shown in red and green, respectively.

4.4.1.3 Generation of variant ITGB3 expression constructs

In order to examine the effects of the seven *ITGB3* missense variants, site-directed mutagenesis was carried out to introduce the corresponding single nucleotide changes into pcDNA3.1 bearing the wild-type *ITGB3* cDNA as described in section 2.2.2.11. Following mutagenesis, sequence analysis of the recombinant expression plasmids was conducted to confirm the presence of the desired alteration and also that no further changes had been introduced into the *ITGB3* cDNA. Sequence analysis of the recombinant plasmids revealed the successful introduction of the alterations predicting the p.Trp11Arg, p.Pro189Ser, p.Glu200Lys, p.Trp264Leu, p.Ser317Phe, p.Cys554Arg and p.Ile665Thr substitutions, with only the desired alteration being present in all cases (Figure 4.4).

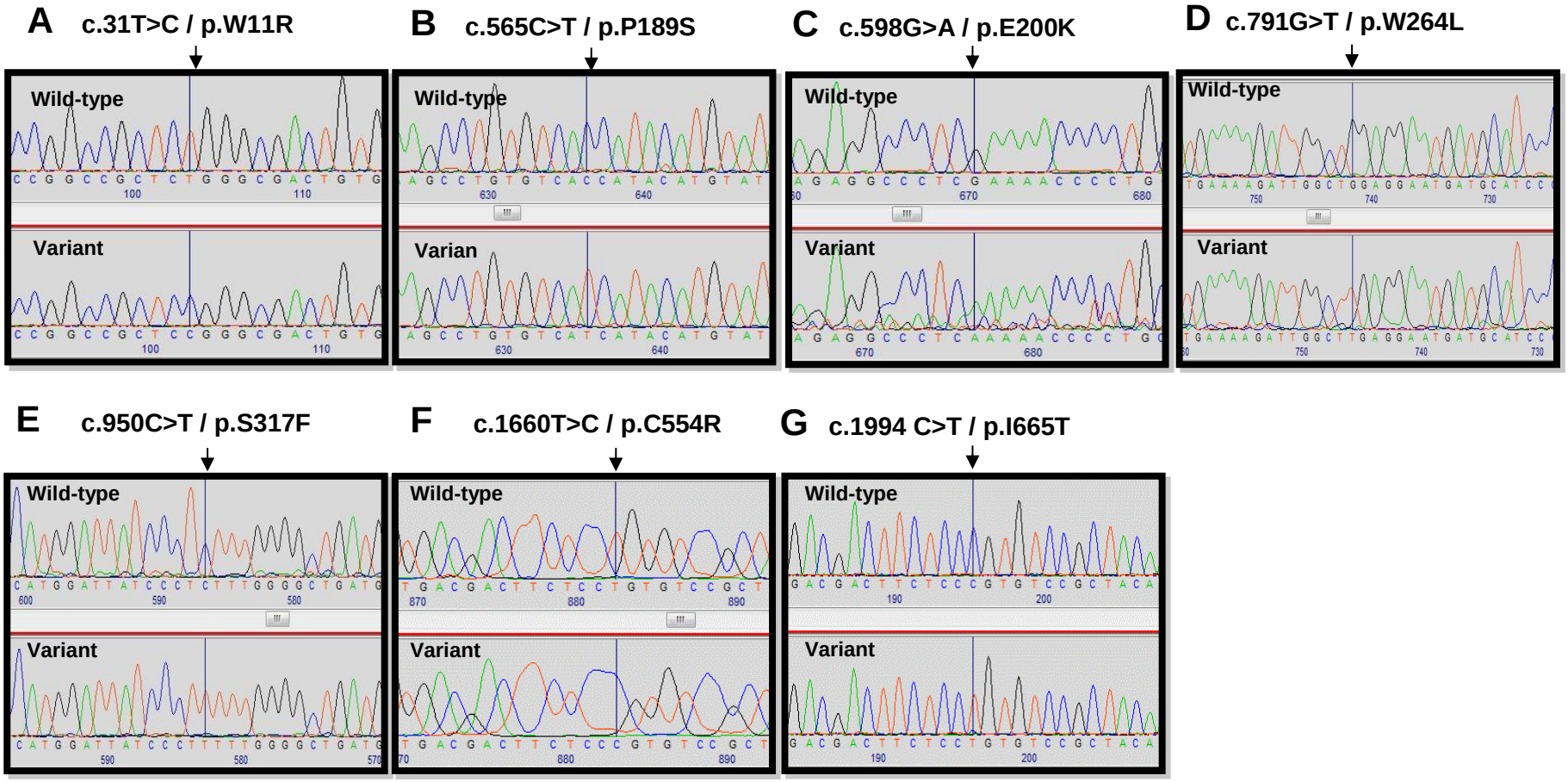

Figure 4.4 Sequence chromatograms displaying fragments of the wild-type and recombinant *ITGB3* expression plasmids showing the positions of single nucleotide changes introduced by site-directed mutagenesis. The chromatograms demonstrate the introduction of mutations to derive the (A) p.Trp11Arg, (B) p. Pro189Ser, (C) p.Glu200Lys, (D) p.Trp264Leu, (E) p.Ser317Phe, (F) p.Cys554Arg and (G) p.Ile665Thr β3 variants. The black arrows indicate the positions of nucleotide changes.

4.4.2 Membrane expression of $\alpha_{IIb}\beta_3$ in CHO cells expressing β_3 variants

To further characterise the p.Trp11Arg, p.Pro189Ser, p.Glu200Lys, p.Trp264Leu, p.Ser317Phe, p.Cys554Arg and p.Ile665Thr variants that were predicted to occur as a result of *ITGB3* defects identified in index cases with GT, CHO cells were co-transfected with wild-type *ITGA2B* cDNA and either wild-type or variant *ITGB3* cDNA. CHO cells were also transfected with the empty expression plasmid (pcDNA3.1) to act as a negative control and to measure background fluorescence of the antibodies. Following 48 hours of transfection, the cells were incubated with monoclonal antibodies against α_{IIb}, β_3 and $\alpha_{IIb}\beta_3$ receptor complex, and surface expression of $\alpha_{IIb}\beta_3$ was assessed using flow cytometry. In addition, cells co-transfected with wild-type *ITGB3* and *ITGA2B* cDNAs were stained with antibody isotypes to assess non-specific binding of the anti-integrin antibodies.

Flow cytometric analysis demonstrated a complete lack of surface expression of $\alpha_{IIb}\beta_3$ in cells expressing the p.Trp11Arg, p.Trp264Leu and p.Ser317Phe variants when compared with cells expressing the wild-type β_3 ($p<0.0001$). There was a 96% reduction ($p<0.0001$) in membrane expression of $\alpha_{IIb}\beta_3$ in cells expressing the p.Pro189Ser variant when compared with cells expressing the wild-type receptor, while co-expression of the p.Trp11Arg and p.Pro189Ser variants (in order to mimic the compound heterozygous genotype of the patient) resulted in a 95% reduction in $\alpha_{IIb}\beta_3$ expression ($p<0.0001$). CHO cells expressing the p.Cys554Arg and p.Cys547Trp variants showed a significant reduction ($p<0.0001$) in $\alpha_{IIb}\beta_3$ expression, by 58% and 31% when compared with wild-type receptor, respectively. Interestingly, CHO cells expressing the p.Glu200Lys and p.Ile665Thr variants demonstrated similar surface expression of $\alpha_{IIb}\beta_3$ to that observed in cells expressing the wild-type receptor ($p=0.39$, $p=0.35$, respectively) (Figures 4.5 and 4.6)

These findings were confirmed by repeating the transfection and then assessing receptor expression by flow cytometry using an anti $\alpha_{IIb}\beta_3$ antibody (Figures 4.7 and 4.8). Consistent with the findings above, flow cytometric analysis showed a complete absence of membrane $\alpha_{IIb}\beta_3$ expression in cells expressing the p.Trp11Arg, p.Trp264Leu and p.Ser317Phe variants compared to cells expressing wild-type β_3 ($p<0.0001$). CHO cells expressing the p.Pro189Ser, p.Cys554Arg and p.Cys547Trp variants showed significant 94%, 37% and 36% reductions in $\alpha_{IIb}\beta_3$ expression, respectively, when compared with cells expressing wild-type receptor, and co-expression of the p.Trp11Arg and p.Pro189Ser variants results in a 95% reduction in a

$\alpha_{IIb}\beta_3$ expression ($p<0.0001$). CHO cells expressing the p.Glu200Lys and p.Ile665Thr variants showed similar surface expression of $\alpha_{IIb}\beta_3$ to that observed in cells expressing the wild-type receptor ($p=0.96$, $p=0.9$, respectively).

An interesting observation was the high percentage (36%) of CHO cells expressing the p.Pro189Ser variant that stained positive with the anti-β_3 PE antibody, compared to the 1% which stained positive using the antibody to the $\alpha_{IIb}\beta_3$ receptor complex (Figure 4.5). This suggested that the p.Pro189Ser variant can be expressed on the surface of the CHO cells without forming a heterodimer with α_{IIb} and raised the possibility that the p. Pro189Ser variant may be capable of forming a heterodimer with endogenous α_v in CHO cells resulting in expression of $\alpha_v\beta_3$ (vitronectin receptor) at the cell surface. This finding suggests that the p.Pro189Ser variant is unable to bind to α_{IIb} but is still capable of binding to endogenously expressed α_v (more details in section 4.4.3).

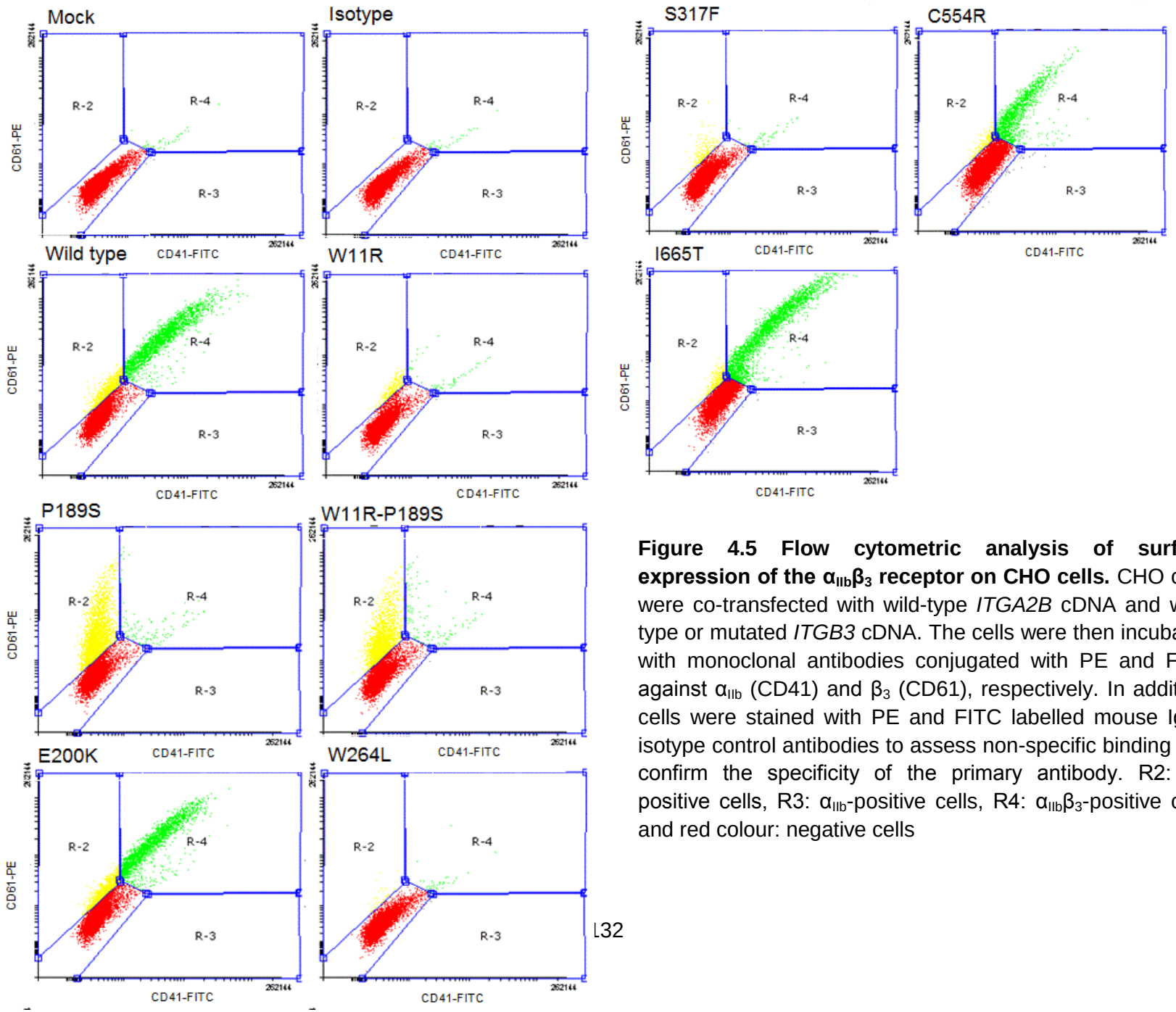

Figure 4.5 Flow cytometric analysis of surface expression of the $\alpha_{IIb}\beta_3$ receptor on CHO cells. CHO cells were co-transfected with wild-type *ITGA2B* cDNA and wild-type or mutated *ITGB3* cDNA. The cells were then incubated with monoclonal antibodies conjugated with PE and FITC against α_{IIb} (CD41) and β_3 (CD61), respectively. In addition, cells were stained with PE and FITC labelled mouse IgG1 isotype control antibodies to assess non-specific binding and confirm the specificity of the primary antibody. R2: β_3-positive cells, R3: α_{IIb}-positive cells, R4: $\alpha_{IIb}\beta_3$-positive cells and red colour: negative cells

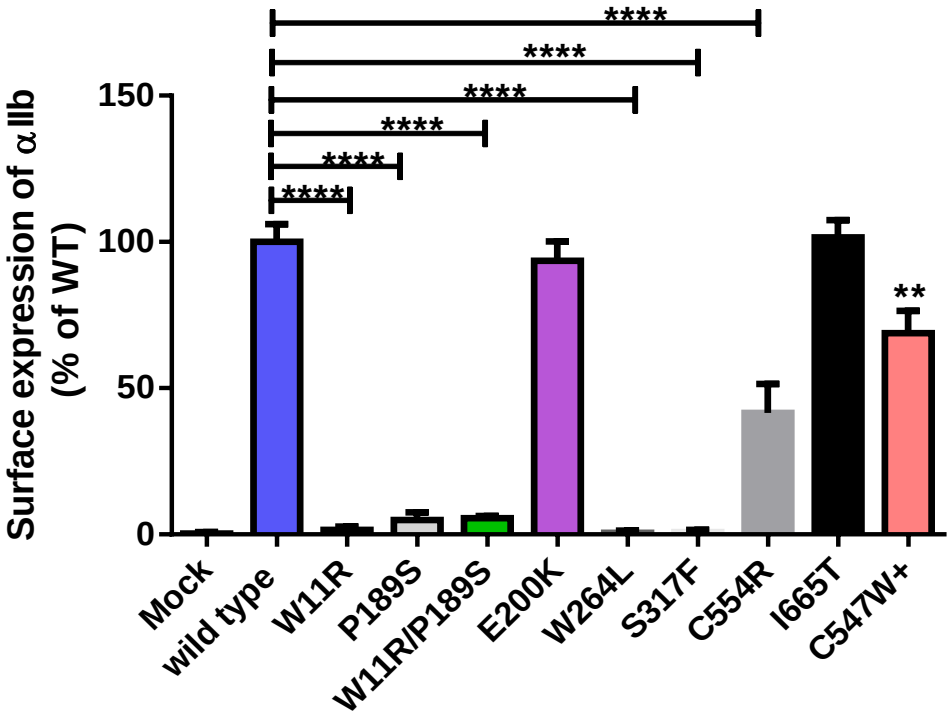

Figure 4.6 Flow cytometric analysis of surface α_{IIb} expression on transfected CHO cells. Membrane expression of α_{IIb} on CHO cells expressing β_3 variants relative to that in cells expressing the wild-type receptor (normalized to 100%). CHO cells were transfected with wild-type *ITGA2B* cDNA and either wild-type or variant *ITGB3* cDNA, or mock transfected with empty pcDNA3.1 vector as a negative control. Cells were incubated with anti-α_{IIb} monoclonal antibody conjugated with FITC. The figure shows a severe reduction in expression of the α_{IIb} receptor by CHO cells expressing the p.Trp11Arg, p.Pro189Ser, p.Trp264Leu and p.Ser317Phe variants. The co-transfection of p.Trp11Arg and p.Pro189Ser constructs demonstrates 95% reduction in the level of membrane expression of α_{IIb} compared to wild-type receptor. The p.Cys554Arg and p.Cys547Trp variants led to a significant reduction in surface expression of α_{IIb}, to 42% and 69% of the levels observed in cells expressing wild-type receptor, respectively. The p.Glu200Lys and p.Ile665Thr variants are expressed at similar levels to the wild-type receptor. The data represent the mean of 5 independent experiments with error bars representing the standard deviation. ****p<0.0001,**p<0.01, One-way ANOVA, followed Dunnett's test.+ indicates data provided by A. Almusbahi (Masters project, 2014)(Almusbahi 2014).

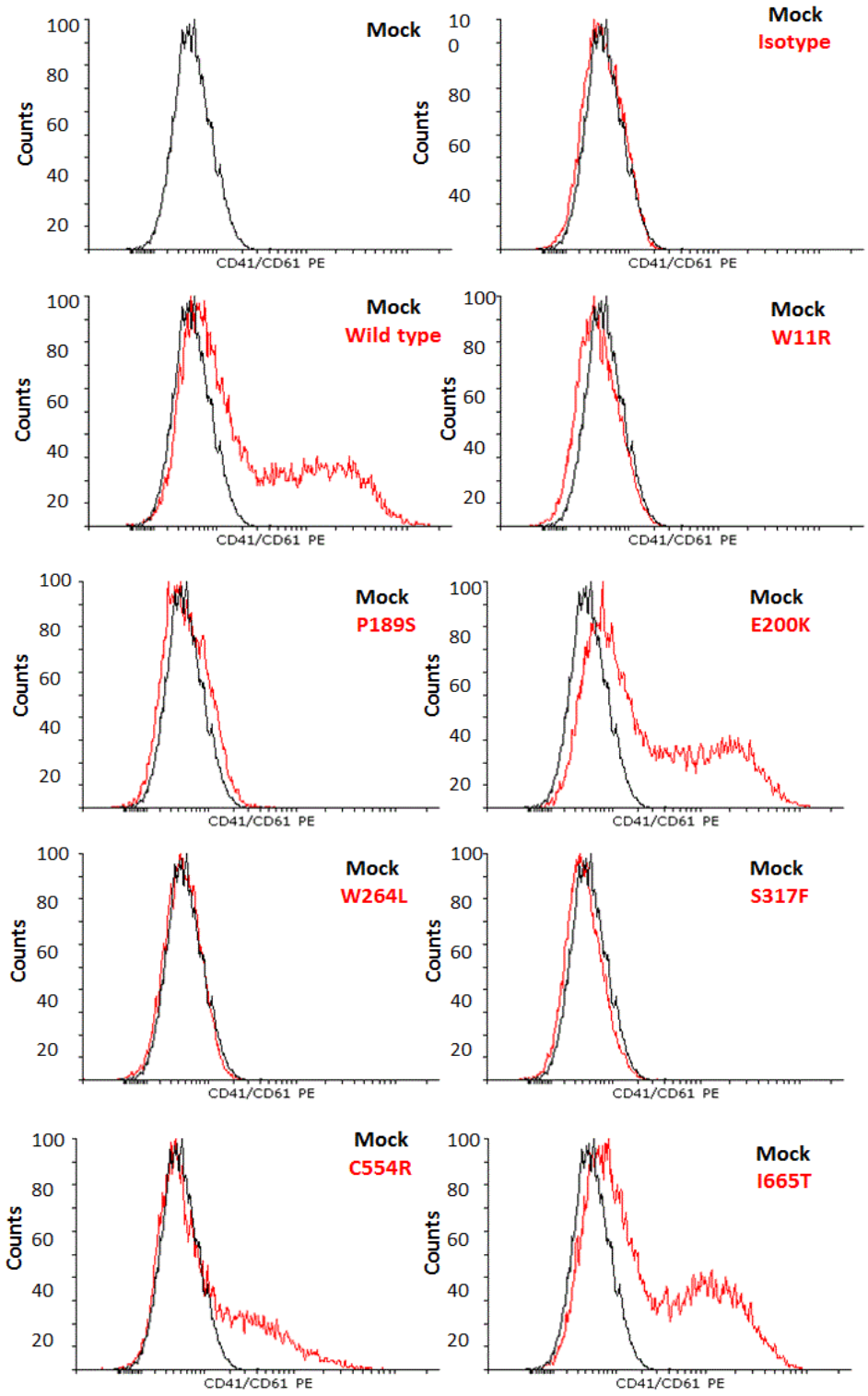

Figure 4.7 Flow cytometric analysis of surface expression of the $\alpha_{IIb}\beta_3$ receptor on CHO cells using anti-$\alpha_{IIb}\beta_3$ antibody. CHO cells were transfected with wild-type *ITGA2B* cDNA and wild-type or variant *ITGB3* cDNA. The cells were then incubated with a PE-conjugated monoclonal antibody against $\alpha_{IIb}\beta_3$. Cells were also stained with a PE-conjugated mouse IgG1 isotype control antibody to assess non-specific binding and confirm the specificity of the primary antibody.

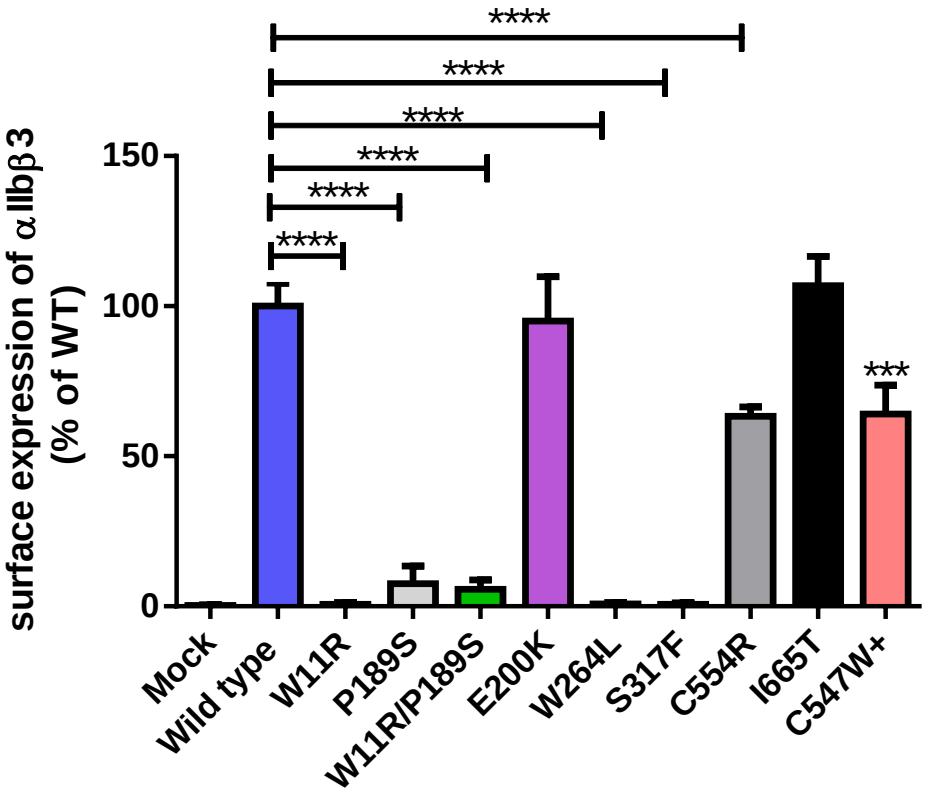

Figure 4.8 Flow cytometric analysis of surface $\alpha_{IIb}\beta_3$ expression on transfected CHO cells detected using anti-$\alpha_{IIb}\beta_3$ antibody. Membrane expression of $\alpha_{IIb}\beta_3$ by CHO cells expressing β_3 variants relative to cells expressing the wild-type receptor (normalized to 100%). CHO cells were transfected with wild-type *ITGA2B* cDNA and either wild-type or variant *ITGB3* cDNA, or mock transfected with empty pcDNA3.1 as a negative control. Cells were incubated with PE-conjugated monoclonal antibody against $\alpha_{IIb}\beta_3$.The figure shows a severe reduction in expression of the $\alpha_{IIb}\beta_3$ receptor by CHO cells expressing the p.Trp11Arg, p.Pro189Ser, p.Trp264Leu and p.Ser317Phe variants. Co-transfection of the p.Trp11Arg and p.Pro189Ser constructs causes a 95% reduction in membrane expression of $\alpha_{IIb}\beta_3$ compared to wild-type receptor. Cells expressing the p.Glu200Lys and p.Ile665Thr variants showed similar levels of the receptor to cells expressing the wild-type receptor. CHO cells expressing the p.Cys554Arg and p.Cys547Trp variants demonstrated a significant reduction in surface $\alpha_{IIb}\beta_3$ expression (by 37% and 36% compared to wild-type, respectively). The data represent the mean of 5 independent experiments with error bars representing the standard deviation. ****p<0.0001, One-way ANOVA followed by Dunnett's test. + indicates data provided by A. Almusbahi (Masters project, 2014).

4.4.3 Membrane expression of $\alpha_v\beta_3$ in CHO cells expressing β_3 variants

β3 is also able to form a heterodimer with the integrin α_v, to form the vitronectin receptor. While CHO cells do not express α_{IIb}, they have been shown to endogenously express α_v, therefore allowing assessment of the ability of β_3 variants to combine with α_v (Chen*, et al* 2001, Schaffner-Reckinger*, et al* 1998). CHO cells were transfected with wild-type *ITGA2B* cDNA and either wild-type or variant *ITGB3* cDNA. The empty plasmid (pcDNA3.1) was also transfected into the CHO cells to act as a negative control and to measure background fluorescence of the antibody. The cells were incubated with monoclonal antibody against the $\alpha_v\beta_3$ integrin, and surface expression was assessed using flow cytometry.

Flow cytometric analysis demonstrated an absence of surface expression of $\alpha_v\beta_3$ in cells expressing the p.Trp11Arg, p.Trp264Leu and p.Ser317Phe variants. Cells expressing the p.Cys554Arg, p.Cys547Trp and p.Glu200Lys variants showed significant reductions in $\alpha_v\beta_3$ expression by 92%, 90% and 78% respectively compared to wild-type ($p<0.0001$). Cells expressing the p.Pro189Ser variant showed a 22% reduction in $\alpha_v\beta_3$ expression compared with cells expressing wild-type β_3 ($p<0.001$). This contrasted with the dramatic reduction in $\alpha_{IIb}\beta_3$ expression observed in cells expressing the p.Pro189Ser variant along with wild-type α_{IIb} (see Figure 4.6). The co-transfection of p.Trp11Arg and p.Pro189Ser constructs (representing the heterozygous form in the patient) caused a moderate reduction by 57% compared to wild-type receptor ($p<0.0001$). Finally, surface $\alpha_v\beta_3$ receptor expression in cells expressing the p.Ile665Thr variant were similar to those observed in cells expressing the wild-type receptor ($p=0.76$) (Figure 4.9).

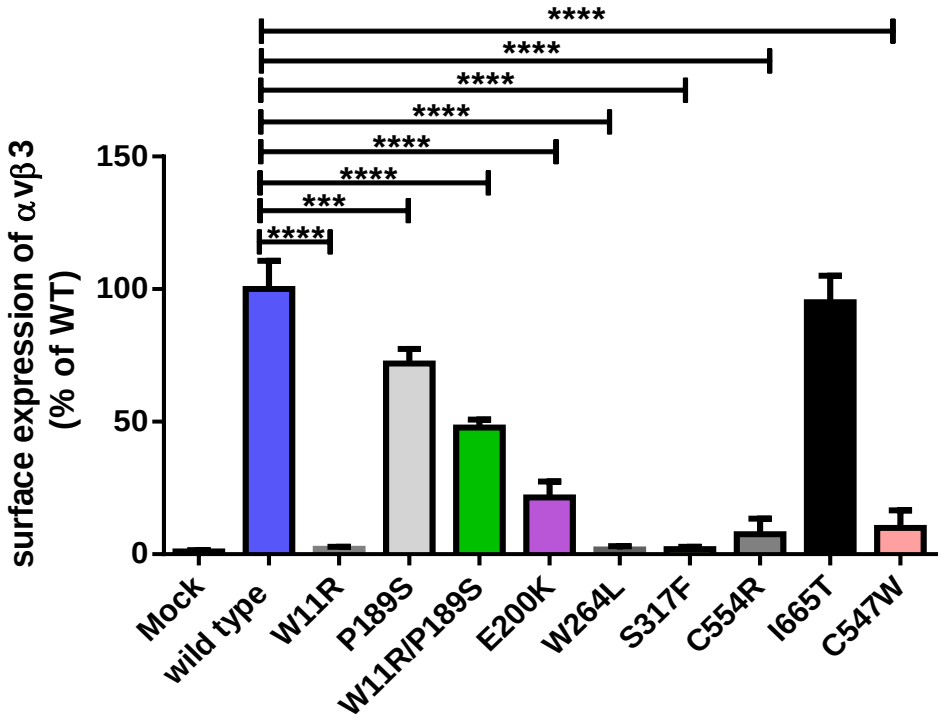

Figure 4.9 Flow cytometric analysis of surface $\alpha_v\beta_3$ expression on CHO cells expressing β_3 variants. Membrane expression of $\alpha_v\beta_3$ by CHO cells expressing β_3 variants relative to that in cells expressing the wild-type receptor (normalized to 100%). CHO cells were transfected with wild-type *ITGA2B* cDNA and either wild-type or variant *ITGB3* cDNA, or mock transfected with empty pcDNA3.1 as a negative control. Cells were incubated with FITC-conjugated monoclonal antibody against $\alpha_v\beta_3$. The figure shows a complete absence of surface expression of the $\alpha_v\beta_3$ receptor by CHO cells expressing the p.Trp11Arg, p.Trp264Leu and p.Ser317Phe variants while low levels were detected in cells expressing the p.Cys554Arg (8%), p.Cys547Trp (10%), and p.Glu200Lys (22%), whereas a reduction in expression was observed for the p.Pro189Ser variant, displaying 78% expression compared to wild-type. The co-transfection of p.Trp11Arg and p.Pro189Ser constructs showed 43% expression of $\alpha_v\beta_3$ compared to wild-type receptor. The p.Ile665Thr showed a similar level of $\alpha_v\beta_3$ receptor to cells expressing the wild-type receptor. The data represents the mean of 5 independent experiments with error bars representing the standard deviation. ***p<0.001; ****p<0.0001; One-way ANOVA, followed by Dunnett's test.

4.4.4 Total expression of β_3 in CHO cells expressing β_3 variants

The lack of membrane expression of $\alpha_{IIb}\beta_3$ in cells expressing the p.Trp11Arg, p.Pro189Ser, p.Trp264Leu and p.Ser317Phe β_3 variants could be explained by a failure of the plasmid to drive β_3 expression, or by a failure of the variant β_3 subunits to form heterodimers with the α_{IIb} chain and hence to be transported to the cell surface. The possibility that the β_3 variants were retained intracellularly was therefore investigated by carrying out intracellular staining of the variant β_3 subunits. CHO cells were transfected with wild-type *ITGA2B* cDNA and either wild-type or variant *ITGB3* cDNA. The empty vector, pcDNA3.1, was also transfected into the CHO cells as a negative control and to measure the background fluorescence of the antibodies. The cells were then fixed and permeabilized as described in section 2.2.2.16 to allow intracellular staining of the proteins. The cells were incubated with monoclonal antibody against β_3, and total β_3 expression was assessed using flow cytometry.

There was an apparent absence of β_3 expression in CHO cells transfected with the p.Trp11Arg expression construct with the level being reduced by 99% compared with that of cells expressing wild-type β_3 ($p<0.0001$) (Figure 4.10). There was a reduction in β_3 expression in CHO cells expressing the p.Pro189Ser, p.Trp264Leu, p.Ser317Leu, p.Cys554Arg and p.Cys547Trp variants with the levels being reduced by 29% ($p<0.01$), 37% ($p<0.001$), 23% ($p<0.05$), 23% ($p<0.05$) and 34% ($p<0.01$) respectively, compared with wild-type (Figure 4.10). The co-transfection of p.Trp11Arg and p.Pro189Ser constructs on CHO cells (representing a heterozygous form in patient) showed 51% ($p<0.0001$) reduction in β_3 expression compared to wild-type β_3 expression. The p.Glu200Lys and p.Ile665Thr variants were expressed at similar levels to those observed in cells expressing the wild-type receptor ($p=0.97$ and $p=0.99$) (Figure 4.10). It was not possible to examine total expression of α_{IIb} due to non-specific binding of the anti-α_{IIb} antibody intracellularly.

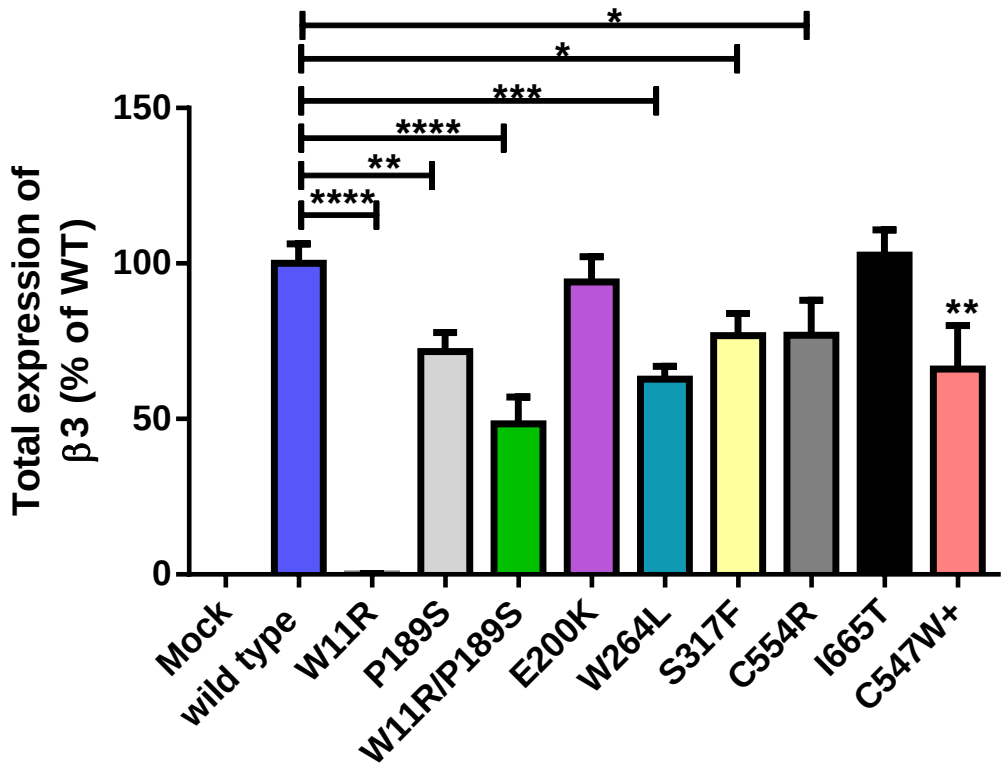

Figure 4.10 Flow cytometric analysis of total β_3 expression in CHO cells expressing variant *ITGB3* cDNAs. Total β_3 variant expression relative to that of wild-type β_3 (normalized to 100%). CHO cells were transfected with wild-type *ITGA2B* cDNA and either wild-type or variant *ITGB3* cDNA, or mock transfected with empty pcDNA3.1 as a negative control. The cells were fixed and permeabilized before being incubated with PE-conjugated monoclonal antibody against β_3. The figure shows an absence of β_3 subunits in CHO cells expressing the p.Trp11Arg variant, while cells expressing the p.Pro189Ser, Trp264Leu, and p.Ser317Phe, p.Cys554Arg and p.Cys547Trp variants show reductions in expression levels by 29%, 37%, 23%, 23% and 34%, respectively. Co-transfection of p.Trp11Arg and p.Pro189Ser constructs on CHO cells showed 51% reduction in total β_3 expression. CHO cells expressing the p.Glu200Lys and p.Ile665Thr variants demonstrated β_3 subunit levels comparable to those of wild-type. The data represents the mean of 3 independent experiments with error bars representing the standard deviation. ****p<0.0001; *** p<0.001; **p<0.01; * p<0.05, One-way ANOVA followed by Dunnett's test. + indicates data provided by A. Almusbahi (Masters project, 2014).

4.4.5 The p.Trp11Arg variant is not susceptible to proteasomal degradation

The complete absence of β_3 expression, both on the cell membrane and intracellularly, in CHO cells transfected with the p.Trp11Arg expression construct may reflect an increased susceptibility of the p.Trp11Arg β_3 subunit to proteasomal degradation. This possibility was investigated by treatment of transfected cells with 10µm or 20µm MG-132, a cell-permeable proteasome inhibitor (Section 4.3.1). The cells were then fixed and permeabilized as described in section 2.2.2.16 to allow intracellular staining of the of total β_3.There was a lack of expression of β_3 in CHO cells expressing the p.Trp11Arg variant with the level being reduced by 99% compared with that of the wild-type receptor at the two concentrations of MG-132 and different time points tested ($p<0.0001$) (Figure 4.11). The absence of any apparent accumulation of the p.Trp11Arg variant in cells where proteasome was inhibited, suggested that either the p.Trp11Arg variant was not targeted for proteasome degradation, or that the p.Trp11Arg variant was not stably expressed at the protein level.

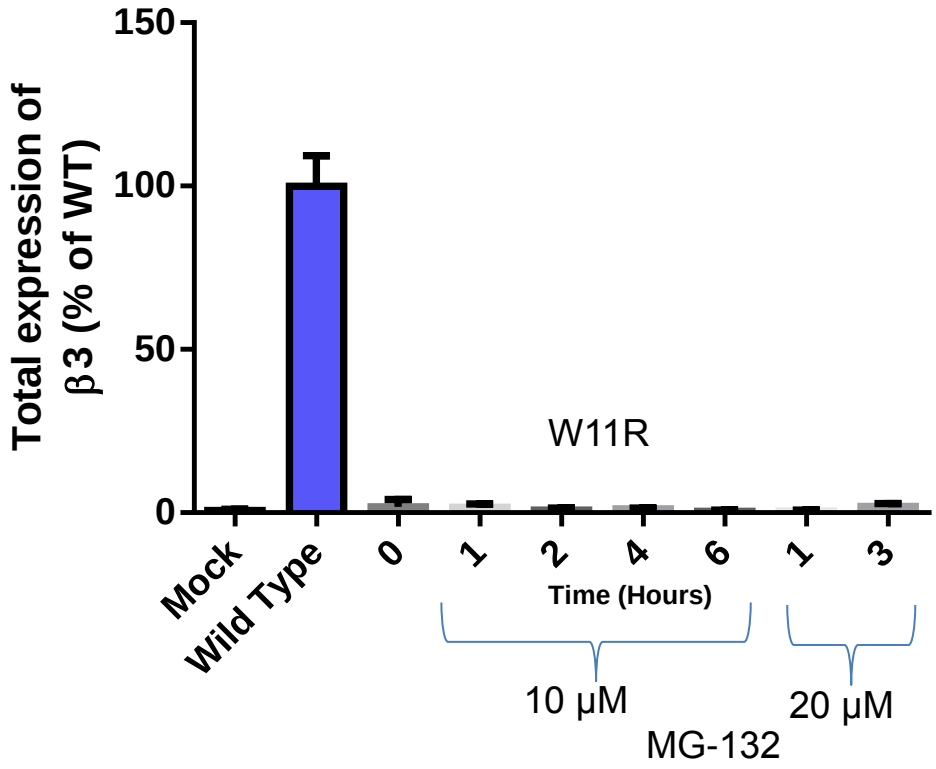

Figure 4.11 Total β_3 expression in CHO cells expressing the p.Trp11Arg variant following proteasome inhibition using MG-132. Total p.Trp11Arg variant expression is shown relative to that of wild-type β_3 (normalized to 100%). CHO cells were transfected with wild-type *ITGA2B* cDNA and either wild-type or p.Trp11Arg cDNA, or mock transfected with empty pcDNA3.1 as a negative control. Forty-eight hours post-transfection, cells were treated with 10μm or 20μm MG-132 or DMSO for the indicated time. The cells were then fixed and permeabilized before incubation with an anti-β_3 monoclonal antibody conjugated to PE. The results show no apparent accumulation of p.Trp11Arg β_3 in cells following proteasome inhibition at the indicated MG-132 concentrations and time points. The data represent the mean of 5 independent experiments with error bars representing the standard deviation. Statistical analyses were calculated by Two-way ANOVA.

4.4.6 The p.Trp11Arg variant is expressed normally at the RNA level

The failure of proteasome inhibition to cause accumulation of the p.Trp11Arg variant in CHO cells may be explained by a lack of expression of the variant, as opposed to its rapid degradation after expression. This possibility was investigated by examining expression of the p.Trp11Arg variant at the RNA level. Following transfection of CHO cells with the p.Trp11Arg and wild-type β_3 constructs, RNA was isolated, and any genomic or plasmid DNA remaining in the preparation was removed by digestion. Reverse transcription was carried out to generate cDNA before PCR was performed using two different sets of primers to amplify fragments of the *ITGB3* cDNA and the plasmid backbone (see Section 4.3.2). Importantly, *ITGB3* RNA was detected in the cells transfected with the p.Trp11Arg expression construct in similar amounts to those observed in cells expressing the wild-type β_3 construct (Figure 4.12 A). Densitometric analysis of the results showed an approximate 10% reduction in *ITGB3* RNA expression in cells transfected with the p.Trp11Arg variant which was not significant, ($p=0.54$) (Figure 4.12 B).

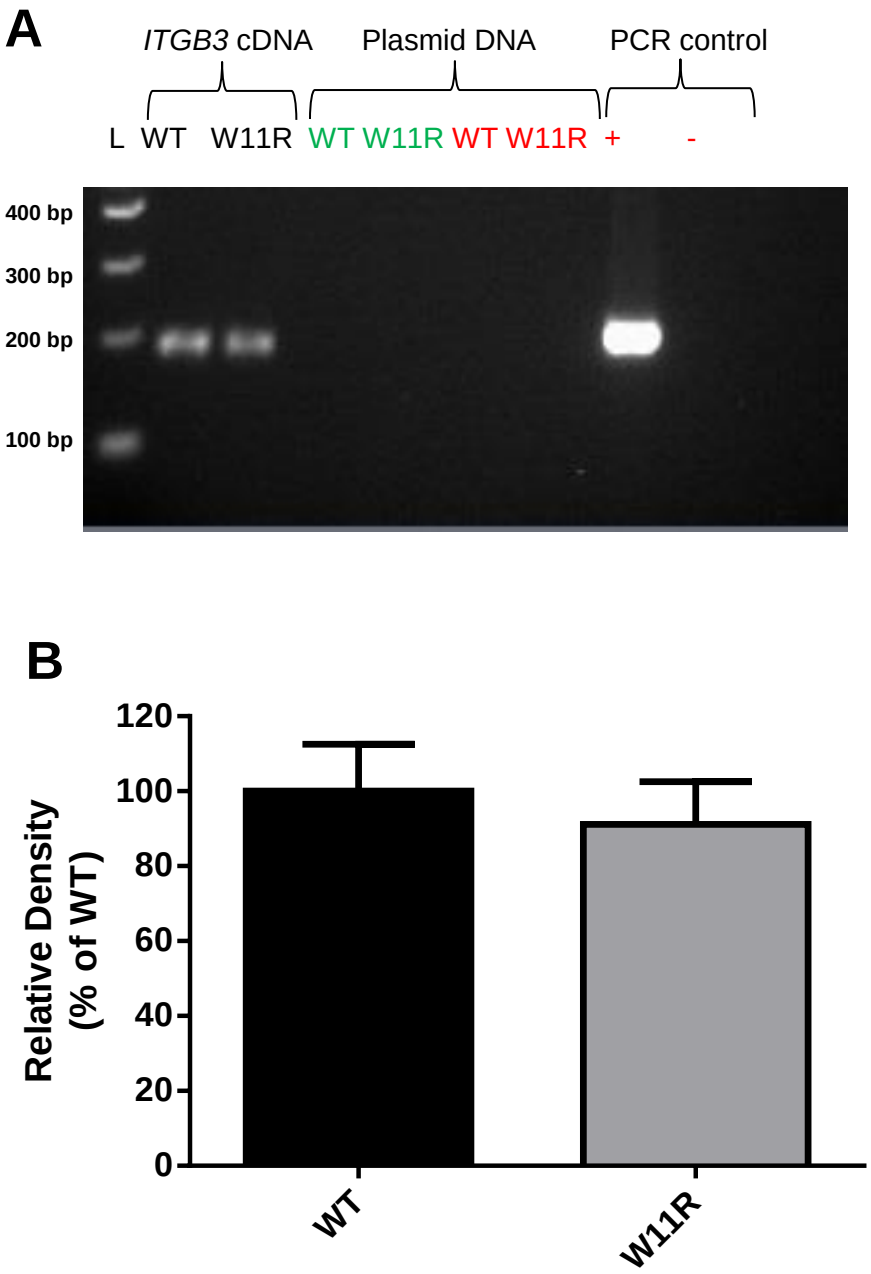

Figure 4.12 mRNA expression levels for the p.Trp11Arg variant. A) Electrophoresis of amplified *ITGB3* cDNA fragments. Fragments of the *ITGB3* mRNA and pcDNA3.1 backbone were amplified using two different sets of primers. Similar mRNA expression levels were observed in cells transfected with wild-type *ITGB3* and the p.Trp11Arg variant. In addition, no product was amplified using vector-specific primers either before (green) or after (red) reverse transcription, indicating the absence of contaminating plasmid DNA, while a product was amplified from the positive control of the plasmid backbone (+). (-) indicates the no template control B) Densitometric analysis of the amplified *ITGB3* cDNA fragments using ImageJ. No difference in wild-type and p.Trp11Arg mRNA expression levels was observed (p=0.54, unpaired students t-test). The data represents the mean of 3 independent experiments with error bars representing the standard deviation.

4.4.7 Evaluation of intracellular β_3 and α_{IIb} expression in cells transfected with β_3 variants

To further elucidate the mechanism for reduced membrane expression of $\alpha_{IIb}\beta_3$ in CHO cells transfected with the p.Trp11Arg p.Pro189Ser, p.Trp264Leu, p.Ser317Phe, p.Cys547Trp and p.Cys554Arg β_3 expression constructs, expression of α_{IIb} and β_3 subunits was analysed by SDS-PAGE of CHO cell lysates under reducing conditions followed by Western blotting of the separated proteins and immunodetection of α_{IIb} and β_3 using polyclonal antibodies as described in section 2.2.2.18. Lysates from cells expressing the p.Glu200Lys and p.Ile665Thr β_3 variants were also analysed to confirm the normal expression of $\alpha_{IIb}\beta_3$ that was observed in cells expressing these variants. The size of pro-α_{IIb} is estimated to be 136 kDa while the mature α_{IIb} and β_3 subunits are 125 kDa and 85 kDa, respectively.

Three immunoreactive protein species having molecular weights of 136 kDa, 125 kDa and 85kDa, and corresponding to pro-α_{IIb}, mature-α_{IIb} and β_3 respectively, were detected in lysates from cells expressing the wild-type β_3, and the p.Glu200Lys and p.Ile665Thr β_3 variants. In contrast, lysates from cells expressing the p.Trp11Arg, p.Pro189Ser, p.Trp264Leu and p.Ser317Phe β_3 subunits revealed the presence of only pro-α_{IIb} and β_3 indicating a failure in processing of pro-α_{IIb} to mature α_{IIb} in the presence of these β_3 variants. Analysis of the lysate from cells expressing the p.Cys554Arg β_3 variant revealed the 85kDa β_3 species as expected. However, α_{IIb} was expressed predominantly as pro-α_{IIb}, and only a trace of mature-α_{IIb} could be detected (Figure 4.13). Interestingly, the β_3 subunit appeared to be expressed at lower concentrations in CHO cells expressing the p.Trp264Leu and p.Ser317Phe variants than in cells expressing the wild-type and other variants of β_3 (Figure 4.13).

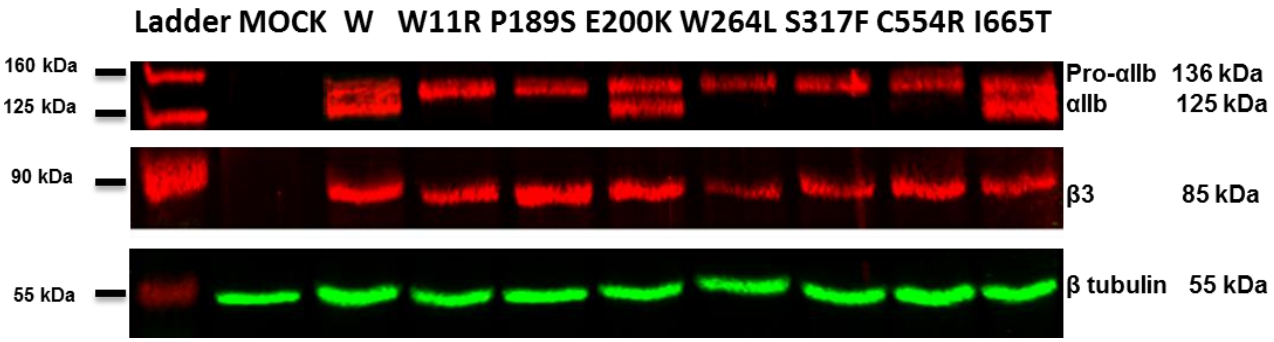

Figure 4.13 Electrophoresis and Western blot analysis of lysates from CHO cells expressing β_3 variants. CHO cells were transfected with wild-type *ITGA2B* cDNA and either wild-type or variant *ITGB3* cDNA, or mock transfected with empty pcDNA3.1 as a negative control. Cell lysates were subjected to electrophoresis in 8% SDS polyacrylamide gels under reducing conditions and then transferred to a nitrocellulose membrane before immunodetection of β_3, α_{IIb} and β-tubulin. The lysates from cells expressing wild-type β_3 and the p.Glu200Lys and p.Ile665Thr showed three immunoreactive protein species at 136,125 and 85kDa, corresponding to pro-α_{IIb}, mature-α_{IIb} and β_3 subunits, respectively. In contrast, western blotting on lysates from cells expressing p.Trp11Arg, p.Pro189Ser, p.Trp264Leu, and p.Ser317Phe demonstrated only two protein species at 136 and 85kDa, corresponding to pro-α_{IIb} and β_3, respectively. The lysate from cells expressing the p.Cys554Arg variant showed three immunoreactive protein species at 136, 125 and 85kDa, corresponding to pro-α_{IIb}, mature-α_{IIb} and β_3 subunits, respectively. However, α_{IIb} was expressed predominantly as pro-α_{IIb}, and only a trace of mature-α_{IIb} could be detected. The β_3 species in lysates from cells expressing the p.Trp264Leu and p.Ser317Phe variants appeared to be present at lower concentrations to those of other variants. β tubulin was used as a loading control.

4.4.8 Activation capacity of β_3 variants

As membrane $\alpha_{IIb}\beta_3$ expression was normal (compared to wild-type) or moderately reduced in CHO cells expressing the p.Glu200Lys, p.Cys554Arg and p.Ile665Thr variants, the ability of the recombinant $\alpha_{IIb}\beta_3$ receptors to undergo the conformational change that occurs on activation and to bind ligand was investigated by flow cytometry. Activation of $\alpha_{IIb}\beta_3$ was measured using FITC-conjugated PAC-1 which binds only to the active form of the receptor, while ligand binding was assessed using fibrinogen conjugated with Alexa Fluor® 488. Cells were transfected and harvested as described in section 2.2.2.13 and then treated with 20µM DTT (to activate the receptor) or PBS as a control (resting). Cells were then incubated either with the fluorescently labelled PAC-1 or fibrinogen.

4.4.8.1 The p.Cys554Arg and p.Cys547Trp variants show spontaneous activation

The flow cytometric analysis of cells expressing the p.Cys554Arg and p.Cys547Trp variants showed an increased ability to bind both PAC-1 ($p<0.001$ and $p<0.0001$) and fibrinogen ($p<0.01$ and $p<0.0001$) compared to cells expressing wild-type β_3, and without treatment with DTT to activate the receptor (Figure 4.14A and C). Compared to wild-type, the activation index, which corrects for the level of surface receptor expression, showed 6 and 4 folds increase in cells expressing the p.Cys554Arg variant for both PAC-1 ($p<0.0001$) and fibrinogen ($p<0.001$) binding, respectively (Figures 4.14B and D). While the cells expressing p.Cys547Trp variant showed approximately 5.5 and 7.5 folds increase in binding to PAC-1 ($p<0.0001$) and Fibrinogen ($p<0.0001$), respectively (Figure 4.14B and D).

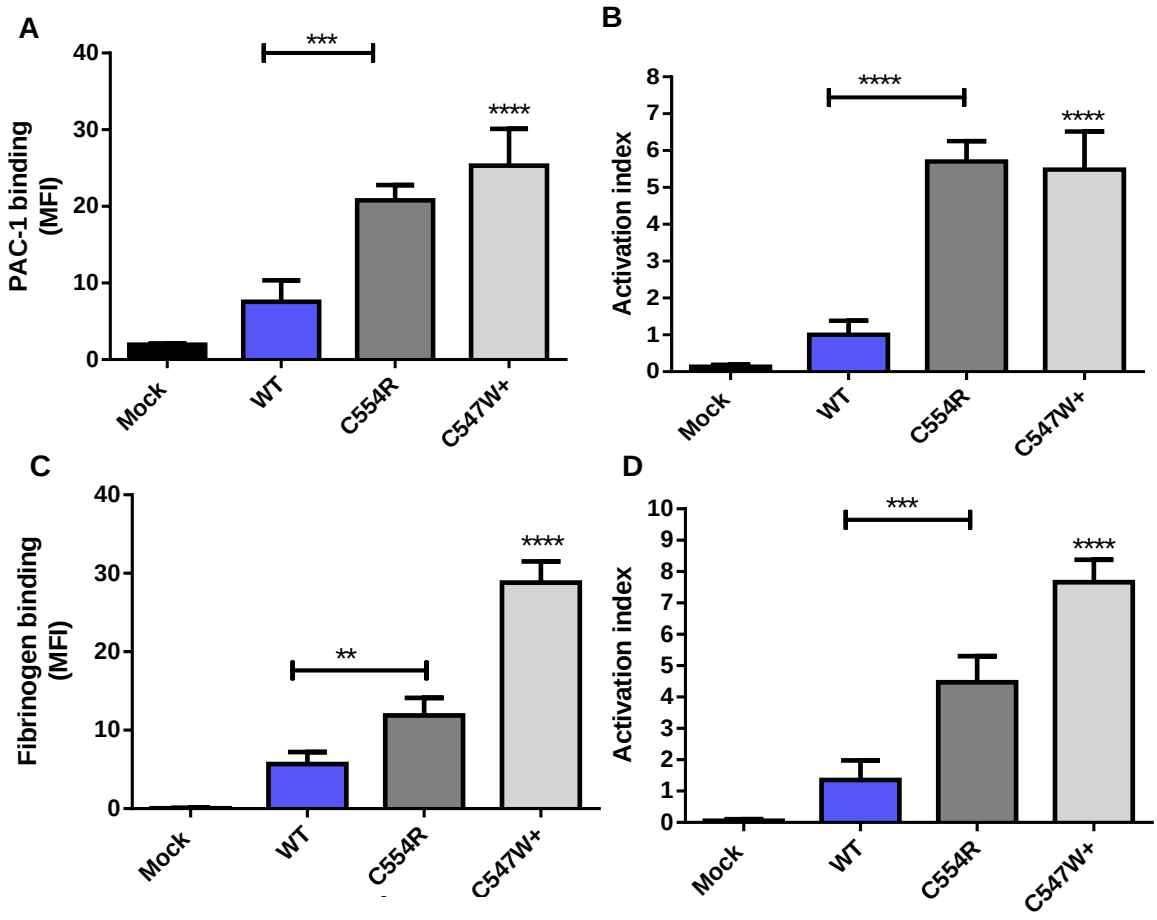

Figure 4.14 Spontaneous binding of PAC-1 and fibrinogen to $\alpha_{IIb}\beta_3$ on CHO cells expressing the p.Cys554Arg and p.Cys547Trp β_3 variants. CHO cells were transfected with wild-type *ITGA2B* cDNA and either wild-type or variant *ITGB3* cDNA, or mock transfected with empty pcDNA3.1 as a negative control. Cells were incubated with either FITC-conjugated PAC-1 or Alexa Fluor® 488-conjugated fibrinogen and analysed by flow cytometry. (A) PAC-1 binding to resting CHO cells; (B) the activation index which is the ratio between PAC-1 binding and surface expression of the variants (corrected for the level of membrane receptor expression). (C) Fibrinogen binding to resting CHO cells; (D) Ratio between fibrinogen binding and surface expression of the variants (corrected for the level of membrane receptor expression). The results show that $\alpha_{IIb}\beta_3$ receptors formed using the p.Cys554Arg and p.Cys547Trp β_3 variants bind spontaneously to PAC-1 and fibrinogen. The data represents the mean of 4 independent experiments with error bars representing the standard deviation of the mean. Statistical analyses were calculated by one-way ANOVA followed by Dunnett's test. ****,p<0.0001; ***,p<0.001,**p<0.01. MFI: mean fluorescence intensity. + indicates data provided by A. Almusbahi (Masters project, 2014)

4.4.8.2 The p.Glu200Lys variant is activated normally while the p.Ile665Thr variant shows aberrant activation

The flow cytometric analysis showed no difference in activation was observed between wild-type cells and cells expressing the p.Glu200Lys (p=0.4) or p.Ile665Thr (p=0.26) variants under resting conditions (Figure 4.15). Following activation with DTT, the $\alpha_{IIb}\beta_3$ in cells expressing the p.Glu200Lys variant was able to bind to both PAC-1 and fibrinogen at levels that were comparable to those of wild-type (p=0.97). In contrast, there was a minor, but significant reduction in PAC-1 (30%) and fibrinogen (15%) binding in cells expressing the p.Ile665Thr variant (Figure 4.15).

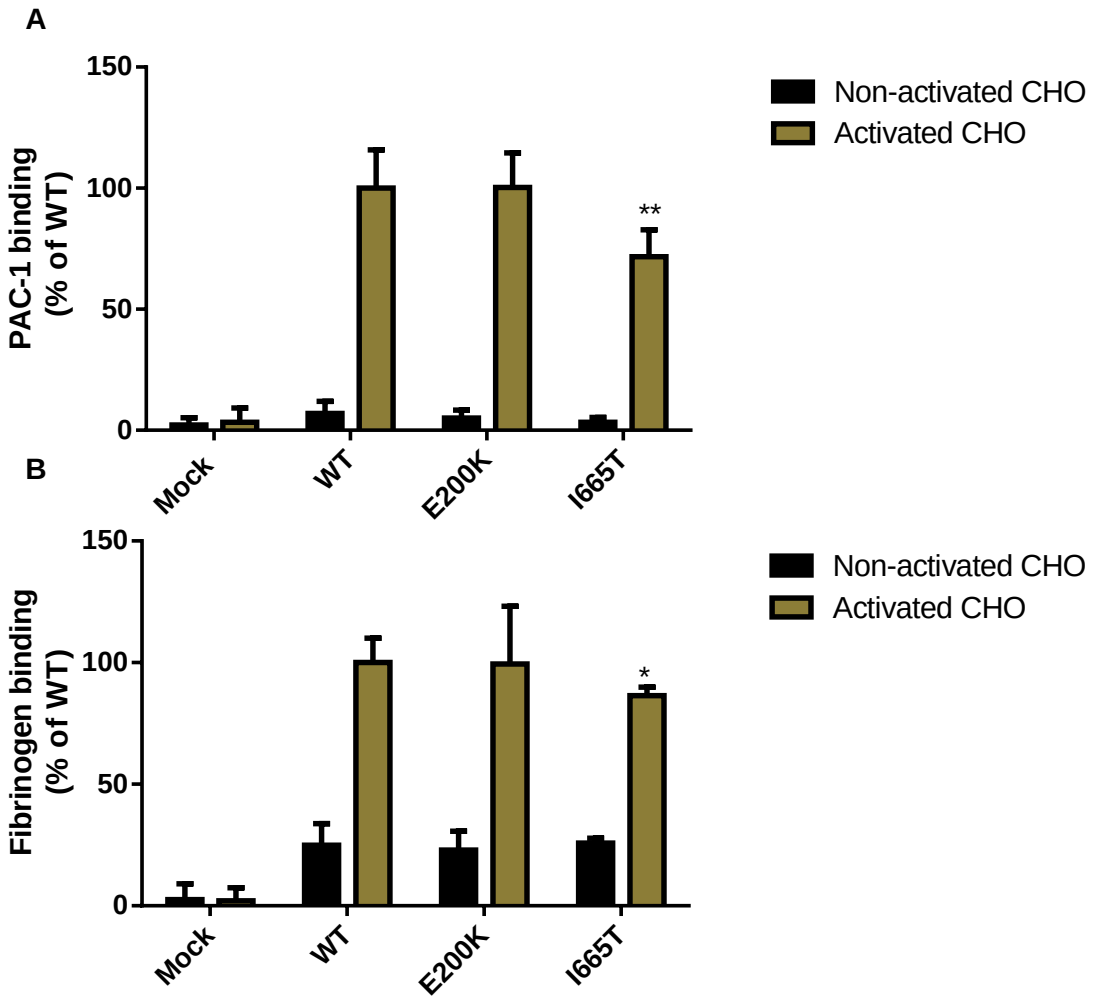

Figure 4.15 $\alpha_{IIb}\beta_3$ activation in CHO cells expressing the p.Glu200Lys and p.Ile665Thr variants. PAC-1 (A) and fibrinogen (B) binding to resting and activated CHO cells. Cells were transfected with wild-type *ITGA2B* cDNA and either wild-type or mutated *ITGB3* cDNA (p.Glu200Lys and p.Ile665Thr), or mock transfected with empty pcDNA3.1 vector as a negative control. Cells were incubated with 20µM DTT (activated) or PBS (resting/non-activated) at 37°C. Cells were then incubated either with PAC-1 conjugated to FITC or soluble fibrinogen conjugated to Alexa Fluor®488 and binding analysed by flow cytometry. Compared to wild-type, PAC-1 and fibrinogen binding were reduced by 30% and 15% respectively in cells expressing p.Ile665Thr, while PAC-1 and fibrinogen binding were similar to wild-type in cells expressing p.Glu200Lys. The data represents the mean of 5 independent experiments with error bars representing the standard deviation of the mean. Statistical analyses were calculated by one-way ANOVA followed by Dunnett's test **,$p<0.01$; *,$p<0.05$.

4.4.8.3 The p.Glu200Lys variant does not alter the rate of integrin activation

The $\alpha_{IIb}\beta_3$ receptor bearing the p.Glu200Lys substitution showed similar surface expression to the wild-type receptor. Furthermore, binding to PAC-1 and fibrinogen were comparable to that observed with the wild-type receptor following treatment with 20mM DTT to induce the conformational change that is associated with activation. To investigate the possibility that the p.Glu200Lys substitution has a more subtle effect on the rate of receptor activation, cells were transfected as previously described (see 2.2.2.13) and treated for 5 minutes with four different concentrations of DTT: 1mM, 5mM, 10mM and 20mM prior to incubation with FITC-conjugated PAC-1 and analysis by flow cytometry. PAC-1 binding of cells expressing the p.Glu200Lys variant was similar to wild-type at all concentrations of DTT used to induce receptor activation (Figure 4.16).

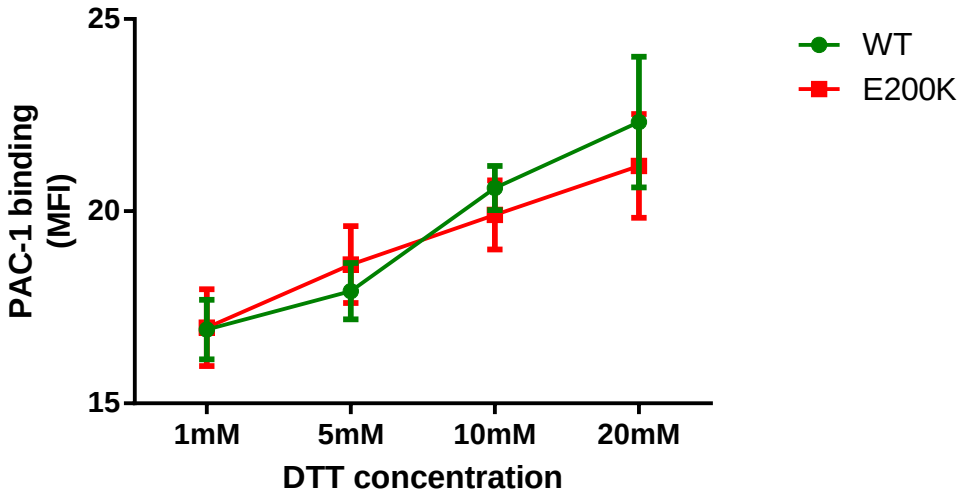

Figure 4.16 PAC-1 binding of $\alpha_{IIb}\beta_3$ in CHO cells expressing the p.Glu200Lys variant following receptor activation with DTT. Cells were transfected with wild-type *ITGA2B* cDNA and either wild-type or mutated *ITGB3* cDNA (p.Glu200Lys). Cells were treated with the indicated concentrations of DTT at 37°C for 5 minutes before incubation with FITC-conjugated PAC-1 and assessment of binding by flow cytometry. Analysis of PAC-1 binding showed a similarity between cells expressing p.Glu200Lys to those expressing wild-type at all DTT concentrations. The data represents the standard deviation of the mean of 4 independent experiments. Statistical analyses were calculated by Two-way ANOVA.

4.4.9 A c.598G>A transition in *ITGB3* does not disturb splicing of the *ITGB3* mRNA

4.4.9.1 In silico prediction of the effects of the c.598G>A transition on ESE sequences

Given that the p.Glu200Lys variant behaved similarly to wild-type β_3 in terms of its membrane expression and ability to bind PAC-1 and fibrinogen, its association with GT remains to be explained. The possibility that the c.598G>A transition which predicts the p.Glu200Lys substitution is deleterious to platelet $\alpha_{IIb}\beta_3$ expression at the RNA level, through causing aberrant splicing, was therefore considered. Preliminary evaluation of the c.698G>A transition showed that it did not disturb, or introduce a cryptic donor or acceptor splice site in *ITGB3* (see section 3.3.3). The possibility that it disturbed an exonic splice enhancer sequence was therefore investigated using the bioinformatic prediction tools ESE-finder and RESCUE-ESE (Cartegni*, et al* 2003, Fairbrother*, et al* 2002). The c.598G>A transition was predicted to decrease the probability of an Serine/Arginine-rich splicing factor (SRSF)-2 motif from 4.1 to 3.6, and also to disrupt SRSF1 and SRSF1 (IgM-BRCA1) motifs using the ESE-finder tool. The RESCUE-ESE tool also predicted the loss of the SRSF1 and SRSF1 (IgM-BRCA1) motifs as a result of the c.698G>A transition (Table 4.6).

Table 4.6 Predictions of ESE sequences spanning the c.698G>A transition in *ITGB3*.

***ITGB3* variant**	**ESE-finder**			**RESCUE-ESE**	
C.598G>A	Motif	Sequence^{+} (WT/variant)	Score (WT/variant)	Sequence^{+} (WT/variant)	Match^{x} (WT/variant)
	SRSF1	CCCTC(G/A)A	2.4/b.t*.	C(G/A)AAAA	1/0
	SRSF1 (IgM-BRCA1)	CCCTC(G/A)A	3.1/b.t.	(G/A)AAAAC	1/0
	SRSF2	GGCCCTC(G/A)	4.1/3.6		

The default threshold values were used with the ESE-finder algorithm, and were as follows: SRSF1: 1.956, SRSF1 (IgM-BRCA1): 1.867 and SRSF2: 2.383. +Putative splicing regulatory sequences, *b.t., below threshold, xMatch, presence (1) or absence (0) of putative ESEs.

4.4.9.2 The c.598G>A nucleotide substitution predicting the p.Glu200Lys substitution does not disrupt exon splicing

Given the comparable levels of membrane expression and similar binding to PAC-1 antibody and fibrinogen of $\alpha_{IIb}\beta_3$ in cells expressing the p.Glu200Lys variant to wild-type cells, the effect of this genetic alteration may stem from an alteration in the splicing mechanism of the *ITGB3* gene. In addition, the platelets from the patient was not available, hence the confirmation of these findings on the patient was not possible. As a result, ESE dependent splicing assay was used to determine the effect of C.598G>A on exon splice enhancer *in vitro*. The potential for the c.598G>A nucleotide change to affect *ITGB3* RNA splicing was investigated using ESE-finder and RESCUE-ESE. *In silico* analysis predicted the c.598G>A transition disturbs an exon splice enhancer (ESE) site. To investigate this possibility, a 31 bp fragment corresponding to nucleotides c.583-c.613 of the *ITGB3* gene (bearing c.598G or c.598A) was inserted in the plasmid pcDNA-Dup (see section 4.3.3). RNA was extracted from CHO cells transfected with the wild-type or mutated pcDNA-Dup and cDNA was generated by reverse transcription. The PCR was then used to amplify the region of cDNA encompassing the two *BHH* exons and the inserted *ITGB3* fragment and the products were analysed by electrophoresis. As expected, the positive control, which contains binding sites for the splicing regulatory protein Serine/Arginine-Rich Splicing Factor 1 (SRSF1), resulted in inclusion of the middle exon in the transcript, while the negative control, which contains intronic sequence derived from *BRCA2* intron-11 without known regulatory elements, excluded the middle exon from the transcript produced (Gaildrat*, et al* 2012, Tournier*, et al* 2008). Both the wild-type and mutated (c.598G>A) minigenes resulted in the inclusion of the middle exon of the spliced transcript (Figure 4.17), suggesting the c.598G>A mutation does not disturb the ESE site within the *ITGB3* gene.

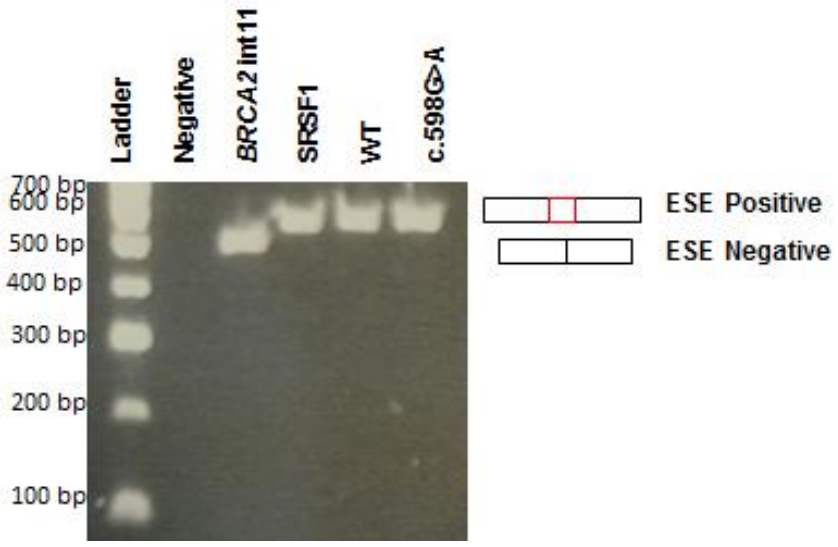

Figure 4.17 Electrophoresis of amplified ESE-dependent splicing products. PCR products of the minigene following electrophoresis in 2% agarose. Amplification of cDNA from cells transfected with the negative control, *BRCA2*int11, produced a fragment corresponding to the two exons without the inserted middle exon, while amplification from cells transfected with the positive control, SRSF1, produces a larger fragment that includes the middle exon containing the functional exon splice enhancer (ESE) regulatory element. Similar to the positive control, pcDNA-dup plasmids containing the *ITGB3* fragment corresponding to both wild-type and mutated c.598G>A alleles produced fragments of similar size to the positive control indicating they also contain ESE regulatory elements and they do not disturb splicing. Results are representative of two independent experiments. Negative: no template control.

4.5 Discussion

GT is an autosomal recessive platelet disorder characterised by a quantitative and/or qualitative deficiency in $\alpha_{IIb}\beta_3$, an integrin receptor that is expressed at high density on the platelet membrane. This disorder is rare in the UK, where it affects approximately 1 in 1 million people. GT patients experience subcutaneous bleeding episodes that vary from mild to life threatening in severity due to a failure in platelet aggregation and thus thrombus formation. A previous study carried out by the Haemostasis Research Group, the University of Sheffield investigated the spectrum of *ITGB3* and *ITGA2B* defects underlying GT in 37 unrelated index cases recruited through haemophilia centres throughout the UK (Al-Marwani 2009). Fourteen candidate defects were identified within *ITGB3,* of which twelve predicted missense substitutions in β_3. The research described in this chapter aimed to characterise the possible pathogenic effects of eight of these missense defects, one predicting an amino acid substitution in the signal peptide of β_3 (p.Trp11Arg), four predicting substitutions in the ligand binding domain of β_3 (p.Pro189Ser, p.Glu200Lys, p.Trp264Leu and p.Ser317Phe), two causing substitutions in the cysteine rich domain (p.Cys547Trp and p.Cys554Arg) and one affecting the β-tail domain (p.Ile665Thr). All but one of these missense defects were novel. The p.Cys547Trp defect had been described previously, although it had not been characterised (Kannan*, et al* 2009). The remaining four missense substitutions, p.Arg119Gln p.Leu143Trp, p.Asp145Asn and p.Arg240Gln, have been reported and characterised previously (Almusbahi 2014, Bajt*, et al* 1992, Basani*, et al* 1997, Loftus*, et al* 1990).

In silico methods were used to generate several hypotheses relating to the eight missense defects affecting β_3 studied here which are detailed in the previous chapter. In the work described in this chapter, these hypotheses were investigated using *in vitro* methods and a summary of the main findings is shown in Table 4.7. *In vitro* studies demonstrated a complete absence of membrane expression of $\alpha_{IIb}\beta_3$ and $\alpha_v\beta_3$ in CHO cells expressing the p.Trp11Arg, p.Trp264Leu and p.Ser317Phe variants, supporting the hypothesis that these amino acid substitutions are deleterious to the β_3 subunit and will result in a severe reduction or complete absence of membrane expression of the $\alpha_{IIb}\beta_3$ and $\alpha_v\beta_3$ receptors. In contrast, it was hypothesised that the p.Pro189Ser substitution would result in abnormal heterodimer formation between β_3 and α_{IIb} and the absence of $\alpha_{IIb}\beta_3$ receptor expression but it would have a less deleterious effect on heterodimer formation between β_3 and α_v. The results of the *in vitro* studies supported this hypothesis. Thus, the p.Pro189Ser substitution caused a severe reduction in the membrane expression of $\alpha_{IIb}\beta_3$ and a milder reduction in $\alpha_v\beta_3$ receptor expression.

Although the p.Pro189Ser, p.Trp264Leu and p.Ser317Phe substitutions all involve residues in the ligand binding domain, it was not possible to assess their effects on ligand binding due to their failure to be membrane expressed. The p.Cys547Trp and p.Cys554Arg substitutions resulted in reduced membrane expression of the $\alpha_{IIb}\beta_3$ receptors that were spontaneously active, supporting the hypothesis that these two variants would be associated with reduced membrane expression of $\alpha_{IIb}\beta_3$ and the accompanying functional defects. The hypothesis that the p.Ile665Thr substitution would result in a qualitative defect in $\alpha_{IIb}\beta_3$ was also supported as the p.Ile665Thr variant resulted in an $\alpha_{IIb}\beta_3$ receptor that was expressed at similar levels to the wild-type receptor, but also showed an impaired ability to undergo activation. The prediction that the p.Glu200Lys substitution would not be deleterious to the expression or function of $\alpha_{IIb}\beta_3$ or $\alpha_v\beta_3$ was partially supported by the results, which showed the levels of $\alpha_{IIb}\beta_3$ expression, and binding to fibrinogen and PAC-1 on cells expressing this variant which were comparable to those observed in cells expressing the wild-type receptor. However, the p.Glu200Lys substitution also caused a reduction in $\alpha_v\beta_3$ expression. In summary, with the exception of the p.Glu200Lys variant, data have been obtained which support the pathogenicity of all the variants studied in GT.

Table 4.7 Summary of the characteristics of the β_3 variants studied.

ITGB3 **variant / Nucleotide change**	**Surface expression (α_{IIb} and β_3 subunits / $\alpha_{IIb}\beta_3$ receptor) (% of WT)**	**PAC-1 / fibrinogen binding (% of WT)**	**Spontaneous binding to PAC-1 / Fibrinogen (Fold)**	**Western blotting**
p.Trp11Arg / c.31T>C	Absence	N/A	N/A	Pro-α_{IIb} β_3
p.Pro189Ser / c.565C>T	4 / 6	N/A	N/A	Pro-α_{IIb} β_3
p.Glu200Lys / c.598G>A	93 / 95	100/99.5	Absence	Pro-α_{IIb} Mature-α_{IIb} β_3
p.Trp264Leu / c.791G>T	Absence	N/A	N/A	Pro-α_{IIb} β_3
p.Ser317Phe / c.950C>T	Absence	N/A	N/A	Pro-α_{IIb} β_3
p.Cys547Trp /c.1641C>G	69/ 64	N/A	6/4	N/A
p.Cys554Arg /c.1660T>C	42/63	N/A	5.5/7.5	Pro-α_{IIb} Trance of Mature-α_{IIb} β_3
p.Ile665Thr / c.1994T>C	101/106	70/85	Absence	Pro-α_{IIb} Mature-α_{IIb} β_3

N/A: Not applicable

The *ITGB3* defects predicting the p.Trp11Arg (c.31T>C) and p.Pro189Ser (c.565C>T) substitutions were inherited as compound heterozygous defects in a 46 year old Caucasian male with a history of moderate bleeding symptoms including epistaxis. The patient had a bleeding score of 5 when assessed subjectively by the referring clinician on a scale of 1 to 10, where 1 is minor and 10 is severe bleeding. As described in Chapter 3, the bioinformatic analysis revealed that the tryptophan (Trp) residue at position 11 and proline (Pro) residue at position 189 are highly conserved across species and among human β-integrin family members, suggesting that they are important for the structural integrity of the β_3 chain. When a number of online prediction tools were used to predict the possible effects of these substitutions, the results consistently predicted that the p.Trp11Arg and p.Pro189Ser substitutions cause significant damage to the structure and function of the protein.

The c.31T>C transition predicted the substitution of a hydrophobic amino acid, tryptophan, with the polar positively charged amino acid arginine (Arg) at amino acid position 11 of the signal peptide in the hydrophobic region of the signal peptide of β_3. As no other defects have, to our knowledge, been identified within this region, this was the first study to investigate a β_3 signal peptide defect. The signal peptide is an N-terminal peptide sequence present in many membrane proteins, which plays an important role in mediating the targeting of nascent proteins to, and translocation across the ER. Signal peptides have a tripartite structure comprising a positively charged amino terminal region (n-region), a hydrophobic core region (h-region) and a polar carboxyl-terminal region (c-region). Thus, amino acid substitutions within signal peptides can vary in their effects depending on where they are located, with substitutions in the n- and h- regions potentially altering translocation efficiency, while substitutions in the c-region can disturb signal peptide cleavage (Heijne 1990, von Heijne 1998). Bioinformatic predictions indicated that Trp11 is located in the hydrophobic region of the β_3 signal peptide which is considered to play a crucial role in signal peptide function, particularly in ER translocation. Therefore, a significant defect in this region may impair the ability of the protein to enter the ER affecting protein translocation (Heijne, 1990; Oliver, 1985; von Heijne, 1998). Importantly, *in vitro* expression of the p.Trp11Arg variant demonstrated a complete loss of surface expression of the $\alpha_{IIb}\beta_3$ integrin on CHO cells, indicating that the wild-type α_{IIb} subunit and the p.Trp11Arg variant were unable to form the heterodimer that is essential for surface expression of the $\alpha_{IIb}\beta_3$ receptor (Duperray*, et al* 1989, Rosa and McEver 1989). In addition, no β_3 could be detected in transfected CHO cells after permeabilising the cells to allow intracellular staining using a monoclonal antibody. The

possibility that the absence of β_3 was due to its rapid removal by proteasome was investigated (Duperray*, et al* 1987, Duperray*, et al* 1989). However, inhibition of proteasome through treatment with MG-132 did not lead to accumulation of the β_3 subunit. The expression of pro-α_{IIb}, mature-α_{IIb} and β_3 in lysates from cells expressing the p.Trp11Arg variant was also examined using SDS-PAGE and western blotting. Briefly, $\alpha_{IIb}\beta_3$ biogenesis starts with the formation of pro-α_{IIb} and β_3 subunits independently from *ITAG2B* and *ITGB3* mRNAs before translocating into the ER. The subunits are then subjected to carbohydrate modifications and then they bind to each other to form the pro-$\alpha_{IIb}\beta_3$ complex. The signal peptides are then removed and pro-$\alpha_{IIb}\beta_3$ is transported to the Golgi where the integrin undergoes further post translational modification and maturation. As a result, pro-α_{IIb} is processed to its mature form (heavy and light chains) and the mature receptor is expressed on the platelet membrane (Bray*, et al* 1986, Duperray*, et al* 1989, Nurden*, et al* 2013). Interestingly, immunoblot analysis of lysates from cells expressing the p.Trp11Arg variant demonstrated the presence of both β_3 and pro-α_{IIb} but the absence of mature α_{IIb}, suggesting that the biogenesis of α_{IIb} fails to progress beyond pro-α_{IIb} as a result of impaired binding between β_3 and pro-α_{IIb}, thereby results in the absence of a stable receptor on the cell membrane.

Failure to detect the p.Trp11Arg variant following intracellular staining and flow cytometry contrasts with its obvious presence when detected by western blotting, and is most likely explained by the use of a monoclonal antibody for the former, and a polyclonal antibody for the latter, analyses. This suggests that the failure to detect the variant by flow cytometry was due to misfolding of the protein and lack of exposure of the epitope required to bind the monoclonal antibody. While this work was in progress, there was a report of a GT patient who was compound heterozygous for the c.31T>C defect and a novel defect predicting a p.Cys532Arg substitution in β_3. The patient was a German female with a prolonged bleeding time and a history of severe bleeding symptoms. Platelets from the patient failed to aggregate normally and platelet membrane expression of $\alpha_{IIb}\beta_3$ was significantly reduced (Sandrock-Lang*, et al* 2015). The p.Trp11Arg variant was also identified in a 58 year old French female with a history of moderate bleeding symptoms including gingivorrhagia, easy bruising, oesophegal bleeding and menorrhagia. This variant was inherited as a homozygous defect and platelets from the patient failed to aggregate and showed less than 5% of the normal $\alpha_{IIb}\beta_3$ levels on their surface (Nurden*, et al* 2015). Collectively, these results suggest that the tryptophan residue at position 11 in the β_3 signal peptide is an important amino acid and its substitution by arginine leads to the disturbance of the normal biogenesis

of $\alpha_{IIb}\beta_3$, causing a complete loss of surface expression and contributing to the bleeding symptoms observed in the patient.

The p.Pro189Ser substitution predicted by the c.565C>T transition in *ITGB3* was co-inherited in the UK GT patient with the c.31T>C transition discussed above. This substitution occurs within the ligand binding domain of the β_3 subunit. Depending on their location, substitutions in this domain have been shown to interrupt heterodimer formation, disturb $\alpha_{IIb}\beta_3$ structure and expression and impair ligand binding (Nurden*, et al* 2013, Zhu*, et al* 2008). Our *in vitro* expression studies demonstrated a 94-96% reduction in $\alpha_{IIb}\beta_3$ receptor density on CHO cells expressing the p.Pro189Ser variant of β_3, while total expression of the p.Pro189Ser variant was reduced by 29% compared to that of the wild-type subunit. Interestingly, the wild-type β_3 subunit and the p.Pro189Ser variant were both observed to traffic to the cell surface independently of α_{IIb}. This finding indicates that the p.Pro189Ser substitution in β_3 impairs binding to α_{IIb} and the formation of the $\alpha_{IIb}\beta_3$ complex but it does not impair cell surface expression of β_3 on CHO cells. Given that complex formation is a prerequisite for the transport and cell surface expression of $\alpha_{IIb}\beta_3$, this suggested that the p.Pro189Ser substitution impairs the ability of the β_3 chain to form heterodimers with α_{IIb} but does not affect its ability to form a heterodimer with the endogenous α_v subunit that is known to be expressed by Chinese hamster ovary cells (Butta*, et al* 2003, Chen*, et al* 2001). To investigate this possibility, membrane expression of $\alpha_v\beta_3$ on CHO cells expressing p.Pro189Ser β_3 was assessed using an antibody to the $\alpha_v\beta_3$ receptor. The results revealed that the p.Pro189Ser β_3 variant was expressed as $\alpha_v\beta_3$ in 78% of the levels observed in cells expressing the wild-type β_3.

There have been other examples of *ITGB3* defects leading to substitutions in β_3 that have had differential effects on the ability of β_3 to form $\alpha_{IIb}\beta_3$ and $\alpha_v\beta_3$ receptors, where substitutions in β_3 have been shown to impair the expression of $\alpha_{IIb}\beta_3$ but not the $\alpha_v\beta_3$ receptor. Examples include the p.Leu222Pro, p.His306Pro and p.Ser188Leu amino acid substitutions, all of which caused a selective reduction in surface expression of $\alpha_{IIb}\beta_3$, but not of the $\alpha_v\beta_3$ receptor (Coller*, et al* 1991, Jackson*, et al* 1998, Morel-Kopp*, et al* 2001, Tadokoro*, et al* 2002). The p.Leu222Pro variant was identified in a patient with mild bleeding symptoms who was diagnosed as having type II GT. Expression studies in CHO cells showed a significant reduction in the surface expression of $\alpha_{IIb}\beta_3$ when wild-type β_3 was replaced by a p.Leu222Pro β_3 variant. Both the full length and mature forms of α_{IIb} and β_3 were detected in cell lysates, suggesting that the p.Leu222Pro β_3 subunit was able to associate with α_{IIb} but still failed to traffic to the cell

surface. In contrast, the p.Leu222Pro substitution in β_3 did not affect surface expression of $\alpha_v\beta_3$ (Morel-Kopp*, et al* 2001). The p.His306Pro β_3 variant was identified in a Japanese patient who was diagnosed with type I GT. Flow cytometry analysis of platelets from the patient revealed a 94% reduction in membrane expression of $\alpha_{IIb}\beta_3$ compared to control platelets but 47% of the levels of $\alpha_v\beta_3$ that were observed on control platelets. Expression of the p.His306Pro variant in T293 cells showed a severe reduction (75%) in the membrane expression of $\alpha_{IIb}\beta_3$ but levels of the $\alpha_v\beta_3$ receptor that were comparable to those of the wild-type. The authors suggested that the differences in *ex vivo* and *in vitro* expression levels observed in their study may reflect overexpression of the $\alpha_{IIb}\beta_3$ protein in a heterologous system. Immunoblotting of lysates from cells expressing the p.His306Pro variant showed levels of pro-α_{IIb} and β_3 which were comparable to those of the wild-type but low levels of mature α_{IIb}. In addition, pulse chase analysis demonstrated that α_{IIb} was present mainly as pro-$\alpha_{IIb,}$ suggesting protein retention in the ER and abnormal intracellular trafficking to the Golgi (Tadokoro*, et al* 2002). The p.Ser188Leu variant was identified in an 11 year old Caucasian male with a history of easy bruising, epistaxis and mucocutaneous bleeding whose platelets expressed 16-27% of the $\alpha_{IIb}\beta_3$ receptor levels observed on control platelets. Immunoblotting of platelet lysates showed a 70% reduction in the total $\alpha_{IIb}\beta_3$ receptor levels compared to the control platelets. Further characterisation of this variant *in vitro* revealed that surface expression of $\alpha_{IIb}\beta_3$ on COS-7 cells expressing the p.Ser188Leu β_3 subunit was reduced to 15-30% of the receptor levels observed in cells expressing wild-type β_3. Although both pro-α_{IIb} and the p.Ser188Leu β_3 were detected in cell lysates, there was a complete absence of mature-α_{IIb}. These results suggested that the pro-α_{IIb} and β_3 formed a heterodimer which was unstable and degraded or retained in the ER (Jackson*, et al* 1998). The p.Ser188Leu β_3 variant was further characterised by Tadokoro*, et al* (2002) who showed that it formed an $\alpha_v\beta_3$ receptor in T293 cells that was expressed at levels that were similar to those seen with the wild-type β_3. These findings, and those of the present study, suggest that the structural integrity of the region encompassing Ser188 and Pro189 is important for $\alpha_{IIb}\beta_3$ heterodimer formation, but less so for formation of the $\alpha_v\beta_3$ receptor.

Data from the current study contributed to a collaborative project which used molecular dynamic analysis to investigate the effects of the p.Pro189Ser substitution on the molecular structures of $\alpha_{IIb}\beta_3$ and $\alpha_v\beta_3$ (Laguerre*, et al* 2013). The p.Pro189Ser variant was also identified in a 49 year old French female with a history of bleeding symptoms and whose platelets displayed an aggregation profile that was consistent with a diagnosis of GT. This variant was inherited as a homozygous defect and platelets from

the patient failed to aggregate and showed less than 9% of the normal $\alpha_{IIb}\beta_3$ levels on their surface compared to that of the surface $\alpha_{IIb}\beta_3$ levels detected on the platelets of a control subject. The main findings of the molecular dynamic analysis were that substitution of serine for proline at amino acid position 189 in $\alpha_{IIb}\beta_3$ resulted in an 11% increase in intra subunit hydrogen bonds, but a decrease in global hydrogen bonding as well as disruption of an α-helix (amino acid residues 285-260) and consequently of the interaction that occurs between Phe52, Ala128, Trp141, Gly201, Tyr319 and Phe450 in α_{IIb} and Arg287 in β3. In contrast, the presence of a serine residue at position 189 in the β3 subunit of $\alpha_v\beta_3$ resulted in a 43% increase in inter subunit hydrogen bonds without changing the global hydrogen bond network. In addition, the structural changes in the α-helix (amino acid residues 285-290) of β_3 allowed an increase in the extent of interaction between Arg287 in β_3 and the β-propeller domain of the α_v subunit. In addition, this study also confirmed our finding (see Chapter 3) that the strong interaction in the region of Pro189, that occurs between Arg242 in β3 and Asp154 in α_{IIb}, does not occur in $\alpha_v\beta_3$ and that substitution of Pro189 with serine results in the formation of a new hydrogen bond with His143 in $\alpha_v\beta_3$. Thus, these results suggested that the p.Pro189Ser substitution has a destabilising effect on the structure of $\alpha_{IIb}\beta_3$ while making $\alpha_v\beta_3$ even more rigid (Laguerre*, et al* 2013).

The p.Trp11Arg and p.Pro189Ser substitutions were inherited as compound heterozygous defects by the GT patient recruited to the UK cohort and the *in vitro* co-expression of both of these β3 variants with wild-type α_{IIb} to mimic the compound heterozygous status of the patient revealed significant reductions in both the cell membrane and total expression of the receptor, confirming the pathogenicity of these variants and their likely contribution to the bleeding symptoms observed in the patient.

The c.791G>T (p.Trp264Leu) and c.950 C>T (p.Ser317Phe) defects in *ITGB3* were inherited as homozygous defects in two index cases with GT, the former in a 12 year old Caucasian female with a bleeding score of 10, and the latter in a 31 year old African female with a bleeding score of 8. Both index cases had also developed isoantibodies (alloantibodies) to $\alpha_{IIb}\beta_3$ in response to blood transfusions, implying a complete absence of $\alpha_{IIb}\beta_3$ on their platelets (Fiore*, et al* 2012). The c.791G>T transversion predicted substitution of the hydrophobic tryptophan residue at position 264 by a hydrophobic leucine residue, while the c.950C>T transition predicted substitution of an uncharged serine residue by a hydrophobic phenylalanine residue at position 317. Both of these substitutions affected residues in the β I domain, defects which have been associated with either disturbing fibrinogen binding or membrane expression of $\alpha_{IIb}\beta_3$ (Ambo*, et al* 1998, Basani*, et al* 1997, Loftus*, et al* 1990).

Both the p.Trp264Leu and p.Ser317Phe substitutions involved highly conserved residues, suggesting that these amino acids may be important for the structural and functional integrity of the integrin. The latter was consistent with the results obtained using a number of online prediction tools which predicted these substitutions to be pathogenic (for further details see Chapter 3). The p.Trp264Leu and p.Ser317Phe variants were co-expressed with wild-type α_{IIb} in CHO cells to allow further characterisation. Total β_3 expression was reduced by 37% in cells expressing the p.Trp264Leu variant and by 23% in cells expressing the p.Ser317Phe variant and there was a complete absence of surface $\alpha_{IIb}\beta_3$ and $\alpha_v\beta_3$ expression on CHO cells expressing both variants. While the analysis of lysates from cells expressing the two variants revealed the presence of β_3 and pro-α_{IIb} but the absence of mature α_{IIb} in both cases, this indicates the failure of the β_3 variants to form the normal pro-$\alpha_{IIb}\beta_3$ heterodimer that then undergoes trafficking to the Golgi. Since the amount of β_3 in lysates from cells expressing the p.Trp264Leu or p.Ser317Phe variants was reduced compared to the wild-type, it could be speculated that these variants are less stable than wild-type β_3 variants. Several missense mutations affecting residues within the ligand binding domains of either α_{IIb} or β_3 have been shown to result in an abrogation of surface expression of $\alpha_{IIb}\beta_3$ and $\alpha_v\beta_3$. Examples include the p.Leu143Trp and p.Cys400Tyr substitutions which were shown to result in reduced surface expression of $\alpha_{IIb}\beta_3$ and $\alpha_v\beta_3$ (Ambo*, et al* 1998, Basani*, et al* 1997). The p.Leu143Trp variant was identified in a Pakistani child whose platelets displayed an aggregation profile that was consistent with a diagnosis of GT and a membrane $\alpha_{IIb}\beta_3$ receptor density that was less than 10% of normal control. *In vitro* investigations in COS-1 cells revealed 85-90% and 75% reductions in membrane expression of $\alpha_{IIb}\beta_3$ and $\alpha_v\beta_3$, respectively. Similar to the findings with the p.Trp264Leu and p.Ser317Phe variants in this study, the analysis of lysates from cells expressing the p.Leu143Trp variant showed an almost complete absence of mature α_{IIb}, while pro-α_{IIb} and β_3 were present at slightly lower levels than the wild-type subunit. These results suggest that the pro-α_{IIb} and β_3 form a heterodimer which is unstable, possibly leading to degradation or retain in the ER (Basani*, et al* 1997, Tadokoro*, et al* 2002). Similarly, the p.Cys400Tyr variant was inherited as a homozygous defect by a 20 year old Chinese female with a clinical history and platelet aggregation profile that were consistent with GT, whose platelets displayed 85% and 81% reductions in the membrane expression of $\alpha_{IIb}\beta_3$ and $\alpha_v\beta_3$ respectively. Further characterisation of the variant in HEK293 cells revealed a marked reduction (75%) in membrane expression of both $\alpha_{IIb}\beta_3$ and $\alpha_v\beta_3$ on cells expressing the p.Cys400Tyr variant, and analysis of the lysates showed a decrease in both β3 and mature α_{IIb} subunit levels compared to wild-type (Grimaldi*, et al* 1996, Tadokoro*, et al* 2002). The

results of the current study suggest that the p.Trp264Leu and p.Ser317Phe variants act similarly to cause the bleeding symptoms in the index cases who inherited these defects. Overall, our results suggested that these variants disturb the normal biogenesis, possibly by either affecting heterodimer formation or intracellular trafficking, causing an absence of surface expression of both $\alpha_v\beta_3$ and $\alpha_{IIb}\beta_3$.

The c.1641C>G and c.1660T>C alterations in *ITGB3* were inherited as homozygous defects in two index cases with GT who both had subjective bleeding scores of 3. These defects predicted the substitution of cysteine (Cys) residues with Tryptophan and Arginine at amino acid positions 547 and 554, respectively, in β_3. Cys547 and Cys554 are both highly conserved in β_3 across species and in other human β-integrin family members and online bioinformatic tools consistently predicted the p.Cys547Trp and the p.Cys554Arg substitutions to be pathogenic (see Chapter 3). Cys547 and Cys554 are located in the cysteine rich repeats of β_3 and form disulphide bonds with Cys534 and Cys568 in epidermal growth factor-like domains 2 (EGF-2) and 3 (EGF-3), respectively (see Chapter 3). In a parallel study, which was carried out under my supervision as part of a Master's project, the p.Cys547Trp variant resulted in an approximate one-third reduction in $\alpha_{IIb}\beta_3$ receptor density on CHO cells compared to wild-type $\alpha_{IIb}\beta_3$, and a similar reduction in the total amount of p.Cys547Trp β_3 variant was expressed. Interestingly, the p.Cys547Trp variant showed spontaneous activation as was evidenced by its ability to bind PAC-1 and labelled fibrinogen under non-activating conditions (Almusbahi 2014). Similarly, in the current study, compared to wild-type, cell surface levels of $\alpha_{IIb}\beta_3$ were reduced by approximately 50%, and total β3 levels were reduced by 23% in CHO cells expressing the p.Cys554Arg β3 variant, compared with wild-type. An analysis of lysates from cells expressing the p.Cys554Arg variant revealed the presence of pro-α_{IIb} and β3 in abundance, while only trace amounts of mature α_{IIb} could be detected which suggests that the p.Cys554Arg substitution in β_3 does not completely prevent heterodimer formation and maturation of $\alpha_{IIb}\beta_3$ but may lead to abnormal folding of the subunit, which may in turn impair receptor biogenesis. Interestingly, $\alpha_{IIb}\beta_3$ in CHO cells expressing the p.Cys554Arg variant also demonstrated spontaneous activation, and was able to bind PAC-1 and fibrinogen under non-activating conditions. These findings suggest that these substitutions cause a change in the conformation of $\alpha_{IIb}\beta_3$ which forces the integrin to adopt a high affinity state, exposing the ligand binding epitope and facilitating PAC-1 and fibrinogen binding. Unlike $\alpha_{IIb}\beta_3$, membrane expression of $\alpha_v\beta_3$-p.Cys547Trp and -p.Cys554Arg was markedly reduced compared to wild-type by approximately 92% and 90%, respectively indicating the substitutions affect the ability of β_3 to bind α_v.

The cysteine rich repeat domain, where the p.Cys547Trp and p.Cys554Arg substitutions occur, plays an important structural and functional role in $\alpha_{IIb}\beta_3$ (Kamata*, et al* 2004, Milet-Marsal*, et al* 2002a, Mor-Cohen*, et al* 2012). As mentioned previously (Section 1.3.3.4), the β_3 subunit incorporates 56 pairs of cysteine residues which cluster within the cysteine rich repeat domain to form four EGF-like domains, each of which contains four disulphide bonds that occur in a specific pattern, 1-5, 2-4, 3-6 and 7-8, in all but the EGF-1 domain, which lacks the bond between residues 2 and 4 (Zhu*, et al* 2008). Several studies have reported amino acid substitutions in the cysteine-rich domain in patients with GT, which are associated with a complete absence to normal $\alpha_{IIb}\beta_3$ expression levels and accompanied by constitutive activation of the receptor (Milet-Marsal*, et al* 2002a, Ruan*, et al* 1999, Ruiz*, et al* 2001).

Mor-Cohen*, et al* (2012) studied the effects of single and double substitutions of the cysteine residues in the Cys529-Cys499 bond in the EGF-2 domain. Substituting either of these cysteine residues with a serine residue resulted in the expression of an $\alpha_{IIb}\beta_3$ receptor which was activated spontaneously and expressed at levels comparable to those of the wild-type receptor. The double substitutions caused a slight reduction in $\alpha_{IIb}\beta_3$ expression to 64% of the wild-type levels and resulted in a receptor that was locked in the activated conformation. The authors proposed that the Cys529-Cys499 disulphide bond is essential to stabilise the integrin in a low affinity state but less important for EGF-2 folding and protein structure. Two further substitutions, which were identified in cases with GT, p.Cys483Tyr in the EGF-1 domain and p.Cys568Arg in the EGF-3 domain, were associated with the complete absence of membrane $\alpha_{IIb}\beta_3$ expression in platelets from the affected patients and a significant reduction in α_{IIb} and β_3 protein levels (Hourdille*, et al* 1986, Milet-Marsal*, et al* 2002a, Ruan*, et al* 1999). *In vitro* studies of p.Cys483Tyr and Cys568Arg showed that pro-$\alpha_{IIb}\beta_3$ was formed but the variants disturbed the maturation process in Golgi (Milet-Marsal*, et al* 2002a). Milet-Marsal et al. (2002) claimed that Cys568 formed a disulphide bond with Cys573 and showed that single (p.Cys568Arg and p.Cys573Ala) and double (p.Cys568Arg-p.Cys573Ala) substitutions of these cysteine residues had similar effects, reducing the expression of $\alpha_{IIb}\beta_3$ by approximately 79%, 90% and 85% respectively. However, our modelling studies, using the recent crystal structure of $\alpha_{IIb}\beta_3$ (3FCS) (Zhu et al., 2008), showed that Cys568 formed a disulphide bond with Cys554 rather than Cys573, a finding that is supported by other studies (Mor-Cohen*, et al* 2012, Mor-Cohen*, et al* 2008). Thus, an amino acid substitution at Cys568 causes a severe defect in membrane expression, while at Cys554 it causes a moderate reduction in surface expression, accompanied by functional defects of $\alpha_{IIb}\beta_3$. Interestingly, this may suggest

that the Cys554 and Cys568 residues have two different roles: to maintain normal stability of EGF-3 folding and to stabilise inactive conformation of the integrin, respectively.

In another interesting study, platelets from patients who were homozygous for a defect predicting a p.Cys575Arg substitution in the EGF-3 domain showed $\alpha_{IIb}\beta_3$ expression levels which were less than 15% of those seen on control platelets. Further characterisation of the naturally occurring p.Cys575Arg variant and an artificial p.Cys575Ser variant showed these resulted in constitutively active $\alpha_{IIb}\beta_3$ receptors that were expressed at 16-20% of the levels of wild-type $\alpha_{IIb}\beta_3$ (Mor-Cohen*, et al* 2007). Analysis of the lysates revealed marked reductions in both mature α_{IIb} and β_3 and cellular localisation studies showed that $\alpha_{IIb}\beta_3$ harbouring these mutations were retained in the ER (Mor-Cohen*, et al* 2007). Cys575 is known to form a disulphide bond with Cys584, and the p.Cys584Ser substitution had similar deleterious effects on surface and intracellular expression of $\alpha_{IIb}\beta_3$ and caused constitutive activation (Mor-Cohen*, et al* 2008). These studies suggested that the Cys575-Cys584 bond plays a primary role in folding of the EGF-3 domain and stabilising the resting conformation of the integrin. Interestingly, a study involving variants in which Cys586 (EGF-3) and Cys609 (EGF-4) were substituted by serine residues and expressed in Baby Hamster Kidney (BHK) cells revealed $\alpha_{IIb}\beta_3$ membrane expression that was 60-80% of that of wild-type. In addition, the integrin demonstrated spontaneous activation when only Cys586 was mutated. This result suggested that the free thiol group of Cys609 is involved in integrin activation, possibly through a disulphide exchange dependent mechanism (Mor-Cohen*, et al* 2012).

The physiological effects of constitutive $\alpha_{IIb}\beta_3$ activation were investigated in a murine model engineered to express the p.Cys586Arg (EGF-3) variant, which was characterised by reduced expression of constitutively active $\alpha_{IIb}\beta_3$ receptors in platelets from a GT patient with the defect (Fang*, et al* 2013, Ruiz*, et al* 2001). Murine platelets bearing the mutated $\alpha_{IIb}\beta_3$ showed relatively normal expression of $\alpha_{IIb}\beta_3$ receptors which were locked in the activated conformation. Furthermore, the platelets bound spontaneously to fibrinogen in the absence of surface p-selectin expression, and failed to aggregate when exposed to fibrinogen prior to a physiological agonist, unlike washed platelets, which were able to aggregate in the presence of added fibrinogen and a physiological agonist. These findings suggested that spontaneous binding to fibrinogen disturbs the normal ability of platelets to aggregate upon activation. The mutation led to increased mortality in the mice, and was associated with significant pathological changes, including spleen enlargement, abnormal platelet and

megakaryocyte morphology, intestinal bleeding and increased hemosiderin, indicating an increased haemorrhagic tendency (Fang*, et al* 2013). These findings suggested that spontaneous occupancy of the $\alpha_{IIb}\beta_3$ integrin interferes with platelet function and structure, leading to life threatening bleeding consistent with GT, and explained why constitutive activation of $\alpha_{IIb}\beta_3$ results in bleeding rather than thrombotic symptoms.

In a similar way to some of the EGF domain variants described above, our results showed that the release of the free thiol groups of Cys568, as a result of the p.Cys554Arg substitution (Cys554 forms a disulphide bond with Cys568) and Cys534 as a result of the p.Cys547Trp substitution (Cys 547 forms a disulphide bond with Cys 534) result in spontaneous activation of $\alpha_{IIb}\beta_3$.

The c.1994T>C transition in *ITGB3* was inherited as a homozygous defect in a 16 year old Yemeni male index case with GT, who had a bleeding score of 7 when assessed subjectively by the referring clinician. The c.1994T>C transition predicted a p.Ile665Thr substitution in the extracellular β tail domain of β_3. Ile665 was found to be highly conserved in β_3 across species but less conserved among human β-integrin family members and the p.Ile665Thr substitution was predicted to be deleterious by only three of the five online tools used in the study of β_3. Structural modelling showed that Ile665 is located in a region containing six cysteine residues which are known to form three disulphide bonds, between Cys634 and Cys681, between Cys640 and Cys661, and between Cys643 and Cys657.

The p.Ile665Thr variant was characterised further following its expression in CHO cells. These studies demonstrated total β_3 and $\alpha_{IIb}\beta_3$ expression levels which were comparable to wild-type. Similarly, membrane $\alpha_v\beta_3$ expression was also comparable to that of wild-type in CHO cells expressing the p.Ile665Thr variant. Furthermore, analysis of the cell lysates confirmed the presence of pro-α_{IIb}, mature α_{IIb} and β_3, at similar levels to those in cells expressing the wild-type receptor, indicating normal biogenesis and expression of $\alpha_{IIb}\beta_3$ bearing the p.Ile665Thr variant. However, following activation of the receptor by treatment with dithiothreitol (DTT), it showed a significant decrease in binding of both PAC-1 and fibrinogen, which suggested that the p.Ile665Thr substitution in β_3 causes impaired activation of $\alpha_{IIb}\beta_3$ and disrupts its ability to undergo the normal conformational change that is required to allow it to bind its ligand.

To date, little has been done to characterise the β tail domain of β_3, and the main functions of this domain remain uncertain. To my knowledge, only one other naturally occurring non-synonymous defect, predicting a p.His652Leu substitution in this domain, has been identified (Vinciguerra*, et al* 2001). While this variant has not been

characterised, a review of GT classified the p.His652Leu variant as a non-functional integrin defect (Nurden*, et al* 2012b). According to the study by Butta*, et al* (2003) which investigated the role of residues within the β tail domain of β_3, internal deletion of the residues spanning 642 to 716, 680 to 716 and 711 to 716 did not disturb surface expression of $\alpha_{IIb}\beta_3$ but did result in receptors that were locked in an activated state. The study also proposed that the residues between 711 and 716 were responsible for spontaneous activation (Butta*, et al* 2003). The crystal structure of β_3 shows that there are four disulphide bonds in the region between residues 642 and 716, Cys634-Cys681, Cys640-Cys661, Cys643-Cys657 and Cys689-Cys713 (Xiong*, et al* 2001). Thus, it has been proposed that the interaction between Cys689 and Cys713 is the most likely to be responsible for maintaining the integrin in its resting (bent) conformation, and that disruption of this bond is likely to result in spontaneous activation of the integrin. This was supported by the finding that substitution of Cys713 by alanine had a similar effect to that observed when residues 711-716 were deleted from the β tail (Butta*, et al* 2003). Other studies have shown that disruption of the Cys640-Cys661 and Cys643-Cys657 bonds does not result in spontaneous integrin activation (Kamata*, et al* 2004, Mor-Cohen*, et al* 2008). In contrast to the findings of Butta*, et al* (2003), they showed a moderate reduction in the surface expression of $\alpha_{IIb}\beta_3$ in cells expressing a p.Cys643Ser variant but not with p.Cys640Ser and p.Cys634Ser-p.Cys681Ser variants, indicating a role for the Cys643-Cys651 disulphide bond in stable expression of the receptor. Overall however, these studies suggest that the integrity of the β tail domain is less important for $\alpha_{IIb}\beta_3$ surface expression than it is for integrin activation, which is consistent with our findings for the p.Ile665Thr variant (Kamata*, et al* 2004, Mor-Cohen*, et al* 2008). Interestingly, all the β tail domain studies mentioned above focused on characterising those residues which, when deleted or mutated, resulted in spontaneous activation of the receptor and those residues that determine the capacity of the receptor to undergo DTT or antibody induced activation have not been characterised. For example, it would be interesting to explore whether the Cys640-Cys661 and Cys643-Cys657 disulphide bonds play a role in the conformational change that occurs in receptor activation. It is also possible that the p.Ile665Thr substitution reduces the flexibility of the β tail domain that is required to undergo the conformational change in response to activation. The study by Butta*, et al* (2003) also showed that deletion of the residues between 642 and 716 did not impair the surface expression of $\alpha_v\beta_3$, suggesting that the region of the β tail which includes Ile665 is less important for $\alpha_v\beta_3$ integrity, a suggestion that is supported by the finding that membrane expression of $\alpha_v\beta_3$ was similar to wild-type in CHO cells expressing the Ile665Thr variant.

In contrast to the above findings, the substitution of the negatively charged Glutamate (Glu) residue by the positively charged Lysine (Lys) residue at amino acid position 200 in the ligand binding domain of β_3 (p.Glu200Lys), which was predicted by the c.598G>A defect in *ITGB3*, did not appear to disrupt the expression or activation of $\alpha_{IIb}\beta_3$. The p.Glu200Lys substitution was inherited as a homozygous defect in a 13 year old Guatemalan male with a history of mild bleeding symptoms who had a bleeding score of 3 when assessed subjectively by the referring clinician. Bioinformatic studies showed that the Glutamate residue at amino acid position 200 in β_3 was not highly conserved across vertebrate species or among other human β-integrin family members and the p.Glu200Lys substitution was predicted to be benign using several bioinformatic tools. Structural studies revealed no associations between Glu200 and other residues in β_3, suggesting it may not be essential for protein structure. Nevertheless, its location on the surface of β_3 suggests it may have a role in protein function, possibly through interacting with other molecules.

In vitro expression of the p.Glu200Lys β_3 variant with wild-type α_{IIb} resulted in surface and total expression levels of $\alpha_{IIb}\beta_3$ comparable to those of wild-type, and western blot analysis of cell lysates revealed no abnormalities in pro-α_{IIb}, mature α_{IIb} and β_3 distribution, suggesting that this variant does not disturb $\alpha_{IIb}\beta_3$ biogenesis. The $\alpha_{IIb}\beta_3$ receptor bearing the p.Glu200Lys β_3 variant bound PAC-1 and fibrinogen similarly to the wild-type receptor following activation by reduction with DTT, indicating that it undergoes the conformational change that is required for integrin activation normally. The activation of the variant $\alpha_{IIb}\beta_3$ receptor using various concentrations of DTT was also shown to be normal compared to wild-type, implying that the integrin bearing p.Glu200Lys β_3 is expressed and activated similarly to the wild-type receptor. Other possible explanations for the association of this variant with GT were therefore sought. The c.598G>A transition that predicts the p.Glu200Lys substitution was also predicted to alter the exonic splicing enhancer (ESE) regulatory elements and potentially to disrupt splicing of the *ITGB3* mRNA. However, no evidence to support a defect in splicing was obtained following *in vitro* investigations. Interestingly, the p.Glu200Lys variant was shown to result in a 78% reduction in surface expression of $\alpha_v\beta_3$ in CHO cells compared to wild-type, suggesting Glu200 is required for the interaction of β_3 with α_v, and is less critical for the assembly of $\alpha_{IIb}\beta_3$. Given the role of $\alpha_v\beta_3$ in angiogenesis and in wound healing, the association of the p.Glu200Lys variant with GT may therefore be a consequence of disturbed blood vessel repair following injury (Dufourcq*, et al* 2002, Ramjaun and Hodivala-Dilke 2009).

Unfortunately, attempts to re-recruit the index case with the p.Glu200Lys defect were not successful. However, further clinical information supplied about the patient revealed that he also had macrothrombocytopenia, leading us to speculate that the p.Glu200Lys variant may be interfering with megakaryopoiesis. Preliminary work to investigate this hypothesis, carried out by the Haemostasis Research Group in Sheffield, revealed that when seeded on immobilised fibrinogen, CHO cells expressing the p.Glu200Lys variant demonstrated increased formation of proplatelet-like protrusions and an increase in protrusion length compared to cells expressing wild-type β_3. This may translate to an increase in the rate of proplatelet production, producing fewer, but larger platelets, as demonstrated previously by Ghaevert et al. (2007) and therefore accounting for the observed macrothrombocytopenia in the patient.

4.6 Conclusion

The results presented here provide insights into the potential pathogenic effects of 8 missense mutations in *ITGB3* that were identified in GT patients in the UK. It was found that the p.Trp11Arg substitution failed to stably express the β_3 integrin, and caused a severe reduction in surface and intracellular expression of $\alpha_{IIb}\beta_3$ and $\alpha_v\beta_3$ *in vitro*. Interestingly, there was a severe reduction in membrane expression of $\alpha_{IIb}\beta_3$ in cells expressing the p.Pro189Ser variant while increasing expression levels of $\alpha_v\beta_3$. This indicates that β_3 bearing p.Pro189Ser retains the ability to bind to α_v but possibly disrupts interactions with α_{IIb}. The homozygous variants predicting the p.Trp264Leu and p.Ser317Phe variants of β_3 were expressed at detectable levels in CHO cells but failed to form normal heterodimers with α_{IIb} and α_v, resulting in the absence of $\alpha_{IIb}\beta_3$ and $\alpha_v\beta_3$ receptors on the cell membrane. The p.Cys547Trp and p.Cys554Arg substitutions caused a partial reduction in the membrane expression of $\alpha_{IIb}\beta_3$ on CHO cells; however this caused the integrin, present on the surface, to remain in a high-affinity state. The p.Ile665Thr substitution results in normal expression of $\alpha_{IIb}\beta_3$ and $\alpha_v\beta_3$, but showed impaired activation of the $\alpha_{IIb}\beta_3$ receptor. In contrast, the p.Glu200Lys substitution showed normal expression and activation. However, this variant severely reduced the expression levels of $\alpha_v\beta_3$, which may affect proplatelet formation. Overall, the majority of these variants supported the hypotheses generated, with the exception of p.Glu200Lys, which is yet to confirm an association with GT. Importantly these studies highlight the roles of some amino acid residues within the β_3 protein, thus aiding our understanding of the molecular basis of GT. In addition, this study is considered to be the first to investigate the effect of a mutation within the signal peptide of the β_3 protein.

Chapter 5: Functional Characterisation of α_{IIb} Variants

5.1 Introduction

In addition to the eight missense alterations affecting *ITGB3* that were the focus of the studies described in Chapter 4, the UK survey of patients with Glanzmann thrombasthenia also identified five non-synonymous alterations affecting *ITGA2B,* which predicted amino acid substitutions in different domains of the α_{IIb} subunit (Table 5.1). Three of the missense changes were novel. These were the c.1475T>C, c.2010C>A and c.2094G>T variants, which predicted p.Leu492Pro, p.Asn670Lys and p.Glu698Asp substitutions respectively. The other two alterations, c.1186G>A and c.1787T>C, predicting p.Asp396Asn and p.Ile596Thr substitutions, which were each identified in two index cases, had been described previously, but had not been characterised to any extent (Ruan*, et al* 1998, Vijapurkar*, et al* 2009). These five variants, which were associated with variable clinical symptoms and bleeding severities, will form the focus of the studies in this chapter (Table 5.1).

The bioinformatic studies described in Chapter 3 predicted four of the amino acid substitutions, affecting residues in the β propeller domain (p.Asp396Asn), the thigh domain (p.Leu492Pro and p.Ile596Thr) and the calf-1 domain (p.Asn670Lys), to have pathogenic effects. The c.2094G>T transversion was predicted to exert its pathogenic effects either through disrupting *ITGA2B* RNA splicing, or through the p.Glu698Asp substitution, though the former was considered to be more likely than the latter amino acid change since this was predicted to be benign (Sections 3.3.2 and 3.3.3). However, both possibilities were considered in further studies of this variant. Investigation into the effects of these five variants will further our understanding of the molecular basis of Glanzmann thrombasthenia and will highlight the roles of specific residues within α_{IIb} with regards to the structure and function of the $\alpha_{IIb}\beta_3$ integrin.

Table 5.1 Clinical features of index cases with inherited defects in *ITGA2B*.

Nucleotide change	Predicted amino acid substitution	Genotype	Treatment	Anti-$\alpha_{IIb}\beta_3$*	Bleeding symptoms/ score[x]
c.1186G>A	p.Asp396Asn	Homozygous	RBC, Platelets, rVIIa	Unknown	Epistaxis / 5
c.1186G>A	p.Asp396Asn	Homozygous	Platelets, rVIIa	Unknown	Epistaxis / 7
c.1475T>C	p.Leu492Pro	Compound heterozygous	None	No	Epistaxis / 1
c.1787T>C	p.Ile596Thr	Homozygous	Platelets	Unknown	Epistaxis, Menorrhagia and Gastrointestinal bleeding / 7
c.1787T>C	p.Ile596Thr	Homozygous	RBC, Platelets, rVIIa	No	Epistaxis, Menorrhagia and Gastrointestinal bleeding / 7
c.2010C>A	p.Asn670Lys	Homozygous	None	Unknown	Epistaxis / 7
c.2094G>T	p.Glu698Asp/ splicing defect	Homozygous	Platelets	No	Epistaxis and Menorrhagia / 4

*Indicates whether patients developed antibodies to $\alpha_{IIb}\beta_3$ in response to platelet transfusion. [x]Bleeding severity, assessed subjectively by the referring clinician on a scale of 1 to 10, where 1 is minor and 10 is severe bleeding. RBC: red blood cells; rVIIa:recombinant factor VIIa.

5.2 Aims and hypothesis

Based on the *in silico* analyses presented in Chapter 3, and published data relating to α_{IIb} structure and function, we hypothesise that:

- The p.Asp396Asn, p.Leu492Pro and p.IIe596Thr amino acid substitutions mediate their pathogenicity by interfering with the intracellular assembly of the $\alpha_{IIb}\beta_3$ receptor and causing a failure in the expression of the receptor on the platelet membrane.
- The p.Asn670Lys substitution in α_{IIb} will result in an $\alpha_{IIb}\beta_3$ receptor that shows reduced or normal surface expression on platelets but which will have altered integrin function.
- The c.2094G>T results in aberrant splicing of the *ITGA2B* RNA.

The above hypotheses will be investigated by assessing the expression and function of $\alpha_{IIb}\beta_3$ following co-expression of recombinant *ITGA2B* cDNAs bearing the above five candidate defects and a wild-type *ITGB3* expression construct in CHO cells. The results of this study help to elucidate how alterations of the β propeller, thigh and calf-1 domains in the α_{IIb} subunit can lead to GT, thereby furthering our understanding of the molecular basis of the disease. In addition, characterisation of the region between the thigh and calf-1 domains (α_{IIb} genu), which contains a putative calcium binding site, may yield insights into the function of this region and the nearby calcium binding site.

5.3 Methods

5.3.1 Investigation of the predicted effects of the c.2094G>T *ITGA2B* transversion

5.3.1.1 Description of pET-01

The exontrap pET-01 vector contains two exons of a eukaryotic phosphatase gene separated by 600 bp of intronic sequence. The intron is framed by a 5´ donor splice site and a 3´ acceptor splice site of a eukaryotic exon. The intron also contains a multiple cloning site to facilitate cloning and insertion of DNA sequences of interest (Figure 5.1)(Duyk*, et al* 1990). The vector was used here to investigate the potential effects on splicing of a single nucleotide substitution in the donor splice site of exon 20 of *ITGA2B*. The features of the vector are shown in Figure 5.1 while the sequence of the vector is provided in **Appendix 3**.

5.3.1.2 pET-01 preparation and purification

The vector pET-01 was suspended in distilled water at a concentration of 10 ng/µl. Competent *E.coli*, strain NM-554 (45 µl) were then transformed with 1 ng of pET-01 DNA as described in section 2.2.2.7. Following overnight growth, a single colony was used to inoculate 250 ml LB broth (25 g/l) containing 100 µg/ml ampicillin and the culture incubated for 16-18 hours at 37°C, 200 rpm. Plasmid DNA was extracted and purified using the Qiagen plasmid Maxi kit (see section 2.2.2.9).

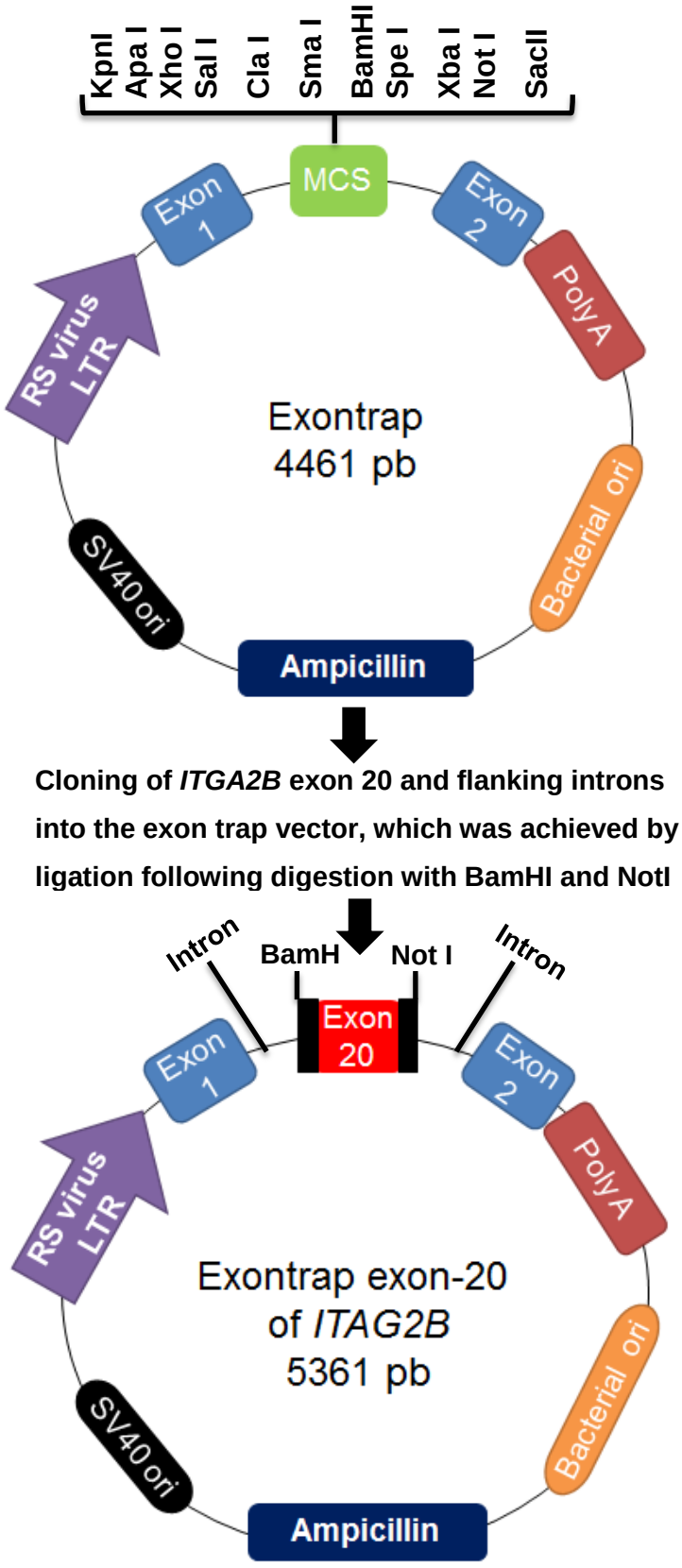

Figure 5.1 Vector map of pET-01 (exontrap) and cloning strategy. A fragment corresponding to exon 20 of *ITGA2B* and 706 bp of flanking intronic sequence was cloned into pET01 using the restriction enzymes BamHI and NotI.

5.3.1.3 PCR amplification of exon 20 of ITGA2B

A DNA fragment corresponding to exon 20 of *ITGA2B* and its flanking intronic sequences (Reference Sequence: NM_000419) was amplified from genomic DNA using the primers shown in table 5.2. Primers were designed to incorporate restriction sites and M13 tails to facilitate directional cloning. PCR was performed using Q5® Hot Start High-Fidelity DNA Polymerase (NEB, Massachusetts, USA) and carried out using a GeneAmp ABI 9700 Thermal cycler (Life Technologies Ltd, California, USA). The PCR mixture comprised the following: 1_X Q5 reaction buffer (2 mM $MgCl_2$), 200 µM dNTPs, 0.5 µM forward and reverse primers, 10 ng DNA template and 0.02 U/µl DNA polymerase. Thermocycling began with an initial denaturation step at 98°C for 30 seconds (secs), followed by 35 cycles of denaturation at 98°C for 10 secs, annealing at 68°C for 30 secs and extension at 72°C for 30 secs, followed by a final extension step at 72°C for 2 minutes. PCR products were then subjected to agarose gel electrophoresis to assess the efficiency of the reaction, and estimate product yield (see section 2.2.2.1).

Table 5.2 Oligonucleotide primers used to amplify exon 20 of *ITGA2B* and its flanking intronic sequences.

Primer	Direction	Primer (5' to 3')*	Restriction site
***ITGA2B* exon 20F**	Forward	TGTAAAACGACGGCCAGTGGATCCTGAGGAGGCCTCC CATTCTG	BamHI
***ITGA2B* exon 20R**	Reverse	CAGGAAACAGCTATGACCGCGGCCGCCTTCAGGAAG GCAGTTCCAAG	NotI

* Restriction sites are highlighted in red

5.3.1.4 Restriction digestion of pET-01 and PCR product

To facilitate directional cloning of the PCR product corresponding to exon 20 of *ITGA2B* and its flanking intronic sequences into pET-01, both the PCR product and the vector were subjected to restriction digestion with BamHI and NotI (NEB, Massachusetts, USA). Digestion of 5 µg pET-01 was carried out overnight at 37°C in a final volume of 50 µl containing 1x NEB cutsmart buffer, 50 units of BamHI and 50 units of NotI. Similarly, 1 µg of PCR product was digested for 3 hours at 37°C with 10 units of BamHI and 10 units of NotI diluted in 1x NEB cutsmart buffer in a final volume of 50 µl. The digested plasmid and PCR product were subjected to electrophoresis in 0.7% and 2% agarose gel, respectively and purified as described in sections 2.2.2.1 and

2.2.2.2. The purified PCR product and vector were quantified using a Nano Drop 1000 Microfluid Spectrophotometer (Section 2.2.2.3).

5.3.1.5 Ligation of PCR product with pET-01

The digested and purified PCR product (insert) and pET-01 (vector) were ligated using T4 DNA ligase (Promega, Fitchburg, USA). The ligation reactions contained a fixed amount of the vector (100 ng) combined with varying amounts of the insert in order to achieve a range of vector:insert DNA ratios by size (see Table 5.3). The amounts of insert required to achieve the desired ratios were determined using the equation below, where the size of the insert was 0.85kb, and the size of the vector was 4.5kb. The ligation reactions were incubated at room temperature for 3 hours, before heat inactivating the ligase at 70°C for 10 minutes.

$$\frac{\text{ng of vector} \times \text{Size of insert (kb)}}{\text{Size of vector (kb)}} \text{ X ratio of } \frac{\text{Insert}}{\text{Vector}}$$

Table 5.3 Conditions used to ligate exon 20 of *ITGA2B* with pET-01.

Reagents	**Vector:Insert ratio**			
	1:1	**1:3**	**1:5**	**Control**
dH_2O	6	4	2	7
Vector	100 ng (1µl)	100 ng (1µl)	100 ng (1µl)	100 ng (1µl)
Insert	19 ng (1µl)	57 ng (3µl)	95 ng (5µl)	19 ng (1µl)
10x ligase buffer	1µl	1µl	1µl	1µl
T4 DNA Ligase	1 unit (1µl)	1 unit (1µl)	1 unit (1µl)	-

5.3.1.6 Transformation of competent E.coli with recombinant plasmid

Each ligation reaction (10 µl) was added to 45 µl of competent *E.coli*, NM-554 with gentle mixing, before incubating the sample on ice for 20-30 minutes. The cells were then subjected to a 60-90 second heat-pulse at 42°C, before being incubated on ice for a further 2 minutes. A 0.5 ml aliquot of preheated (42°C) LB broth (22 g/L) was then added, and the samples incubated at 37°C, with shaking at 200 rpm, for 30 minutes before plating on LB agar (11.1g/300ml) plates containing 100 µg/ml ampicillin. Agar

plates were incubated overnight at 37°C. Single colonies were then used to inoculate 5 ml samples of LB broth (25 g/L) containing 100 µg/ml ampicillin. The *E.coli* were grown and the plasmid DNA isolated and purified as described earlier (Section 2.2.2.8). Plasmids were screened for the presence of the insert (exon 20 and its flanking introns) by sequencing (Section 2.2.2.10). The desired plasmid containing the insertion was then purified using the Qiagen plasmid Maxi kit (Section 2.2.2.9).

5.3.1.7 Site-directed mutagenesis and transformation of E.coli

The desired nucleotide substitution (c.2094G>T) was introduced into wild-type *ITGA2B* pET-01 using the Quikchange lightning site-directed mutagenesis kit (Agilent Technologies, California, USA) according to the manufacturer's instructions and as described in section 2.2.2.11.

5.3.1.8 Transfection of CHO cells and PCR analysis

CHO cells were transfected with the wild-type and mutated *ITGA2B* pET-01 plasmids using the protocol described in section 2.2.2.13. RNA was then extracted and cDNA generated as described in sections 2.2.2.4 and 2.2.2.6 using the primers shown in table 5.4. PCR was performed using OneTaq® DNA Polymerase (NEB, Massachusetts, USA) and carried out using a GeneAmp ABI 9700 Thermal cycler (Life Technologies Ltd, USA). The PCR mixture comprised the following: 1x OneTaq standard reaction buffer, 200 µM dNTPs, 0.2 µM forward and reverse primers, 100 ng cDNA template and 0.025 U/µl OneTaq® DNA polymerase. Thermocycling began with an initial denaturation step at 94°C for 30 secs, followed by 35 cycles of denaturation at 94°C for 10 secs, annealing at 47°C for 30 secs and extension at 68°C for 30 secs, followed by a final extension step at 68°C for 5 minutes. The PCR products were then subjected to agarose gel electrophoresis to assess the efficiency of the reaction, and estimate product size (see section 2.2.2.1).

Table 5.4 Oligonucleotide primers used to amplify cDNA derived from pET-01 plasmids.

Primer	Direction	Primer (5'to 3')
pET-01 –AMP-F	Forward	GGATTCTTCTACACACCC
pET-01 –AMP-R	Reverse	CGGGCCACCTCCAGTG

5.3.1.9 Deletion of exon 20 from ITGA2B pcDNA3.1

The deletion of exon 20 (c.1947_2094del) from the wild-type *ITGA2B* expression plasmid was achieved using the Quikchange lightning site-directed mutagenesis kit and primers designed using QuikChange Primer Design at (http://www.genomics.agilent.com/) (Table 5.5). The PCR and transformation were carried out as described in section 2.2.2.11.

Table 5.5 Oligonucleotide primers used to delete exon 20 from the *ITGA2B* cDNA.

Mutation	Exon	Forward primer (5' to 3')	Reverse primer (5' to 3')
c.1947_2094del	20	TCAGCTCACTGCCAGCGT GGCTTTGAGAGAC	GTCTCTCAAAGCCACGCTGG CAGTGAGCTGA

5.3.2 Deglycosylation of α_{IIb} using Endoglycosidase (Endo) H

Endo H was purchased from New England Biolabs (Massachusetts, USA). Twenty five µg of protein was denatured with Glycoprotein Denaturing Buffer (5% SDS, 0.4 M DTT) by incubation at 100°C for 5-10 minutes. The reaction was then mixed with G5 Reaction Buffer (0.5 M Sodium Citrate, pH 5.5) and two units of Endo H added before incubation at 37°C for 1 hour. Samples were prepared and assessed by Western blot as described in section 2.2.2.18.

5.4 Results

5.4.1 Generation of variant *ITGA2B* expression constructs

In order to investigate the *in vitro* effects of the five *ITGA2B* variants, site-directed mutagenesis was carried out to introduce the corresponding single nucleotide changes into pcDNA3.1 bearing the wild-type *ITGA2B* cDNA as described in section 2.2.2.11. Following mutagenesis, sequence analysis of the recombinant expression plasmids confirmed the presence of the desired alterations and that no further changes had been introduced into the *ITGA2B* cDNA (Figure 5.2).

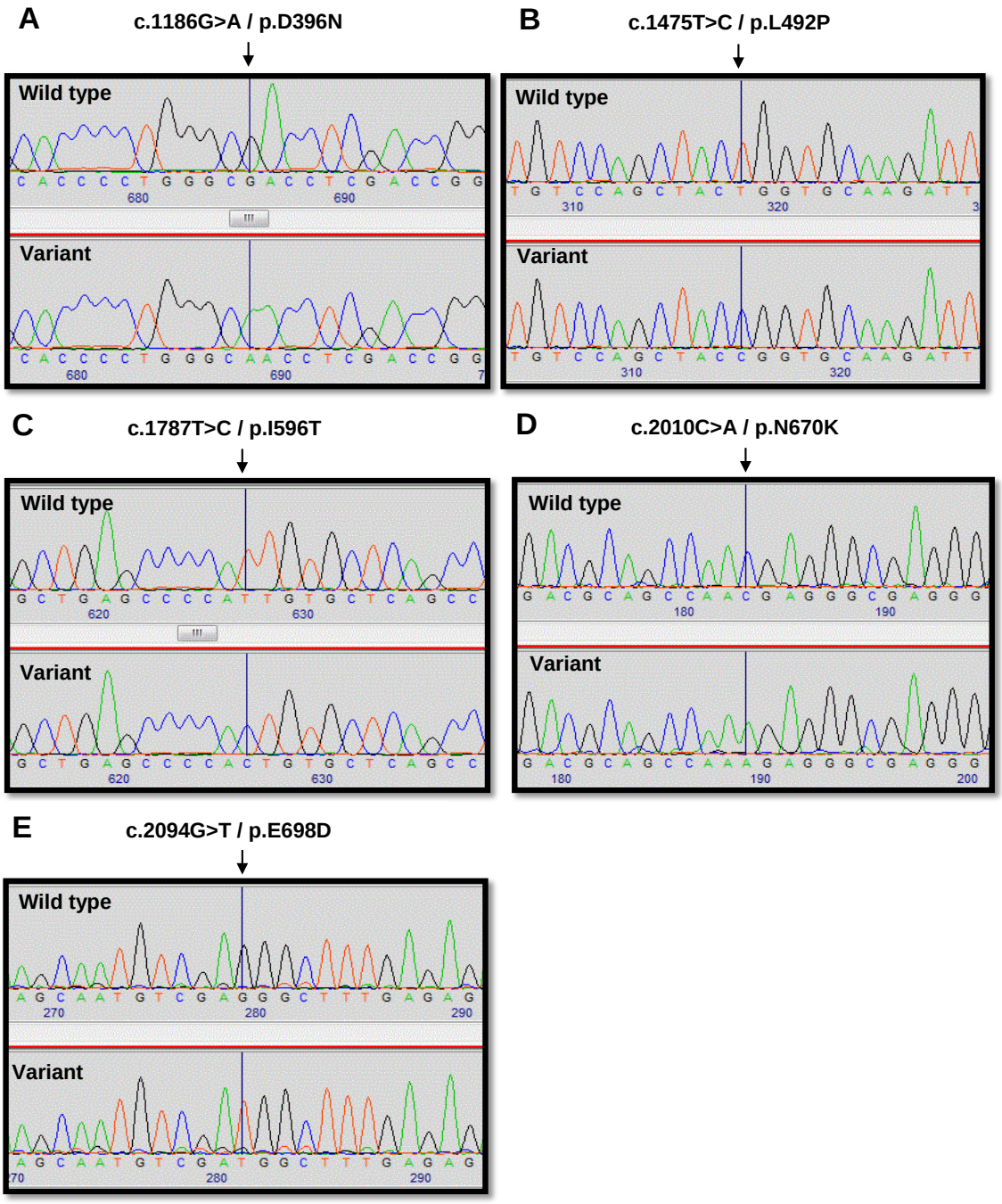

Figure 5.2 Sequence chromatograms of recombinant *ITGA2B* expression plasmids showing the positions of single nucleotide changes introduced by site-directed mutagenesis. The chromatograms demonstrate the introduction of mutations to derive the (A) p.D396N, (B) p.L492P, (C) p.I596T, (D) p.N670K and (E) p.E698D substitutions. The black arrows indicate the positions of nucleotide changes.

5.4.2 Membrane expression of $\alpha_{IIb}\beta_3$ in CHO cells expressing α_{IIb} variants

In order to further characterise the effects of the p.Asp396Asn, p.Leu492Pro, p.Ile596Thr, p.Asn670Lys and p.Glu698Asp substitutions that were predicted to occur as a result of *ITGA2B* defects identified in index cases with GT, CHO cells were transfected with wild-type *ITGB3* cDNA and either wild-type or variant *ITGA2B* cDNA. As a negative control, and to allow assessment of the background fluorescence of the antibodies, CHO cells were also transfected with the empty expression plasmid (pcDNA3.1). Following 48 hours of transfection, the cells were incubated with monoclonal antibodies against α_{IIb}, β_3 and the $\alpha_{IIb}\beta_3$ receptor complex, to assess surface expression using flow cytometry. In addition, cells co-transfected with wild-type *ITGB3* and *ITGA2B* cDNAs were stained with isotype controls for the corresponding antibody to assess non-specific binding of the antibodies.

Flow cytometric analysis revealed significant 94% and 90% reductions in membrane expression of $\alpha_{IIb}\beta_3$ in cells expressing the p.Asp396Asn and p.Ile596Thr α_{IIb} variants ($p<0.0001$) respectively, when compared with cells expressing wild-type α_{IIb}. Cells expressing the p.Leu492Pro α_{IIb} variant showed a 79% reduction in surface expression of $\alpha_{IIb}\beta_3$ compared to wild-type ($p<0.0001$). Interestingly, CHO cells expressing the p.Asn670Lys and p.Glu698Asp α_{IIb} variants demonstrated similar surface expression of $\alpha_{IIb}\beta_3$ to that observed in cells expressing the wild-type receptor ($p=0.63$, $p=0.77$, respectively) (Figures 5.3 and 5.4).

These findings were confirmed by repeating the transfections and then assessing receptor expression by flow cytometry using an antibody against the $\alpha_{IIb}\beta_3$ complex (Figure 5.5 and 5.6). Thus, compared to cells expressing the wild-type receptor, flow cytometric analysis revealed reductions in surface expression of $\alpha_{IIb}\beta_3$ of 95%, 90% and 60% in cells expressing the p.Asp396Asn, p.Ile596Thr and p.Leu492Pro α_{IIb} variants, respectively ($p<0.0001$), while $\alpha_{IIb}\beta_3$ expression was similar to that of wild-type cells in those cells expressing the p.Asn670Lys (91%; $p=0.09$) and p.Glu698Asp (110%; $p=0.06$) α_{IIb} variants.

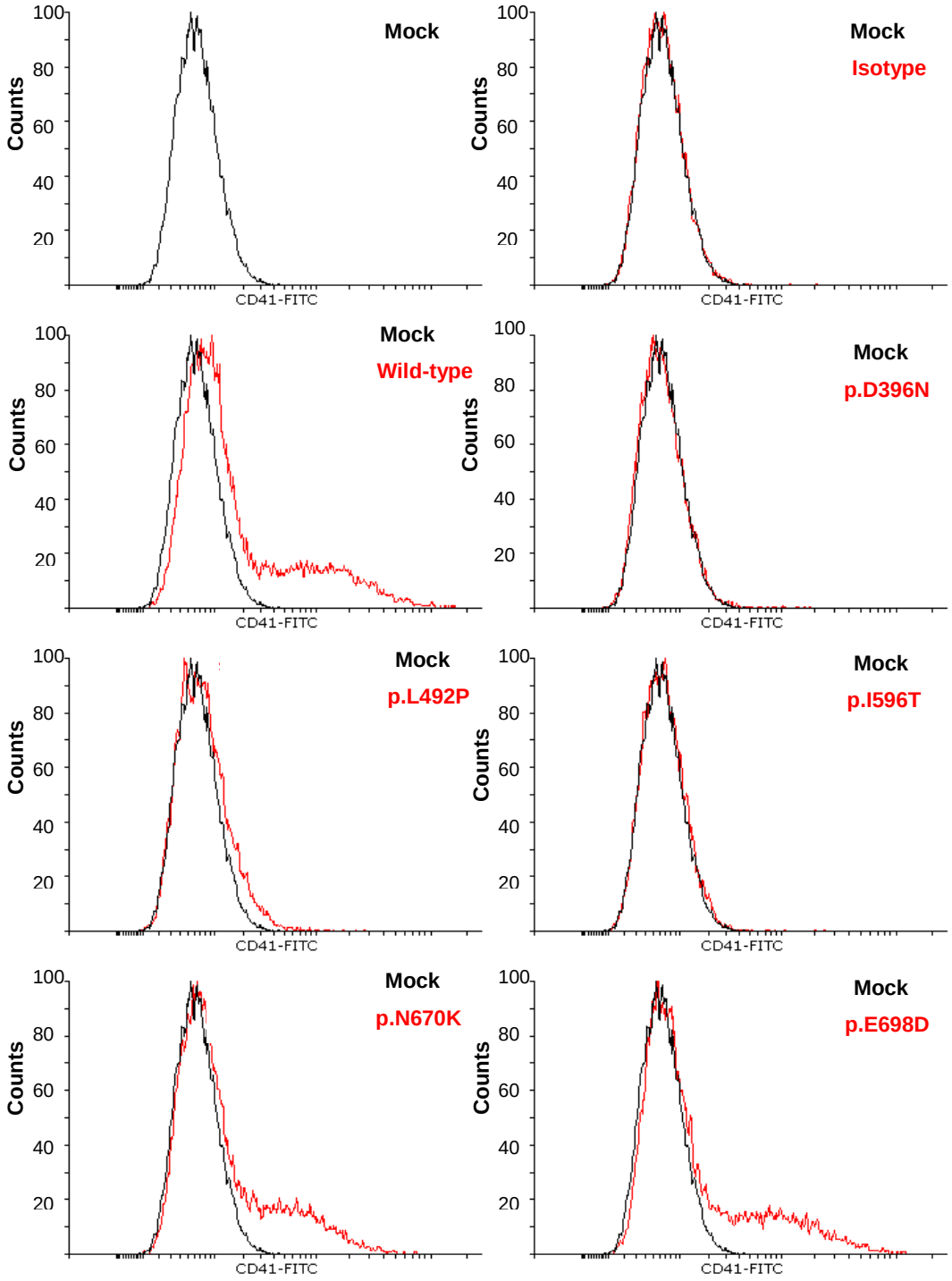

Figure 5.3 Flow cytometric analysis of surface expression of $\alpha_{IIb}\beta_3$ in CHO cells using an antibody against α_{IIb}. CHO cells were transfected with wild-type *ITGB3* cDNA and wild-type or variant *ITGA2B* cDNAs as indicated. Following 48 hours of transfection, the cells were then incubated with a FITC-conjugated monoclonal antibody against the α_{IIb} subunit. Cells were also stained with a FITC-conjugated mouse IgG1 isotype control antibody to assess non-specific binding and confirm the specificity of the primary antibody.

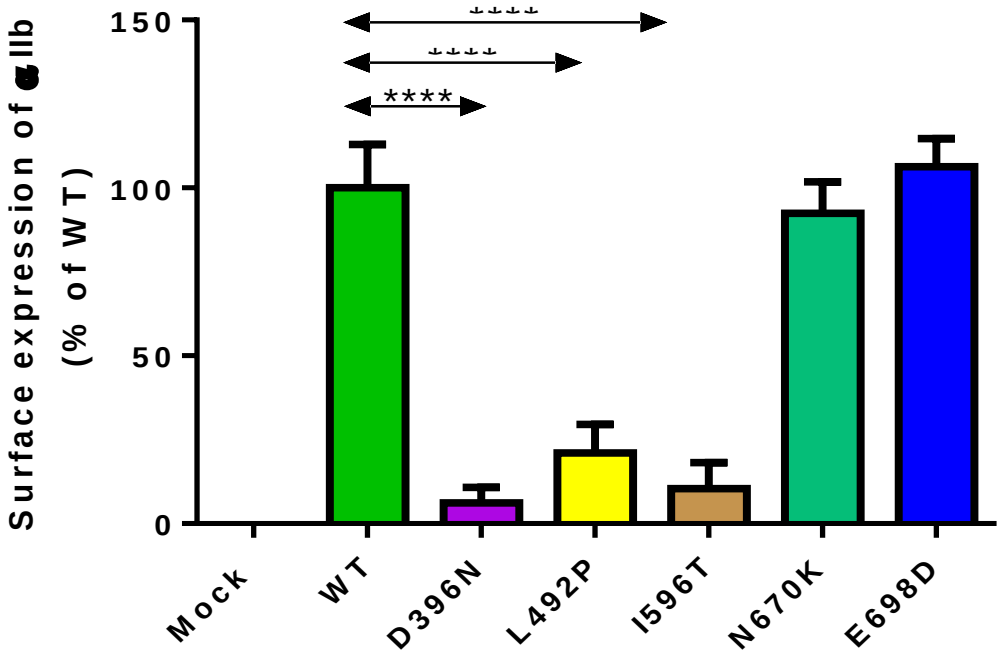

Figure 5.4 Flow cytometric analysis of surface α_{IIb} expression on transfected CHO cells using anti-α_{IIb} antibody. Membrane expression of α_{IIb} on CHO cells expressing the indicated α_{IIb} variants relative to that in cells expressing the wild-type receptor (normalized to 100%). CHO cells were transfected with wild-type *ITGB3* cDNA and either wild-type or variant *ITGA2B* cDNA, or mock transfected with empty pcDNA3.1 as a negative control. Cells were incubated with anti-α_{IIb} monoclonal antibody conjugated with FITC. There were significant reductions in α_{IIb} expression in CHO cells expressing the p.Asp396Asn, p.Leu492Pro and p.Ile596Thr variants by approximately 94%, 79% and 90%, respectively. Cells expressing the p.Asn670Lys and p.Glu698Asp variants showed similar levels of $\alpha_{IIb}\beta_3$ receptor expression to those expressing the wild-type receptor. The data represent the mean of 5 independent experiments with error bars representing the standard deviation. ****,p<0.0001, One-way ANOVA, followed by Dunnett's test.

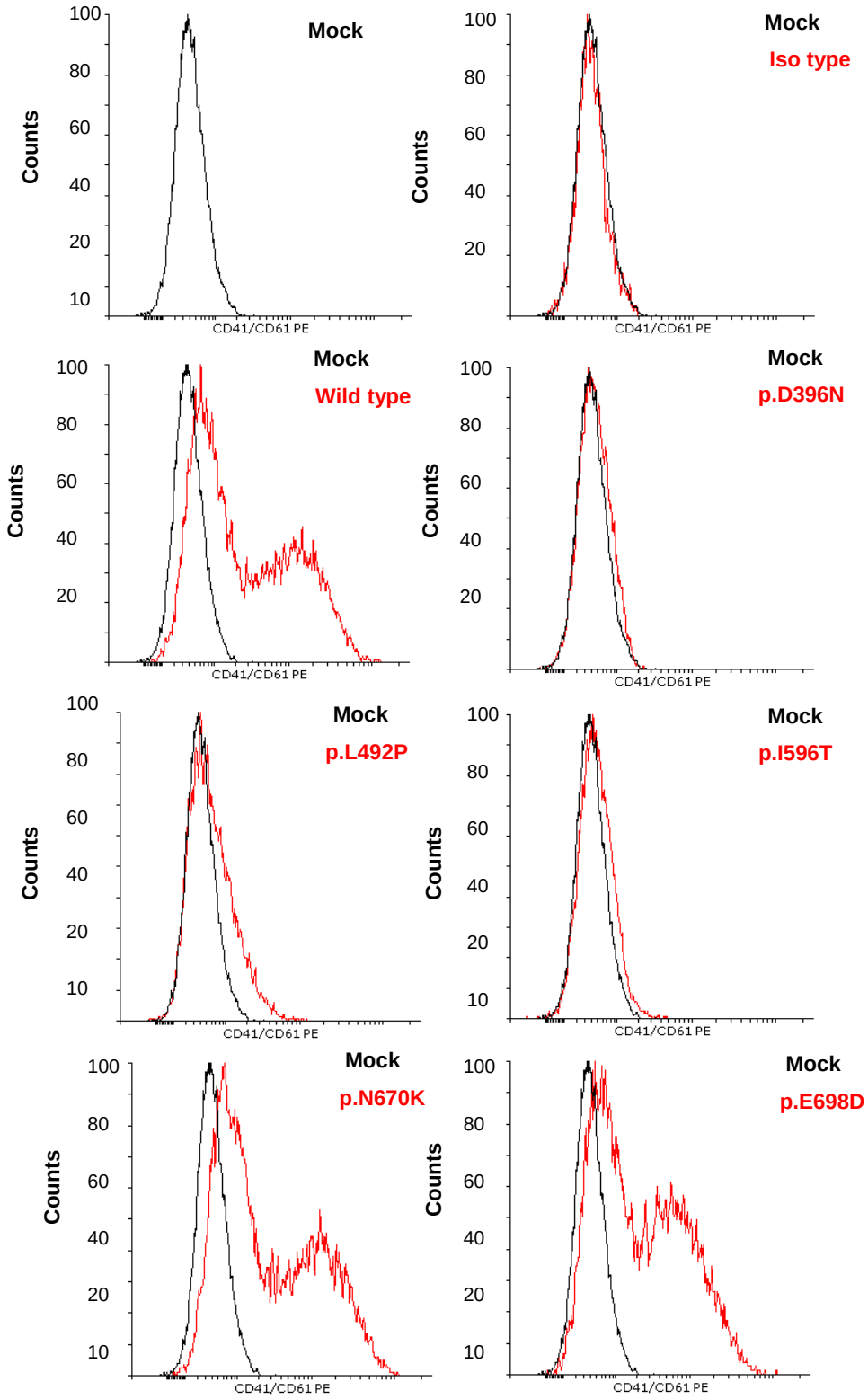

Figure 5.5 Flow cytometric analysis of surface expression of $\alpha_{IIb}\beta_3$ in CHO cells using an antibody against the $\alpha_{IIb}\beta_3$ complex. CHO cells were transfected with wild-type *ITGB3* cDNA and wild-type or variant *ITGA2B* cDNAs as indicated. The cells were then incubated with a PE-conjugated monoclonal antibody against $\alpha_{IIb}\beta_3$ (CD41/CD61). Cells were also stained with a PE mouse IgG1 isotype control antibody to assess non-specific binding and confirm the specificity of the primary antibody.

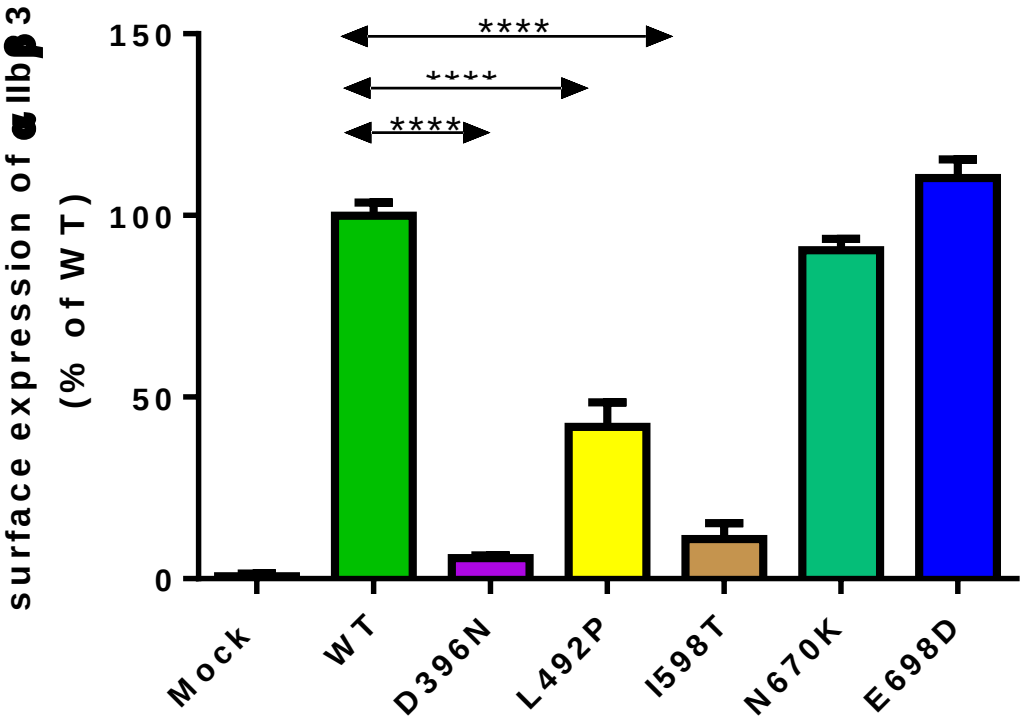

Figure 5.6 Flow cytometric analysis of surface $\alpha_{IIb}\beta_3$ expression on transfected CHO cells using an anti-$\alpha_{IIb}\beta_3$ antibody. Membrane expression of $\alpha_{IIb}\beta_3$ on CHO cells expressing the indicated α_{IIb} variants relative to cells expressing the wild-type receptor (normalized to 100%). CHO cells were transfected with wild-type *ITGB3* cDNA and either wild-type or variant *ITGA2B* cDNA, or mock transfected with empty pcDNA3.1 as a negative control. Cells were incubated with anti-$\alpha_{IIb}\beta_3$ monoclonal antibody conjugated with PE. Significant reductions in surface $\alpha_{IIb}\beta_3$ expression were observed in CHO cells expressing the p.Asp396Asn (95%), p.Leu492Pro (60%) and p.Ile596Thr (90%) variants. Cells expressing the p.Asn670Lys and p.Glu698Asp variants showed similar levels of $\alpha_{IIb}\beta_3$ receptor expression to those expressing the wild-type receptor. The data represent the mean of 5 independent experiments with error bars representing the standard deviation. ****,p<0.0001, One-way ANOVA, followed by Dunnett's test.

5.4.3 Activation capacity of α_{IIb} variants

Given that surface $\alpha_{IIb}\beta_3$ expression in CHO cells expressing the p.Asn670Lys and pGlu698Asp variants of α_{IIb} was comparable to that of cells expressing the wild-type receptor, and that the p.Leu492Pro α_{IIb} variant resulted in a receptor that was surface expressed at moderate levels, the ability of these recombinant $\alpha_{IIb}\beta_3$ receptors to undergo the conformational change that occur upon activation to enable ligand-binding was investigated by flow cytometry.

Activation of $\alpha_{IIb}\beta_3$ was assessed using FITC-conjugated PAC-1, an antibody which binds only to the active conformation of the receptor, while ligand binding was assessed using fibrinogen conjugated to an Alexa Fluor® 488 tag. Cells were transfected and harvested as described in section 2.2.2.13 and then treated with 20µM DTT (to activate the receptor) or PBS as a control (resting), before being incubated with fluorescently labelled PAC-1 or fibrinogen and analysed by flow cytometry.

Under resting conditions, without activation of the receptor by treatment with DTT, cells expressing the p.Asn670Lys, pGlu698Asp and p.Leu492Pro α_{IIb} variants behaved similarly to cells expressing the wild-type receptor. Following activation of $\alpha_{IIb}\beta_3$ by treatment with DTT, binding to both PAC-1 and fibrinogen was similar to that of the wild-type receptor in cells expressing the p.Glu698Asp α_{IIb} variant receptor ($p=0.9$). In contrast, there was almost a complete absence of PAC-1 and fibrinogen-binding in cells expressing the p.Leu492Pro ($p<0.0001$) variant, while a severe reduction in PAC-1 (53%) and fibrinogen (40%) binding was detected in cells expressing the p.Asn670Lys variant ($p<0.001$) (Figure 5.7), suggesting the p.Leu492Pro and p.Asn670Lys substitutions cause impaired integrin activation.

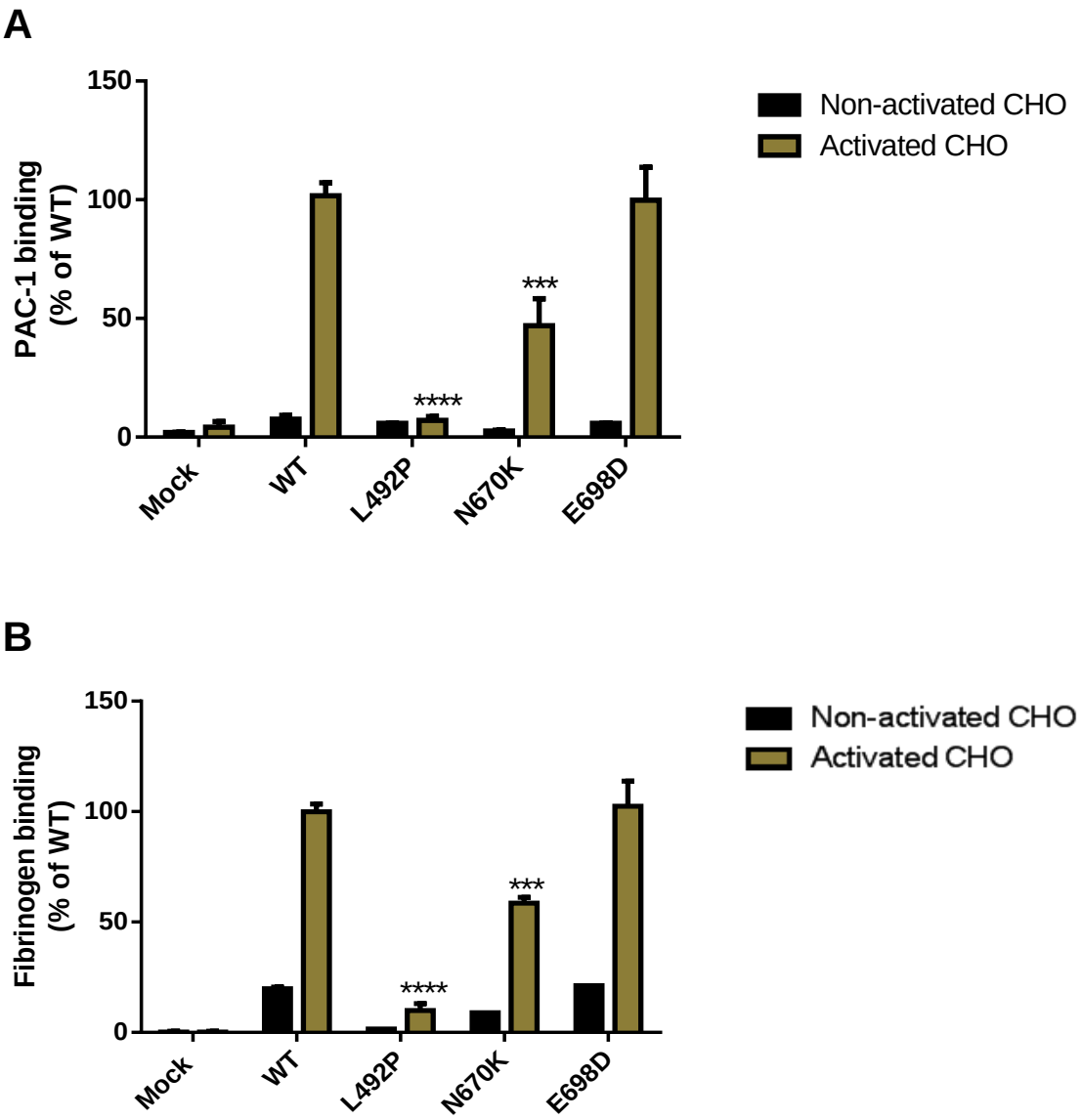

Figure 5.7 $\alpha_{IIb}\beta_3$ activation in CHO cells expressing p.Leu492Pro, p.Asn670Lys and p.Glu698Asp α_{IIb} variants. PAC-1 (A) and fibrinogen (B) binding to resting and activated CHO cells expressing α_{IIb} variants. Cells were transfected with wild-type *ITGB3* cDNA and either wild-type or variant *ITGA2B* cDNA, or mock transfected with empty pcDNA3.1 as a negative control. Cells were incubated with 20µM DTT (activated) or PBS (resting/non-activated) at 37°C. Cells were then incubated either with PAC-1 conjugated to FITC or soluble fibrinogen conjugated to Alexa Fluor®488 and binding analysed by flow cytometry. Compared to cells expressing the wild-type receptor, PAC-1 binding showed 93% and 53% reductions in cells expressing the p.Leu492Pro and p.Asn670Lys variants, respectively while binding was similar to the wild-type receptor in cells expressing the p.Glu698Asp variant. Similarly, cells expressing the p.Leu492Pro and p.Asn670Lys variants showed 90% and 40% reductions in fibrinogen binding, respectively while cells expressing p.E698D variant demonstrated comparable fibrinogen binding to that of the wild-type receptor. The data represents the mean of 3 independent experiments with error bars representing the standard deviation of the mean. Statistical analyses were calculated by one-way ANOVA, followed by Dunnett's test ****,p<0.0001; ***,p<0.001.

5.4.4 Immunoblot analysis of lysates from CHO cells expressing wild-type and variant forms of α_{IIb}

To further elucidate the mechanism for reduced membrane expression of $\alpha_{IIb}\beta_3$ in CHO cells transfected with the p.Asp396Asn, p.Leu492Pro, p.Ile596Thr α_{IIb} expression constructs, expression of α_{IIb} subunits was analysed by SDS-PAGE of CHO cell lysates under reducing conditions followed by Western blot analysis. Lysates from cells expressing the p.Asn670Lys and p.Glu698Asp α_{IIb} variants were also analysed to confirm the normal surface expression levels of $\alpha_{IIb}\beta_3$ that were observed in cells expressing these variants. CHO cells were transfected with wild-type *ITGB3* cDNA and either wild-type or variant *ITGA2B* cDNA, or mock transfected with empty pcDNA3.1 plasmid as a negative control. Following 48 hours of transfection, cell lysates were subjected to electrophoresis in 8% polyacrylamide gels containing SDS under reducing conditions. Following electrophoresis, proteins were transferred to a nitrocellulose membrane by Western blotting and the α_{IIb} subunit then immunologically detected (Section 2.2.2.18). Pro-α_{IIb} and mature-α_{IIb} are estimated to be 136 kDa and 125 kDa in size, respectively.

As expected, lysates from cells expressing wild-type α_{IIb} and the p.Asn670Lys and p.Glu698Asp variants of α_{IIb} displayed two immunoreactive bands of 136kDa and 125kDa, corresponding to pro-α_{IIb} and mature-α_{IIb}, respectively (Figure 5.7). In contrast, a single 136kDa protein species, which corresponding to pro-α_{IIb}, was observed in lysates from cells expressing the p.Leu492Pro and p.Ile596Thr α_{IIb} variants, indicating a failure in processing of both of these variants to the mature α_{IIb} (Figure 5.8). Interestingly, a single α_{IIb} immunoreactive species, having a molecular weight of approximately 200kDa was detected in lysates from cells expressing the p.Asp396Asn α_{IIb} variant.

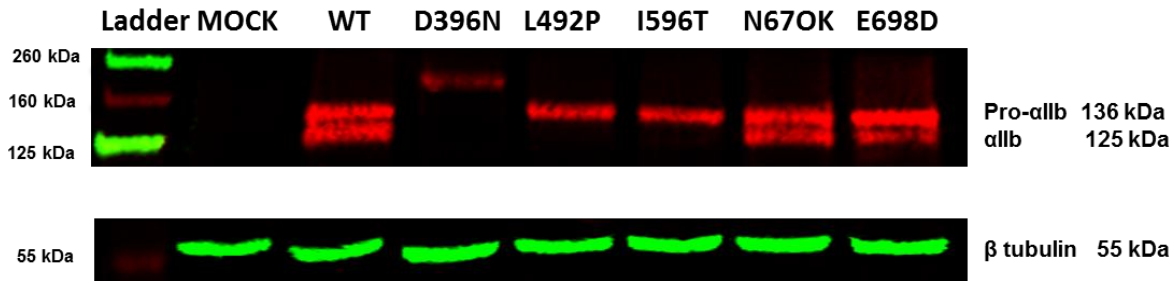

Figure 5.8 Electrophresis and Western blot analysis of lysates from CHO cells expressing α_{IIb} variants. CHO cells were transfected with wild-type *ITGB3* cDNA and either wild-type or variant *ITGA2B* cDNA, or mock transfected with empty pcDNA3.1 plasmid as a negative control. Cell lysates were subjected to electrophoresis in 8% SDS polyacrylamide gels under reducing conditions and then transferred to a nitrocellulose membrane before immunodetection of α_{IIb} and β-tubulin. Lysates from cells expressing wild-type α_{IIb}, and the p.Asn670Lys and p.Glu698Asp variants displayed two immunoreactive protein species at 136kDa and 126kDa, corresponding to pro-α_{IIb} and mature α_{IIb}, respectively. In contrast, lysates from cells expressing the p.Leu492Pro and p.Ile596Thr variants demonstrated the presence only of pro-α_{IIb} (136kDa). A single immunoreactive species, having a molecular weight of approximately 200kDa was observed in cells expressing the p.Asp396Asn α_{IIb} variant. β tubulin was used as a loading control.

5.4.5 Aberrant N-linked glycosylation, or binding to β_3 do not explain the high molecular weight of the p.Asp396Asn α_{IIb} subunit

Previous studies revealed that the processing of pro-α_{IIb} into its mature form is associated with N-linked glycosylation, and that the molecular weight of pro-α_{IIb} was reduced following treatment of cell lysates with Endoglycosidase H which cleaves the unprocessed high mannose carbohydrate chains which are added to specific asparagine residues of glycoproteins in the ER. Thus, inhibition of N-linked glycosylation has been shown to result in the absence of mature-α_{IIb} (Duperray*, et al* 1987, Freeze and Kranz 2008). Calvete*, et al* (1989) previously identified five N-linked glycosylation sites at asparagine residues 46, 280, 601, 711 and 962 of α_{IIb}, all of which occur in classical Asn-X-Ser/Thr consensus sequences. The possibility that the high molecular weight form of α_{IIb} which was observed in CHO cells expressing the p.Asp396Asn variant could be due to aberrant glycosylation was considered. The p.Asp396Asn substitution occurs in a triad of residues, Asn396-Leu397-Asp398, which is not in a consensus sequence for N-linked glycosylation. However, prediction of N-linked glycosylation sites in the wild-type α_{IIb} and p.Asp396Asn variant using NetNGlyc1.0 (http://www.cbs.dtu.dk/services/NetNGlyc/) showed that the substitution increased the potential for glycosylation at this position (Figure 5.9).

The possibility that the increased size of the α_{IIb} in cells expressing the p.Asp396Asn was due to additional glycosylation was examined by treating cell lysates with Endoglycosidase (Endo) H prior to SDS-PAGE and western blotting. There was a slight reduction in the size of the α_{IIb} species in cells expressing the p.Asp396Asn variant, but not to the size of the wild-type α_{IIb} treated with Endo H, suggesting that the difference in molecular weight between the wild-type α_{IIb} and p.Asp396Asn variant is unlikely to be the result of abnormal N-linked glycosylation (Figure 5.10).

The possibility that the high molecular weight form of α_{IIb} represented a complex of α_{IIb} with β_3 that resists reduction was also examined. Thus, immunoblots of lysates from cells expressing the wild-type α_{IIb} and p.Asp396Asn variant were probed with a β_3 antibody. However, the high molecular weight form of α_{IIb} did not react with the anti- β_3 antibody, and the only β_3 species that was observed was the of the expected size of 85kDa (Figure 5.11).

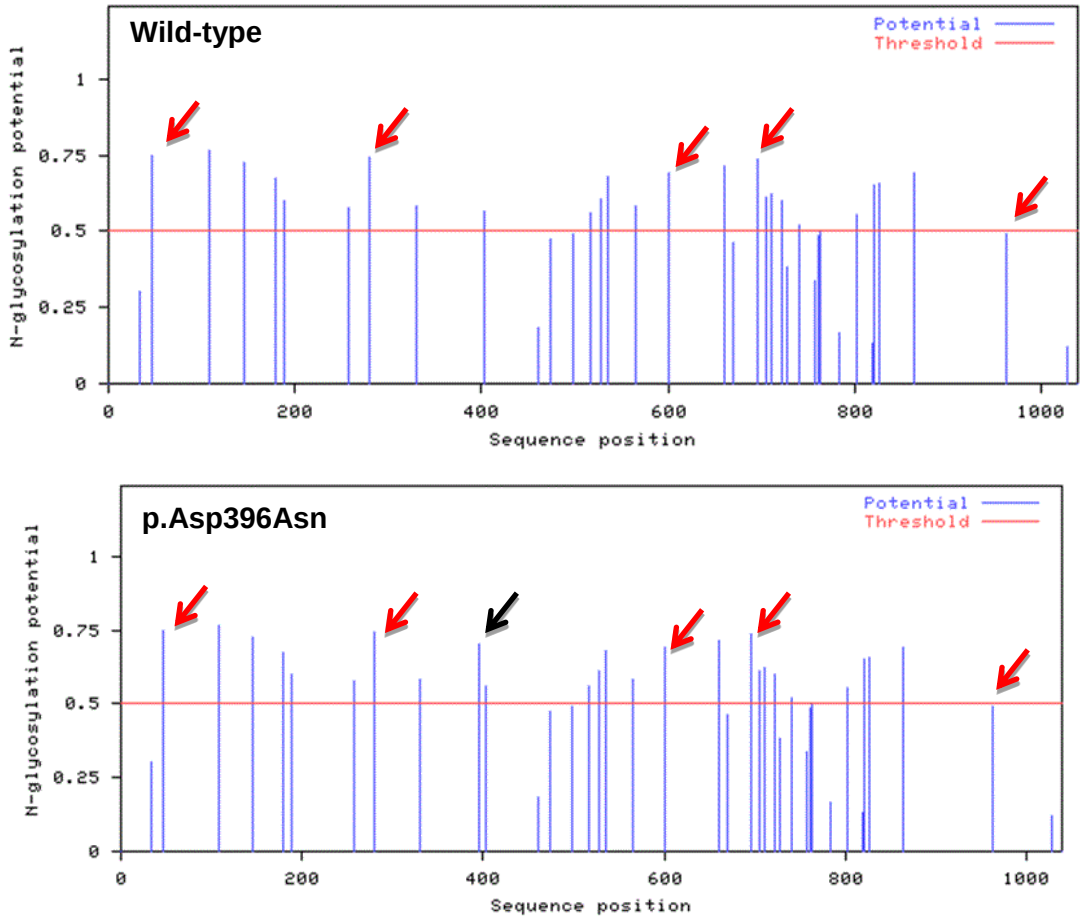

Figure 5.9 Potential for N-glycosylation across the amino acid sequence of wild-type α_{IIb} and the p.Asp396Asn variant predicted using NetNGlyc 1.0. As expected, asparagine residues 46, 280, 601, 711 and 962, which occur within the consensus sequence Asn-X-Ser/Thr, all show high potential for N-linked glycosylation, as indicated by the red arrows in the upper panel. The p.Asp396Asn substitution introduces an asparagine residue that has a high potential for N-glycosylation (score: 0.7037), as is indicated with a black arrow in the lower panel.

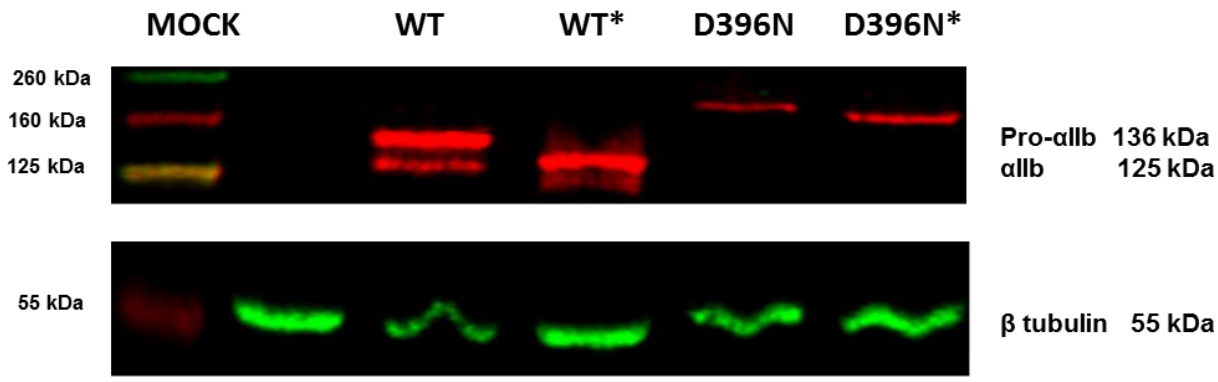

Figure 5.10 Electrophoresis and Western blot analysis of lysates from CHO cells expressing the p.Asp396Asn α_{IIb} variant following treatment with Endo H. CHO cells were transfected with wild-type *ITGB3* cDNA and either wild-type or variant *ITGA2B* cDNA, or mock transfected with empty pcDNA3.1 plasmid as a negative control. Cell lysates were incubated with Endo H or buffer before being subjected to electrophoresis in 8% SDS polyacrylamide gels under reducing conditions and then transferred to a membrane for immunodetection of α_{IIb} and β-tubulin. Cells expressing the p.Asp396Asn variant show a single α_{IIb} species with a molecular weight of approximately 200 kDa, in contrast to cells expressing wild-type α_{IIb} which show the presence of pro- and mature-α_{IIb}. After Endo H treatment, a modest reduction in size was observed for both wild-type and variant α_{IIb}. β tubulin was used as a loading control. * : cell lysates treated with Endo H.

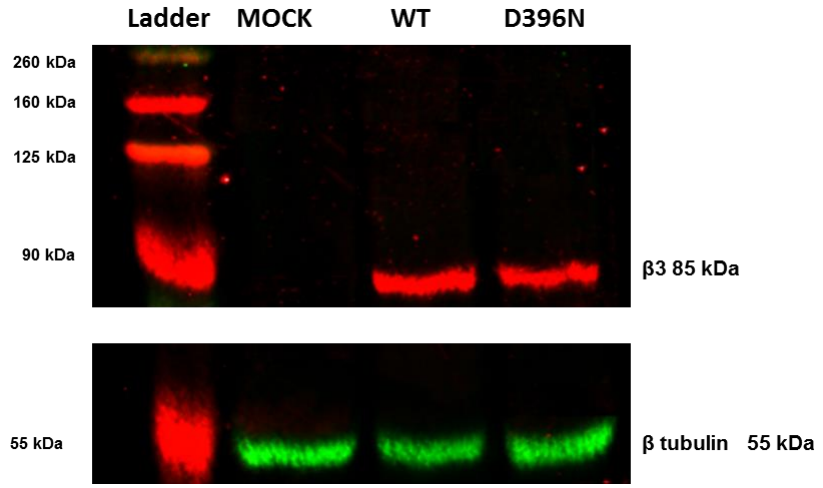

Figure 5.11 Electrophoresis and Western blot analysis of β_3 in lysates from CHO cells expressing the p.Asp396Asn α_{IIb} variant. A single protein species of the expected molecular weight of 85kDa was observed in lysates from cells expressing wild-type α_{IIb} and the p.Asp396Asn. β tubulin was used as a loading control.

5.4.6 Investigation of the potential effects of the c.2094G>T transversion on *ITGA2B* splicing

Primers were designed to amplify a DNA fragment of 851 bp spanning nucleotides +10831 to +11682 of *ITGA2B* from genomic DNA (Section 5.3.1). PCRs were performed over a range of annealing temperatures (57-68°C), with a single fragment of the expected size being selectively amplified at 68°C (Figure 5.12).

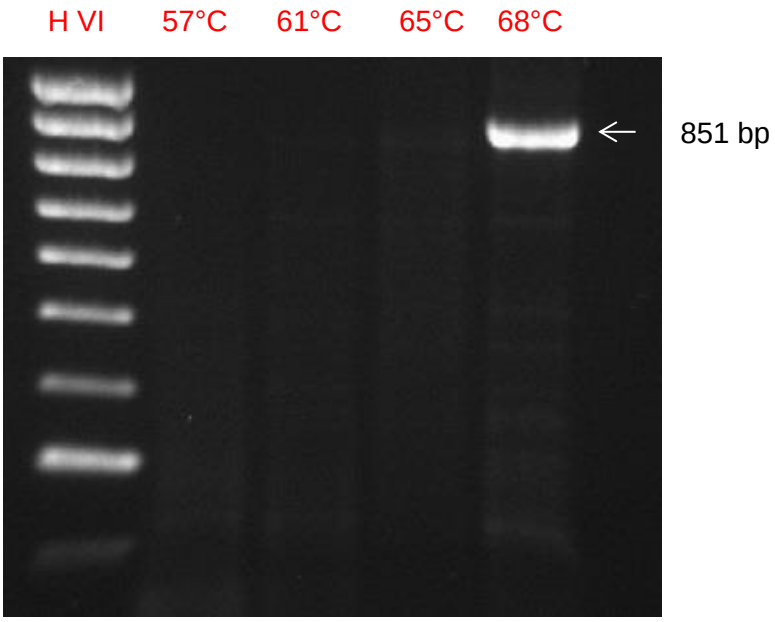

Figure 5.12 Electrophoresis of amplified *ITGA2B* fragment. Electrophoresis in 2% agarose of an 851 bp fragment of *ITGA2B* which was amplified at the indicated annealing temperatures. A single DNA fragment of the expected size was amplified at 68°C. H IV: hyperladder IV.

The 851 bp fragment of *ITGA2B* was cloned into pET-01 as described (Section 5.3.1) and sequencing of DNA from a recombinant plasmid confirmed the presence of the expected insert sequence in the recombinant pET01-*ITGA2B* plasmid (Figure 5.13).

Figure 5.13 Sequence analysis of recombinant pET01-*ITGA2B* plasmid. Alignment of the recombinant pET01-*ITGA2B* plasmid sequence with that of empty pET-01 demonstrates the presence of an 851 bp insert corresponding to exon 20 and flanking introns (intron 19 and intron 20) of *ITGA2B*. The text highlighted in yellow indicates the BamHI (GGATCC) and NotI (GCGGCCGC) sites that were used to facilitate cloning. Exon sequence is shown in upper case and intron in lower case.

Having successfully derived the recombinant pET01-*ITGA2B* plasmid, site-directed mutagenesis was carried out to introduce the c.2094G>T substitution at the 5' end of the exon 20 sequence (see Section 5.3.1.7). Sequence analysis of the mutated plasmid confirmed the presence of the desired alteration and that no further changes had been introduced into the pET01 plasmid (Figure 5.14).

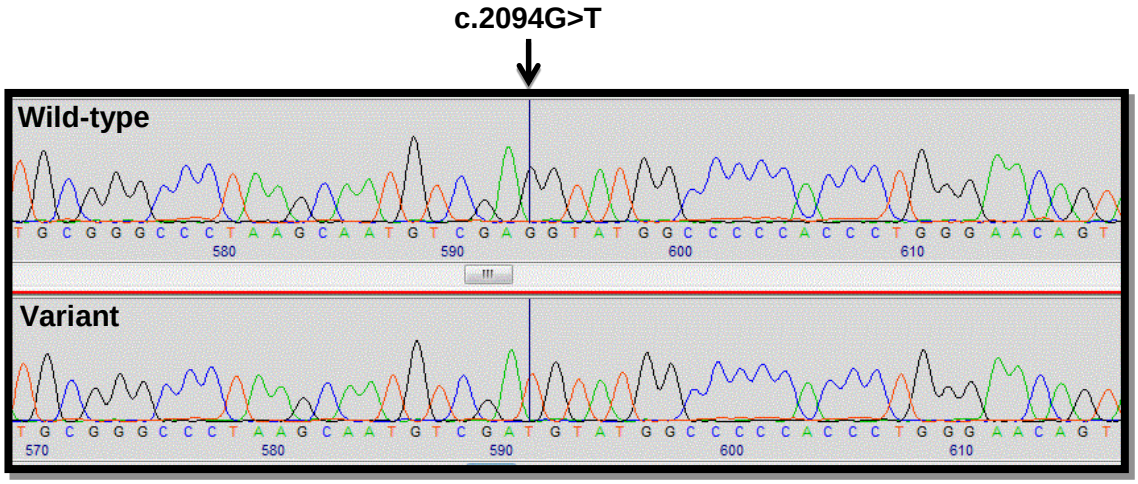

Figure 5.14 Sequence chromatograms of *ITGA2B*-pET01 fragments showing the position of the single nucleotide change introduced by site-directed mutagenesis. The chromatograms confirm introduction of the c.2094G>T alteration.

To investigate the effects of the c.2094G>T transversion in *ITGA2B* on splicing of the *ITGA2B* RNA, the wild-type *ITGA2B*-pET01, mutant *ITGA2B*-pET01 and empty pET01 plasmids were transfected into CHO cells as previously described (see Section 5.3.1.8). Forty eight hours post transfection, mRNA was extracted from the cells and reverse transcribed to generate cDNA, before amplifying a cDNA fragment using primers that bind to sequences in the exons located upstream and downstream of the inserted *ITGA2B* sequence (Section 5.3.1.8). The PCR products were then analysed by electrophoresis in 0.7% agarose (Section 2.2.2.1).

A fragment of the expected size of 113 bp was amplified from cells transfected with empty pET01 indicating removal of the intron sequences derived from the vector. Two fragments of 113 bp and 262 bp were amplified from cells transfected with wild-type pET01-*ITGA2B*, which corresponded to the expected fragments expected after removal of the intron sequences from the exontrap vector and those introduced in the *ITGA2B* fragment, respectively. Interestingly, a single fragment of 113 bp was amplified from cDNA derived from cells transfected with the mutated pET01-*ITGA2B*-2094T plasmid, indicating that the c.2094G>T substitution resulted in exon 20 skipping (Figure 5.15).

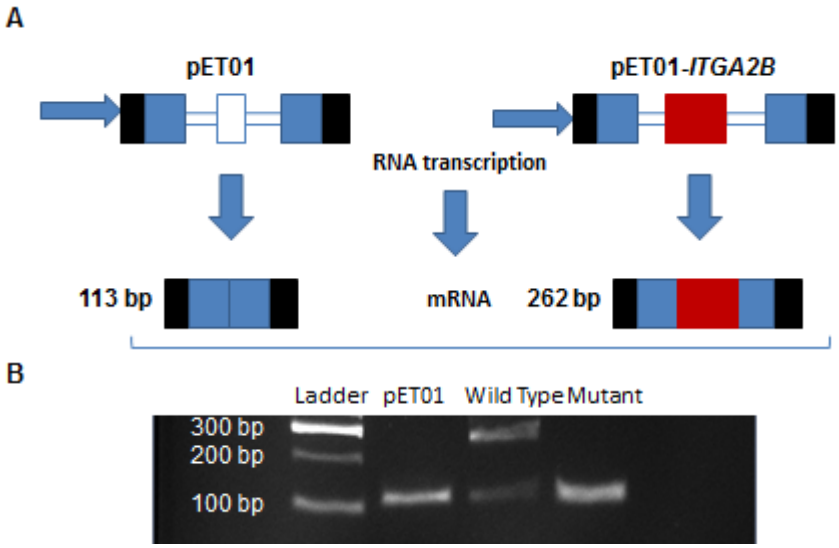

Figure 5.15 The c.2094G>T transversion in *ITGA2B* results in skipping of exon 20. A) A schematic representation of pET01 and the wild-type pET01-*ITGA2B* vector showing the sizes of the mRNA transcripts expected following removal of the exons from pET01 (113 bp) and the inserted *ITGA2B* sequence (262 bp). B) Electrophoresis of PCR amplified cDNA fragments derived from CHO cells transfected with pET01, wild-type pET01-*ITGA2B* and mutated pET-*ITGA2B*-2094T.

5.4.6.1 Deletion mutagenesis of exon 20

The skipping of exon 20, and its exclusion from the *ITGA2B* mRNA that occurs as a result of the c.2094G>T defect is predicted to lead to a frameshift and introduction of a premature stop codon, (c.1947_2094del; p.Thr650Alafs*24) (**Appendix 4**). To further investigate the effect of the c.1947_2094del defect, exon 20 was deleted from wild-type *ITGA2B* cDNA using the QuikChange® Lightning Site-Directed Mutagenesis Kit and its absence confirmed by direct sequencing (Section 5.3.1.9; Figure 5.16).

Figure 5.16 Sequence analysis of wild-type and recombinant *ITGA2B* expression plasmids following deletion of exon 20. Alignment of the wild-type and mutated pcDNA3.1 *ITGA2B* expression plasmid sequences confirms the introduction of the c.1947_2094del defect.

5.4.6.2 The c.1947_2094del ITGA2B defect reduces expression of $\alpha_{IIb}\beta_3$ in CHO cells

CHO cells were transfected with wild-type *ITGB3* cDNA and either wild-type or c.1947_2094del *ITGA2B* cDNA. Flow cytometric analysis revealed a 96-98% reduction in surface expression of the $\alpha_{IIb}\beta_3$ receptor in CHO cells expressing the c.1947_2094del *ITGA2B* variant (Figure 5.17). Western blot analysis of the cell lysates revealed an almost complete absence of both pro-α_{IIb} and mature α_{IIb} in the cells transfected with the c.1947_2094del *ITGA2B* variant (Figure 5.18).

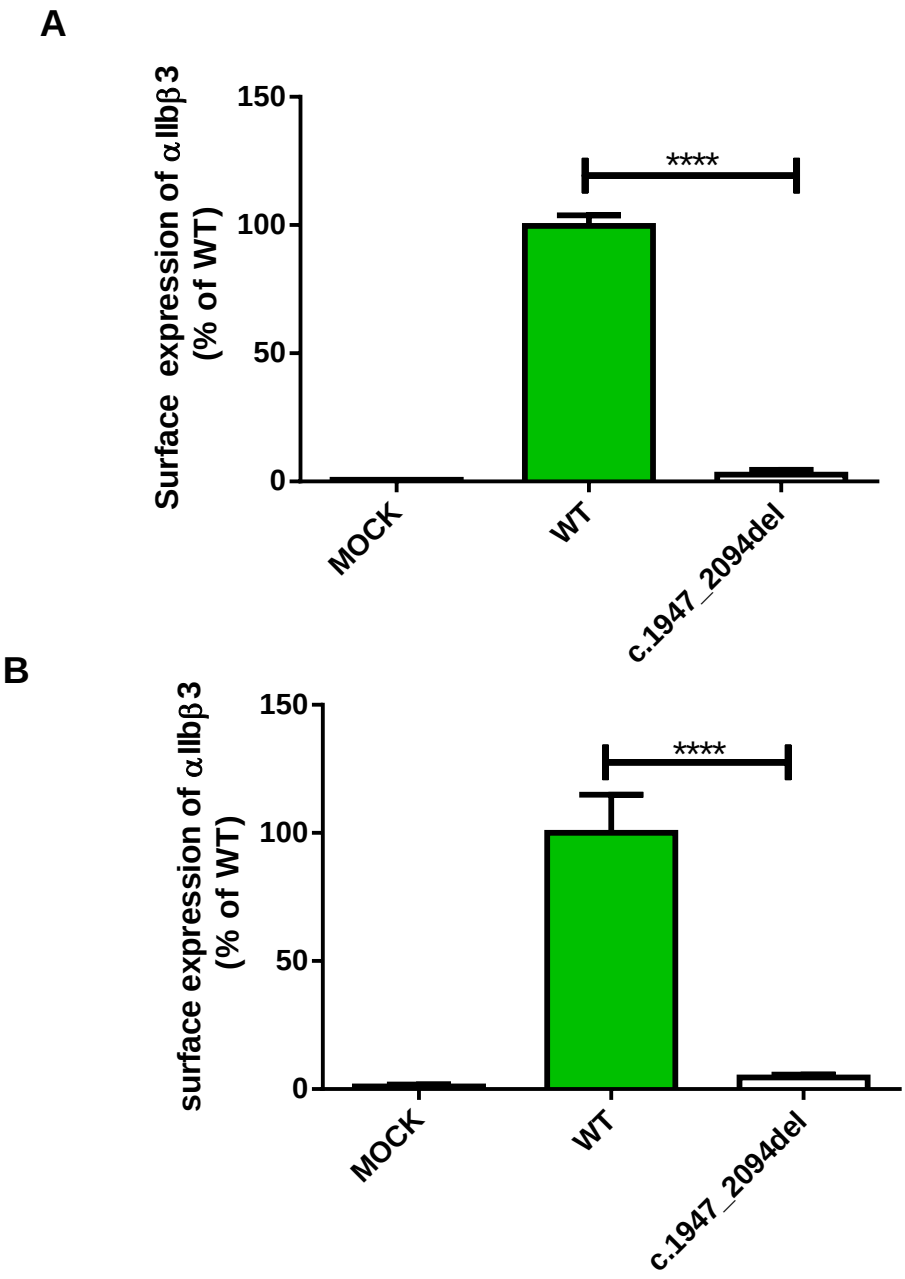

Figure 5.17 Flow cytometric analysis of surface $\alpha_{IIb}\beta_3$ expression in transfected CHO cells expressing c.1947_2094del. CHO cells were transfected with wild-type *ITGB3* cDNA and either wild-type or variant *ITGA2B* cDNA, or mock transfected with empty pcDNA3.1 vector as a negative control. Cells were incubated either with anti-α_{IIb} and β_3 monoclonal antibodies conjugated with FITC and PE, respectively (A) or with a PE-conjugated anti-$\alpha_{IIb}\beta_3$ (B). The expression level of $\alpha_{IIb}\beta_3$ was normalized to that of cells expressing the wild-type receptor. The flow cytometric analysis demonstrated a 96-98% reduction in surface expression of the $\alpha_{IIb}\beta_3$ receptor on CHO cells expressing the c.1947_2094del variant, when compared with wild-type. The data represent the mean of 3 independent experiments with error bars representing the standard deviation. ****,p<0.0001, One-way ANOVA, followed by Dunnett's test.

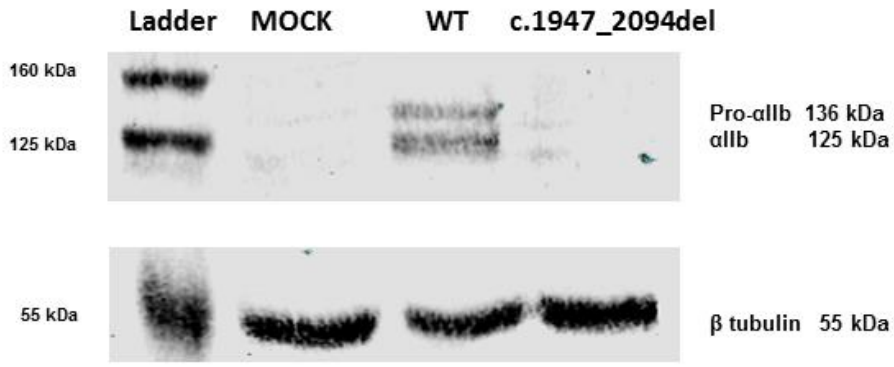

Figure 5.18 Western blot analysis of CHO cell lysates expressing c.1947_2094del under reduced conditions. CHO cells were transfected with wild-type *ITGB3* cDNA and either wild-type or mutated *ITGA2B* cDNA, or mock transfected with empty vector pcDNA3.1 as a negative control. Cell lysates were electrophoresed in an 8% SDS-polyacrylamide gel, and Western blotted prior to detection of α_{IIb} and β-tubulin. Pro-α_{IIb} and mature α_{IIb} were almost absent in cells transfected with the c.1947_2094del variant of *ITGA2B*. β tubulin (55 kDa) was detected using a mouse anti-β tubulin and used as a loading control.

5.5 Discussion

The studies summarised in this chapter aimed to characterise five non-synonymous *ITGA2B* defects which were identified in index cases with GT, who were recruited as part of a previous survey to characterise the molecular defects underlying GT in the UK. Two of the defects have been described in other GT cases, but none of them had been characterised to any extent. Four of the defects, c.1186G>A, c.1475T>C, c.1787T>C and c.2010C>A, predicted p.Asp396Asn, p.Leu492Pro, p.Ile596Thr and p.Asn670Lys amino acid substitutions in α_{IIb}. The fifth defect, a c.2094G>T transversion in exon 20 of *ITGA2B,* was predicted to cause aberrant splicing of the *ITGA2B* RNA, though the less likely possibility that it could result in a p.Glu698Asp substitution was also investigated.

The key findings of the *in vitro* studies described in this chapter are summarised in Table 5.6. The p.Asp396Asn, p.Leu492Pro and p.Ile596Thr α_{IIb} variants resulted in a significantly reduced surface expression of $\alpha_{IIb}\beta_3$ in CHO cells. In contrast, the p.Asn670Lys variant did not interfere with integrin expression but resulted in impaired activation of $\alpha_{IIb}\beta_3$. The c.2094G>T transversion caused aberrant splicing and exclusion of exon 20 from the *ITGA2B* RNA. Thus, my findings confirm the pathogenicity of these five defects, and the likelihood that they cause or contribute to the bleeding tendency that was observed in the index cases who inherited the defects.

Table 5.6 Summary of in vitro studies on candidate *ITGA2B* defects

***ITGA2B* variants**	**Nucleotide change**	**Surface expression (α_{IIb} and β_3 subunits / $\alpha_{IIb}\beta_3$ receptor) (% of WT)**	**PAC-1 / fibrinogen binding (% of WT)**	**Western blotting**
p.Asp396Asn	c.1186G>A	6 / 5	N/A	Pro-α_{IIb}
p.Leu492Pro	c.1475T>C	21 / 40	Almost absent	Pro-α_{IIb}
p.Ile596Thr	c.1787T>C	10 / 10	N/A	Pro-α_{IIb}
p.Asn670Lys	c.2010C>A	92 / 91	47 / 60	Pro-α_{IIb} Mature-α_{IIb}
p.Glu698Asp	c.2094G>T	106 / 110	Comparable level	Pro-α_{IIb} Mature-α_{IIb}
c.1947_2094del	c.2094G>T	4 / 2	N/A	Absence

N/A : Not applicable

The c.1186G>A transition predicted the substitution of a negatively charged aspartate residue, by an uncharged asparagine residue at position 396 of the α_{IIb} subunit. This defect was identified in two GT cases recruited through the UK cohort, both of whom inherited it as a homozygous defect. The cases were 16 and 29 year old males of Pakistani origin who had severe bleeding histories, and subjective bleeding scores of 7 and 5, respectively. As stated earlier (Section 3.3.5.2), Asp396 forms part of the calcium binding site in blade-6 of the α_{IIb} β propeller domain. *In silico* analysis showed that this residue is highly conserved across species and in other human α-integrin family members and its substitution by asparagine was predicted to be deleterious to the α_{IIb} subunit.

A 94% reduction in surface expression of $\alpha_{IIb}\beta_3$ was observed in CHO cells expressing the p.Asp396Asn α_{IIb} variant, suggesting that this variant was unable to form a stable heterodimer with β_3. Interestingly, analysis of cell lysates revealed the presence of a 200kDa α_{IIb} subunit, a higher molecular weight than expected. This ultimately affects the surface expression of $\alpha_{IIb}\beta_3$. It was shown however that this does not result from enhanced N-linked glycosylation or aberrant binding to β_3. The presence of a larger α_{IIb} protein could be due to lack of reduction of the $\alpha_{IIb}\beta_3$ complex prior to electrophoresis since a complex of the two proteins would be expected to have a molecular weight of approximately 221kDa. However, this was considered unlikely as all other samples migrated at the expected size, and the high molecular weight form of α_{IIb} was not immunoreactive to the anti-β_3 antibody. A failure to separate the complex into its monomeric subunits is therefore unlikely to explain the high molecular weight form of α_{IIb}. Post-translational modifications can also explain an increase in protein size. Although the presence of asparagine at residue 396 in α_{IIb} does not match the consensus sequence for N-linked glycosylation, it was predicted to create a new potential site using an online prediction tool. The possibility that the p.Asp396Asn substitution resulted in additional N-linked glycosylation was therefore assessed by treating protein extracts with Endoglycosidase H (Endo H) which cleaves N-linked glycans between the two N-acetylglucosamine residues that are attached to the asparagine residues in the protein chain (Calvete*, et al* 1989, Duperray*, et al* 1987, Freeze and Kranz 2008). Endo H treatment resulted in a slight decrease in size of both wild-type α_{IIb} and the p.Asp396Asn variant, but the p.Asp396Asn variant was still larger than the expected size and the wild-type control, suggesting that the high molecular weight form is unlikely to be due to differences in N-linked glycosylation, but do not exclude the possibility that it is due to abnormal O-linked glycosylation, or to more complex types of N-linked glycosylation (Calvete*, et al* 1989). It is also possible that the

p.Asp396Asn variant does not fold normally and has adopted a conformation that migrates at a lower rate than the wild-type subunit.

This interesting finding requires further investigation to determine why this protein has a higher molecular weight. This could involve further analysis using other glycosidases such as Peptide-N-Glycosidase F (PNGase F) which cleaves complex oligosaccharides from proteins, or by inhibiting glycosylation to determine whether it explains the increase in size (Duperray*, et al* 1987, Freeze and Kranz 2008). Mass spectrometry could also be used to determine the nature and sequence of this high molecular weight α_{IIb} subunit.

Of the 78 deleterious missense mutations reported in the α_{IIb} subunit, fifty-three involve residues within the β-propeller domain. These have been classified into two groups, those which interfere with α_{IIb} biosynthesis, and those which disrupt $\alpha_{IIb}\beta_3$ complex formation. However, the majority of GT causing substitutions that occur in the β-propeller domain result in a lack of surface expression of $\alpha_{IIb}\beta_3$ due to their deleterious effects on protein biosynthesis, including intracellular trafficking and maturation of the protein, and not on defects in heterodimer formation (Nelson*, et al* 2005, Nurden*, et al* 2013). Residues 1 to 233 of α_{IIb}, which comprise blades 1-3 of the β propeller, have been shown to be crucial for heterodimer formation, and it has been suggested that the residues in blades 4-7 are less important for complex formation (McKay*, et al* 1996). However, the only mutation which has been identified in the β propeller and shown to cause a defect in complex formation involved substitution of Phe202 which binds to Arg287 in β_3 by cysteine at the interface between α_{IIb} and β_3 (Rosenberg*, et al* 2004). Substitutions of other residues in blades 1-3, such as p.Pro157His and p.Gly159Ser, impair progression of pro-$\alpha_{IIb}\beta_3$ from the endoplasmic reticulum (ER) to the Golgi apparatus, and lead to ER retention of the receptor (Nelson*, et al* 2005, Shen*, et al* 2009). There are four calcium-binding sites in blades 4-7 and several mutations have been identified in the vicinity of these, including p.Asp396Asn (Vijapurkar*, et al* 2009). The calcium-binding sites are coordinated by negatively charged amino acids, such as aspartate and glutamate, and by the oxygen atoms of the backbone carbonyl groups. While their function in the β-propeller remains to be fully elucidated they have been shown to play a crucial role in α_{IIb} biogenesis and stability as well as in maintaining the rigidity between α_{IIb} and β_3. For example, although deletion of residues Val456 and Asp457 in the fourth calcium-binding site in blade 7 does not affect the ability of the α_{IIb} to form a heterodimer with β_3, the receptor fails to translocate to the Golgi, thereby resulting in a significant reduction in membrane expression of $\alpha_{IIb}\beta_3$ (Basani*, et al* 1996). Interestingly, in a previous study, while deletion of each of the four calcium-

binding domains in the β propeller was shown not to disturb pro-α_{IIb} synthesis, or impair heterodimer formation, the pro-$\alpha_{IIb}\beta_3$ dimers failed to undergo maturation and expression on the surface membrane, indicating that these deletions disrupted the progression of pro-$\alpha_{IIb}\beta_3$ from the ER to the Golgi for maturation (Basani*, et al* 1996). Importantly, the current results suggest that a single amino acid substitution in the calcium binding site has similar effects on α_{IIb} integrin function to those of whole binding site deletion, indicating that each residue is essential and required for the functioning of the calcium-binding sites. This would be supported by the finding that several other amino acid substitutions affecting these domains, including p.Gly273Asp, p.Val329Phe, p.Glu355Lys, p.Arg358His, p.IIe405The and p.Gly418Asp, impair progression of pro-$\alpha_{IIb}\beta_3$ from the ER to the Golgi, and result in reduced surface expression of the receptor (Milet-Marsal*, et al* 2002b, Mitchell*, et al* 2003, Wilcox*, et al* 1995, Wilcox*, et al* 1994).

Overall, our results indicate that the p.Asp396Asn substitution disturbs $\alpha_{IIb}\beta_3$ biogenesis, possibly by destabilising the β propeller domain and interfering with integrin maturation and intracellular trafficking, ultimately resulting in reduced membrane expression of $\alpha_{IIb}\beta_3$. Given that this substitution directly affects the calcium binding site of the β propeller domain; these findings support previous suggestions that an intact calcium binding site is a prerequisite for correct folding of the β propeller domain, which is in turn essential for heterodimer formation with β_3 and intracellular trafficking of the receptor to the membrane.

We investigated two *ITGA2B* defects which predicted amino acid substitutions in the thigh domain of α_{IIb}, a c.1475T>C transition predicting a p.Leu492Pro substitution and a c.1787T>C transition predicting a p.Ile596Thr substitution. The c.1475T>C transition was identified in a 6 year old Pakistani female with a history of mild bleeding symptoms and a bleeding score of 1, who was compound heterozygous for the defect, having a frame-shift defect on the second allele. The c.1787T>C transition was identified in two Caucasian female index cases, who were both homozygous for the defect. Both cases had severe bleeding symptoms including epistaxis, menorrhagia and gastrointestinal bleeding, and had a bleeding score of 7 when assessed subjectively by the referring clinician. The c.1787T>C transition occurs in the codon for Ile596, which is a highly conserved residue both across species and also among other human α-integrin family members. Online bioinformatic tools consistently predicted this variant to be deleterious to the α_{IIb} subunit. Leu492, the residue substituted as a result of the c.1475T>C transition, was not highly conserved across species, or among α-integrins, but its substitution by proline was predicted to be deleterious to α_{IIb}. While the p.Leu492Pro variant is novel, there have been two previous reports of the p.Ile596Thr variant (Ruan,

et al 1998, Sandrock*, et al* 2012). Thus, Ruan*, et al* (1998) reported a 5 year old Swiss boy who was compound heterozygous for defects predicting the p.Ile596Thr substitution on one allele, and a p.Glu324Lys substitution on the other allele. The boy had a history of frequent subcutaneous bleeding, and his platelets displayed an aggregation profile that was consistent with GT, as well as a 98% reduction in membrane expression of $\alpha_{IIb}\beta_3$ compared to the wild-type control. More recently, the p.Ile596Thr variant was reported as a homozygous defect in a patient with moderate bleeding symptoms whose platelets showed a similar profile to the Swiss case (Sandrock*, et al* 2012).

Co-expression of the p.Leu492Pro and p.Ile596Thr α_{IIb} variants in CHO cells with wild-type β_3 resulted in the appearance of $\alpha_{IIb}\beta_3$ at levels which were 21-40% of those seen in cells expressing the wild-type receptor in the case of the p.Leu492Pro variant and 10% of wild-type levels in the case of the p.Ile596Thr variant. Interestingly, analysis of cell lysates revealed the presence of only the pro-α_{IIb} subunit, and there was a complete absence of mature α_{IIb}, suggesting that the p.Leu492Pro and p.Ile596Thr substitutions interfere with protein folding of the thigh domain, thereby interfering with intracellular trafficking and maturation of $\alpha_{IIb}\beta_3$ and causing a reduction in the membrane expression of the receptor.

Eight missense substitutions affecting residues in the thigh domain have previously been identified in patients with GT; p.Pro507Arg, p.Ile518Asn, p.Arg551Trp, p.Arg551Gln, p.Ala581Asp p.Cys575Arg, p.Val630Gly and p.Gln626His. However, whilst they were all identified in GT patients suffering from a bleeding tendency, they are not being characterised and their pathogenic effects remain unclear. In addition, these mutations were identified in GT patients classified as type I GT, which suggests that the surface expression of these variants was less than 10% of the normal control (D'Andrea*, et al* 2002, Nurden*, et al* 2015, Nurden*, et al* 2012b, Peretz*, et al* 2006). Collectively, these results suggested that a single missense mutation in the thigh domain can significantly reduce the surface expression and that these mutations are likely to be responsible for the bleeding observed in the patients. Our results for p.Leu492Pro and p.Ile596Thr supported and confirmed the results of previous studies, indicating that the thigh domain may play an important role in integrin biogenesis and the intracellular trafficking and maturation of $\alpha_{IIb}\beta_3$, resulting in a severe reduction in surface expression. Therefore, their pathogenic defects will contribute to or be responsible for the bleeding symptoms in the patient.

The c.2010C>A transversion in *ITGA2B*, which predicted a p.Asn670Lys substitution in the calf-1 domain, was identified as a homozygous defect in a female index case of Caucasian origin, who had a history of moderate bleeding, which had been subjectively scored as 7 on a scale of 1 to 10. Asn670 is highly conserved in α_{IIb} across species, and also among other human α-integrin family members, and the online bioinformatics tools consistently predicted this variant to be deleterious to α_{IIb}. Analysis of CHO cells following co-transfection with *ITGA2B* cDNA encoding the p.Asn670Lys variant with wild-type β_3 revealed levels of $\alpha_{IIb}\beta_3$ receptor expression on the surface of the cells which were comparable to wild-type. In addition, analysis of the cell lysates revealed the presence of both pro-α_{IIb} and mature α_{IIb} at similar concentrations to those of cells expressing wild-type α_{IIb}, confirming the normal biogenesis of the α_{IIb} variant.

As a result of the p.Asn670Lys variant did not significantly interfere with integrin biogenesis and surface expression, activation analysis was performed to investigate the ability of integrins bearing this variant to undergo a conformation change in response to activation. Prior to activation, the receptor bearing p.Asn670Lys failed to bind to the PAC-1 antibody and the labelled fibrinogen, suggesting that the integrin was in a resting, bent conformation and was behaving normally compared to the wild-type. Following activation with DTT, there was a significant reduction in PAC-1 and fibrinogen binding in cells expressing p.Asn670Lys by 53% and 40%, respectively. These results suggest the p.Asn670Lys substitution is expressed at similar levels to wild-type but has impaired activation.

According to the extensive review of *ITGA2B* and *ITGB3* defects published in 2012 (Nurden*, et al* 2012b), and the online GT database http://sinaicentral.mssm.edu/intranet/research/glanzmann (January, 2016), six amino acid substitutions involving residues in the calf-1 domain have been identified in patients with GT; p.Leu684Arg, p.Cys705Arg, p.Leu752Val, p.Arg755Pro, p.Pro772Arg and p.Gln778Pro. With the exception of the p.Gln778Pro substitution, all of these have been identified in cases with type I GT, and were therefore characterised by platelet membrane expression levels of $\alpha_{IIb}\beta_3$ that were less than 5% of the normal control. The p.Cys705Arg and p.Gln778Pro variants have been further characterised (D'Andrea*, et al* 2002, Pillitteri*, et al* 2010, Tadokoro*, et al* 1998, Vijapurkar*, et al* 2009). The p.Cys705Arg variant was identified as a compound heterozygous defect along with a splicing mutation (c.624+2C>A) and expression of the variant in CHO cells recapitulated the approximate 90% reduction in membrane expression of the receptor that was observed in platelets (D'Andrea*, et al* 2002). The p.Gln778Pro variant was identified as a homozygous defect in a Japanese female with a prolonged bleeding

time and a history of moderate mucocutaneous bleeding. The patient's platelets failed to aggregate in response to all agonists except ristocetin. Flow cytometry and immunoprecipitation of transfected 293T cells using an antibody against $\alpha_{IIb}\beta_3$ displayed a moderate reduction (70-80%) in surface expression of $\alpha_{IIb}\beta_3$. Immunoblotting analysis of cell lysates revealed a comparable level of pro-α_{IIb}, but a reduction in mature α_{IIb} when compared with wild-type control cells, indicating that the mutation interferes with intracellular trafficking and maturation of the integrin, causing a moderate reduction in membrane expression. Importantly, the mutation gave rise to quantitative defects and did not affect ligand binding. Indeed, the p.Gln778Pro variant demonstrated binding to PAC-1 which was comparable to that of the wild-type receptor (Tadokoro*, et al* 1998).

Interestingly, the p.Asn670Lys substitution investigated here would appear to result in the first variant involving a residue in the calf-1 domain, which did not interfere with integrin biogenesis and membrane expression of $\alpha_{IIb}\beta_3$, and instead caused a qualitative defect and a reduction in the capacity of the receptor to undergo the conformational change that allows binding of fibrinogen and mediates platelet aggregation. As discussed in Chapter 3, Asn670 is located close to the putative calcium-binding domain between the thigh and calf-1 domains, and interacts with the calcium binding residues, including Glu673. The function of this calcium-binding domain is still unclear. Its function in $\alpha_{IIb}\beta_3$ has been proposed based on the crystal structure of the extracellular domain of $\alpha_v\beta_3$ and $\alpha_{IIb}\beta_3$. In the resting state, the leg domain of α_{IIb} and α_v is bent between the thigh and calf-1 domains in the genu region with the head domain pointing towards the cell membrane (Xiong*, et al* 2001, Zhu*, et al* 2008). This suggests that the genu may be responsible for providing the extension for the change in structural conformation that occurs in response to integrin activation, leading to exposed ligand binding epitopes in the head domain of $\alpha_v\beta_3$ and $\alpha_{IIb}\beta_3$. In support of this, electron microscopic analysis of $\alpha_v\beta_3$ suggested that, in response to activation, the integrin undergoes a conformational rearrangement in the extracellular domains of both β_3 and α_v. Importantly, upon activation, the α_v subunit undergoes a single structural change, possibly from the genu region (Takagi*, et al* 2002). In support of the above findings, Xie*, et al* (2004) studied the conformational rearrangement of $\alpha_L\beta_2$, a receptor for intercellular adhesion molecules (ICAMs) 1-4, using two specific monoclonal antibodies which bound to the genu and thigh domains. In the resting state, both antibodies failed to bind to their epitopes in the genu-thigh region, indicating that the key residues for these antibodies are completely shielded and possibly blocked by the calf-1 domain and nearby EGF-2 of the β subunit. In contrast, upon integrin

activation, these antibodies bound to their epitopes, indicating a rearrangement of the thigh-genu region in response to integrin activation. In addition, mutations in Ca^{2+} coordination residues, such as p.Asp749Ala and p.Glu787Ala in α_L, resulted in a failure of both antibodies to bind to the integrin, suggesting that the integrity of Ca^{2+} coordination is required for activation (Xie*, et al* 2004). These results suggested that the thigh-genu linker, and its Ca^{2+} binding site, essentially provide the required extension for the structural rearrangements that take place in the receptor upon activation and would lead us to predict that mutations in nearby regions would lead to altered integrin rearrangements. In support of previous studies, our results show that the p.Asn670Lys variant severely reduces the ability of the integrin to bind PAC-1 and fibrinogen, suggesting that this change disturbs the normal flexibility of the thigh-genu and the Ca^{2+} binding site. Thus, the integrin was partially locked in a bent conformation, unable to fully extend in response to activation.

The c.2094G>T transversion in *ITGA2B*, which predicted a p.Glu698Asp substitution in the calf-1 domain, was identified as a homozygous defect in a female index case of Caucasian origin, who had a history of moderate bleeding, which had been subjectively scored as 4 on a scale of 1 to 10. Glu698 was found to be less conserved in α_{IIb} across species and not conserved among human α-integrin family members, and its substitution by aspartate was a neutral change. Analysis of CHO cells following co-transfection with *ITGA2B* cDNA encoding the p.Glu698Asp variant with wild-type β_3, showed that p.Glu698Asp substitution did not interfere with the biogenesis, surface expression and activation of $\alpha_{IIb}\beta_3$ integrin and indeed did not explain the phenotypic data gathered from the patient. The data on this variant was revisited, confirming the original findings. However, it was also noted that the reference sequence used to interpret the sequence results had been removed from the sequence databanks, and replaced with an updated sequence which differed by two codons from the original reference sequence. Interestingly, an examination of the updated *ITGA2B* sequence shows that c.2094G is the last nucleotide in exon 20 where it forms part of the donor splice site consensus sequence. The c.2094G>T substitution was thus predicted to result in the loss of the donor splice site using several bioinformatic tools. Since it was not possible to examine platelet RNA from the patient, the effect of the c.2094G>T transversion on mRNA splicing was evaluated using an exontrap vector system, demonstrating that it resulted in the skipping of exon 20 from the *ITGA2B* RNA. The removal of exon 20 was predicted to result in a frameshift and the introduction of a premature stop codon 24 amino acids after the alanine residue at position 650, p.Thr650Alafs*24. *In vitro* expression of an *ITGA2B* cDNA that lacked exon 20, with the

β_3 cDNA subunit, showed a lack of $\alpha_{IIb}\beta_3$ expression in the CHO cells. This was confirmed by immunoblot analysis which failed to demonstrate the presence of either pro-α_{IIb} or mature α_{IIb}, suggesting that any truncated α_{IIb} protein that is made is rapidly degraded or that the mRNA is subjected to nonsense mediated decay.

The majority of mutations that give rise to defects in RNA splicing occur in the invariant GT and AG dinucleotides of the donor and acceptor splice sites of intron as these dinucleotides are crucial to proper mRNA splicing and are able to distinguish coding from the non-coding sequence. However, other nucleotides located near the donor and acceptor sites have also been reported to cause splicing defects. Importantly, nucleotide substitutions within the consensus acceptor (c/agG) and donor (A/CAGgta/gag) splice site sequences are most commonly associated with splicing defects. Although point mutation in exons is commonly linked to amino acid substitution and the appearance of a dysfunctional protein, exonic nucleotide changes have been associated with splicing defects, and are shown to lead either to exon skipping or to the activation of alternative splice sites, or "cryptic sites" (Antonarakis*, et al* 2001, Krawczak*, et al* 1992). A number of exonic splice site defects in *ITGA2B* have been associated with GT. For example, the c.1878G>C transversion occurred in the last nucleotide of exon 18 and was predicted to cause a p.Gln626His substitution. Flow cytometric analysis of COS-7 cells expressing this variant revealed membrane $\alpha_{IIb}\beta_3$ expression levels that were comparable with those of cells expressing the wild-type receptor. However, while the patient's platelets contained normal levels of *ITGB3* mRNA, the *ITGA2B* mRNA could not be detected*,* indicating its likely rapid degradation. Although the study did not further characterise this mutation to determine the consequence of the nucleotide change at the exon18-intron18 junction, it is likely that the c.1878G>C transversion results in abnormal mRNA splicing, leading either to exon skipping or to the introduction of a cryptic splice site. As a consequence, the aberrant *ITGA2B* mRNA might be eliminated by nonsense-mediated mRNA decay, explaining the complete lack of *ITGA2B* mRNA in these patients (Jallu*, et al* 2010, Sandrock*, et al* 2012). Jayo*, et al* (2006) identified a novel mutation in exon 27 of *ITGA2B*, while c.2829C>T was predicted to cause a p.Pro943Leu substitution. The defect was inherited with a nonsense mutation (c.1750C>T) in exon 17 on the second allele in a 2 year old Chinese girl diagnosed with GT. Analysis of the patient's platelets demonstrated a 90% reduction in $\alpha_{IIb}\beta_3$ receptor density compared with a normal control. Sequence analysis of α_{IIb} cDNA derived from the patient's mRNA demonstrated a lack of expression of the c.1750C>T allele, while there was an increase in cDNA derived from the c.2829C>T allele, which also lacked exon 28. *In vitro* expression of

the p.Pro944Leu variant showed an 80% reduction in $\alpha_{IIb}\beta_3$ receptor density compared to wild-type expression. An exontrapping experiment showed that the wild-type and mutated constructs (c.2829C>T) generate two fragments corresponding to two RNA species, one containing exon 28, and a second in which exon 28 was deleted, respectively. Interestingly, there was a 100% increase in the intensity of the fragment corresponding to the RNA species in which exon 28 was deleted when compared to the corresponding fragment derived from the wild-type construct. The result suggests that the c.2829C>T transition disrupts RNA splicing in this region, leading to exon 28 skipping (Jayo*, et al* 2006). Similarly, our results would suggest that the c.2094G>T transversion mediates its pathogenicity by causing skipping of exon 20 during mRNA splicing, and resulting in the failure to express the α_{IIb} subunit.

5.6 Conclusion

The results presented here provide insights into the potential pathogenic effects of 5 non-synonymous substitutions affecting residues in α_{IIb} that were identified in GT patients in the UK. The p.Asp396Asn and p.Ile596Thr variants failed to undergo processing in the ER to the mature α_{IIb} subunit, and were consequently associated with the failure of $\alpha_{IIb}\beta_3$ to be surface expressed in CHO cells. The p.Leu492Pro variant led to a severe reduction in surface expression and impaired integrin activation. In contrast, the p.Asn670Lys variant was expressed at comparable levels to the wild-type receptor, but remained partially locked in a low affinity state upon activation, disturbing the ability of the integrin to bind fibrinogen. In addition, characterisation of the p.Asn670Lys variant provided the first experimental evidence for the essential role of the thigh-genu region in mediating the conformational change of $\alpha_{IIb}\beta_3$ in response to activation. Finally, the c.2094G>T transversion caused exon 20 skipping during mRNA splicing, leading to a complete absence of the α_{IIb} subunit from the transfected cells. Our results provide evidence to support the pathogenicity of all five variants.

Chapter 6: General discussion, final summary and future work

6.1 General discussion

Glanzmann thrombasthenia is an autosomal recessive platelet bleeding disorder due to genetic defects in either *ITGA2B* or *ITGB3,* which code for the α_{IIb} and β_3 integrin subunits, respectively. Twelve non-synonymous defects and one splicing defect were previously identified in *ITGA2B* and *ITGB3* in 14 index cases with GT recruited in the UK, of which 9 were novel and the remainder not yet characterised. The variants identified were predicted to affect residues in different domains of the two integrin subunits. The aim of this project was therefore to investigate the pathogenicity of these variants in GT by characterising their effects on the expression and function of the $\alpha_{IIb}\beta_3$ receptor. The results of this work contribute to our understanding of the molecular basis of GT and of the functions of 12 different amino acid residues in the β_3 and α_{IIb} subunits. These variants had variable effects on $\alpha_{IIb}\beta_3$ ranging from causing a complete or severe quantitative reduction in membrane $\alpha_{IIb}\beta_3$ that mirrored the platelet profiles observed in types I and II GT, to causing qualitative defects characterised by spontaneous or impaired receptor activation similar to those observed in variant type GT. In contrast, further studies will be required to examine whether the presence of the p.Glu200Lys variant is responsible for the bleeding symptoms observed in the index case who had inherited this defect.

Six variants were found to result in quantitative $\alpha_{IIb}\beta_3$ defects. In brief, *in silico* analysis predicted that the *ITGB3* defects predicting the p.Trp11Arg, p.Pro189Ser, p.Trp264Leu and p.Ser317Phe substitutions in β_3 and the *ITGA2B* defects predicting the p.Asp396Asn and p.Ile596Thr substitutions in α_{IIb} are deleterious. An analysis of lysates from cells expressing these variants revealed the presence of β_3 and pro-α_{IIb}, and the absence of mature α_{IIb} in all cases, indicating that the receptors bearing these variants were unable to undergo the process of maturation in the Golgi, possibly due to impaired intracellular trafficking, or indeed due to failure to exit the ER. Similar findings have been reported for other variants which fail to exit the ER, examples of which include the β_3-p.Leu143Trp, β_3-p.His306Pro, α_{IIb}-p.Glu355Lys and α_{IIb}-p.Ile405Thr variants (Basani*, et al* 1997, Milet-Marsal*, et al* 2002b, Tadokoro*, et al* 2002). Immunohistochemistry of cells expressing these variants could potentially identify the mechanism resulting in impaired maturation and membrane expression of $\alpha_{IIb}\beta_3$.

Variant type GT is the least common form of the disorder and is characterised by $\alpha_{IIb}\beta_3$ expression levels that are greater than 20% of the normal levels and are usually associated with functional defects (Nurden*, et al* 2013). There are two subtypes of

variant GT depending on whether the functional defect is characterised by impaired integrin activation or spontaneous activation of the receptor (gain of function mutation).

A number of missense mutations have previously been identified that cause impaired activation of $\alpha_{IIb}\beta_{3,}$ preventing it from binding to its ligand and thereby affecting platelet aggregation. The majority of these amino acid substitutions occur in the head domain of α_{IIb} and β_3 where fibrinogen binds to $\alpha_{IIb}\beta_3$ in response to integrin activation. In most of the previously described cases, the defects disrupted the ligand binding domain and cation binding sites preventing the integrin from undergoing the conformational change required for integrin extension and activation (Bajt*, et al* 1992, Djaffar and Rosa 1993, Nurden*, et al* 2012b). In the current study, 3 variants were associated with a non-functional integrin, one of which, α_{IIb}_p.Leu492Pro, also resulted in reduced surface expression and a receptor that was locked in a low affinity state and unable to bind to PAC-1 or fibrinogen. In contrast, the other two variants, α_{IIb}_p.Asn670Lys and β_3_p.Ile665Thr were expressed at levels which were comparable to those of wild-type $\alpha_{IIb}\beta_3$, but failed to bind to PAC-1 and fibrinogen. In contrast to previous variants which showed defects in ligand binding as a result of amino acid substitutions in the α_{IIb} and β_3 ligand binding domains, residues α_{IIb}_Leu492, α_{IIb}_Asn670 and β_3_IIe665 are located in the Thigh and calf-1 domain of α_{IIb} and the β-tail domain of β_3, respectively. Therefore, this study provides the first examples of 'loss of function' defects as a result of amino acid substitutions in the α_{IIb}-thigh, α_{IIb}-calf-1 and β_3-β-tail domains.

The second subtype of variant type GT is characterised by a normal or reduced level of $\alpha_{IIb}\beta_3$ accompanied by spontaneous activation. Several non-synonymous mutations have been identified in GT patients and associated with spontaneous binding of $\alpha_{IIb}\beta_3$ to PAC-1 and fibrinogen with, or without, interfering with membrane expression. The majority of these mutations affect residues located in the β_3 subunit particularly within the cysteine rich domains (Mor-Cohen*, et al* 2007, Nurden*, et al* 2012b, Ruiz*, et al* 2001). In the current study, two *ITGB3* mutations predicted to cause p.Cys547Trp and p.Cys554Arg substitutions were investigated. *In silico* analysis showed p.Cys547 and Cys554 form disulphide bonds with Cys534 and Cys568, respectively, which are lost when they are substituted by tryptophan and arginine residues, respectively. *In vitro* analysis showed that the p.Cys547Trp and p.Cys554Arg substitutions result in moderate reductions in membrane expression of $\alpha_{IIb}\beta_3$, which was able to bind spontaneously to fibrinogen and PAC-1, demonstrating that these disulphide bonds are important for maintaining the integrin in the resting state, and supporting previous findings that the EGF domains in β_3 play important roles in maintaining the structural

and functional integrity of β_3 (Mor-Cohen*, et al* 2007, Ruan*, et al* 1999, Ruiz*, et al* 2001).

Gain-of-function mutations have been associated with thrombocytopenia in GT patients (Ruiz*, et al* 2001). Although GT is usually characterised by normal platelet counts and morphology, some cases do present with thrombocytopenia and platelet anisocytosis (Nurden*, et al* 2013). In addition, heterozygous defects in either *ITGA2B* or *ITGB3* have been shown to result in GT-like thrombocytopenia. These defects, examples of which include β_3-p.Arg995Gln, β_3-p.Asp723His, β_3-p.(Asp621_Glu660del) and α_{IIb}-p.Gly991Cys, mainly affect residues located in the cytoplasmic domain which have also been associated with spontaneous activation of $\alpha_{IIb}\beta_3$ (Ghevaert*, et al* 2008, Kashiwagi*, et al* 2013, Kunishima*, et al* 2011). It is thought that the presence of the receptor in an active conformation may trigger continuous outside-in-signalling, leading to impaired cytoskeletal rearrangement, possibly by preventing actin turnover during polymerization (Bury*, et al* 2016). Supporting this suggestion, further characterisation of CD34+ stem cells isolated from a patient with the β_3-p.Asp723His variant suggested that the production of large dysfunctional platelets resulted from an increase in the rate and size of proplatelet formation. Furthermore, the β3-p.Asp723His and other variants mentioned earlier showed spontaneous activation when expressed in CHO cells, and formation of proplatelet-like protrusions when the transfected cells were plated on fibrinogen (Ghevaert*, et al* 2008, Kashiwagi*, et al* 2013, Kunishima*, et al* 2011). Preliminary studies to investigate the ability of β_3 variants to direct formation of proplatelet-like protrusions in CHO cells, which were carried out by members of the Haemostasis Research Group in Sheffield showed an increase in the number and length of proplatelet-like protrusions in CHO cells expressing the p.Cys554Arg and p.Cys547Trp variants, compared to cells expressing the wild-type receptor. Unfortunately, the significance of these findings remains unclear as data relating to platelet count were not available for the patients who were identified as having these defects, though it would obviously be of interest to know if they had a history of thrombocytopenia.

The c.2094G>T transversion in *ITGA2B* was originally predicted to cause a benign non-synonymous p.Glu698Asp substitution in α_{IIb}. Further *in silico* analysis predicted that the c.2094G>T transversion was more likely to disturb the exon 20 donor splice site in *ITGA2B*. *In vitro* investigations showed the p.Glu698Asp substitution had no effect on $\alpha_{IIb}\beta_3$ expression or activation supporting the *in silico* predictions, whereas expression studies to analyse the effect of the c.2094G>T alteration on splicing demonstrated the exclusion of exon 20 from the *ITGA2B* RNA, which was predicted to

introduce a premature stop codon 24 amino acids downstream, p.Thr650Alafs*24. The frameshift defect resulted in a complete loss of the calf-2, transmembrane and cytoplasmic domains of the α_{IIb} subunit. As expected, *in vitro* investigations of the p.Thr650Alafs*24 variant displayed a complete absence of membrane and intracellular expression of the $\alpha_{IIb}\beta_3$ receptor. Therefore, the c.2094G>T transversion was likely to mediate its pathogenicity through a splicing defect resulting in the bleeding symptoms presented by the patient.

In addition to binding α_{IIb} to form the fibrinogen receptor, β_3 also has the ability to bind α_v to form $\alpha_v\beta_3$, the vitronectin receptor, which is expressed on platelets at a very low copy number (50-100) when compared to $\alpha_{IIb}\beta_3$. Nonetheless mutations in β_3 have been shown to cause differential binding to α_v and α_{IIb} (Mor-Cohen*, et al* 2012, Tadokoro*, et al* 2002). The vitronectin receptor plays an important role in angiogenesis and in blood vessel repair following the formation of a haemostatic plug (Dufourcq*, et al* 2002, Ramjaun and Hodivala-Dilke 2009). $\alpha_v\beta_3$ receptor expression was examined for all β_3 variants investigated in the current study. For the majority of variants, a reduction in membrane expression of $\alpha_{IIb}\beta_3$ was accompanied by a similar reduction in $\alpha_v\beta_3$ receptor expression. However, there were four variants where this was not the case. Thus, while the p.Pro189Ser β_3 variant failed to form a heterodimer with α_{IIb}, it was still able to heterodimerise with α_v to form a receptor that was surface expressed on CHO cells at 78% of the levels seen in cells expressing wild-type β_3. These findings supported the structural modelling and molecular dynamics studies, which predicted that the presence of a serine residue at position 189 would stabilise the interaction with α_v but would reduce the stability of the interaction with α_{IIb} (Laguerre*, et al* 2013). The p.Cys547Trp and p.Cys554Arg substitutions both caused a moderate reduction in $\alpha_{IIb}\beta_3$ expression but led to a severe reduction in $\alpha_v\beta_3$ expression to approximately 10% of the levels observed in cells expressing the wild-type receptor.

The homozygous variant, which predicted the substitution of a glutamate residue by a lysine residue at position 200 (p.Glu200Lys) in β_3 was predicted to be benign by the majority of the computational tools used. In accordance with this, expression of the p.Glu200Lys variant in CHO cells revealed membrane expression levels of $\alpha_{IIb}\beta_3$ that were comparable to those of wild-type β_3, as were total β_3 expression levels and there were no differences detected in α_{IIb} maturity. The integrin was also able to undergo activation normally. These findings suggested that this variant does not alter the biogenesis, intracellular trafficking, membrane expression and activation of $\alpha_{IIb}\beta_3$. However, there was a dramatic reduction in the surface expression of $\alpha_v\beta_3$ in the presence of the p.Glu200Lys variant. In addition to platelets, $\alpha_v\beta_3$ is highly expressed

on endothelial cells, smooth muscle cells and osteoclasts (Dufourcq*, et al* 2002, Ramjaun and Hodivala-Dilke 2009). Vitronectin was shown to be highly expressed in response to vascular damage and blocking of the $\alpha_v\beta_3$ receptor or vitronectin caused a reduction in the neointima cell count and neointima formation in a rat model, a finding that was explained by the *in vitro* demonstration of a role for $\alpha_v\beta_3$ in smooth muscle cell migration (Dufourcq*, et al* 2002). Thus, it is not surprising that antagonism of β_3 and $\alpha_v\beta_3$ antagonism have been associated with suppressed angiogenesis *in vitro* (Ramjaun and Hodivala-Dilke 2009). Therefore, a reduction in $\alpha_v\beta_3$ may account for the mild bleeding that was experienced by the index case in whom this variant was identified, although it does not explain the diagnosis of GT. While the index case was unavailable for further study, additional clinical data, which became available during the course of this study, suggested that this index case has a history of macrothrombocytopenia. Preliminary work carried out by members of the Haemostasis Research Group revealed that CHO cells expressing the p.Glu200Lys β_3 variant, when seeded on immobilised fibrinogen, show an increase in the formation of proplatelet-like protrusions and an increase in protrusion length compared to cells expressing wild-type β_3. One might speculate that this finding could translate to an increase in the rate of proplatelet production, producing fewer, but larger platelets, as demonstrated previously by Ghevaert*, et al* (2008) and therefore accounting for the macrothrombocytopenia observed in the patient, although this would be unusual as the p.Glu200Lys variant contrasts with other variants that are associated with thrombocytopenia in that it does not exhibit spontaneous activation (Ghevaert*, et al* 2008, Kashiwagi*, et al* 2013, Kunishima*, et al* 2011).

Fibrinogen has been shown to be present in murine bone marrow where it is required for the formation of proplatelets and for platelet release from MKs via interactions with $\alpha_{IIb}\beta_3$ (Larson and Watson 2006). The reports of mutations in *ITGA2B* and *ITGB3* which have been associated with thrombocytopenia would support a role for $\alpha_{IIb}\beta_3$ in proplatelet formation (Ghevaert*, et al* 2008, Kashiwagi*, et al* 2013, Kunishima*, et al* 2011). However, this role is not supported by the results of Balduini*, et al* (2008) who demonstrated that $\alpha_{IIb}\beta_3$ was essential for the adhesion and spreading of human megakaryocytes on fibrinogen but not for proplatelet formation (Balduini*, et al* 2008). In addition, mice lacking α_{IIb} did not display any abnormalities in platelet count and morphology, while β3-knockdown mice only showed a mild reduction in platelet number (Hodivala-Dilke*, et al* 1999, Tronik-Le Roux*, et al* 2000). Therefore, the role of $\alpha_{IIb}\beta_3$ in proplatelet formation requires further investigation. It is plausible that $\alpha_v\beta_3$ ligand-binding may play a role in the cytoskeletal rearrangement of the megakaryocyte and

may be required for proplatelet formation, and that the p.Glu200Lys substitution in β_3 disturbs this process, resulting in macrothrombocytopenia.

6.2 Limitations of this study

The work described in this project has provided evidence supporting the pathogenicity of 13 candidate *ITGA2B* and *ITGB3* variants identified in cases with GT. A major limitation of the work presented here was that the majority of the studies relied on cell-based models, and the lack of availability of the index cases for follow up investigations meant that it was not possible to confirm the *in vitro* findings by assessing the surface expression and function of platelet integrin receptors on platelets from the index cases, or to assess platelet RNA levels in those cases where defects were predicted to result in aberrant splicing. While the CHO cell line is an established model for investigating these variants *in vitro* and has been widely used for the characterisation of integrin variants associated with GT, CHO cells are not derived from human tissue and do not show endogenous expression of $\alpha_{IIb}\beta_3$. A second limitation of this work was that the outside-in signalling via $\alpha_{IIb}\beta_3$ receptor has not been investigated.

A third limitation of this study was that it took advantage of the presence of α_v in CHO cells line to examine the interaction between human β_3 and hamster α_v, which may not be the same as that with human α_v. Interestingly, this approach demonstrated differential interactions of the p.Pro189Ser and p.Glu200Lys β_3 variants with human α_{IIb} and hamster α_v. It would be interesting to follow up on these by assessing the interaction with human α_v *in vitro*, or indeed to assess the expression of both $\alpha_{IIb}\beta_3$ and $\alpha_v\beta_3$ on platelets from the index case who inherited this defect. Another shortcoming of the study concerned the use of certain antibodies. For example, detection of the chimeric $\alpha_v\beta_3$ receptor was undertaken using anti-human $\alpha_v\beta_3$, although the α_v subunit was derived from a hamster, and it is possible that the results may have been different using an antibody that was specific for the chimeric receptor. Importantly, intracellular staining of the p.Trp11Arg β_3 variant appeared to be absent when detected by flow cytometry using a monoclonal antibody that bound to wild-type β_3, but was present in similar quantities to the wild-type variant when detected in lysates using a polyclonal antibody.

6.3 Conclusions

The primary aims of this study were to confirm the pathogenicity of a subset of novel and uncharacterised non-synonymous variants in both *ITGA2B* and *ITGB3* that were previously identified in index cases diagnosed with GT and recruited through different UK haemophilia centres. An additional aim was to provide insight into the structural and functional mechanisms of the $\alpha_{IIb}\beta_3$ integrin, by characterising 13 different amino acid substitutions affecting six different domains in α_{IIb} and β_3. A summary of the project's main findings is shown in Figure 6.1

In silico analysis suggested that all variants were pathogenic to $\alpha_{IIb}\beta_3$ with the exception of the p.Glu200Lys β_3 variant. *In vitro* studies in CHO cells showed that β_3-p.Trp11Arg, β_3-p.Pro189Ser, β_3-Trp264Leu and β_3-Ser317Phe, α_{IIb}-p.Asp396Asn and α_{IIb}-Ile596Thr result in a severe reduction of $\alpha_{IIb}\beta_3$ membrane expression with an absence of mature-α_{IIb}, indicating possible prevention of intracellular trafficking and maturation of pro-$\alpha_{IIb}\beta_3$. In contrast, cells expressing the β_3_p.Ile665Thr and α_{IIb}_p.Asn670Lys variants have $\alpha_{IIb}\beta_3$ receptors that are expressed normally, but show impaired activation, while the α_{IIb}_p.Pro492Leu variant results in a severe reduction in both surface expression and activation of $\alpha_{IIb}\beta_3$.

Interestingly, cells expressing β_3_p.Cys547Trp and β_3_p.Cys554Arg show a moderate reduction in surface expression of $\alpha_{IIb}\beta_3$, but are able to spontaneously bind fibrinogen. This is due to the loss of disulphide bonds within the structure that normally maintain the receptor in a low affinity conformation, and their disturbance results in the receptor becoming locked in a high-affinity conformation that is constitutively active.

The c.2094G>T variant results in exon 20 skipping of *ITGA2B,* leading to a frameshift deletion and introduction of a premature stop codon, p.Thr650Alafs*24. Expression studies investigating the effects of the p.Thr650Alafs*24 variant showed a complete absence of membrane and intracellular expression of $\alpha_{IIb}\beta_3$, suggesting that this variant is likely to mediate its pathogenicity through aberrant splicing.

The p.Glu200Lys variant does not appear to affect the expression or function of $\alpha_{IIb}\beta_3$, but does seem to impair $\alpha_v\beta_3$ biogenesis and expression. Further work is necessary to confirm its association with GT.

6.4 Future work

While the findings reported in this thesis confirm the pathogenicity of all but one of the variants investigated, and advance our understanding of the molecular basis of GT, the results of this work raise some interesting questions, which could be addressed in further studies. Our study showed that six variants were associated with an almost complete absence of $\alpha_{IIb}\beta_3$ membrane expression with a further three resulting in moderate reductions in expression. These variants are likely to cause protein retention, which could be confirmed using immunofluorescent staining of α_{IIb} and β_3 and possible markers of the ER and Golgi to assess co-localisation. The study highlights a number of mutations that appear to affect cytoskeletal rearrangement. It would therefore be interesting to assess cell adhesion, spreading and proplatelet formation for p.Glu200Lys, p.Cys547Trp and p.Cys554Arg variants. The p.Asn670Lys variant is the first GT associated variant to be characterised, which is located in the vicinity of a genu calcium binding site and results in the disturbance of integrin activation by approximately 50%. This calcium binding site is coordinated by the 632-Asp-Cys-Gly-Glu-Asp-Asp-Val-Cys-Val-640 motif and Glu673 (Zhu*, et al* 2008). Therefore, further characterisation of this region may provide additional information for the development of novel anti-platelet drugs. It would also be interesting to follow up on the increase in the molecular weight of α_{IIb} that was observed in cells expressing the p.Asp396Asn variant, either by mass spectrometry or by further probing its glycosylation using inhibitors of glycosylation or other deglycosylases to determine the reasons for its increased molecular weight.

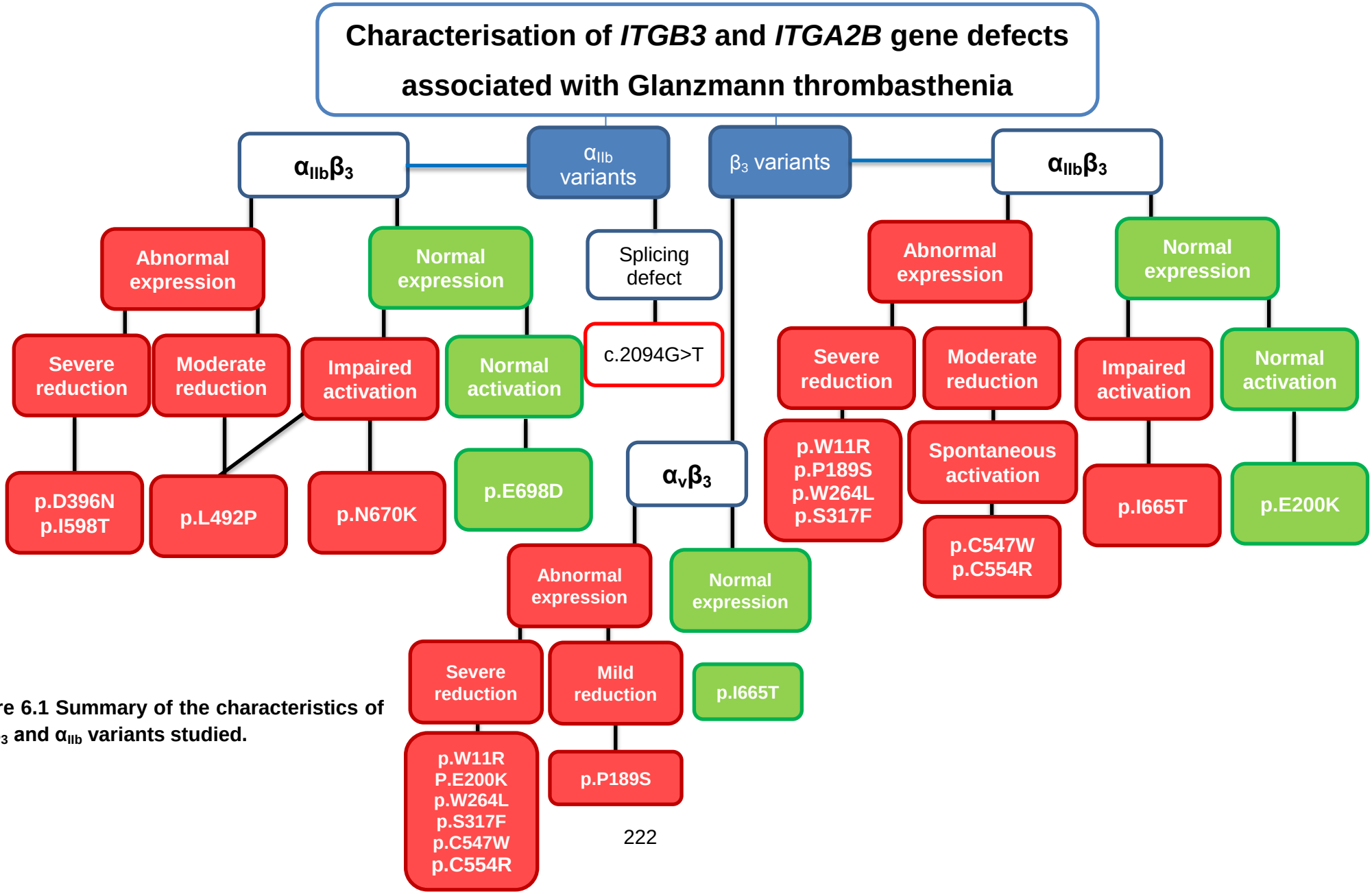

Figure 6.1 Summary of the characteristics of the β_3 and α_{IIb} variants studied.

Bibliography

Adair, B.D., Xiong, J.P., Maddock, C., Goodman, S.L., Arnaout, M.A. & Yeager, M. (2005) Three-dimensional EM structure of the ectodomain of integrin {alpha}V{beta}3 in a complex with fibronectin. *J Cell Biol,* **168,** 1109-1118.

Akashi, K., Traver, D., Miyamoto, T. & Weissman, I.L. (2000) A clonogenic common myeloid progenitor that gives rise to all myeloid lineages. *Nature,* **404,** 193-197.

Al-Marwani, A. (2009) Molecular Genetic of inherited platelet Bleeding Disorders. *PhD Thesis***,** University of Sheffield

Almusbahi, A. (2014) Investigation of Molecular Basis of Glanzmann's Thrombasthenia. *Master Thesis,* **,** Uinversity of Sheffield.

Ambo, H., Kamata, T., Handa, M., Taki, M., Kuwajima, M., Kawai, Y., Oda, A., Murata, M., Takada, Y., Watanabe, K. & Ikeda, Y. (1998) Three novel integrin beta3 subunit missense mutations (H280P, C560F, and G579S) in thrombasthenia, including one (H280P) prevalent in Japanese patients. *Biochem Biophys Res Commun,* **251,** 763-768.

Anthis, N.J., Wegener, K.L., Ye, F., Kim, C., Goult, B.T., Lowe, E.D., Vakonakis, I., Bate, N., Critchley, D.R., Ginsberg, M.H. & Campbell, I.D. (2009) The structure of an integrin/talin complex reveals the basis of inside-out signal transduction. *EMBO J,* **28,** 3623-3632.

Antonarakis, S.E., Krawczak, M. & Cooper, D.N. (2001) The nature and mechanisms of human gene mutation.

Arnaout, M.A., Mahalingam, B. & Xiong, J.P. (2005) Integrin structure, allostery, and bidirectional signaling. *Annu Rev Cell Dev Biol,* **21,** 381-410.

Atkinson, B.T., Jarvis, G.E. & Watson, S.P. (2003) Activation of GPVI by collagen is regulated by alpha2beta1 and secondary mediators. *J Thromb Haemost,* **1,** 1278-1287.

Bajt, M.L., Ginsberg, M.H., Frelinger, A.L., 3rd, Berndt, M.C. & Loftus, J.C. (1992) A spontaneous mutation of integrin alpha IIb beta 3 (platelet glycoprotein IIb-IIIa) helps define a ligand binding site. *J Biol Chem,* **267,** 3789-3794.

Bajt, M.L. & Loftus, J.C. (1994) Mutation of a ligand binding domain of beta 3 integrin. Integral role of oxygenated residues in alpha IIb beta 3 (GPIIb-IIIa) receptor function. *J Biol Chem,* **269,** 20913-20919.

Balduini, A., Pallotta, I., Malara, A., Lova, P., Pecci, A., Viarengo, G., Balduini, C.L. & Torti, M. (2008) Adhesive receptors, extracellular proteins and myosin IIA orchestrate proplatelet formation by human megakaryocytes. *J Thromb Haemost,* **6,** 1900-1907.

Balduini, C.L., Iolascon, A. & Savoia, A. (2002) Inherited thrombocytopenias: from genes to therapy. *Haematologica,* **87,** 860-880.

Basani, R.B., Brown, D.L., Vilaire, G., Bennett, J.S. & Poncz, M. (1997) A Leu117-->Trp mutation within the RGD-peptide cross-linking region of beta3 results in Glanzmann thrombasthenia by preventing alphaIIb beta3 export to the platelet surface. *Blood,* **90,** 3082-3088.

Basani, R.B., French, D.L., Vilaire, G., Brown, D.L., Chen, F., Coller, B.S., Derrick, J.M., Gartner, T.K., Bennett, J.S. & Poncz, M. (2000) A naturally occurring mutation near the amino terminus of alphaIIb defines a new region involved in ligand binding to alphaIIbbeta3. *Blood,* **95,** 180-188.

Basani, R.B., Vilaire, G., Shattil, S.J., Kolodziej, M.A., Bennett, J.S. & Poncz, M. (1996) Glanzmann thrombasthenia due to a two amino acid deletion in the fourth calcium-binding domain of alpha IIb: demonstration of the importance of calcium-binding domains in the conformation of alpha IIb beta 3. *Blood,* **88,** 167-173.

Bauren, G. & Wieslander, L. (1994) Splicing of Balbiani ring 1 gene pre-mRNA occurs simultaneously with transcription. *Cell,* **76,** 183-192.

Bellucci, S. & Caen, J. (2002) Molecular basis of Glanzmann's Thrombasthenia and current strategies in treatment. *Blood Rev,* **16,** 193-202.

Bellucci, S., Damaj, G., Boval, B., Rocha, V., Devergie, A., Yacoub-Agha, I., Garderet, L., Ribaud, P., Traineau, R., Socie, G. & Gluckman, E. (2000) Bone marrow transplantation in severe Glanzmann's thrombasthenia with antiplatelet alloimmunization. *Bone Marrow Transplant,* **25,** 327-330.

Bellucci, S., Devergie, A., Gluckman, E., Tobelem, G., Lethielleux, P., Benbunan, M., Schaison, G. & Boiron, M. (1985) Complete correction of Glanzmann's thrombasthenia by allogeneic bone-marrow transplantation. *Br J Haematol,* **59,** 635-641.

Bennett, J.S., Berger, B.W. & Billings, P.C. (2009) The structure and function of platelet integrins. *J Thromb Haemost,* **7 Suppl 1,** 200-205.

Bernardi, B., Guidetti, G.F., Campus, F., Crittenden, J.R., Graybiel, A.M., Balduini, C. & Torti, M. (2006) The small GTPase Rap1b regulates the cross talk between platelet integrin alpha2beta1 and integrin alphaIIbbeta3. *Blood,* **107,** 2728-2735.

Borders, C.L., Jr., Broadwater, J.A., Bekeny, P.A., Salmon, J.E., Lee, A.S., Eldridge, A.M. & Pett, V.B. (1994) A structural role for arginine in proteins: multiple hydrogen bonds to backbone carbonyl oxygens. *Protein Sci,* **3,** 541-548.

Bouaouina, M., Lad, Y. & Calderwood, D.A. (2008) The N-terminal domains of talin cooperate with the phosphotyrosine binding-like domain to activate beta1 and beta3 integrins. *J Biol Chem,* **283,** 6118-6125.

Boudreaux, M.K. & Lipscomb, D.L. (2001) Clinical, biochemical, and molecular aspects of Glanzmann's thrombasthenia in humans and dogs. *Vet Pathol,* **38,** 249-260.

Bray, P.F., Rosa, J.-P., Johnston, G.I., Shiu, D.T., Cook, R.G., Lau, C., Kan, Y.W., McEver, R.P. & Shuman, M.A. (1987) Platelet glycoprotein IIb. Chromosomal localization and tissue expression. *Journal of Clinical Investigation,* **80,** 1812.

Bray, P.F., Rosa, J.P., Lingappa, V.R., Kan, Y.W., McEver, R.P. & Shuman, M.A. (1986) Biogenesis of the platelet receptor for fibrinogen: evidence for separate precursors for glycoproteins IIb and IIIa. *Proc Natl Acad Sci U S A,* **83,** 1480-1484.

Bray, P.F. & Shuman, M. (1990) Identification of an abnormal gene for the GPIIIa subunit of the platelet fibrinogen receptor resulting in Glanzmann's thrombasthenia. *Blood,* **75,** 881-888.

Briscoe, A.D., Gaur, C. & Kumar, S. (2004) The spectrum of human rhodopsin disease mutations through the lens of interspecific variation. *Gene,* **332,** 107-118.

Broos, K., Feys, H.B., De Meyer, S.F., Vanhoorelbeke, K. & Deckmyn, H. (2011) Platelets at work in primary hemostasis. *Blood Rev,* **25,** 155-167.

Bury, L., Falcinelli, E., Chiasserini, D., Springer, T.A., Italiano, J.E., Jr. & Gresele, P. (2016) Cytoskeletal perturbation leads to platelet dysfunction and thrombocytopenia in variant forms of Glanzmann thrombasthenia. *Haematologica,* **101,** 46-56.

Bury, L., Malara, A., Gresele, P. & Balduini, A. (2012) Outside-in signalling generated by a constitutively activated integrin alphaIIbbeta3 impairs proplatelet formation in human megakaryocytes. *PLoS One,* **7,** e34449.

Butta, N., Arias-Salgado, E.G., Gonzalez-Manchon, C., Ferrer, M., Larrucea, S., Ayuso, M.S. & Parrilla, R. (2003) Disruption of the beta3 663-687 disulfide bridge confers constitutive activity to beta3 integrins. *Blood,* **102,** 2491-2497.

Caen, J., Castaldi, P., Leclerc, J., Inceman, S., Larrieu, M., Probst, M. & Bernard, J. (1966) Congenital bleeding disorders with long bleeding time and normal platelet count: I. Glanzmann's thrombasthenia (report of fifteen patients). *The American Journal of Medicine,* **41,** 4-26.

Caen, J. & Cousin, C. (1962) In vivo" disorder of platelet adhesiveness in Willebrand's disease and Glanzmann's thrombasthenias. *NOUVELLE REVUE FRANCAISE D HEMATOLOGIE,* **2,** 685-&.

Caen, J.P. (1989) 5 Glanzmann's thrombasthenia. *Baillière's Clinical Haematology,* **2,** 609-625.

Calabrese, R., Capriotti, E., Fariselli, P., Martelli, P.L. & Casadio, R. (2009) Functional annotations improve the predictive score of human disease-related mutations in proteins. *Hum Mutat,* **30,** 1237-1244.

Calvete, J.J. & Gonzalez-Rodriguez, J. (1986) Isolation and biochemical characterization of the alpha- and beta-subunits of glycoprotein IIb of human platelet plasma membrane. *Biochem J,* **240,** 155-161.

Calvete, J.J., Henschen, A. & Gonzalez-Rodriguez, J. (1989) Complete localization of the intrachain disulphide bonds and the N-glycosylation points in the alpha-subunit of human platelet glycoprotein IIb. *Biochem J,* **261,** 561-568.

Calvete, J.J., Schafer, W., Henschen, A. & Gonzalez-Rodriguez, J. (1990) Characterization of the beta-chain N-terminus heterogeneity and the alpha-chain C-terminus of human platelet GPIIb. Posttranslational cleavage sites. *FEBS Lett,* **272,** 37-40.

Cartegni, L., Wang, J., Zhu, Z., Zhang, M.Q. & Krainer, A.R. (2003) ESEfinder: A web resource to identify exonic splicing enhancers. *Nucleic Acids Res,* **31,** 3568-3571.

Chang, Y., Bluteau, D., Debili, N. & Vainchenker, W. (2007) From hematopoietic stem cells to platelets. *J Thromb Haemost,* **5 Suppl 1,** 318-327.

Chen, P., Melchior, C., Brons, N.H., Schlegel, N., Caen, J. & Kieffer, N. (2001) Probing conformational changes in the I-like domain and the cysteine-rich repeat of human beta 3 integrins following disulfide bond disruption by cysteine mutations: identification of cysteine 598 involved in alphaIIbbeta3 activation. *J Biol Chem,* **276,** 38628-38635.

Chen, Y.P., Djaffar, I., Pidard, D., Steiner, B., Cieutat, A.M., Caen, J.P. & Rosa, J.P. (1992) Ser-752-->Pro mutation in the cytoplasmic domain of integrin beta 3 subunit and defective activation of platelet integrin alpha IIb beta 3 (glycoprotein IIb-IIIa) in a variant of Glanzmann thrombasthenia. *Proc Natl Acad Sci U S A,* **89,** 10169-10173.

Choi, W.S., Rice, W.J., Stokes, D.L. & Coller, B.S. (2013) Three-dimensional reconstruction of intact human integrin alphaIIbbeta3: new implications for activation-dependent ligand binding. *Blood,* **122,** 4165-4171.

Chrzanowska-Wodnicka, M., Smyth, S.S., Schoenwaelder, S.M., Fischer, T.H. & White, G.C., 2nd (2005) Rap1b is required for normal platelet function and hemostasis in mice. *J Clin Invest,* **115,** 680-687.

Coller, B.S., Cheresh, D.A., Asch, E. & Seligsohn, U. (1991) Platelet vitronectin receptor expression differentiates Iraqi-Jewish from Arab patients with Glanzmann thrombasthenia in Israel. *Blood,* **77,** 75-83.

Cong, N.V., Uzan, G., Gross, M.S., Jegou-Foubert, C., Frachet, P., Boucheix, C., Marguerie, G. & Frezal, J. (1988) Assignment of human platelet GP2B (GPIIb) gene to chromosome 17, region q21.1-q21.3. *Hum Genet,* **80,** 389-392.

Cramer, E.M., Norol, F., Guichard, J., Breton-Gorius, J., Vainchenker, W., Masse, J.M. & Debili, N. (1997) Ultrastructure of platelet formation by human megakaryocytes cultured with the Mpl ligand. *Blood,* **89,** 2336-2346.

Crazzolara, R., Maurer, K., Schulze, H., Zieger, B., Zustin, J. & Schulz, A.S. (2015) A new mutation in the KINDLIN-3 gene ablates integrin-dependent leukocyte, platelet, and osteoclast function in a patient with leukocyte adhesion deficiency-III. *Pediatr Blood Cancer,* **62,** 1677-1679.

Crittenden, J.R., Bergmeier, W., Zhang, Y., Piffath, C.L., Liang, Y., Wagner, D.D., Housman, D.E. & Graybiel, A.M. (2004) CalDAG-GEFI integrates signaling for platelet aggregation and thrombus formation. *Nat Med,* **10,** 982-986.

D'Andrea, G., Colaizzo, D., Vecchione, G., Grandone, E., Di Minno, G. & Margaglione, M. (2002) Glanzmann's thrombasthenia: identification of 19 new mutations in 30 patients. *Thromb Haemost,* **87,** 1034-1042.

Daly, M.E., Leo, V.C., Lowe, G.C., Watson, S.P. & Morgan, N.V. (2014) What is the role of genetic testing in the investigation of patients with suspected platelet function disorders? *Br J Haematol,* **165,** 193-203.

Daniel, J.L., Dangelmaier, C., Jin, J., Kim, Y.B. & Kunapuli, S.P. (1999) Role of intracellular signaling events in ADP-induced platelet aggregation. *Thromb Haemost,* **82,** 1322-1326.

Di Minno, G., Coppola, A., Di Minno, M.N. & Poon, M.C. (2009) Glanzmann's thrombasthenia (defective platelet integrin alphaIIb-beta3): proposals for management between evidence and open issues. *Thromb Haemost,* **102,** 1157-1164.

Djaffar, I. & Rosa, J.P. (1993) A second case of variant of Glanzmann's thrombasthenia due to substitution of platelet GPIIIa (integrin beta 3) Arg214 by Trp. *Hum Mol Genet,* **2,** 2179-2180.

Du, X. (2007) Signaling and regulation of the platelet glycoprotein Ib-IX-V complex. *Curr Opin Hematol,* **14,** 262-269.

Dufourcq, P., Couffinhal, T., Alzieu, P., Daret, D., Moreau, C., Duplaa, C. & Bonnet, J. (2002) Vitronectin is up-regulated after vascular injury and

vitronectin blockade prevents neointima formation. *Cardiovasc Res,* **53,** 952-962.

Duperray, A., Berthier, R., Chagnon, E., Ryckewaert, J.J., Ginsberg, M., Plow, E. & Marguerie, G. (1987) Biosynthesis and processing of platelet GPIIb-IIIa in human megakaryocytes. *J Cell Biol,* **104,** 1665-1673.

Duperray, A., Troesch, A., Berthier, R., Chagnon, E., Frachet, P., Uzan, G. & Marguerie, G. (1989) Biosynthesis and assembly of platelet GPIIb-IIIa in human megakaryocytes: evidence that assembly between pro-GPIIb and GPIIIa is a prerequisite for expression of the complex on the cell surface. *Blood,* **74,** 1603-1611.

Duyk, G.M., Kim, S.W., Myers, R.M. & Cox, D.R. (1990) Exon trapping: a genetic screen to identify candidate transcribed sequences in cloned mammalian genomic DNA. *Proc Natl Acad Sci U S A,* **87,** 8995-8999.

Emambokus, N.R. & Frampton, J. (2003) The glycoprotein IIb molecule is expressed on early murine hematopoietic progenitors and regulates their numbers in sites of hematopoiesis. *Immunity,* **19,** 33-45.

Eng, E.T., Smagghe, B.J., Walz, T. & Springer, T.A. (2011) Intact alphaIIbbeta3 integrin is extended after activation as measured by solution X-ray scattering and electron microscopy. *J Biol Chem,* **286,** 35218-35226.

Escolar, G., Krumwiede, M. & White, J.G. (1986) Organization of the actin cytoskeleton of resting and activated platelets in suspension. *Am J Pathol,* **123,** 86-94.

Escolar, G. & White, J.G. (1991) The platelet open canalicular system: a final common pathway. *Blood Cells,* **17,** 467-485; discussion 486-495.

Fairbrother, W.G., Yeh, R.F., Sharp, P.A. & Burge, C.B. (2002) Predictive identification of exonic splicing enhancers in human genes. *Science,* **297,** 1007-1013.

Fang, J., Nurden, P., North, P., Nurden, A.T., Du, L.M., Valentin, N. & Wilcox, D.A. (2013) C560Rbeta3 caused platelet integrin alphaII b beta3 to bind fibrinogen continuously, but resulted in a severe bleeding syndrome and increased murine mortality. *J Thromb Haemost,* **11,** 1163-1171.

Fiore, M., Firah, N., Pillois, X., Nurden, P., Heilig, R. & Nurden, A.T. (2012) Natural history of platelet antibody formation against alphaIIbbeta3 in a French cohort of Glanzmann thrombasthenia patients. *Haemophilia,* **18,** e201-209.

Fitzgerald, L.A., Steiner, B., Rall, S., Lo, S.-S. & Phillips, D. (1987) Protein sequence of endothelial glycoprotein IIIa derived from a cDNA clone. Identity with platelet glycoprotein IIIa and similarity to" integrin". *Journal of Biological Chemistry,* **262,** 3936-3939.

Freeze, H.H. & Kranz, C. (2008) Endoglycosidase and Glycoamidase Release of N-Linked Glycans. *Current Protocols in Immunology***,** 12.14. 11-12.14. 25.

Gaildrat, P., Krieger, S., Di Giacomo, D., Abdat, J., Revillion, F., Caputo, S., Vaur, D., Jamard, E., Bohers, E., Ledemeney, D., Peyrat, J.P., Houdayer, C., Rouleau, E., Lidereau, R., Frebourg, T., Hardouin, A., Tosi, M. & Martins, A. (2012) Multiple sequence variants of BRCA2 exon 7 alter splicing regulation. *J Med Genet,* **49,** 609-617.

George, J.N., Caen, J.P. & Nurden, A.T. (1990) Glanzmanns thrombasthenia - the spectrum of clinical-disease. *Blood,* **75,** 1383-1395.

Ghevaert, C., Salsmann, A., Watkins, N.A., Schaffner-Reckinger, E., Rankin, A., Garner, S.F., Stephens, J., Smith, G.A., Debili, N., Vainchenker, W., de Groot, P.G., Huntington, J.A., Laffan, M., Kieffer, N. & Ouwehand, W.H. (2008) A nonsynonymous SNP in the ITGB3 gene disrupts the conserved membrane-proximal cytoplasmic salt bridge in the alphaIIbbeta3 integrin and cosegregates dominantly with abnormal proplatelet formation and macrothrombocytopenia. *Blood,* **111,** 3407-3414.

Gonzalez-Manchon, C., Arias-Salgado, E.G., Butta, N., Martin, G., Rodriguez, R.B., Elalamy, I., Parrilla, R. & Favier, R. (2003) A novel homozygous splice junction mutation in GPIIb associated with alternative splicing, nonsense-mediated decay of GPIIb-mRNA, and type II Glanzmann's thrombasthenia. *J Thromb Haemost,* **1,** 1071-1078.

Grimaldi, C.M., Chen, F., Scudder, L.E., Coller, B.S. & French, D.L. (1996) A Cys374Tyr homozygous mutation of platelet glycoprotein IIIa (beta 3) in a Chinese patient with Glanzmann's thrombasthenia. *Blood,* **88,** 1666-1675.

Grimaldi, C.M., Chen, F., Wu, C., Weiss, H.J., Coller, B.S. & French, D.L. (1998) Glycoprotein IIb Leu214Pro mutation produces glanzmann thrombasthenia with both quantitative and qualitative abnormalities in GPIIb/IIIa. *Blood,* **91,** 1562-1571.

Hagen, I., Nurden, A., Bjerrum, O.J., Solum, N.O. & Caen, J. (1980) Immunochemical evidence for protein abnormalities in platelets from patients with Glanzmann's thrombasthenia and Bernard-Soulier syndrome. *Journal of Clinical Investigation,* **65,** 722.

Haghighi, A., Borhany, M., Ghazi, A., Edwards, N., Tabaksert, A., Fatima, N., Shamsi, T.S. & Sayer, J.A. (2015) Glanzmann thrombasthenia in Pakistan: molecular analysis and identification of novel mutations. *Clin Genet*.

Handagama, P., Scarborough, R.M., Shuman, M.A. & Bainton, D.F. (1993) Endocytosis of fibrinogen into megakaryocyte and platelet alpha-

granules is mediated by alpha IIb beta 3 (glycoprotein IIb-IIIa). *Blood,* **82,** 135-138.

Hauschner, H., Mor-Cohen, R., Seligsohn, U. & Rosenberg, N. (2012) A mutation in the beta3 cytoplasmic tail causes variant Glanzmann thrombasthenia by abrogating transition of alphaIIb beta3 to an active state. *J Thromb Haemost,* **10,** 289-297.

Heijne, G. (1990) The signal peptide. *The Journal of Membrane Biology,* **115,** 195-201.

Hodivala-Dilke, K.M., McHugh, K.P., Tsakiris, D.A., Rayburn, H., Crowley, D., Ullman-Cullere, M., Ross, F.P., Coller, B.S., Teitelbaum, S. & Hynes, R.O. (1999) beta 3-integrin-deficient mice are a model for Glanzmann thrombasthenia showing placental defects and reduced survival. *Journal of Clinical Investigation,* **103,** 229-238.

Hourdille, P., Fialon, P., Belloc, F., Namur, M., Boisseau, M.R. & Nurden, A.T. (1986) Megakaryocytes from the marrow of a patient with Glanzmann's thrombasthenia lacked GP IIb-IIIa complexes. *Thromb Haemost,* **56,** 66-70.

Hoylaerts, M.F., Yamamoto, H., Nuyts, K., Vreys, I., Deckmyn, H. & Vermylen, J. (1997) von Willebrand factor binds to native collagen VI primarily via its A1 domain. *Biochem J,* **324 (Pt 1),** 185-191.

Israels, S.J., McNicol, A., Robertson, C. & Gerrard, J.M. (1990) Platelet storage pool deficiency: diagnosis in patients with prolonged bleeding times and normal platelet aggregation. *Br J Haematol,* **75,** 118-121.

Italiano, J.E., Jr., Lecine, P., Shivdasani, R.A. & Hartwig, J.H. (1999a) Blood platelets are assembled principally at the ends of proplatelet processes produced by differentiated megakaryocytes. *J Cell Biol,* **147,** 1299-1312.

Italiano, J.E., Lecine, P., Shivdasani, R.A. & Hartwig, J.H. (1999b) Blood platelets are assembled principally at the ends of proplatelet processes produced by differentiated megakaryocytes. *Journal of Cell Biology,* **147,** 1299-1312.

Iwasaki, H., Mizuno, S., Wells, R.A., Cantor, A.B., Watanabe, S. & Akashi, K. (2003) GATA-1 converts lymphoid and myelomonocytic progenitors into the megakaryocyte/erythrocyte lineages. *Immunity,* **19,** 451-462.

Jackson, D.E., White, M.M., Jennings, L.K. & Newman, P.J. (1998) A Ser162-->Leu mutation within glycoprotein (GP) IIIa (integrin beta3) results in an unstable alphaIIbbeta3 complex that retains partial function in a novel form of type II Glanzmann thrombasthenia. *Thromb Haemost,* **80,** 42-48.

Jallu, V., Dusseaux, M., Panzer, S., Torchet, M.F., Hezard, N., Goudemand, J., de Brevern, A.G. & Kaplan, C. (2010) AlphaIIbbeta3 integrin: new allelic

variants in Glanzmann thrombasthenia, effects on ITGA2B and ITGB3 mRNA splicing, expression, and structure-function. *Hum Mutat,* **31,** 237-246.

Jayo, A., Conde, I., Lastres, P., Martinez, C., Rivera, J., Vicente, V. & Gonzalez-Manchon, C. (2010) L718P mutation in the membrane-proximal cytoplasmic tail of beta 3 promotes abnormal alpha IIb beta 3 clustering and lipid microdomain coalescence, and associates with a thrombasthenia-like phenotype. *Haematologica,* **95,** 1158-1166.

Jayo, A., Pabon, D., Lastres, P., Jimenez-Yuste, V. & Gonzalez-Manchon, C. (2006) Type II Glanzmann thrombasthenia in a compound heterozygote for the alpha IIb gene. A novel missense mutation in exon 27. *Haematologica,* **91,** 1352-1359.

Jennings, L.K. & Phillips, D.R. (1982) Purification of glycoproteins IIb and III from human platelet plasma membranes and characterization of a calcium-dependent glycoprotein IIb-III complex. *J Biol Chem,* **257,** 10458-10466.

Jin, Y., Dietz, H.C., Montgomery, R.A., Bell, W.R., McIntosh, I., Coller, B. & Bray, P.F. (1996) Glanzmann thrombasthenia. Cooperation between sequence variants in cis during splice site selection. *J Clin Invest,* **98,** 1745-1754.

Johnson, A., Goodall, A.H., Downie, C.J., Vellodi, A. & Michael, D.P. (1994) Bone marrow transplantation for Glanzmann's thrombasthenia. *Bone Marrow Transplant,* **14,** 147-150.

Kamata, T., Ambo, H., Puzon-McLaughlin, W., Tieu, K.K., Handa, M., Ikeda, Y. & Takada, Y. (2004) Critical cysteine residues for regulation of integrin alphaIIbbeta3 are clustered in the epidermal growth factor domains of the beta3 subunit. *Biochem J,* **378,** 1079-1082.

Kannan, M., Ahmad, F., Yadav, B.K., Kumar, R., Choudhry, V.P. & Saxena, R. (2009) Molecular defects in ITGA2B and ITGB3 genes in patients with Glanzmann thrombasthenia. *J Thromb Haemost,* **7,** 1878-1885.

Kashiwagi, H., Kunishima, S., Kiyomizu, K., Amano, Y., Shimada, H., Morishita, M., Kanakura, Y. & Tomiyama, Y. (2013) Demonstration of novel gain-of-function mutations of alphaIIbbeta3: association with macrothrombocytopenia and glanzmann thrombasthenia-like phenotype. *Mol Genet Genomic Med,* **1,** 77-86.

Kasirer-Friede, A., Kahn, M.L. & Shattil, S.J. (2007) Platelet integrins and immunoreceptors. *Immunol Rev,* **218,** 247-264.

Kaushansky, K. (2009) Determinants of platelet number and regulation of thrombopoiesis. *Hematology Am Soc Hematol Educ Program***,** 147-152.

Kessler, O., Jiang, Y. & Chasin, L.A. (1993) Order of intron removal during splicing of endogenous adenine phosphoribosyltransferase and dihydrofolate reductase pre-mRNA. *Mol Cell Biol,* **13,** 6211-6222.

Kiyoi, T., Tomiyama, Y., Honda, S., Tadokoro, S., Arai, M., Kashiwagi, H., Kosugi, S., Kato, H., Kurata, Y. & Matsuzawa, Y. (2003) A naturally occurring Tyr143His alpha IIb mutation abolishes alpha IIb beta 3 function for soluble ligands but retains its ability for mediating cell adhesion and clot retraction: comparison with other mutations causing ligand-binding defects. *Blood,* **101,** 3485-3491.

Kondo, M., Weissman, I.L. & Akashi, K. (1997) Identification of clonogenic common lymphoid progenitors in mouse bone marrow. *Cell,* **91,** 661-672.

Krawczak, M., Reiss, J. & Cooper, D.N. (1992) The mutational spectrum of single base-pair substitutions in mRNA splice junctions of human genes: causes and consequences. *Hum Genet,* **90,** 41-54.

Kunishima, S., Kashiwagi, H., Otsu, M., Takayama, N., Eto, K., Onodera, M., Miyajima, Y., Takamatsu, Y., Suzumiya, J., Matsubara, K., Tomiyama, Y. & Saito, H. (2011) Heterozygous ITGA2B R995W mutation inducing constitutive activation of the alphaIIbbeta3 receptor affects proplatelet formation and causes congenital macrothrombocytopenia. *Blood,* **117,** 5479-5484.

Kurosawa, S., Stearns-Kurosawa, D.J., Hidari, N. & Esmon, C.T. (1997) Identification of functional endothelial protein C receptor in human plasma. *J Clin Invest,* **100,** 411-418.

Laguerre, M., Sabi, E., Daly, M., Stockley, J., Nurden, P., Pillois, X. & Nurden, A.T. (2013) Molecular dynamics analysis of a novel beta3 Pro189Ser mutation in a patient with glanzmann thrombasthenia differentially affecting alphaIIbbeta3 and alphavbeta3 expression. *PLoS One,* **8,** e78683.

Lanza, F., Stierle, A., Fournier, D., Morales, M., Andre, G., Nurden, A.T. & Cazenave, J.P. (1992) A new variant of Glanzmann's thrombasthenia (Strasbourg I). Platelets with functionally defective glycoprotein IIb-IIIa complexes and a glycoprotein IIIa 214Arg----214Trp mutation. *J Clin Invest,* **89,** 1995-2004.

Larson, M.K. & Watson, S.P. (2006) Regulation of proplatelet formation and platelet release by integrin alpha IIb beta3. *Blood,* **108,** 1509-1514.

Leslie, M. (2010) Cell biology. Beyond clotting: the powers of platelets. *Science,* **328,** 562-564.

Levine, R.F., Hazzard, K.C. & Lamberg, J.D. (1982) The significance of megakaryocyte size. *Blood,* **60,** 1122-1131.

Li, A., Guo, Q., Kim, C., Hu, W. & Ye, F. (2014) Integrin alphaI b tail distal of GFFKR participates in inside-out alphaI b beta3 activation. *J Thromb Haemost,* **12,** 1145-1155.

Lockyer, S., Okuyama, K., Begum, S., Le, S., Sun, B., Watanabe, T., Matsumoto, Y., Yoshitake, M., Kambayashi, J. & Tandon, N.N. (2006) GPVI-deficient mice lack collagen responses and are protected against experimentally induced pulmonary thromboembolism. *Thromb Res,* **118,** 371-380.

Loftus, J.C., O'Toole, T.E., Plow, E.F., Glass, A., Frelinger, A.L., 3rd & Ginsberg, M.H. (1990) A beta 3 integrin mutation abolishes ligand binding and alters divalent cation-dependent conformation. *Science,* **249,** 915-918.

Malinin, N.L., Zhang, L., Choi, J., Ciocea, A., Razorenova, O., Ma, Y.Q., Podrez, E.A., Tosi, M., Lennon, D.P., Caplan, A.I., Shurin, S.B., Plow, E.F. & Byzova, T.V. (2009) A point mutation in KINDLIN3 ablates activation of three integrin subfamilies in humans. *Nat Med,* **15,** 313-318.

Mansour, W., Einav, Y., Hauschner, H., Koren, A., Seligsohn, U. & Rosenberg, N. (2011) An alphaIIb mutation in patients with Glanzmann thrombasthenia located in the N-terminus of blade 1 of the beta-propeller (Asn2Asp) disrupts a calcium binding site in blade 6. *J Thromb Haemost,* **9,** 192-200.

Marguerie, G.A., Plow, E.F. & Edgington, T.S. (1979) Human platelets possess an inducible and saturable receptor specific for fibrinogen. *Journal of Biological Chemistry,* **254,** 5357-5363.

Maynard, D.M., Heijnen, H.F., Horne, M.K., White, J.G. & Gahl, W.A. (2007) Proteomic analysis of platelet alpha-granules using mass spectrometry. *J Thromb Haemost,* **5,** 1945-1955.

McColl, M.D. & Gibson, B.E. (1997) Sibling allogeneic bone marrow transplantation in a patient with type I Glanzmann's thrombasthenia. *Br J Haematol,* **99,** 58-60.

McKay, B.S., Annis, D.S., Honda, S., Christie, D. & Kunicki, T.J. (1996) Molecular requirements for assembly and function of a minimized human integrin alphaIIbbeta3. *J Biol Chem,* **271,** 30544-30547.

McNicol, A. & Israels, S.J. (1999) Platelet dense granules: structure, function and implications for haemostasis. *Thromb Res,* **95,** 1-18.

Metcalf, D. (1999) Stem cells, pre-progenitor cells and lineage-committed cells: are our dogmas correct? *Ann N Y Acad Sci,* **872,** 289-303; discussion 303-284.

Michiels, C. (2003) Endothelial cell functions. *J Cell Physiol,* **196,** 430-443.

Milet-Marsal, S., Breillat, C., Peyruchaud, O., Nurden, P., Combrie, R., Nurden, A. & Bourre, F. (2002a) Two different beta3 cysteine substitutions alter alphaIIb beta3 maturation and result in Glanzmann thrombasthenia. *Thromb Haemost,* **88,** 104-110.

Milet-Marsal, S., Breillat, C., Peyruchaud, O., Nurden, P., Combrie, R., Nurden, A.T. & Bourre, F. (2002b) Analysis of the amino acid requirement for a normal alphaIIbbeta3 maturation at alphaIIbGlu324 commonly mutated in Glanzmann thrombasthenia. *Thromb Haemost,* **88,** 655-662.

Miller, M.P. & Kumar, S. (2001) Understanding human disease mutations through the use of interspecific genetic variation. *Hum Mol Genet,* **10,** 2319-2328.

Mitchell, W.B., Li, J., French, D.L. & Coller, B.S. (2006) alphaIIbbeta3 biogenesis is controlled by engagement of alphaIIb in the calnexin cycle via the N15-linked glycan. *Blood,* **107,** 2713-2719.

Mitchell, W.B., Li, J., Murcia, M., Valentin, N., Newman, P.J. & Coller, B.S. (2007) Mapping early conformational changes in alphaIIb and beta3 during biogenesis reveals a potential mechanism for alphaIIbbeta3 adopting its bent conformation. *Blood,* **109,** 3725-3732.

Mitchell, W.B., Li, J.H., Singh, F., Michelson, A.D., Bussel, J., Coller, B.S. & French, D.L. (2003) Two novel mutations in the alpha IIb calcium-binding domains identify hydrophobic regions essential for alpha IIbbeta 3 biogenesis. *Blood,* **101,** 2268-2276.

Mooney, S.D. & Klein, T.E. (2002) The functional importance of disease-associated mutation. *BMC Bioinformatics,* **3,** 24.

Mor-Cohen, R., Rosenberg, N., Einav, Y., Zelzion, E., Landau, M., Mansour, W., Averbukh, Y. & Seligsohn, U. (2012) Unique disulfide bonds in epidermal growth factor (EGF) domains of beta3 affect structure and function of alphaIIbbeta3 and alphavbeta3 integrins in different manner. *J Biol Chem,* **287,** 8879-8891.

Mor-Cohen, R., Rosenberg, N., Landau, M., Lahav, J. & Seligsohn, U. (2008) Specific cysteines in beta3 are involved in disulfide bond exchange-dependent and -independent activation of alphaIIbbeta3. *J Biol Chem,* **283,** 19235-19244.

Mor-Cohen, R., Rosenberg, N., Peretz, H., Landau, M., Coller, B.S., Awidi, A. & Seligsohn, U. (2007) Disulfide bond disruption by a beta 3-Cys549Arg mutation in six Jordanian families with Glanzmann thrombasthenia causes diminished production of constitutively active alpha IIb beta 3. *Thromb Haemost,* **98,** 1257-1265.

Morel-Kopp, M.C., Melchior, C., Chen, P., Ammerlaan, W., Lecompte, T., Kaplan, C. & Kieffer, N. (2001) A naturally occurring point mutation in the beta3 integrin MIDAS-like domain affects differently alphavbeta3 and alphaIIbbeta3 receptor function. *Thromb Haemost,* **86,** 1425-1434.

Moser, M., Nieswandt, B., Ussar, S., Pozgajova, M. & Fassler, R. (2008) Kindlin-3 is essential for integrin activation and platelet aggregation. *Nat Med,* **14,** 325-330.

Nachman, R.L., Leung, L., Kloczewiak, M. & Hawiger, J. (1984) Complex formation of platelet membrane glycoproteins IIb and IIIa with the fibrinogen D domain. *Journal of Biological Chemistry,* **259,** 8584-8588.

Nelson, E.J., Li, J., Mitchell, W.B., Chandy, M., Srivastava, A. & Coller, B.S. (2005) Three novel beta-propeller mutations causing Glanzmann thrombasthenia result in production of normally stable pro-alphaIIb, but variably impaired progression of pro-alphaIIbbeta3 from endoplasmic reticulum to Golgi. *J Thromb Haemost,* **3,** 2773-2783.

Ng, P.C. & Henikoff, S. (2001) Predicting deleterious amino acid substitutions. *Genome Res,* **11,** 863-874.

Nurden, A. & Nurden, P. (2011) Advances in our understanding of the molecular basis of disorders of platelet function. *J Thromb Haemost,* **9 Suppl 1,** 76-91.

Nurden, A.T. (2006) Glanzmann thrombasthenia. *Orphanet J Rare Dis,* **1,** b1.

Nurden, A.T. & Caen, J.P. (1974) An abnormal platelet glycoprotein pattern in three cases of Glanzmann's thrombasthenia. *Br J Haematol,* **28,** 253-260.

Nurden, A.T., Fiore, M., Nurden, P. & Pillois, X. (2011) Glanzmann thrombasthenia: a review of ITGA2B and ITGB3 defects with emphasis on variants, phenotypic variability, and mouse models. *Blood,* **118,** 5996-6005.

Nurden, A.T., Freson, K. & Seligsohn, U. (2012a) Inherited platelet disorders. *Haemophilia,* **18 Suppl 4,** 154-160.

Nurden, A.T., Pillois, X., Fiore, M., Alessi, M.C., Bonduel, M., Dreyfus, M., Goudemand, J., Gruel, Y., Benabdallah-Guerida, S., Latger-Cannard, V., Negrier, C., Nugent, D., Oiron, R.D., Rand, M.L., Sie, P., Trossaert, M., Alberio, L., Martins, N., Sirvain-Trukniewicz, P., Couloux, A., Canault, M., Fronthroth, J.P., Fretigny, M., Nurden, P., Heilig, R. & Vinciguerra, C. (2015) Expanding the Mutation Spectrum Affecting alphaIIbbeta3 Integrin in Glanzmann Thrombasthenia: Screening of the ITGA2B and ITGB3 Genes in a Large International Cohort. *Hum Mutat,* **36,** 548-561.

Nurden, A.T., Pillois, X. & Nurden, P. (2012b) Understanding the genetic basis of Glanzmann thrombasthenia: implications for treatment. *Expert Rev Hematol,* **5,** 487-503.

Nurden, A.T., Pillois, X. & Wilcox, D.A. (2013) Glanzmann thrombasthenia: state of the art and future directions. *Semin Thromb Hemost,* **39,** 642-655.

Nurden, A.T., Rosa, J.P., Fournier, D., Legrand, C., Didry, D., Parquet, A. & Pidard, D. (1987) A variant of Glanzmann's thrombasthenia with abnormal glycoprotein IIb-IIIa complexes in the platelet membrane. *J Clin Invest,* **79,** 962-969.

Nutt, S.L., Metcalf, D., D'Amico, A., Polli, M. & Wu, L. (2005) Dynamic regulation of PU.1 expression in multipotent hematopoietic progenitors. *J Exp Med,* **201,** 221-231.

O'Toole, T.E., Loftus, J.C., Plow, E.F., Glass, A.A., Harper, J.R. & Ginsberg, M.H. (1989) Efficient surface expression of platelet GPIIb-IIIa requires both subunits. *Blood,* **74,** 14-18.

Odell, T.T., Jackson, C.W. & Friday, T.J. (1970) Megakaryocytopoiesis in rats with special reference to polyploidy. *Blood-the Journal of Hematology,* **35,** 775-&.

Oliver, D. (1985) Protein Secretion in Escherichia Coli. *Annual Review of Microbiology,* **39,** 615-648.

Patel, S.R., Richardson, J.L., Schulze, H., Kahle, E., Galjart, N., Drabek, K., Shivdasani, R.A., Hartwig, J.H. & Italiano, J.E., Jr. (2005) Differential roles of microtubule assembly and sliding in proplatelet formation by megakaryocytes. *Blood,* **106,** 4076-4085.

Peretz, H., Rosenberg, N., Landau, M., Usher, S., Nelson, E.J., Mor-Cohen, R., French, D.L., Mitchell, B.W., Nair, S.C., Chandy, M., Coller, B.S., Srivastava, A. & Seligsohn, U. (2006) Molecular diversity of Glanzmann thrombasthenia in southern India: new insights into mRNA splicing and structure-function correlations of alphaIIbbeta3 integrin (ITGA2B, ITGB3). *Hum Mutat,* **27,** 359-369.

Phillips, D.R. & Agin, P.P. (1977) Platelet membrane defects in Glanzmann's thrombasthenia: evidence for decreased amounts of two major glycoproteins. *Journal of Clinical Investigation,* **60,** 535.

Pillitteri, D., Pilgrimm, A.K. & Kirchmaier, C.M. (2010) Novel Mutations in the GPIIb and GPIIIa Genes in Glanzmann Thrombasthenia. *Transfus Med Hemother,* **37,** 268-277.

Poncz, M., Rifat, S., Coller, B.S., Newman, P.J., Shattil, S.J., Parrella, T., Fortina, P. & Bennett, J.S. (1994) Glanzmann thrombasthenia secondary

to a Gly273-->Asp mutation adjacent to the first calcium-binding domain of platelet glycoprotein IIb. *J Clin Invest,* **93,** 172-179.

Radley, J.M. & Haller, C.J. (1982) The demarcation membrane system of the megakaryocyte: a misnomer? *Blood,* **60,** 213-219.

Ramjaun, A.R. & Hodivala-Dilke, K. (2009) The role of cell adhesion pathways in angiogenesis. *Int J Biochem Cell Biol,* **41,** 521-530.

Rappsilber, J., Ryder, U., Lamond, A.I. & Mann, M. (2002) Large-scale proteomic analysis of the human spliceosome. *Genome Res,* **12,** 1231-1245.

Reed, R. (2000) Mechanisms of fidelity in pre-mRNA splicing. *Curr Opin Cell Biol,* **12,** 340-345.

Reichert, N., Seligsohn, U. & Ramot, B. (1975) Clinical and genetic aspects of Glanzmann's thrombasthenia in Israel: report of 22 cases. *Thromb Diath Haemorrh,* **34,** 806-820.

Riddel, J.P., Jr., Aouizerat, B.E., Miaskowski, C. & Lillicrap, D.P. (2007) Theories of blood coagulation. *J Pediatr Oncol Nurs,* **24,** 123-131.

Rosa, J.P., Bray, P.F., Gayet, O., Johnston, G.I., Cook, R.G., Jackson, K.W., Shuman, M.A. & McEver, R.P. (1988) Cloning of glycoprotein IIIa cDNA from human erythroleukaemia cells and localization of the gene to chromosome 17. *Blood,* **72,** 593-600.

Rosa, J.P. & McEver, R.P. (1989) Processing and assembly of the integrin, glycoprotein IIb-IIIa, in HEL cells. *J Biol Chem,* **264,** 12596-12603.

Rosenberg, N., Landau, M., Luboshitz, J., Rechavi, G. & Seligsohn, U. (2004) A novel Phe171Cys mutation in integrin alpha causes Glanzmann thrombasthenia by abrogating alphabeta complex formation. *J Thromb Haemost,* **2,** 1167-1175.

Ruan, J., Peyruchaud, O., Alberio, L., Valles, G., Clemetson, K., Bourre, F. & Nurden, A.T. (1998) Double heterozygosity of the GPIIb gene in a Swiss patient with Glanzmann's thrombasthenia. *Br J Haematol,* **102,** 918-925.

Ruan, J., Schmugge, M., Clemetson, K.J., Cazes, E., Combrie, R., Bourre, F. & Nurden, A.T. (1999) Homozygous Cys542-->Arg substitution in GPIIIa in a Swiss patient with type I Glanzmann's thrombasthenia. *Br J Haematol,* **105,** 523-531.

Ruiz, C., Liu, C.Y., Sun, Q.H., Sigaud-Fiks, M., Fressinaud, E., Muller, J.Y., Nurden, P., Nurden, A.T., Newman, P.J. & Valentin, N. (2001) A point mutation in the cysteine-rich domain of glycoprotein (GP) IIIa results in the expression of a GPIIb-IIIa (alphaIIbbeta3) integrin receptor locked in

a high-affinity state and a Glanzmann thrombasthenia-like phenotype. *Blood,* **98,** 2432-2441.

Sandrock-Lang, K., Oldenburg, J., Wiegering, V., Halimeh, S., Santoso, S., Kurnik, K., Fischer, L., Tsakiris, D.A., Sigl-Kraetzig, M., Brand, B., Buhrlen, M., Kraetzer, K., Deeg, N., Hund, M., Busse, E., Kahle, A. & Zieger, B. (2015) Characterisation of patients with Glanzmann thrombasthenia and identification of 17 novel mutations. *Thromb Haemost,* **113,** 782-791.

Sandrock, K., Halimeh, S., Wiegering, V., Kappert, G., Sauer, K., Deeg, N., Busse, E. & Zieger, B. (2012) Homozygous point mutations in platelet glycoprotein ITGA2B gene as cause of Glanzmann thrombasthenia in 2 families. *Klin Padiatr,* **224,** 174-178.

Savage, B., Almus-Jacobs, F. & Ruggeri, Z.M. (1998) Specific synergy of multiple substrate-receptor interactions in platelet thrombus formation under flow. *Cell,* **94,** 657-666.

Schaffner-Reckinger, E., Gouon, V., Melchior, C., Plancon, S. & Kieffer, N. (1998) Distinct involvement of beta3 integrin cytoplasmic domain tyrosine residues 747 and 759 in integrin-mediated cytoskeletal assembly and phosphotyrosine signaling. *J Biol Chem,* **273,** 12623-12632.

Schulze, H., Korpal, M., Hurov, J., Kim, S.W., Zhang, J., Cantley, L.C., Graf, T. & Shivdasani, R.A. (2006) Characterization of the megakaryocyte demarcation membrane system and its role in thrombopoiesis. *Blood,* **107,** 3868-3875.

Schwarz, J.M., Cooper, D.N., Schuelke, M. & Seelow, D. (2014) MutationTaster2: mutation prediction for the deep-sequencing age. *Nat Methods,* **11,** 361-362.

Shen, W.Z., Ding, Q.L., Jin, P.P., Wang, X.F., Jiang, Y.Z., Li, S.M. & Wang, H.L. (2009) A novel Pro126His beta propeller mutation in integrin alpha IIb causes Glanzmann thrombasthenia by impairing progression of pro-alpha IIb beta 3 from endoplasmic reticulum to Golgi. *Blood Cells Molecules and Diseases,* **42,** 44-50.

Stegner, D. & Nieswandt, B. (2011) Platelet receptor signaling in thrombus formation. *J Mol Med (Berl),* **89,** 109-121.

Stevens, R.F. & Meyer, S. (2002) Fanconi and Glanzmann: the men and their works. *Br J Haematol,* **119,** 901-904.

Sunyaev, S., Ramensky, V., Koch, I., Lathe, W., 3rd, Kondrashov, A.S. & Bork, P. (2001) Prediction of deleterious human alleles. *Hum Mol Genet,* **10,** 591-597.

Tadokoro, S., Tomiyama, Y., Honda, S., Arai, M., Yamamoto, N., Shiraga, M., Kosugi, S., Kanakura, Y., Kurata, Y. & Matsuzawa, Y. (1998) A Gln747--

>Pro substitution in the IIb subunit is responsible for a moderate IIbbeta3 deficiency in Glanzmann thrombasthenia. *Blood,* **92,** 2750-2758.

Tadokoro, S., Tomiyama, Y., Honda, S., Kashiwagi, H., Kosugi, S., Shiraga, M., Kiyoi, T., Kurata, Y. & Matsuzawa, Y. (2002) Missense mutations in the beta(3) subunit have a different impact on the expression and function between alpha(IIb)beta(3) and alpha(v)beta(3). *Blood,* **99,** 931-938.

Takagi, J., Petre, B.M., Walz, T. & Springer, T.A. (2002) Global conformational rearrangements in integrin extracellular domains in outside-in and inside-out signaling. *Cell,* **110,** 599-511.

Tavtigian, S.V., Greenblatt, M.S., Lesueur, F. & Byrnes, G.B. (2008) In silico analysis of missense substitutions using sequence-alignment based methods. *Hum Mutat,* **29,** 1327-1336.

Thusberg, J. & Vihinen, M. (2009) Pathogenic or not? And if so, then how? Studying the effects of missense mutations using bioinformatics methods. *Hum Mutat,* **30,** 703-714.

Tjio JH & Puck, T.T. (1958) GENETICS OF SOMATIC MAMMALIAN CELLS : II. CHROMOSOMAL CONSTITUTION OF CELLS IN TISSUE CULTURE. The Journal of Experimental Medicine. *Journal of Experimental Medicine,* **108 (2),** 259-268.

Tokgoz, H., Torun Ozkan, D., Caliskan, U. & Akar, N. (2015) Novel mutations of integrin alphaIIb and beta3 genes in Turkish children with Glanzmann's thrombasthenia. *Platelets,* **26,** 779-782.

Toogeh, G., Sharifian, R., Lak, M., Safaee, R., Artoni, A. & Peyvandi, F. (2004) Presentation and pattern of symptoms in 382 patients with Glanzmann thrombasthenia in Iran. *Am J Hematol,* **77,** 198-199.

Tournier, I., Vezain, M., Martins, A., Charbonnier, F., Baert-Desurmont, S., Olschwang, S., Wang, Q., Buisine, M.P., Soret, J., Tazi, J., Frebourg, T. & Tosi, M. (2008) A large fraction of unclassified variants of the mismatch repair genes MLH1 and MSH2 is associated with splicing defects. *Hum Mutat,* **29,** 1412-1424.

Tozer, E.C., Baker, E.K., Ginsberg, M.H. & Loftus, J.C. (1999) A mutation in the alpha subunit of the platelet integrin alphaIIbbeta3 identifies a novel region important for ligand binding. *Blood,* **93,** 918-924.

Tronik-Le Roux, D., Roullot, V., Poujol, C., Kortulewski, T., Nurden, P. & Marguerie, G. (2000) Thrombasthenic mice generated by replacement of the integrin alphaIIb gene: Demonstration that transcriptional activation of this megakaryocytic locus precedes lineage commitment. *Blood,* **96,** 1399-1408.

Varga-Szabo, D., Pleines, I. & Nieswandt, B. (2008) Cell adhesion mechanisms in platelets. *Arterioscler Thromb Vasc Biol,* **28,** 403-412.

Vijapurkar, M., Ghosh, K. & Shetty, S. (2009) Novel mutations in GP IIb gene in Glanzmann's thrombasthenia from India. *Platelets,* **20,** 35-40.

Vinciguerra, C., Bordet, J.C., Beaune, G., Grenier, C., Dechavanne, M. & Negrier, C. (2001) Description of 10 new mutations in platelet glycoprotein IIb (alphaIIb) and glycoprotein IIIa (beta3) genes. *Platelets,* **12,** 486-495.

von Heijne, G. (1998) Life and death of a signal peptide. *Nature,* **396,** 111, 113.

Ward, C.M., Kestin, A.S. & Newman, P.J. (2000) A Leu262Pro mutation in the integrin beta(3) subunit results in an alpha(IIb)-beta(3) complex that binds fibrin but not fibrinogen. *Blood,* **96,** 161-169.

Watson, S.P., Herbert, J.M. & Pollitt, A.Y. (2010) GPVI and CLEC-2 in hemostasis and vascular integrity. *J Thromb Haemost,* **8,** 1456-1467.

Wenceldrake, J.D., Plow, E.F., Kunicki, T.J., Woods, V.L., Keller, D.M. & Ginsberg, M.H. (1986) Localization of internal pools of membrane-glycoproteins involved in platelet adhesive responses. *American Journal of Pathology,* **124,** 324-334.

Westrup, D., Santoso, S., Follert-Hagendorff, K., Bassus, S., Just, M., Jablonka, B. & Kirchmaier, C.M. (2004) Glanzmann thrombasthenia Frankfurt I is associated with a point mutation Thr176Ile in the N-terminal region of alpha IIb subunit integrin. *Thromb Haemost,* **92,** 1040-1051.

White, J.G. (1969) The dense bodies of human platelets: inherent electron opacity of the serotonin storage particles. *Blood,* **33,** 598-606.

White, J.G. (2007) Platelet Structure. In: *Platelets* (ed. by Michelson, A.D.). Academic Press, London ,UK.

White, J.G. & Rao, G.H. (1998) Microtubule coils versus the surface membrane cytoskeleton in maintenance and restoration of platelet discoid shape. *Am J Pathol,* **152,** 597-609.

Wilcox, D.A., Paddock, C.M., Lyman, S., Gill, J.C. & Newman, P.J. (1995) Glanzmann thrombasthenia resulting from a single amino acid substitution between the second and third calcium-binding domains of GPIIb. Role of the GPIIb amino terminus in integrin subunit association. *J Clin Invest,* **95,** 1553-1560.

Wilcox, D.A., Wautier, J.L., Pidard, D. & Newman, P.J. (1994) A single amino acid substitution flanking the fourth calcium binding domain of alpha IIb prevents maturation of the alpha IIb beta 3 integrin complex. *J Biol Chem,* **269,** 4450-4457.

Xiao, T., Takagi, J., Coller, B.S., Wang, J.H. & Springer, T.A. (2004) Structural basis for allostery in integrins and binding to fibrinogen-mimetic therapeutics. *Nature,* **432,** 59-67.

Xie, C., Shimaoka, M., Xiao, T., Schwab, P., Klickstein, L.B. & Springer, T.A. (2004) The integrin alpha-subunit leg extends at a Ca2+-dependent epitope in the thigh/genu interface upon activation. *Proc Natl Acad Sci U S A,* **101,** 15422-15427.

Xiong, J.P., Mahalingham, B., Alonso, J.L., Borrelli, L.A., Rui, X., Anand, S., Hyman, B.T., Rysiok, T., Muller-Pompalla, D., Goodman, S.L. & Arnaout, M.A. (2009) Crystal structure of the complete integrin alphaVbeta3 ectodomain plus an alpha/beta transmembrane fragment. *J Cell Biol,* **186,** 589-600.

Xiong, J.P., Stehle, T., Diefenbach, B., Zhang, R., Dunker, R., Scott, D.L., Joachimiak, A., Goodman, S.L. & Arnaout, M.A. (2001) Crystal structure of the extracellular segment of integrin alpha Vbeta3. *Science,* **294,** 339-345.

Xu, Z., Chen, X., Zhi, H., Gao, J., Bialkowska, K., Byzova, T.V., Pluskota, E., White, G.C., 2nd, Liu, J., Plow, E.F. & Ma, Y.Q. (2014) Direct interaction of kindlin-3 with integrin alphaIIbbeta3 in platelets is required for supporting arterial thrombosis in mice. *Arterioscler Thromb Vasc Biol,* **34,** 1961-1967.

Yang, J., Ma, Y.Q., Page, R.C., Misra, S., Plow, E.F. & Qin, J. (2009) Structure of an integrin alphaIIb beta3 transmembrane-cytoplasmic heterocomplex provides insight into integrin activation. *Proc Natl Acad Sci U S A,* **106,** 17729-17734.

Zhou, Z., Licklider, L.J., Gygi, S.P. & Reed, R. (2002) Comprehensive proteomic analysis of the human spliceosome. *Nature,* **419,** 182-185.

Zhu, J., Boylan, B., Luo, B.H., Newman, P.J. & Springer, T.A. (2007) Tests of the extension and deadbolt models of integrin activation. *J Biol Chem,* **282,** 11914-11920.

Zhu, J., Luo, B.H., Xiao, T., Zhang, C., Nishida, N. & Springer, T.A. (2008) Structure of a complete integrin ectodomain in a physiologic resting state and activation and deactivation by applied forces. *Mol Cell,* **32,** 849-861.

Appendices

8.1 Appendix 1: pcDNA 3.1 - *ITAG2B* and pcDNA 3.1 - *ITGB3* plasmids

The pcDNA 3.1 expression vector, initially derived from pcDNA 3, is designed to deliver non-replication transient and a high level of stable expressions in the most common mammalian hosts. This vector has a variety of different elements and features that are important for making stable mRNA and protein. These elements include selectable markers (Neomycin and Ampicillin), multiple cloning sites, origin of replication, strong promoter (Human cytomegalovirus), ribosomal binding sites and transcriptional termination sequences. Full details of these elements and features and their functions are highlighted in Table A1.

pcDNA-*ITAG2B* and pcDNA-*ITGB3* were made available as a kind gift from Professor Nelly Kieffer, University of Luxembourg. In brief, the α_{IIb} (*ITGA2B*) and β_3 (*ITGB3*) cDNAs were amplified from mRNA of *ITGA2B* and *ITGB3* of the human erythroleukaemic (HEL) cell line. The pcDNA 3.1 and both *ITGA2B* and *ITGB3* cDNA were digested by XbaI and HindIII. The digested cDNA were then ligated into pcDNA3.1, Figure A1.

Table A1 Elements and features within the pcDNA 3.1 vector

Feature	Function
Human cytomegalovirus (CMV) immediate-early promoter/enhancer	Permits high-level and efficient expression of inserted recombinant protein
Multiple cloning site	Allows insertion of gene of interest and facilitates cloning
T7 promoter/priming site	Allows for *in vitro* transcription in the sense orientation and sequencing through the insert
f1 origin	Enables replication of single-stranded DNA
Bovine growth hormone (BGH) polyadenylation signal	Efficient transcription termination and mRNA polyadenylation
SV40 early promoter	Enables efficient expression of the neomycin resistance gene
SV40 origin	Episomal replication in cells expressing SV40 large T antigen
SV40 polyadenylation signal	Efficient transcription termination and mRNA polyadenylation
pUC origin	Allows growth and high-copy number replication in *E. coli*
Neomycin resistance gene	Selection marker in mammalian cells
Ampicillin resistance gene (β-lactamase)	Selection marker in *E. coli*

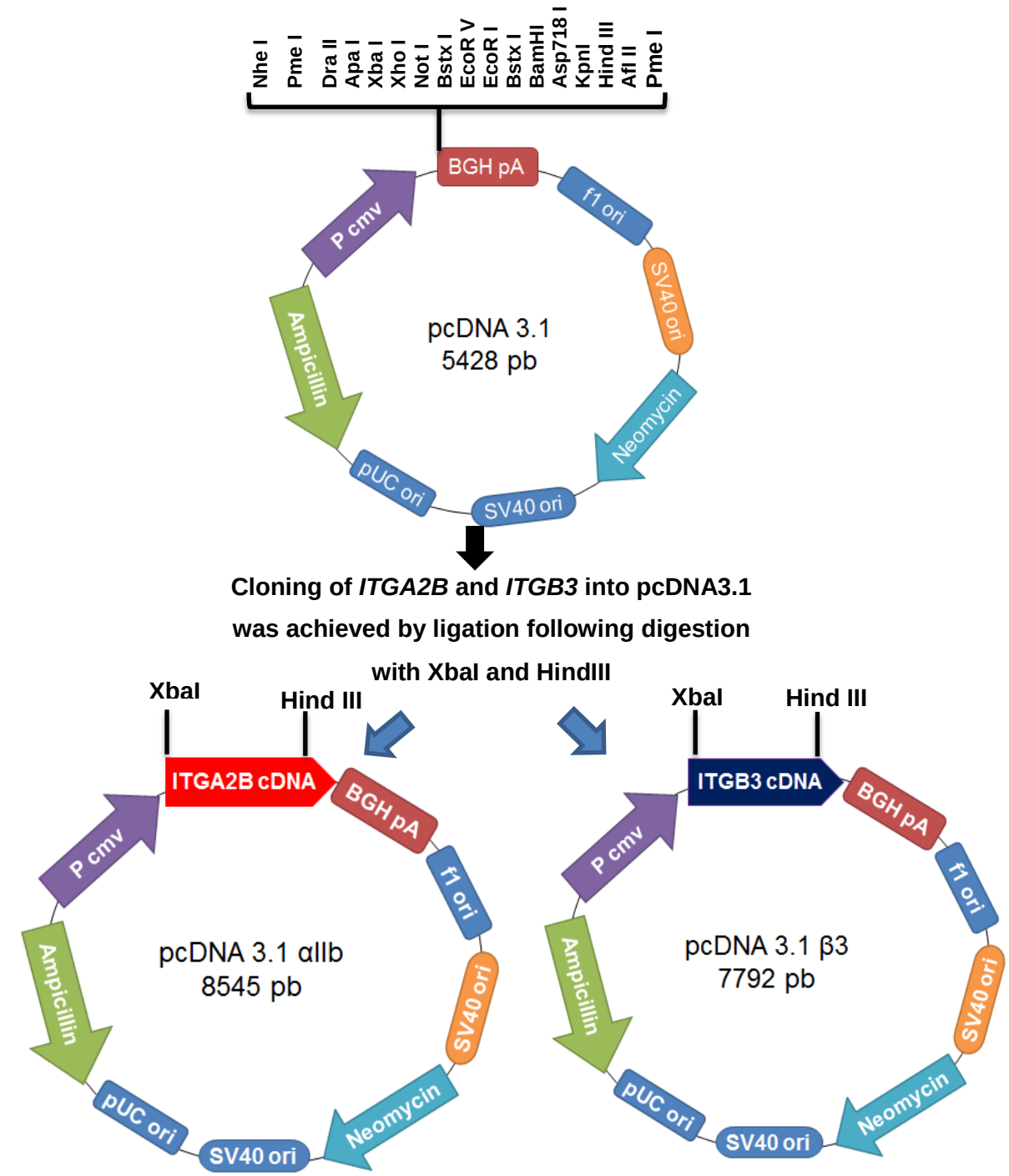

Figure A1 Vector maps of pcDNA3.1, pcDNA 3.1-*ITGA2B* and pcDNA3.1- *ITGB3*. *ITGA2B* and *ITGB3* cDNA were cloned into the pcDNA 3.1 expression construct using the restriction enzymes XbaI and HindIII.

Appendix 1: Sequence of pcDNA3.1-*ITGA2B* and pcDNA3.1- *ITGB3* template

pcDNA3.1-*ITGA2B* sequence:

gacggatcgggagatctcccgatcccctatggtgcactctcagtacaatctgctctgatgccgcatagttaagccagtatctgctccctgcttgtgtgttgg
aggtcgctgagtagtgcgcgagcaaaatttaagctacaacaaggcaaggcttgaccgacaattgcatgaagaatctgcttagggttaggcgttttgcg
ctgcttcgcgatgtacgggccagatatacgcgttgacattgattattgactagttattaatagtaatcaattacggggtcattagttcatagcccatatatgg
agttccgcgttacataacttacggtaaatggcccgcctggctgaccgcccaacgacccccgcccattgacgtcaataatgacgtatgttcccatagtaa
cgccaatagggactttccattgacgtcaatgggtggagtatttacggtaaactgcccacttggcagtacatcaagtgtatcatatgccaagtacgccccc
tattgacgtcaatgacggtaaatggcccgcctggcattatgcccagtacatgaccttatgggactttcctacttggcagtacatctacgtattagtcatcgct
attaccatggtgatgcggttttggcagtacatcaatgggcgtggatagcggtttgactcacggggatttccaagtctccaccccattgacgtcaatggga
gtttgttttggcaccaaaatcaacgggactttccaaaatgtcgtaacaactccgccccattgacgcaaatgggcggtaggcgtgtacggtgggaggtct
atataagcagagctctctggctaactagagaacccactgcttactggcttatcgaaattaatacgactcactatagggagacccaagctggctagcgtt
taaacgggcccTCTAGAGATGGCCAGAGCTTTGTGTCCACTGCAAGCCCTCTGGCTTCTGGAGTGGGTGC
TGCTGCTCTTGGGACCTTGTGCTGCCCCTCCAGCCTGGGCCTTGAACCTGGACCCAGTGCAGCTCAC
CTTCTATGCAGGCCCCAATGGCAGCCAGTTTGGATTTTCACTGGACTTCCACAAGGACAGCCATGGG
AGAGTGGCCATCGTGGTGGGCGCCCCGCGGACCCTGGGCCCCAGCCAGGAGGAGACGGGCGGCG
TGTTCCTGTGCCCCTGGAGGGCCGAGGGCGGCCAGTGCCCCTCGCTGCTCTTTGACCTCCGTGATG
AGACCCGAAATGTAGGCTCCCAAACTTTACAAACCTTCAAGGCCCGCCAAGGACTGGGGGCGTCGGT
CGTCAGCTGGAGCGACGTCATTGTGGCCTGCGCCCCCTGGCAGCACTGGAACGTCCTAGAAAAGAC
TGAGGAGGCTGAGAAGACGCCCGTAGGTAGCTGCTTTTTGGCTCAGCCAGAGAGCGGCCGCCGCGC
CGAGTACTCCCCCTGTCGCGGGAACACCCTGAGCCGCATTTACGTGGAAAATGATTTTAGCTGGGAC
AAGCGTTACTGTGAAGCGGGCTTCAGCTCCGTGGTCACTCAGGCCGGAGAGCTGGTGCTTGGGGCT
CCTGGCGGCTATTATTTCTTAGGTCTCCTGGCCCAGGCTCCAGTTGCGGATATTTTCTCGAGTTACCG
CCCAGGCATCCTTTTGTGGCACGTGTCCTCCCAGAGCCTCTCCTTTGACTCCAGCAACCCAGAGTAC
TTCGACGGCTACTGGGGGTACTCGGTGGCCGTGGGCGAGTTCGACGGGGATCTCAACACTACAGAA
TATGTCGTCGGTGCCCCCACTTGGAGCTGGACCCTGGGAGCGGTGGAAATTTTGGATTCCTACTACC
AGAGGCTGCATCGGCTGCGCGGAGAGCAGATGGCGTCGTATTTTGGGCATTCAGTGGCTGTCACTG
ACGTCAACGGGGATGGGAGGCATGATCTGCTGGTGGGCGCTCCACTGTATATGGAGAGCCGGGCAG
ACCGAAAACTGGCCGAAGTGGGGCGTGTGTATTTGTTCCTGCAGCCGCGAGGCCCCCACGCGCTGG
GTGCCCCCAGCCTCCTGCTGACTGGCACACAGCTCTATGGGCGATTCGGCTCTGCCATCGCACCCCT
GGGCGACCTCGACCGGGATGGCTACAATGACATTGCAGTGGCTGCCCCCTACGGGGGTCCCAGTGG
CCGGGGCCAAGTGCTGGTGTTCCTGGGTCAGAGTGAGGGGCTGAGGTCACGTCCCTCCCAGGTCCT
GGACAGCCCCTTCCCCACAGGCTCTGCCTTTGGCTTCTCCCTTCGAGGTGCCGTAGACATCGATGAC
AACGGATACCCAGACCTGATCGTGGGAGCTTACGGGGCCAACCAGGTGGCTGTGTACAGAGCTCAG
CCAGTGGTGAAGGCCTCTGTCCAGCTACTGGTGCAAGATTCACTGAATCCTGCTGTGAAGAGCTGTG
TCCTACCTCAGACCAAGACACCCGTGAGCTGCTTCAACATCCAGATGTGTGTTGGAGCCACTGGGCA
CAACATTCCTCAGAAGCTATCCCTAAATGCCGAGCTGCAGCTGGACCGGCAGAAGCCCCGCCAGGG
CCGGCGGGTGCTGCTGCTGGGCTCTCAACAGGCAGGCACCACCCTGAACCTGGATCTGGGCGGAAA
GCACAGCCCCATCTGCCACACCACCATGGCCTTCCTTCGAGATGAGGCAGACTTCCGGGACAAGCTG
AGCCCCATTGTGCTCAGCCTCAATGTGTCCCTACCGCCCACGGAGGCTGGAATGGCCCCTGCTGTC
GTGCTGCATGGAGACACCCATGTGCAGGAGCAGACACGAATCGTCCTGGACTGTGGGGAAGATGAC
GTATGTGTGCCCCAGCTTCAGCTCACTGCCAGCGTGACGGGCTCCCCGCTCCTAGTTGGGGCAGAT
AATGTCCTGGAGCTGCAGATGGACGCAGCCAACGAGGGCGAGGGGGCCTATGAAGCAGAGCTGGC
CGTGCACCTGCCCCAGGGCGCCCACTACATGCGGGCCCTAAGCAATGTCGAGGGCTTTGAGAGACT
CATCTGTAATCAGAAGAAGGAGAATGAGACCAGGGTGGTGCTGTGTGAGCTGGGCAACCCCATGAAG
AAGAACGCCCAGATAGGAATCGCGATGTTGGTGAGCGTGGGGAATCTGGAAGAGGCTGGGGAGTCT
GTGTCCTTCCAGCTGCAGATACGGAGCAAGAACAGCCAGAATCCAAACAGCAAGATTGTGCTGCTGG
ACGTGCCGGTCCGGGCAGAGGCCCAAGTGGAGCTGCGAGGGAACTCCTTTCCAGCCTCCCTGGTGG
TGGCAGCAGAAGAAGGTGAGAGGGAGCAGAACAGCTTGGACAGCTGGGGACCCAAAGTGGAGCACA
CCTATGAGCTCCACAACAATGGCCCTGGGACTGTGAATGGTCTTCACCTCAGCATCCACCTTCCGGG
ACAGTCCCAGCCCTCCGACCTGCTCTACATCCTGGATATACAGCCCCAGGGGGGCCTTCAGTGCTTC
CCACAGCCTCCTGTCAACCCTCTCAAGGTGGACTGGGGGCTGCCCATCCCCAGCCCCTCCCCCATTC
ACCCGGCCCATCACAAGCGGGATCGCAGACAGATCTTCCTGCCAGAGCCCGAGCAGCCCTCGAGGC
TTCAGGATCCAGTTCTCGTAAGCTGCGACTCGGCGCCCTGTACTGTGGTGCAGTGTGACCTGCAGGA
GATGGCGCGCGGGCAGCGGGCCATGGTCACGGTGCTGGCCTTCCTGTGGCTGCCCAGCCTCTACC
AGAGGCCTCTGGATCAGTTTGTGCTGCAGTCGCACGCATGGTTCAACGTGTCCTCCCTCCCCTATGC
GGTGCCCCCGCTCAGCCTGCCCCGAGGGGAAGCTCAGGTGTGGACACAGCTGCTCCGGGCCTTGG

AGGAGAGGGCCATTCCAATCTGGTGGGTGCTGGTGGGTGTGCTGGGTGGCCTGCTGCTGCTCACCA
TCCTGGTCCTGGCCATGTGGAAGGTCGGCTTCTTCAAGCGGAACCGGCCACCCCTGGAAGAAGATG
ATGAAGAGGGGGAGTGATGGTGCAGCCTACACTATTCTAGCAGGAGGGTTGGGCGTGCTACCTGCA
CCGCCCCTTCTCCAACAAGTTGCCTCCAAGCTTTGGGTTGGAGCTGTTCCATTGGGTCCTCTTGGTGT
CGTTTCCCTCCCAACAGAGCTGGGCTACCCCCCCTCCTGCTGCCTAATAAAGAGACTGAGCCCTGAA
GCTTaagtttaaaccgctgatcagcctcgactgtgccttctagttgccagccatctgttgtttgcccctcccccgtgccttccttgaccctggaaggtgcc
actcccactgtcctttcctaataaaatgaggaaattgcatcgcattgtctgagtaggtgtcattctattctgggggggtggggtggggcaggacagcaagg
gggaggattgggaagacaatagcaggcatgctggggatgcggtgggctctatggcttctgaggcggaaagaaccagctggggctctaggggggtat
ccccacgcgccctgtagcggcgcattaagcgcggcgggtgtggtggttacgcgcagcgtgaccgctacacttgccagcgccctagcgcccgctcctt
tcgctttcttcccttcctttctcgccacgttcgccggctttccccgtcaagctctaaatcgggggctccctttagggttccgatttagtgctttacggcacctcga
ccccaaaaaacttgattagggtgatggttcacgtagtgggccatcgccctgatagacggtttttcgccctttgacgttggagtccacgttctttaatagtgg
actcttgttccaaactggaacaacactcaaccctatctcggtctattcttttgatttataagggattttgccgatttcggcctattggttaaaaaatgagctgatt
taacaaaaatttaacgcgaattaattctgtggaatgtgtgtcagttagggtgtggaaagtccccaggctccccagcaggcagaagtatgcaaagcatg
catctcaattagtcagcaaccaggtgtggaaagtccccaggctccccagcaggcagaagtatgcaaagcatgcatctcaattagtcagcaaccata
gtcccgcccctaactccgcccatcccgcccctaactccgcccagttccgcccattctccgccccatggctgactaatttttttatttatgcagaggccgag
gccgcctctgcctctgagctattccagaagtagtgaggaggcttttttggaggcctaggcttttgcaaaaagctcccgggagcttgtatatccatttttcgga
tctgatcaagagacaggatgaggatcgtttcgcatgattgaacaagatggattgcacgcaggttctccggccgcttgggtggagaggctattcggctat
gactgggcacaacagacaatcggctgctctgatgccgccgtgttccggctgtcagcgcaggggcgcccggttctttttgtcaagaccgacctgtccggt
gccctgaatgaactgcaggacgaggcagcgcggctatcgtggctggccacgacgggcgttccttgcgcagctgtgctcgacgttgtcactgaagcg
ggaagggactggctgctattgggcgaagtgccggggcaggatctcctgtcatctcaccttgctcctgccgagaaagtatccatcatggctgatgcaat
gcggcggctgcatacgcttgatccggctacctgcccattcgaccaccaagcgaaacatcgcatcgagcgagcacgtactcggatggaagccggtct
tgtcgatcaggatgatctggacgaagagcatcaggggctcgcgccagccgaactgttcgccaggctcaaggcgcgcatgcccgacggcgaggat
ctcgtcgtgacccatggcgatgcctgcttgccgaatatcatggtggaaaatggccgcttttctggattcatcgactgtggccggctgggtgtggcggacc
gctatcaggacatagcgttggctacccgtgatattgctgaagagcttggcggcgaatgggctgaccgcttcctcgtgctttacggtatcgccgctcccga
ttcgcagcgcatcgccttctatcgccttcttgacgagttcttctgagcgggactctggggttcgaaatgaccgaccaagcgacgcccaacctgccatca
cgagatttcgattccaccgccgccttctatgaaaggttgggcttcggaatcgttttccgggacgccggctggatgatcctccagcgcggggatctcatgc
tggagttcttcgcccaccccaacttgtttattgcagcttataatggttacaaataaagcaatagcatcacaaatttcacaaataaagcatttttttcactgcat
tctagttgtggtttgtccaaactcatcaatgtatcttatcatgtctgtataccgtcgacctctagctagagcttggcgtaatcatggtcatagctgtttcctgtgtg
aaattgttatccgctcacaattccacacaacatacgagccggaagcataaagtgtaaagcctggggtgcctaatgagtgagctaactcacattaattg
cgttgcgctcactgcccgctttccagtcgggaaacctgtcgtgccagctgcattaatgaatcggccaacgcgcggggagaggcggtttgcgtattggg
cgctcttccgcttcctcgctcactgactcgctgcgctcggtcgttcggctgcggcgagcggtatcagctcactcaaaggcggtaatacggttatccacag
aatcaggggataacgcaggaaagaacatgtgagcaaaaggccagcaaaaggccaggaaccgtaaaaaggccgcgttgctggcgtttttccata
ggctccgccccctgacgagcatcacaaaaatcgacgctcaagtcagaggtggcgaaacccgacaggactataaagataccaggcgtttccccct
ggaagctccctcgtgcgctctcctgttccgaccctgccgcttaccggatacctgtccgcctttctcccttcgggaagcgtggcgctttctcatagctcacgc
tgtaggtatctcagttcggtgtaggtcgttcgctccaagctgggctgtgtgcacgaacccccgttcagcccgaccgctgcgccttatccggtaactatcg
tcttgagtccaacccggtaagacacgacttatcgccactggcagcagccactggtaacaggattagcagagcgaggtatgtaggcggtgctacaga
gttcttgaagtggtggcctaactacggctacactagaagaacagtatttggtatctgcgctctgctgaagccagttaccttcggaaaaagagttggtagc
tcttgatccggcaaacaaaccaccgctggtagcggttttttgtttgcaagcagcagattacgcgcagaaaaaaaggatctcaagaagatcctttgatct
tttctacggggtctgacgctcagtggaacgaaaactcacgttaagggattttggtcatgagattatcaaaaaggatcttcacctagatcctttaaattaaa
aatgaagttttaaatcaatctaaagtatatatgagtaaacttggtctgacagttaccaatgcttaatcagtgaggcacctatctcagcgatctgtctatttcgt
tcatccatagttgcctgactccccgtcgtgtagataactacgatacgggagggcttaccatctggccccagtgctgcaatgataccgcgagacccacg
ctcaccggctccagatttatcagcaataaaccagccagccggaagggccgagcgcagaagtggtcctgcaactttatccgcctccatccagtctatta
attgttgccgggaagctagagtaagtagttcgccagttaatagtttgcgcaacgttgttgccattgctacaggcatcgtggtgtcacgctcgtcgtttggtat
ggcttcattcagctccggttcccaacgatcaaggcgagttacatgatcccccatgttgtgcaaaaaagcggttagctccttcggtcctccgatcgttgtca
gaagtaagttggccgcagtgttatcactcatggttatggcagcactgcataattctcttactgtcatgccatccgtaagatgcttttctgtgactggtgagtac
tcaaccaagtcattctgagaatagtgtatgcggcgaccgagttgctcttgcccggcgtcaatacgggataataccgcgccacatagcagaactttaaa
agtgctcatcattggaaaacgttcttcggggcgaaaactctcaaggatcttaccgctgttgagatccagttcgatgtaacccactcgtgcacccaactga
tcttcagcatcttttactttcaccagcgtttctgggtgagcaaaaacaggaaggcaaaatgccgcaaaaaagggaataagggcgacacggaaatgtt
gaatactcatactcttcctttttcaatattattgaagcatttatcagggttattgtctcatgagcggatacatatttgaatgtatttagaaaaataaacaaatag
gggttccgcgcacatttccccgaaaagtgccacctgacgtc

pcDNA3.1-*ITGB3* sequence :

gacggatcgggagatctcccgatcccctatggtgcactctcagtacaatctgctctgatgccgcatagttaagccagtatctgctccctgcttgtgtgttgg
aggtcgctgagtagtgcgcgagcaaaatttaagctacaacaaggcaaggcttgaccgacaattgcatgaagaatctgcttagggttaggcgttttgcg
ctgcttcgcgatgtacgggccagatatacgcgttgacattgattattgactagttattaatagtaatcaattacggggtcattagttcatagcccatatatgg
agttccgcgttacataacttacggtaaatggcccgcctggctgaccgcccaacgacccccgcccattgacgtcaataatgacgtatgttcccatagtaa
cgccaatagggactttccattgacgtcaatgggtggagtatttacggtaaactgcccacttggcagtacatcaagtgtatcatatgccaagtacgccccc

tattgacgtcaatgacggtaaatggcccgcctggcattatgcccagtacatgaccttatgggactttcctacttggcagtacatctacgtattagtcatcgct
attaccatggtgatgcggttttggcagtacatcaatgggcgtggatagcggtttgactcacggggatttccaagtctccaccccattgacgtcaatggga
gtttgttttggcaccaaaatcaacgggactttccaaaatgtcgtaacaactccgccccattgacgcaaatgggcggtaggcgtgtacggtgggaggtct
atataagcagagctctctggctaactagagaacccactgcttactggcttatcgaaattaatacgactcactatagggagacccaagctggctagcgtt
taaacgggccc<mark>TCTAGA</mark>*CGCCGCGGGAGGCGGACGAGATGCGAGCGCGGCCGCGGCCCCGGCCGCTCT*
GGGCGACTGTGCTGGCGCTGGGGGCGCTGGCGGGCGTTGGCGTAGGAGGGCCCAACATCTGTACC
ACGCGAGGTTGAGCTCCTGCCAGCAGTGCCTGGCTGTGAGCCCCATGTGTGCCTGGTGCTCTGATG
AGGCCCTGCCTCTGGGCTCACCTCGCTGTGACCTGAAGGAGAATCTGCTGAAGGATAACTGTGCCCC
AGAATCCATCGAGTTCCCAGTGAGTGAGGCCCGAGTACTAGAGGACAGGCCCCTCAGCGACAAGGG
CTCTGGAGACAGCTCCCAGGTCACTCAAGTCAGTCCCCAGAGGATTGCACTCCGGCTCCGGCCAGAT
GATTCGAAGAATTTCTCCATCCAAGTGCGGCAGGTGGAGGATTACCCTGTGGACATCTACTACTTGAT
GGACCTGTCTTACTCCATGAAGGATGATCTGTGGAGCATCCAGAACCTGGGTACCAAGCTGGCCACC
CAGATGCGAAAGCTCACCAGTAACCTGCGGATTGGCTTCGGGGCATTTGTGGACAAGCCTGTGTCAC
CATACATGTATATCTCCCCACCAGAGGCCCTCGAAAACCCCTGCTATGATATGAAGACCACCTGCTTG
CCCATGTTTGGCTACAAACACGTGCTGACGCTAACTGACCAGGTGACCCGCTTCAATGAGGAAGTGA
AGAAGCAGAGTGTGTCACGGAACCGAGATGCCCCAGAGGGTGGCTTTGATGCCATCATGCAGGCTA
CAGTCTGTGATGAAAAGATTGGCTGGAGGAATGATGCATCCCACTTGCTGGTGTTTACCACTGATGCC
AAGACTCATATAGCATTGGACGGAAGGCTGGCAGGCATTGTCCAGCCTAATGACGGGCAGTGTCATG
TTGGTAGTGACAATCATTACTCTGCCTCCACTACCATGGATTATCCCTCTTTGGGGCTGATGACTGAG
AAGCTATCCCAGAAAAACATCAATTTGATCTTTGCAGTGACTGAAAATGTAGTCAATCTCTATCAGAAC
TATAGTGAGCTCATCCCAGGGACCACAGTTGGGGTTCTGTCCATGGATTCCAGCAATGTCCTCCAGC
TCATTGTTGATGCTTATGGGAAAATCCGTTCTAAAGTAGAGCTGGAAGTGCGTGACCTCCCTGAAGAG
TTGTCTCTATCCTTCAATGCCACCTGCCTCAACAATGAGGTCATCCCTGGCCTCAAGTCTTGTATGGG
ACTCAAGATTGGAGACACGGTGAGCTTCAGCATTGAGGCCAAGGTGCGAGGCTGTCCCCAGGAGAA
GGAGAAGTCCTTTACCATAAAGCCCGTGGGCTTCAAGGACAGCCTGATCGTCCAGGTCACCTTTGAT
TGTGACTGTGCCTGCCAGGCCCAAGCTGAACCTAATAGCCATCGCTGCAACAATGGCAATGGGACCT
TTGAGTGTGGGGTATGCCGTTGTGGGCCTGGCTGGCTGGGATCCCAGTGTGAGTGCTCAGAGGAGG
ACTATCGCCCTTCCCAGCAGGACGAATGCAGCCCCCGGGAGGGTCAGCCCGTCTGCAGCCAGCGG
GGCGAGTGCCTCTGTGGTCAATGTGTCTGCCACAGCAGTGACTTTGGCAAGATCACGGGCAAGTACT
GCGAGTGTGACGACTTCTCCTGTGTCCGCTACAAGGGGGAGATGTGCTCAGGCCATGGCCAGTGCA
GCTGTGGGGACTGCCTGTGTGACTCCGACTGGACCGGCTACTACTGCAACTGTACCACGCGTACTGA
CACCTGCATGTCCAGCAATGGGCTGCTGTGCAGCGGCCGCGGCAAGTGTGAATGTGGCAGCTGTGT
CTGTATCCAGCCGGGCTCCTATGGGGACACCTGTGAGAAGTGCCCCACCTGCCCAGATGCCTGCAC
CTTTAAGAAAGAATGTGTGGAGTGTAAGAAGTTTGACCGGGGAGCCCTACATGACGAAAATACCTGCA
ACCGTTACTGCCGTGACGAGATTGAGTCAGTGAAAGAGCTTAAGGACACTGGCAAGGATGCAGTGAA
TTGTACCTATAAGAATGAGGATGACTGTGTCGTCAGATTCCAGTACTATGAAGATTCTAGTGGAAAGT
CCATCCTGTATGTGGTAGAAGAGCCAGAGTGTCCCAAGGGCCCTGACATCCTGGTGGTCCTGCTCTC
AGTGATGGGGGCCATTCTGCTCATTGGCCTTGCCGCCCTGCTCATCTGGAAACTCCTCATCACCATC
CACGACCGAAAAGAATTCGCTAAATTTGAGGAAGAACGCGCCAGAGCAAAATGGGACACAGCCAACA
ACCCACTGTATAAAGAGGCCACGTCTACCTTCACCAATATCACGTACCGGGGCACTTAATGATAAGCA
GTCATCCTCAGATCATTATCAGCCTGTGCCACGATTGCAGGAGTCCCTGCCATCATGTTTACAGAGGA
CAGTATTTGTGGGGAGGGATTTGGGGCTCAGAGTGGGGTAGGTTGGGAGAATGTCAGTATGTGGAA
GTGTGGGTCTGTGTGTGTGTATGTGGGGGTCTGTGTGTTTATGTGTGTGTGTTGTGTGTGGGAGTGT
GTAATTTAAAATTGTGATGTGTCCTGATAAGCTGAGCTCCTTAGCCTTTGTCCCAGAATGCCTCCTGCA
GGGATTCTTCCTGCTTAGCTTGAGGGTGACTATGGAGCTGAGCAGGTGTTCTTCATTACCTCAGTGAG
AAGCCAGCTTTCCTCATCAGGCCATTGTCCCTGAAGAGAAGGGCAGGGCTGAGGCCTCTCATTCCAG
AGGAAGGGACACCAAGCCTTGGCTCTACCCTGAGTTCATAAATTTATGGTTCTCAGGCCTGACTCTCA
GCAGCTATGGTAGGAACTGCTGGGCT<mark>AAGCTT</mark>aagtttaaaccgctgatcagcctcgactgtgccttctagttgccagccatctgt
tgtttgcccctcccccgtgccttccttgaccctggaaggtgccactcccactgtcctttcctaataaaatgaggaaattgcatcgcattgtctgagtaggtgt
cattctattctgggggggtggggtggggcaggacagcaagggggaggattgggaagacaatagcaggcatgctggggatgcggtgggctctatggc
ttctgaggcggaaagaaccagctggggctctagggggtatccccacgcgccctgtagcggcgcattaagcgcggcgggtgtggtggttacgcgca
gcgtgaccgctacacttgccagcgccctagcgcccgctcctttcgctttcttcccttcctttctcgccacgttcgccggctttccccgtcaagctctaaatcg
ggggctcccttagggttccgatttagtgctttacggcacctcgaccccaaaaaacttgattagggtgatggttcacgtagtgggccatcgccctgatag
acggtttttcgcccttgacgttggagtccacgttctttaatagtggactcttgttccaaactggaacaacactcaaccctatctcggtctattcttttgatttata
agggattttgccgatttcggcctattggttaaaaaatgagctgatttaacaaaaatttaacgcgaattaattctgtggaatgtgtgtcagttagggtgtggaa
agtccccaggctccccagcaggcagaagtatgcaaagcatgcatctcaattagtcagcaaccaggtgtggaaagtccccaggctccccagcaggc
agaagtatgcaaagcatgcatctcaattagtcagcaaccatagtcccgcccctaactccgcccatcccgcccctaactccgcccagttccgcccattct
ccgccccatggctgactaatttttttttatttatgcagaggccgaggccgcctctgcctctgagctattccagaagtagtgaggaggctttttggaggccta

ggcttttgcaaaaagctcccgggagcttgtatatccattttcggatctgatcaagagacaggatgaggatcgtttcgcatgattgaacaagatggattgc
acgcaggttctccggccgcttgggtggagaggctattcggctatgactgggcacaacagacaatcggctgctctgatgccgccgtgttccggctgtca
gcgcaggggcgcccggttctttttgtcaagaccgacctgtccggtgccctgaatgaactgcaggacgaggcagcgcggctatcgtggctggccacg
acgggcgttccttgcgcagctgtgctcgacgttgtcactgaagcgggaagggactggctgctattgggcgaagtgccggggcaggatctcctgtcatc
tcaccttgctcctgccgagaaagtatccatcatggctgatgcaatgcggcggctgcatacgcttgatccggctacctgcccattcgaccaccaagcga
aacatcgcatcgagcgagcacgtactcggatggaagccggtcttgtcgatcaggatgatctggacgaagagcatcaggggctcgcgccagccga
actgttcgccaggctcaaggcgcgcatgcccgacggcgaggatctcgtcgtgacccatggcgatgcctgcttgccgaatatcatggtggaaaatggc
cgcttttctggattcatcgactgtggccggctgggtgtggcggaccgctatcaggacatagcgttggctacccgtgatattgctgaagagcttggcggcg
aatgggctgaccgcttcctcgtgctttacggtatcgccgctcccgattcgcagcgcatcgccttctatcgccttcttgacgagttcttctgagcgggactctg
gggttcgaaatgaccgaccaagcgacgcccaacctgccatcacgagatttcgattccaccgccgccttctatgaaaggttgggcttcggaatcgttttc
cgggacgccggctggatgatcctccagcgcggggatctcatgctggagttcttcgcccaccccaacttgtttattgcagcttataatggttacaaataaa
gcaatagcatcacaaatttcacaaataaagcatttttttcactgcattctagttgtggtttgtccaaactcatcaatgtatcttatcatgtctgtataccgtcgac
ctctagctagagcttggcgtaatcatggtcatagctgtttcctgtgtgaaattgttatccgctcacaattccacacaacatacgagccggaagcataaagt
gtaaagcctggggtgcctaatgagtgagctaactcacattaattgcgttgcgctcactgcccgctttccagtcgggaaacctgtcgtgccagctgcatta
atgaatcggccaacgcgcggggagaggcggtttgcgtattgggcgctcttccgcttcctcgctcactgactcgctgcgctcggtcgttcggctgcggcg
agcggtatcagctcactcaaaggcggtaatacggttatccacagaatcaggggataacgcaggaaagaacatgtgagcaaaaggccagcaaaa
ggccaggaaccgtaaaaaggccgcgttgctggcgtttttccataggctccgccccctgacgagcatcacaaaaatcgacgctcaagtcagaggtg
gcgaaacccgacaggactataaagataccaggcgtttcccccctggaagctccctcgtgcgctctcctgttccgaccctgccgcttaccggatacctgtc
cgcctttctcccttcgggaagcgtggcgctttctcatagctcacgctgtaggtatctcagttcggtgtaggtcgttcgctccaagctgggctgtgtgcacga
acccccgttcagcccgaccgctgcgccttatccggtaactatcgtcttgagtccaacccggtaagacacgacttatcgccactggcagcagccactg
gtaacaggattagcagagcgaggtatgtaggcggtgctacagagttcttgaagtggtggcctaactacggctacactagaagaacagtatttggtatct
gcgctctgctgaagccagttaccttcggaaaaagagttggtagctcttgatccggcaaacaaaccaccgctggtagcggttttttgtttgcaagcagca
gattacgcgcagaaaaaaggatctcaagaagatcctttgatcttttctacggggtctgacgctcagtggaacgaaaactcacgttaagggattttggt
catgagattatcaaaaaggatcttcacctagatcctttaaattaaaaatgaagttttaaatcaatctaaagtatatatgagtaaacttggtctgacagttac
caatgcttaatcagtgaggcacctatctcagcgatctgtctatttcgttcatccatagttgcctgactccccgtcgtgtagataactacgatacgggagggc
ttaccatctggccccagtgctgcaatgataccgcgagacccacgctcaccggctccagatttatcagcaataaaccagccagccggaagggccga
gcgcagaagtggtcctgcaactttatccgcctccatccagtctattaattgttgccgggaagctagagtaagtagttcgccagttaatagtttgcgcaacg
ttgttgccattgctacaggcatcgtggtgtcacgctcgtcgtttggtatggcttcattcagctccggttcccaacgatcaaggcgagttacatgatcccccat
gttgtgcaaaaaagcggttagctccttcggtcctccgatcgttgtcagaagtaagttggccgcagtgttatcactcatggttatggcagcactgcataattc
tcttactgtcatgccatccgtaagatgcttttctgtgactggtgagtactcaaccaagtcattctgagaatagtgtatgcggcgaccgagttgctcttgcccg
gcgtcaatacgggataataccgcgccacatagcagaactttaaaagtgctcatcattggaaaacgttcttcggggcgaaaactctcaaggatcttacc
gctgttgagatccagttcgatgtaacccactcgtgcacccaactgatcttcagcatcttttactttcaccagcgtttctgggtgagcaaaaacaggaaggc
aaaatgccgcaaaaaagggaataagggcgacacggaaatgttgaatactcatactcttccttttcaatattattgaagcatttatcagggttattgtctca
tgagcggatacatatttgaatgtatttagaaaaataaacaaatagggttccgcgcacatttccccgaaaagtgccacctgacgtc

Key:
Lower case: pCDNA3.1 sequence**;** Upper case: *ITGB3* or *ITGA2B* cDNA sequence,
Yellow highlight: Hind III restriction site; Red highlight: XbaI restriction site

8.2 Appendix 2: pcDNA 3.1 Dup vector sequence

> pcDNA 3.1 Dup vector

GACGGATCGGGAGATCTCCCGATCCCCTATGGTGCACTCTCAGTACAATCTGCTCTGATGCCGCATA
GTTAAGCCAGTATCTGCTCCCTGCTTGTGTGTTGGAGGTCGCTGAGTAGTGCGCGAGCAAAATTTAA
GCTACAACAAGGCAAGGCTTGACCGACAATTGCATGAAGAATCTGCTTAGGGTTAGGCGTTTTGCGC
TGCTTCGCGATGTACGGGCCAGATATACGCGTTGACATTGATTATTGACTAGTTATTAATAGTAATCAA
TTACGGGGTCATTAGTTCATAGCCCATATATGGAGTTCCGCGTTACATAACTTACGGTAAATGGCCCG
CCTGGCTGACCGCCCAACGACCCCCGCCCATTGACGTCAATAATGACGTATGTTCCCATAGTAACGC
CAATAGGGACTTTCCATTGACGTCAATGGGTGGAGTATTTACGGTAAACTGCCCACTTGGCAGTACAT
CAAGTGTATCATATGCCAAGTACGCCCCCTATTGACGTCAATGACGGTAAATGGCCCGCCTGGCATTA
TGCCCAGTACATGACCTTATGGGACTTTCCTACTTGGCAGTACATCTACGTATTAGTCATCGCTATTAC
CATGGTGATGCGGTTTTGGCAGTACATCAATGGGCGTGGATAGCGGTTTGACTCACGGGGATTTCCA
AGTCTCCACCCCATTGACGTCAATGGGAGTTTGTTTTGGCACCAAAATCAACGGGACTTTCCAAAATG
TCGTAACAACTCCGCCCCATTGACGCAAATGGGCGGTAGGCGTGTACGGTGGGAGGTCTATATAAGC
AGAGCTCTCTGGCTAACTAGAGAACCCACTGCTTACTGGCTTATCGAAATTAATACGACTCACTATAG
*GGAGACCCAAGCTGGCTAGCGTTTAAACGGGCCCTCTAGA*CTCGAGACATTTGCTTCTGACACAACT
GTGTTCACTAGCAACCTCAAACAGACACCATGGTGCACCTGACTCCTGAGGAGAAGTCTGCCGTTAC
TGCCCTGTGGGGCAAGGTGAACGTGGATGAAGTTGGTGGTGAGGCCCTGGGCAGgttggtatcaaggttaca
agacaggtttaaggagaccaatagaaactgggcatgtggagacagagaagactcttgggtttctgataggcactgactctctctgcctattggtctatttt
cccacccttagGCTGAATTC*CCACCAGAGGCCCTCA*/GAAAACCCCTGCTATGGGATCC*GGCAG*gttggtatcaa
ggttacaagacaggtttaaggagaccaatagaaactgggcatgtggagacagagaagactcttgggtttctgataggcactgactctctctgcctattg
gtctattttcccacccttagGCTGCTGGTGGTCTACCCTTGGACCCAGAGGTTCTTTGAGTCCTTTGGGGATCTG
TCCACTCCTGATGCTGTTATGGGCAACCCTAAGGTGAAGGCTCATGGCAAGAAAGTGCTCGGTGCCT
TTAGTGATGGCCTGNCTCACCTGGACAACCTCAAGGGCACCTTTGCCACACTGAGTGAGCTGCACTG
TGACAAGCTGCACGTAGATCTganctcggtaccaagcttaagtttaaaccgctgatcagcctcgactgtgccttctagttgccagccatct
gttgtttgcccctcccccgtgccttccttgaccctggaaggtgccactcccactgtcctttcctaataaaatgaggaaattgcatcgcattgtctgagtaggt
gtcattctattctgggggggtggggtggggcaggacagcaagggggaggattgggaagacaatagcaggcatgctggggatgcggtgggctctatg
gcttctgaggcggaaagaaccagctggggctctaggggtatccccacgcgccctgtagcggcgcattaagcgcggcgggtgtggtggttacgcgc
agcgtgaccgctacacttgccagcgccctagcgcccgctcctttcgctttcttcccttcctttctcgccacgttcgccggctttccccgtcaagctctaaatc
gggggctccctttagggttccgatttagtgctttacggcacctcgaccccaaaaaacttgattagggtgatggttcacgtagtgggccatcgccctgata
gacggtttttcgccctttgacgttggagtccacgttctttaatagtggactcttgttccaaactggaacaacactcaaccctatctcggtctattcttttgatttat
aagggattttgccgatttcggcctattggttaaaaaatgagctgatttaacaaaaatttaacgcgaattaattctgtggaatgtgtgtcagttagggtgtgga
aagtccccaggctccccagcaggcagaagtatgcaaagcatgcatctcaattagtcagcaaccaggtgtggaaagtccccaggctccccagcag
gcagaagtatgcaaa*gcatgcatctcaattagtcagcaaccatagtcccgcccctaactccgcccatcccgcccctaactccgcccagttccgcccat*
tctccgccccatggctgactaatttttttttatttatgcagaggccgaggccgcctctgcctctgagctattccagaagtagtgaggaggctttttggaggcct
aggcttttgcaaaaagctcccgggagcttgtatatccattttcggatctgatcaagagacaggatgaggatcgtttcgcatgattgaacaagatggattg
cacgcaggttctccggccgcttgggtggagaggctattcggctatgactgggcacaacagacaatcggctgctctgatgccgccgtgttccggctgtc
agcgcaggggcgcccggttctttttgtcaagaccgacctgtccggtgccctgaatgaactgcaggacgaggcagcgcggctatcgtggctggccac
gacgggcgttccttgcgcagctgtgctcgacgttgtcactgaagcgggaagggactggctgctattgggcgaagtgccggggcaggatctcctgtcat
ctcaccttgctcctgccgagaaagtatccatcatggctgatgcaatgcggcggctgcatacgcttgatccggctacctgcccattcgaccaccaagcg
aaacatcgcatcgagcgagcacgtactcggatggaagccggtcttgtcgatcaggatgatctggacgaagagcatcaggggctcgcgccagccg
aactgttcgccaggctcaaggcgcgcatgcccgacggcgaggatctcgtcgtgacccatggcgatgcctgcttgccgaatatcatggtggaaaatgg
ccgcttttctggattcatcgactgtggccggctgggtgtggcggaccgctatcaggacatagcgttggctacccgtgatattgctgaagagcttggcggc
gaatgggctgaccgcttcctcgtgctttacggtatcgccgctcccgattcgcagcgcatcgccttctatcgccttcttgacgagttcttctgagcgggactct
ggggttcgaaatgaccgaccaagcgacgcccaacctgccatcacgagatttcgattccaccgccgccttctatgaaaggttgggcttcggaatcgtttt
ccgggacgccggctggatgatcctccagcgcggggatctcatgctggagttcttcgcccaccccaacttgtttattgcagcttataatggttacaaataa
agcaatagcatcacaaatttcacaaataaagcatttttttcactgcattctagttgtggtttgtccaaactcatcaatgtatcttatcatgtctgtataccgtcga
cctctagctagagcttggcgtaatcatggtcatagctgtttcctgtgtgaaattgttatccgctcacaattccacacaacatacgagccggaagcataaa
gtgtaaagcctggggtgcctaatgagtgagctaactcacattaattgcgttgcgctcactgcccgctttccagtcgggaaacctgtcgtgccagctgcatt
aatgaatcggccaacgcgcggggagaggcggtttgcgtattgggcgctcttccgcttcctcgctcactgactcgctgcgctcggtcgttcggctgcggc
gagcggtatcagctcactcaaaggcggtaatacggttatccacagaatcaggggataacgcaggaaagaacatgtgagcaaaaggccagcaaa
aggccaggaaccgtaaaaaggccgcgttgctggcgtttttccataggctccgccccctgacgagcatcacaaaaatcgacgctcaagtcagaggt
ggcgaaacccgacaggactataaagataccaggcgtttcccctggaagctccctcgtgcgctctcctgttccgaccctgccgcttaccggatacctgt
ccgcctttctcccttcgggaagcgtggcgctttctatagctcacgctgtaggtatctcagttcggtgtaggtcgttcgctccaagctgggctgtgtgcacg

aacccccgttcagcccgaccgctgcgccttatccggtaactatcgtcttgagtccaacccggtaagacacgacttatcgccactggcagcagccact
ggtaacaggattagcagagcgaggtatgtaggcggtgctacagagttcttgaagtggtggcctaactacggctacactagaagaacagtatttggtat
ctgcgctctgctgaagccagttaccttcggaaaaagagttggtagctcttgatccggcaaacaaaccaccgctggtagcggttttttgtttgcaagcag
cagattacgcgcagaaaaaaaggatctcaagaagatcctttgatcttttctacggggtctgacgctcagtggaacgaaaactcacgttaagggattttg
gtcatgagattatcaaaaaggatcttcacctagatcctttaaattaaaaatgaagttttaaatcaatctaaagtatatatgagtaaacttggtctgacagtta
ccaatgcttaatcagtgaggcacctatctcagcgatctgtctatttcgttcatccatagttgcctgactccccgtcgtgtagataactacgatacgggaggg
cttaccatctggccccagtgctgcaatgataccgcgagacccacgctcaccggctccagatttatcagcaataaaccagccagccggaagggccg
agcgcagaagtggtcctgcaactttatccgcctccatccagtctattaattgttgccgggaagctagagtaagtagttcgccagttaatagtttgcgcaac
gttgttgccattgctacaggcatcgtggtgtcacgctcgtcgtttggtatggcttcattcagctccggttcccaacgatcaaggcgagttacatgatccccc
atgttgtgcaaaaaagcggttagctccttcggtcctccgatcgttgtcagaagtaagttggccgcagtgttatcactcatggttatggcagcactgcataat
tctcttactgtcatgccatccgtaagatgcttttctgtgactggtgagtactcaaccaagtcattctgagaatagtgtatgcggcgaccgagttgctcttgccc
ggcgtcaatacgggataataccgcgccacatagcagaactttaaaagtgctcatcattggaaaacgttcttcggggcgaaaactctcaaggatcttac
cgctgttgagatccagttcgatgtaacccactcgtgcacccaactgatcttcagcatcttttactttcaccagcgtttctgggtgagcaaaaacaggaagg
caaaatgccgcaaaaaagggaataagggcgacacggaaatgttgaatactcatactcttccttttcaatattattgaagcatttatcagggttattgtctc
atgagcggatacatatttgaatgtatttagaaaaataaacaaatagggggttccgcgcacatttccccgaaaagtgccacctgacgt

Key:

Lower case and italics: pCDNA3.1 sequence; Lower case : non-coding sequence; Grey: non-coding *ITGB3* cDNA sequence; Red text: exons 3 and 4 of the human β-globin gene; Underlined text: *ITGB3* insert (c.583 to c.613) cloned into pcDNA 3.1 Dup ; Yellow highlight: EcoRI restriction site; Pink highlight: BamHI restriction site; Blue highlight: Xhol restriction site; Grey highlight: BgIII restriction site.

8.3 Appendix 3 : pET-01-*ITGA2B* exon 20 sequence:

TCAGGATATAGTAGTTTCGCTTTTGCATAGGGAGGGGGAAATGTAGTCTTATGCAATACTCTTGTAGT
CTTGCAACATGCTTATGTAACGATGAGTTAGCAACATGCCTTATAAGGAGAGAAAAAGCACCGTGCAT
GCCGATTGGTGGGAGTAAGGTGGTATGATCGTGGTATGATCGTGCCTTGTTAGGAAGGCAACAGACG
GGTCTAACACGGATTGGACGAACCACTGAATTCCGCATTGCAGAGATATTGTATTTAAGTGCCTAGCT
CGATACAATAAACGCCATTTGACCATTCACCACATTGGTGTGCACCTCAAGCTTCCTGCATGCTGCTG
CTGCTGCTGCTGCTGGGCCTGAGGCTACAGCTCTCCCTGGGCATCATCCCAGTTGAGGAGGAGAAC
CCGGACTTCTGGAACCGCGAGGCAGCCGAGGCCCTGGGTGCCGCCAAGAAGCTGCAGCCTGCACA
GACAGCCGCCAAGAACCTCATCATCTTCCTGGGCGATGGGATGGGGGTGTCTACGGTGACAGCTGC
CAGGATCGATCTGCTTCCTGGCCCTGCTGGGCCTGCTCATCCTCTGGGAGCCCTGGCCTGCCCAGG
CTTTTGTCAACAGCACCTTTGTGGTTCTCACTTGGTGGAAGCTCTCTACCTGGTGTGTGGGGAGCGTG
GATTCTTCTACACACCCATGTCCCGCCGCGAAGTGGAGGACCCACAAGGTAAGCTCTGCTCCTGAAT
TAATTCTATCCCAAGTGCTAACTACCCTGTTTGTCTTTCACCCTTGAGACCTTGTAAATTGTGCCCTAG
GTGTGGAGGGTCTCAGGCTAACCAGTGGGGGGCACATTTCTGTGGGCAGCTAGACATATGTAAACAT
GGTAGCTGCCAGGAAGGAGTGAGAATCCTTCCTTAAGTCTCCTAGGTGGTGACGGGTGGCTAGGCC
CCAGGATAGGTACCGGGCCCCCCCTCGAGGTCGACGGTATCGATAAGCTAATTCCTGCAGCCCGGG
GGATCCgtgaggaggcctcccattctgcccgaccctggccctttctgcctatcatacctgctccacaccttagtcccctcttttcccacatcctgggcc
cagacccaggctccctggcttcactcctctttccccacagGACGGGCTCCCCGCTCCTAGTTGGGGCAGATAATGTCCTG
GAGCTGCAGATGGACGCAGCCAACGAGGGCGAGGGGGCCTATGAAGCAGAGCTGGCCGTGCACCT
GCCCCAGGGCGCCCACTACATGCGGGCCCTAAGCAATGTCGAC/Tgtatggcccccaccctgggaacagtacccgg
gacctgggaggcactggagccttggctctctcatctcccctccctgagagtccctcttctcttctgctttgctgtcaaagatgtaatttttttattttttttttaatttgga
ggaggaatacttgctaatggcacagaattccaaaactctattacaaaaaccagaaaaacaaaaaaggtttaggaaccaaatgttaacaggaacct
ctgttaacatttggtggatttccttccagtctttttttcaatattgactcacactcacataagtatatatttattttttatgttgttaatatagtttataataatgggggtc
atactctaatgttttgtgttttttatttccaaaatgaaaatgcctaaaaagtagtagtgctacagcaatacacacactagcatgtgacagtcccttgagaccc
caccccaagaaaccccccccctccctaccttggcacacaaatctttccagaccttccaagggagcttaaatatatatatatgatgctctgtaatttctttcttg
gaactgccttcctgaaggGCGGCCGCCACCGCGGTGGAGCTCGGTACCTATTTGGGGACCCCATAGAGCAC

TGCACTGACTGAGGGATGGTAACAGGATGTGTAGGTTTTGGAGGCCCATATGTCCATTCATGACCAG
TGACTTGTCTCACAGCCATGCAACCCTTGCCTCCTGTGCTGACTTAGCAGGGGATAAAGTGAGAGAA
AGCCTGGGCTAATCAGGGGGTCGCTCAGCTCCTCCTAACTGGATTGTCCTATGTGTCTTTGCTTCTGT
GCTGCTGATGCTCTGCCCTGTGCTGACATGACCTCCCTGGCAGTGGCACAACTGGAGCTGGGTGGA
GGCCCGTGACCTTCAGACCTTGGCACTGGAGGTGGCCCGGCAGAAGCGCGGCATCGTGGATCAGTG
CTGCACCAGCATCTGCTCTCTCTACCAACTGGAGAACTACTGCAACTAGGCCCACCACTACCCTGTCC
ACCCCTCTGCAATGAATAAAACCTTTGAAAGAGCACTACAAGTTGTGTGTACATGCGTGCATGTGCAT
ATGTGGTGCGGGGGGAACATGAGTGGGGCTGGCTGGAGTGGCGATGATAAGCTGTCAAACATGAGA
ATTCTTGAAGACGAAAGGGCCTCGTGATACGCCTATTTTTATAGGTTAATGTCATGATAATAATGGTTT
CTTAGACGTCAGGTGGCACTTTTCGGGGAAATGTGCGCGGAACCCCTATTTGTTTATTTTTCTAAATAC
ATTCAAATATGTATCCGCTCATGAGACAATAACCCTGATAAATGCTTCAATAATATTGAAAAAGGAAGA
GTATGAGTATTCAACATTTCCGTGTCGCCCTTATTCCCTTTTTTGCGGCATTTTGCCTTCCTGTTTTTGC
TCACCCAGAAACGCTGGTGAAAGTAAAAGATGCTGAAGATCAGTTGGGTGCACGAGTGGGTTACATC
GAACTGGATCTCAACAGCGGTAAGATCCTTGAGAGTTTTCGCCCCGAAGAACGTTTTCCAATGATGAG
CACTTTTAAAGTTCTGCTATGTGGCGCGGTATTATCCCGTGTTGACGCCGGGCAAGAGCAACTCGGT
CGCCGCATACACTATTCTCAGAATGACTTGGTTGAGTACTCACCAGTCACAGAAAAGCATCTTACGGA
TGGCATGACAGTAAGAGAATTATGCAGTGCTGCCATAACCATGAGTGATAACACTGCGGCCAACTTAC
TTCTGACAACGATCGGAGGACCGAAGGAGCTAACCGCTTTTTTGCACAACATGGGGGATCATGTAAC
TCGCCTTGATCGTTGGGAACCGGAGCTGAATGAAGCCATACCAAACGACGAGCGTGACACCACGATG
CCTGCAGCAATGGCAACAACGTTGCGCAAACTATTAACTGGCGAACTACTTACTCTAGCTTCCCGGCA
ACAATTAATAGACTGGATGGAGGCGGATAAAGTTGCAGGACCACTTCTGCGCTCGGCCCTTCCGGCT
GGCTGGTTTATTGCTGATAAATCTGGAGCCGGTGAGCGTGGGTCTCGCGGTATCATTGCAGCACTGG
GGCCAGATGGTAAGCCCTCCCGTATCGTAGTTATCTACACGACGGGGAGTCAGGCAACTATGGATGA
ACGAAATAGACAGATCGCTGAGATAGGTGCCTCACTGATTAAGCATTGGTAACTGTCAGACCAAGTTT
ACTCATATATACTTTAGATTGATTTAAAACTTCATTTTTAATTTAAAAGGATCTAGGCTGCTGCTTGCAA
ACAAAAAAACCACCGCTACCAGCGGTGGTTTGTTTGCCGGATCAAGAGCTACCAACTCTTTTTCCGAA
GGTAACTGGCTTCAGCAGAGCGCAGATACCAAATACTGTCCTTCTAGTGTAGCCGTAGTTAGGCCAC
CACTTCAAGAACTCTGTAGCACCGCCTACATACCTCGCTCTGCTAATCCTGTTACCAGTGGCTGCTGC
CAGTGGCGATAAGTCGTGTCTTACCGGGTTGGACTCAAGACGATAGTTACCGGATAAGGCGCAGCGG
TCGGGCTGAACGGGGGGTTCGTGCACACAGCCCAGCTTGGAGCGAACGACCTACACCGAACTGAGA
TACCTACAGCGTGAGCTATGAGAAAGCGCCACGCTTCCCGAAGGGAGAAAGGCGGACAGGTATCCG
GTAAGCGGCAGGGTCGGAACAGGAGAGCGCACGAGGGAGCTTCCAGGGGGAAACGCCTGGTATCT
TTATAGTCCTGTCGGGTTTCGCCACCTCTGACTTGAGCGTCGATTTTTGTGATGCTCGTCAGGGGGG
CGGAGCCTATGGAAAAACGCCAGCAACGGAGATGCGCCGCGTGCGGCTGCTGGAGATGGCGGACG
CGATGGATATGTTCTGCCAAGGGTTGGTTTGCGCATTCACAGTTCTCCGCAAGAATTGATTGGCTCCA
ATTCTTGGAGTGGTGAATCCGTTAGCGAGGTGCCGCCGGCTTCCATTCAGGTCGAGGTGGCCCGGC
TCCATGCACCGCGACGCAACGCGGGGAGGCAGACAAGGTATAGGGCGGCGCCTACAATCCATGCCA
ACCCGTTCCATGTGCTCGCCGAGGCGGCATAAATCGCCGTGACGATCAGCGGTCCAATGATCGAAGT
TAGGCTGGTAAGAGCCGCGAGCGATCCTTGAAGCTGTCCCTGATGGTCGTCATCTACCTGCCTGGAC
AGCATGGCCTGCAACGCGGGCATCCCGATGCCGCCGGAAGCGAGAAGAATCATAATGGGGAAGGCC
ATCCAGCCTCGCGTCGGGGAGCTTTTTGCAAAAGCCTAGGCCTCCAAAAAAGCCTCCTCACTACTTCT
GGAATAGCTCAGAGGCCGAGGCGGCCTCGGCCTCTGCATAAATAAAAAAAATTAGTCAGCCATGGGG
CGGAGAATGGGCGGAACTGGGCGGAGTTAGGGGCGGGATGGGCGGAGTTAGGGGCGGGACTATG
GTTGCTGACTAATTGAGATGCATGCAAGGAGATGGCGCCCAACAGTCCCCCGGCCACGGGGCCTGC
CACCATACCCACGCCGAAACAAGCGCTCATGAGCCCGAAGTGGCGAGCCCGATCTTCCCCATCGGT
GATGTCGGCGATATAGGCGCCAGCAACCGCACCTGTGGCGCCGGTGATGCCGGCCACGATGCGTCC
GGCGTAGAGGATC

Key:

Upper case: pET01 sequence; Lower case: introns flacking exon-20 *ITGA2B*; Red text: *ITGA2B* exon 20;Yellow highlight: BamHI restriction site; Red highlight: NotI restriction site.

8.4 Appendix 4: Open reading frame of wild-type *ITGA2B* and exon-20 *ITGA2B* deletion

***ITGA2B* Wild-type:**

Met A R A L C P L Q A L W L L E W V L L L L G P C A A P P A W A L N L D P V Q L T F Y A G P N G S
Q F G F S L D F H K D S H G R V A I V V G A P R T L G P S Q E E T G G V F L C P W R A E G G Q C P
S L L F D L R D E T R N V G S Q T L Q T F K A R Q G L G A S V V S W S D V I V A C A P W Q H W N V
L E K T E E A E K T P V G S C F L A Q P E S G R R A E Y S P C R G N T L S R I Y V E N D F S W D K
R Y C E A G F S S V V T Q A G E L V L G A P G G Y Y F L G L L A Q A P V A D I F S S Y R P G I L L W
H V S S Q S L S F D S S N P E Y F D G Y W G Y S V A V G E F D G D L N T T E Y V V G A P T W S W
T L G A V E I L D S Y Y Q R L H R L R G E Q M A S Y F G H S V A V T D V N G D G R H D L L V G A P
L Y M E S R A D R K L A E V G R V Y L F L Q P R G P H A L G A P S L L L T G T Q L Y G R F G S A I A
P L G D L D R D G Y N D I A V A A P Y G G P S G R G Q V L V F L G Q S E G L R S R P S Q V L D S P
F P T G S A F G F S L R G A V D I D D N G Y P D L I V G A Y G A N Q V A V Y R A Q P V V K A S V Q L
L V Q D S L N P A V K S C V L P Q T K T P V S C F N I Q M C V G A T G H N I P Q K L S L N A E L Q L
D R Q K P R Q G R R V L L L G S Q Q A G T T L N L D L G G K H S P I C H T T M A F L R D E A D F R
D K L S P I V L S L N V S L P P T E A G M A P A V V L H G D T H V Q E Q T R I V L D C G E D D V C V
P Q L Q L T A S V T G S P L L V G A D N V L E L Q M D A A N E G E G A Y E A E L A V H L P Q G A H
Y M R A L S N V E G F E R L I C N Q K K E N E T R V V L C E L G N P M K K N A Q I G I A M L V S V G
N L E E A G E S V S F Q L Q I R S K N S Q N P N S K I V L L D V P V R A E A Q V E L R G N S F P A S
L V V A A E E G E R E Q N S L D S W G P K V E H T Y E L H N N G P G T V N G L H L S I H L P G Q S
Q P S D L L Y I L D I Q P Q G G L Q C F P Q P P V N P L K V D W G L P I P S P S P I H P A H H K R D
R R Q I F L P E P E Q P S R L Q D P V L V S C D S A P C T V V Q C D L Q E M A R G Q R A M V T V L
A F L W L P S L Y Q R P L D Q F V L Q S H A W F N V S S L P Y A V P P L S L P R G E A Q V W T Q L
L R A L E E R A I P I W W V L V G V L G G L L L L T I L V L A M W K V G F F K R N R P P L E E D D E E
G E*

Exon-20 *ITGA2B* deletion

Met A R A L C P L Q A L W L L E W V L L L L G P C A A P P A W A L N L D P V Q L T F Y A G P N G S
Q F G F S L D F H K D S H G R V A I V V G A P R T L G P S Q E E T G G V F L C P W R A E G G Q C P
S L L F D L R D E T R N V G S Q T L Q T F K A R Q G L G A S V V S W S D V I V A C A P W Q H W N V
L E K T E E A E K T P V G S C F L A Q P E S G R R A E Y S P C R G N T L S R I Y V E N D F S W D K
R Y C E A G F S S V V T Q A G E L V L G A P G G Y Y F L G L L A Q A P V A D I F S S Y R P G I L L W
H V S S Q S L S F D S S N P E Y F D G Y W G Y S V A V G E F D G D L N T T E Y V V G A P T W S W
T L G A V E I L D S Y Y Q R L H R L R G E Q M A S Y F G H S V A V T D V N G D G R H D L L V G A P
L Y M E S R A D R K L A E V G R V Y L F L Q P R G P H A L G A P S L L L T G T Q L Y G R F G S A I A
P L G D L D R D G Y N D I A V A A P Y G G P S G R G Q V L V F L G Q S E G L R S R P S Q V L D S P
F P T G S A F G F S L R G A V D I D D N G Y P D L I V G A Y G A N Q V A V Y R A Q P V V K A S V Q L
L V Q D S L N P A V K S C V L P Q T K T P V S C F N I Q M C V G A T G H N I P Q K L S L N A E L Q L
D R Q K P R Q G R R V L L L G S Q Q A G T T L N L D L G G K H S P I C H T T M A F L R D E A D F R
D K L S P I V L S L N V S L P P T E A G M A P A V V L H G D T H V Q E Q T R I V L D C G E D D V C V
P Q L Q L T A S V **A L R D S S V I R R R R Met R P G W C C V S W A T P** **Stop**

Figure A2 The predicted amino acid sequence based on the wild-type and exon 20 deletion (c.1947_2094del). The c.2094G>T defect is predicted to lead to a frameshift and introduction of a premature stop codon 24 amino acids after the alanine residue at position 650, (c.1947_2094del; p.Thr650Alafs*24).The text highlighted in pink and black is the normal protein sequence of α_{IIb} while the red text is new amino acid introduced after exon 20 deletion.